Universität
Augsburg
University

Efficient Evaluation and Estimation of Dynamic Stochastic General Equilibrium Models

Kumulative Dissertation
der Wirtschaftswissenschaftlichen Fakultät
der Universität Augsburg
zur Erlangung des Grades eines
Doktors der Wirtschaftswissenschaften
(Dr. rer. pol.)

vorgelegt von

Johannes Maximilian Huber
(M. Sc. Economics and Public Policy)

Erstgutachter: Prof. Dr. Alfred Maußner

Zweitgutachter: Prof. Dr. Burkhard Heer

Vorsitzende der Disputation: Prof. Dr. Kerstin Roeder

Tag der mündlichen Prüfung: 05.07.2022

April 2022

Efficient Evaluation and Estimation of Dynamic Stochastic General Equilibrium Models

– Johannes Maximilian Huber –

Contents

List of Figures

List of Tables

List of Algorithms

List of Acronyms

AKF	augmented Kalman filter
ASKF	augmented steady-state Kalman filter
BCA	business cycle accounting
BE	Bayesian estimation
CR	Chandrasekhar recursion
DARE	discrete algebraic Riccati equation
DSGE	dynamic stochastic general equilibrium
ECB	European Central Bank
GDP	Gross Domestic Product
GMM	generalized method of moments
KF	Kalman filter
MLE	maximum-likelihood estimation
MSE	mean squared error
PCE	polynomial chaos expansion
QoI	quantity of interest
RBC	real business cycle
RDE	Riccati difference equation
RWMH	random walk Metropolis-Hasting
SKF	steady-state Kalman filter
SMM	simulated method of moments
SSM	state-space model
TaRBMH	tailored randomized block Metropolis-Hastings
UKF	univariate treatment of multivariate observation vectors
VAR	vector autoregression
VAT	value-added tax

List of Publications and the Author's Contribution

The thesis includes the following three essays:

FEHRLE, D., C. HEIBERGER, AND J. HUBER (2022): "Polynomial Chaos Expansion: Efficient Evaluation and Estimation of Computational Models".

FEHRLE, D. AND J. HUBER (2022): "Business Cycle Accounting for the German Fiscal Stimulus Program during the Great Recession".

HUBER, J. (2022): "An Augmented Steady-State Kalman Filter to Evaluate the Likelihood of Linear and Time-Invariant State-Space models".

Contributions:

- Huber (2022) is single authored.
- Fehrle and Huber (2022) is joint work with Dr. Daniel Fehrle (Augsburg University), where both contributed about 50 percent.
- Fehrle, Heiberger, and Huber (2022) is joint work with Dr. Daniel Fehrle (Augsburg University) and Dr. Christopher Heiberger (Augsburg University), where all authors contributed about $33.\bar{3}$ percent.

Conference participations:

- Preceding versions of Huber (2022) significantly benefit from comments during presentations at:

  the 32nd BGPE Research Workshop in Passau and the Seminar in Economics at the University of Augsburg.

- Preceding versions of Fehrle and Huber (2022) significantly benefit from comments during presentations at:

  the 34th Annual Congress of the European Economic Association in Manchester, the Doctoral Seminar in Economics at Leipzig University, the 24th Spring Meeting of Young Economists in Brussels, 23rd Theories and Methods in Macroeconomics in Nuremberg, 19th IWH-CIREQ-GW Macroeconometric Workshop at IWH Halle, and the Seminar in Economics at the University of Augsburg.

Chapter 1

Introduction*

> *The outcome of any important macroeconomic policy change is the net effect of forces operating on different parts of the economy. A central challenge facing policymakers is how to assess the relative strength of those forces.[...] Dynamic stochastic general equilibrium (DSGE) models are the leading tool for making such assessments in an open and transparent manner.*
>
> Christiano et al. (2018, pp. 113)

Going back to the seminal work of Kydland and Prescott (1982) and Long and Plosser (1983), over the past four decades, the class of dynamic stochastic general equilibrium (DSGE) models has become one of the dominant analytic frameworks in modern macroeconomics. For instance, Glandon et al. (2022) find that about 42 percent of the "theory-centered" articles published in five leading macroeconomic field journals – the *Journal of Monetary Economics*, the *Journal of Money, Credit and Banking*, the *American Economic Journal: Macroeconomics*, the *Journal of Economic Dynamics and Control*, and the *Review of Economic Dynamics* – from 2016 to 2018, employ DSGE models.[1] Part of the reason for the growing interest in DSGE models is that they provide a consistent framework for analyzing the impact of macroeconomic policy changes. Thereby, as Fernández-Villaverde and Guerrón-Quintana (2021) emphasize, "[t]he class of DSGE economies is not defined by a particular set of assumptions, but rather by an approach to the construction of macroeconomic models." Within this approach, the researcher is forced to formulate the assumptions underlying his analysis in a clear and transparent manner. On the one hand, this transparency marks DSGE models as a frequent target for critics (see, e.g., Stiglitz, 2018). On the other hand, this transparency also prepares the ground to address their shortcomings by adding new features to the DSGE framework.[2] Another reason for the growing interest in DSGE models is the progress in developing new algorithms to evaluate and estimate these models. Most notable here is the tremendous evolution of Bayesian estimation methods in the wake of the seminal articles by Smets and Wouters (2003, 2007), which established DSGE models as an essential part of the monetary policy analysis in central banks around the world.[3]

*I use the pronoun "we" in order to refer to author(s) and reader in this thesis.

[1] Glandon et al. (2022) distinguish the 786 articles in the above journals from 2016 to 2018 into three categories: Those that use "theory-centered" methods, those that employ "econometrics-based" methods, or those that use both. Of the 529 articles that apply theory-centered methods, 42 percent employ DSGE models. Hence, more than one-fourth of all articles in these journals apply DSGE models.

[2] See, e.g., Christiano et al. (2018), who discuss the progress in DSGE modeling in the aftermath of the financial crisis and the Great Recession.

[3] For a collection of prominent DSGE models used in central banks, see Sergi (2020, Tables 1 and 2).

However, since DSGE models typically cannot be assessed analytically, these models' accurate evaluation and estimation can become a time-consuming computational task. This thesis addresses how to estimate and evaluate DSGE models efficiently. Therefore, we first need to define what we understand by an *efficient evaluation* and *estimation* of DSGE models.

At an abstract level, we can think of a DSGE model as a mapping from a set of parameters to some quantity of interest (QoI), e.g., the model's policy function, its impulse response function, its unconditional first and second moments, or its likelihood function for a given set of data. Throughout this thesis, we denote the process of determining the QoI associated with a set of parameters as *evaluation* of the model. Regarding this evaluation process, the term *efficient* has two dimensions: The first dimension of efficiency refers to the time and resources required to evaluate the QoI of the model. The second dimension, in contrast, refers to the accuracy to which we can determine this QoI.

For instance, consider a scenario where we wish to examine how the agents in our model economy respond to a change in macroeconomic policy. Since the so-called policy function represents the agents' responses to changes in the current state of the economy, this function reflects the natural QoI in such analyses. However, evaluating the model's policy function typically requires numerical methods to solve the model's underlying first-order system of (potentially non-linear) expectational difference equations.[4] Following DeJong and Dave (2011), we can categorize these methods into linear and non-linear techniques. The first category draws mainly on contributions by Blanchard and Kahn (1980), Klein (2000), Uhlig (2001), and Sims (2002), while we can separate the latter into local (e.g., higher-order perturbation methods) and global solution techniques (e.g., value functions iteration or projection methods). Compared to non-linear and especially compared to global techniques, linear methods typically involve less computational effort. Hence, if we focus exclusively on minimizing the computational burden, we might consider linear solution techniques more efficient. However, an essential feature of linear solution techniques is that the (approximated) policy function they imply is itself linear, which is why they may become inaccurate if the model's "true" policy function includes non-linear components. Consequently, non-linear techniques are often more efficient in terms of accuracy for these models. Thus, we consider efficiency as the trade-off between accuracy and computational burden. Further, we consider an evaluation procedure more efficient than its competitors i) if it provides higher accuracy and requires the same or a lower computational effort or ii) if it provides the same or a higher accuracy but has a lower computational burden.

Along with their evaluation, this thesis focuses primarily on estimating DSGE models. We define *estimation* as the utilization of formal sampling theory to infer plausible parameter values (or plausible parameter distributions) for which the model can replicate specific patterns observed in the data. In doing so, we follow Christiano et al. (2018) and distinguish estimation from calibration – another strategy to obtain a model's parameters that may involve matching unconditional model and data moments – because the latter does not lean on a formal sampling theory for the solved model. Regarding the estimation of DSGE models, we again define efficiency as the trade-off between the computational burden and the accuracy to which we can estimate the parameters (or their distribution) conditional on some set of observed data.

It is noteworthy that efficient estimation of DSGE models likewise requires efficient evaluation methods. Suppose we want to estimate a model using likelihood-based methods. Both Bayesian and frequentist estimation techniques will require the repeated evaluation of the model's likelihood function. Consequently, an efficient estimation depends not only on the estimation procedure itself – e.g., Bayesian sampling techniques or numerical routines to maximize the likelihood function – but also on the efficiency by which we can evaluate the model's QoI, which in this case, is its likelihood function. An inaccurate evaluation of the likelihood function may lead to inaccuracies in the estimation. In contrast, an accurate but computationally more

[4] Note that throughout this thesis, we focus exclusively on DSGE models expressed in discrete time.

intensive evaluation of the likelihood function can cause the estimation to become infeasible. The same is true for limited-information methods, e.g., the generalized method of moments or the matching of impulse responses.

As outlined above, the challenging aspect of an efficient evaluation and estimation of DSGE models is the trade-off between ensuring that the model's evaluation and estimation are sufficiently accurate, on the one hand, and that it is computationally feasible, on the other. However, the details of this trade-off depend on the research question at hand. The three essays in this thesis consider different approaches and procedures for a more efficient evaluation and estimation of DSGE models. Thereby, the essays cover linear and non-linear solution techniques, as well as likelihood-based and limited-information estimation methods. Chapters 2 and 3 focus on the likelihood-based estimation of DSGE models, employing linear solution techniques to determine the model's policy function. In Chapter 2, we address how to efficiently evaluate the likelihood of those models in terms of computational time required. Chapter 3 proposes a fast and reliable procedure for the maximum-likelihood estimation (MLE) in the context of a business cycle accounting (BCA) application in the spirit of Chari et al. (2007). Chapter 4 discusses a method known as the generalized polynomial chaos expansion (PCE) to obtain a (point-wise) approximation of a model's QoI in terms of a series expansion of the model's parameters. Analyzing the suitability of the PCE for DSGE models, we extend our analysis to non-linear solution techniques for the model's policy function and limited-information methods to estimate its parameters.

In detail, the first essay (Chapter 2), "An Augmented Steady-State Kalman Filter to Evaluate the Likelihood of Linear and Time-Invariant State-Space Models", which is the current version of the working paper by Huber (2022), reviews the celebrated Kalman filter (KF), going back to the seminal work of Kalman (1960), as the standard tool to evaluate the likelihood of linear state-space models. Further, we propose a modified version of this recursive algorithm and show that this augmented steady-state Kalman filter, as we call it, can lower the computational burden associated with the likelihood evaluation of (log-) linearized DSGE models.

Focusing on models solved by linear solution techniques allows us to interpret their (approximated) policy function as linear state-space models (SSMs), which link the behavior of several – except for a potential measurement error – observable variables to the dynamic evolution of a set of state variables. We can infer these (potentially unobservable) states, conditional on the model's parameters and the variables observed up to a certain point in time. In fact, for linear SSMs with Gaussian disturbances, we can use the KF to determine the conditional distribution of the states given the data we have observed so far. Consequently, if initialized at the unconditional mean vector and variance matrix of the model's states, the KF provides the means to evaluate the exact likelihood function of linear and stationary SSMs. However, this recursive algorithm quickly becomes computationally demanding as the model's complexity increases. To reduce the computational burden of the KF, we may exploit the fact that for time-invariant and stationary SSMs, the uncertainty about the model's states converges towards equilibrium as the number of observations increases (see Hamilton, 1994, Chapter 13.5). Hence, initialized at this long-run equilibrium, updating the states' variance matrix becomes redundant, and we can replace the regular KF with a stationary recursion, which we refer to as a steady-state Kalman filter (SKF). Unfortunately, the speed advantage of the SKF comes at the cost of determining a conditional likelihood rather than the exact and unconditional likelihood.

The main contribution of Huber (2022) is to augment the SKF in the manner of de Jong (1988, 1991) so that we may exploit its speed advantage but obtain the model's exact and unconditional likelihood. We find that this augmented steady-state Kalman filter (ASKF) can significantly reduce the computational burden to evaluate the likelihood of medium- to large-scale SSMs, making it particularly useful to estimate DSGE models. At the example of a medium-scale

DSGE model, namely the model introduced by Smets and Wouters (2007), we compare the performance of the ASKF in terms of an efficient likelihood evaluation to three other variants of the KF: A textbook version of the KF (see, e.g., Harvey, 1990; Hamilton, 1994; DeJong and Dave, 2011; Durbin and Koopman, 2012), the Chandrasekhar recursion (CR) suggested by Herbst (2015), and a filter proposed by Koopman and Durbin (2000) that bases on a univariate treatment of multivariate observation vectors (UKF). Apart from minor numerical errors, all filters evaluate the likelihood with the same accuracy since, given the (approximated) linear policy function, they all compute the model's exact likelihood. Hence, the comparison of the four filters focuses on the computational time required to evaluate the model's likelihood function. When compared to the regular KF or the UKF, we find that the ASKF reduces the computational burden by 60 to 80 percent. Furthermore, we find that the ASKF is up to three times faster than the CR.

The second essay (Chapter 3), "Business Cycle Accounting for the German Fiscal Stimulus Program during the Great Recession", is joint work with Daniel Fehrle and the current version of the working paper by Fehrle and Huber (2022). The essay contains a business cycle accounting (BCA) analysis in the spirit of Chari et al. (2007) for the Great Recession in Germany and the related policy measures enacted by the German government to counter it.

BCA analyses employ a so-called prototype economy, representing a real business cycle (RBC) model extended by time-varying distortions in nearly every market. Chari et al. (2007) construct the origins of these distortions, or wedges, as taxes, nominal and real frictions, changes in expectations, etc. While the interpretation of these wedges is non-structural, the parameterization corresponds to ad-valorem taxes, productivity, or government spending. The wedges' driver is a reduced-form Markov process, commonly approximated by a stationary vector autoregression (VAR) with one lag. Using empirical time series, one can estimate the parameters of the VAR process and determine the states of the wedges. These determined wedges are fed back into the model one by one to assess the contribution of each wedge to the fluctuation of macroeconomic aggregates. Our prototype economy includes wedges to the variables government consumption, durables, investment, labor, net exports, and efficiency and we show how to map the measures of the German fiscal stimulus program towards them.[5]

Using the state-space methods discussed in the first essay (Huber, 2022), we estimate 59 parameters – two structural parameters and the 57 parameters of the wedges' underlying VAR process – of our prototype economy via maximum-likelihood. For this purpose, we introduce a reliable and quick procedure to locate the maximum of the likelihood function. This two-step procedure can be summarized as follows: In the first step, we maximize the conditional likelihood received from a SKF, based on the assumption that the initial states are fixed and known in their long-run equilibrium. Besides the SKF's speed advantage, there is also an analytical and unique solution for the maximizing variance matrix of the wedges' VAR process. The estimator obtained with this procedure retains the properties of a maximum-likelihood estimator, yet, it is usually less accurate than the maximum-likelihood estimator based on the commonly used unconditional likelihood. The first-step estimates are thus only the guess for the actual (second-step) estimation, which maximizes the unconditional likelihood function. Using this procedure, we combine the speed and robustness advantages of the conditional maximum-likelihood estimator with the higher efficiency of an unconditional initialization.

In the subsequent BCA analysis, we find that the efficiency wedge mainly drove the crises (62%), followed by the net exports (26%) and the investment wedge (19%). The government consumption wedge and the durables wedge acted counter-cyclically (about -5% each). Furthermore, the labor wedge contributed only 3% to the crisis but induced a fast recovery. These statistics are robust except for the investment wedge. We discuss the results against different

[5] In this context, the term efficiency refers to the efficiency wedge parameterized by a distortion of labor productivity.

market interventions, e.g., we attribute the counter-cyclicality of the durables wedge to the cash for clunkers program.

The third essay (Chapter 4), "Polynomial Chaos Expansion: Efficient Evaluation and Estimation of Computational Models", is joint work with Daniel Fehrle and Christopher Heiberger and the current version of the working paper by Fehrle, Heiberger, and Huber (2022). The essay discusses the suitability of a method known as generalized polynomial chaos expansion (PCE) – going back to Xiu and Karniadakis (2002) – for computational economics and, in particular, for DSGE models.

In a nutshell, we can describe PCE as follows: Considering the model's parameters as (stochastically independent) random variables, the PCE – under some general assumptions – provides the means to represent the model's QoI as a series expansion of its uncertain parameters. Thereby, the polynomials of this Fourier series belong to families that are orthogonal with respect to the densities of the model's parameters. Further, we may determine the coefficients of the truncated Fourier series from the inner product of the mapping from the parameter values to the model's QoI and the orthogonal polynomials. Provided that we cannot compute this inner product analytically, we may employ numerical integration rules, such as Gauss quadratures, which, if the dimensionality of the unknown parameters is not too large, require only a comparably small number of model evaluations. As the number of parameters increases, we can switch to sparse grid methods, such as Smolyak-Gauss quadratures, to approximate the inner product or determine the coefficients using the least-squares method. Given the respective formulae – and compared to the repeated, potentially time-consuming evaluation of the entire model – the repeated evaluation of the model's QoI becomes inexpensive in terms of computational time required.

In the first part of our numerical analysis, we investigate the efficiency of the PCE when used to evaluate the QoIs of the benchmark RBC model. We employ the PCE method to (point-wise) approximate the mapping between the parameters and the model's (approximated) QoIs – its linear solution, a non-linear and global solution, its variables' unconditional second moments, and its impulse response function – in terms of a series expansion of its parameters. The accuracy of this approximation depends on the truncation level and the accuracy of the PCE coefficients, while the computational effort mainly relies on the number of model evaluations required to approximate these PCE coefficients. We analyze the convergence behavior of the PCE – in the sense of the L^2 norm of the approximation error over the parameters' support – and find linear convergence as we increase the truncation level.[6] We also compare the different approaches to derive the PCE coefficients – full-grid quadrature rules, sparse-grid quadrature rules, and the least-squares method – regarding the approximation's accuracy and the computational time required. Our findings suggest that the PCE constructed from a sparse-grid quadrature is most efficient, followed by least squares.

In the second part of our numerical analysis, we employ Monte Carlo experiments to investigate the efficiency of the PCE in the context of parameter estimation. Therefore, we estimate the model's parameters by generalized method of moments (GMM), simulated method of moments (SMM), maximum-likelihood estimation (MLE), and Bayesian estimation (BE) but use PCE to evaluate the QoI for different parameter values. In terms of accuracy and computational time required, we compare these parameter estimates to the estimates obtained by repeatedly solving for the model's QoIs. We find that the PCE-based estimates deviate only negligibly from the benchmark procedure, while the computation time reduces by 99 percent for BE and by 50 percent for GMM, SMM, and MLE.

[6] For this exercise, we use a full-grid quadrature rule with enough nodes to approximate the PCE coefficients accurately since we want to abstract from possible errors in calculating these coefficients.

Bibliography

BLANCHARD, O. J. AND C. M. KAHN (1980): "The Solution of Linear Difference Models under Rational Expectations," *Econometrica*, 48, 1305–1311.

CHARI, V. V., P. J. KEHOE, AND E. R. MCGRATTAN (2007): "Business Cycle Accounting," *Econometrica*, 75, 781–836.

CHRISTIANO, L. J., M. S. EICHENBAUM, AND M. TRABANDT (2018): "On DSGE Models," *Journal of Economic Perspectives*, 32, 113–40.

DE JONG, P. (1988): "The Likelihood for a State Space Model," *Biometrika*, 75, 165–169.

——— (1991): "The Diffuse Kalman Filter," *The Annals of Statistics*, 19, 1073–1083.

DEJONG, D. N. AND C. DAVE (2011): *Structural Macroeconometrics: Second Edition*, Princeton, NJ: Princeton University Press.

DURBIN, J. AND S. J. KOOPMAN (2012): *Time Series Analysis by State Space Methods: Second Edition*, Oxford Statistical Science Series, Oxford, UK: Oxford University Press.

FEHRLE, D., C. HEIBERGER, AND J. HUBER (2022): "Polynomial Chaos Expansion: Efficient Evaluation and Estimation of Computational Models".

FEHRLE, D. AND J. HUBER (2022): "Business Cycle Accounting for the German Fiscal Stimulus Program during the Great Recession".

FERNÁNDEZ-VILLAVERDE, J. AND P. A. GUERRÓN-QUINTANA (2021): "Estimating DSGE Models: Recent Advances and Future Challenges," *Annual Review of Economics*, 13, 229–252.

GLANDON, P. J., K. KUTTNER, S. MAZUMDER, AND C. STROUP (2022): "Macroeconomic Research, Present and Past," Working Paper 29628, National Bureau of Economic Research.

HAMILTON, J. D. (1994): *Time Series Analysis*, Princeton, NJ: Princeton University Press.

HARVEY, A. C. (1990): *Forecasting, Structural Time Series Models and the Kalman Filter*, Cambridge, UK: Cambridge University Press.

HERBST, E. (2015): "Using the "Chandrasekhar Recursions" for Likelihood Evaluation of DSGE Models," *Comput. Econ.*, 45, 693–705.

HUBER, J. (2022): "An Augmented Steady-State Kalman Filter to Evaluate the Likelihood of Linear and Time-Invariant State-Space Models".

KALMAN, R. E. (1960): "A New Approach to Linear Filtering and Prediction Problems," *Journal of Basic Engineering*, 82, 35–45.

KLEIN, P. (2000): "Using the Generalized Schur Form to Solve a Multivariate Linear Rational Expectations Model," *Journal of Economic Dynamics and Control*, 24, 1405–1423.

KOOPMAN, S. J. AND J. DURBIN (2000): "Fast Filtering and Smoothing for Multivariate State Space Models," *Journal of Time Series Analysis*, 21, 281–296.

KYDLAND, F. E. AND E. C. PRESCOTT (1982): "Time to Build and Aggregate Fluctuations," *Econometrica*, 50, 1345–1370.

LONG, J. B. AND C. I. PLOSSER (1983): "Real Business Cycles," *Journal of Political Economy*, 91, 39–69.

SERGI, F. (2020): "The Standard Narrative about DSGE Models in Central Banks' Technical Reports," *The European Journal of the History of Economic Thought*, 27, 163–193.

SIMS, C. A. (2002): "Solving Linear Rational Expectations Models," *Comput. Econ.*, 20, 1–20.

SMETS, F. AND R. WOUTERS (2003): "An Estimated Dynamic Stochastic General Equilibrium Model of the Euro Area," *Journal of the European Economic Association*, 1, 1123–1175.

——— (2007): "Shocks and Frictions in US Business Cycles: A Bayesian DSGE Approach," *American Economic Review*, 97, 586–606.

STIGLITZ, J. E. (2018): "Where Modern Macroeconomics Went Wrong," *Oxford Review of Economic Policy*, 34, 70–106.

UHLIG, H. (2001): "A Toolkit for Analysing Nonlinear Dynamic Stochastic Models Easily," in *Computational Methods for the Study of Dynamic Economies*, ed. by R. Marimon and A. Scott, Oxford, UK: Oxford University Press, 30–61.

XIU, D. AND G. E. KARNIADAKIS (2002): "The Wiener–Askey Polynomial Chaos for Stochastic Differential Equations," *SIAM Journal on Scientific Computing*, 24, 619–644.

Chapter 2

An Augmented Steady-State Kalman Filter to Evaluate the Likelihood of Linear and Time-Invariant State-Space Models

— *Johannes Huber* —

2.1 Introduction

Since their introduction in the 1980s, dynamic stochastic general equilibrium (DSGE) models have become a cornerstone of modern macroeconomics. While the first class of DSGE models mainly consisted of small-scale models with a handful of equations and only a few shocks (e.g., Hansen, 1985; King et al., 1988), the complexity of these models has increased significantly over the past decades (see, e.g., Leeper et al., 2010; Gadatsch et al., 2016; Drygalla et al., 2020). In particular, New-Keynesian models, such as those of Christiano et al. (2005) or Smets and Wouters (2003, 2007), are no longer used only for academic purposes but also for monetary policy analysis.[1] A popular approach to specify the parameters of a (log-) linearized DSGE model is to treat its policy function as a linear (and time-invariant) state-space model (SSM), and estimate this SSM using likelihood-based methods (e.g., Ireland, 2004; An and Schorfheide, 2007; Chari et al., 2007). However, as the complexity of the model increases, the repeated evaluation of the likelihood function can become time-consuming.[2] This paper proposes an algorithm to evaluate the likelihood of linear and time-invariant SSMs. We find that this augmented steady-state Kalman filter (ASKF), as we call it, can significantly reduce the time required to evaluate the likelihood of (log-) linearized DSGE models, such as the one introduced by Smets and Wouters (2007). Although we focus mainly on DSGE models in this paper, the ASKF may also be useful for estimating other linear and time-invariant SSMs such as, e.g., dynamic factor models.

There are two likelihood-based approaches to estimate the parameters of DSGE models, namely the frequentist and the Bayesian approach. The frequentist approach considers the set of unknown parameters as fixed and estimates them by maximum-likelihood. The number of likelihood evaluations within this approach remains manageable for a limited amount of unknown parameters and a well-shaped likelihood function. However, even for well-identified models, due to the curse of dimensionality, maximization of the likelihood function often becomes a difficult task as the dimension of the parameter space rises. Thus, problems with a high-dimensional parameter space often require global search routines, such as simulated annealing, to locate the global maxima (see, e.g., Andreasen, 2010; Šustek, 2011). However, exploring a high-dimensional parameter space usually also requires a considerable amount of

[1] E.g., the European Central Bank uses an open-economy extension of the model by Smets and Wouters (2007), the so-called New Area-Wide Model, for macroeconomic projection exercises.

[2] Herbst (2015) reports that the likelihood is sometimes evaluated up to several million times, for both classical and the Bayesian approach.

likelihood evaluations. Hence, efficient techniques to evaluate the likelihood function become essential as the number of parameters increases.

In contrast to the frequentist approach, Bayesian econometricians treat the unknown parameters as random variables. By combining the information contained in the data (likelihood function) with their prior beliefs about the parameters (prior density), the Bayesian approach seeks to gain information about the (posterior) density of the unknown parameters for a given set of data. From a technical perspective, modern sampling techniques, like the random walk Metropolis-Hasting (RWMH) algorithm used by Smets and Wouters (2007), the tailored randomized block Metropolis-Hastings (TaRBMH) algorithm suggested by Chib and Ramamurthy (2010), or the Sequential Monte Carlo sampler by Herbst and Schorfheide (2014), provide easily accessible ways to generate draws from the posterior distribution, that are often in some ways less challenging than maximizing the likelihood function. However, all three samplers mentioned above require a considerable amount of likelihood evaluations. For example, estimating a medium-scale DSGE model, such as the model by Smets and Wouters (2007), requires up to several million likelihood evaluations, depending on the selected sampling algorithm.[3] Thus not surprisingly, Herbst (2015) reports that, especially in medium to large-scale DSGEs models, the likelihood evaluation eventually becomes one of the bottlenecks in the estimation process.

As mentioned above, we can treat the policy function of (log-) linearized DSGE models as a linear SSM, where we assume that the behavior of a set of time series links to the dynamics of some potentially unobserved states. In the case of linear SSMs with Gaussian disturbances, we may use the so-called Kalman filter (KF) to recursively determine these states' mean vector and variance matrix for a given set of observed data. Consequently, the KF also provides the means to evaluate the likelihood function of the model. However, this recursive algorithm quickly becomes computationally demanding as the model's complexity increases. To reduce the computational burden of the KF, we might exploit the fact that for time-invariant and stationary SSMs, the uncertainty about the model's states converges towards an equilibrium as the number of observations increases. Hence, after a certain number of observations, it is no longer necessary to update the states' variance matrix, and we can replace the regular KF with a stationary recursion, which we refer to as a steady-state Kalman filter (SKF). However, the convergence process of the states' variance matrix can take many periods, especially when estimating DSGE models. Therefore, in this paper, we propose a variant of the KF based on a SKF augmented in the manner of de Jong (1988, 1991). We show that the additional computations caused by augmenting the filter require fewer arithmetic operations than those necessary to update the states' variance matrix. We find that this ASKF can significantly reduce the computational burden of the likelihood evaluation in medium- to large-scale SSMs. Furthermore, we show that for DSGE models without measurement error, where the number of exogenous state variables equals the number of the observable time series, it is usually possible to determine the equilibrium variance matrix of the model's states analytically.

The ASKF adds to a strand of literature that attempts to evaluate the likelihood of linear SSMs more efficiently. For models where the number of observed time series exceeds the number of states, Jungbacker and Koopman (2014) suggest a model transformation that reduces the dimensionality of the observation vector to the dimension of the state vector. This „collapsing of large observation vectors," as Durbin and Koopman (2012) call it, is particularly helpful in the context of dynamic factor models, where we attribute the common dynamics from a typically large number of time series to the movement in a small number of unobserved factors.

[3] Note that Smets and Wouters (2007) generate only 250000 draws from the posterior distribution using the Random Walk Metropolis-Hastings sampler, where each draw is equivalent to one likelihood evaluation. However, as mentioned by Chib and Ramamurthy (2010), a careful exploration of the parameter space to find the mode of the posterior distribution needed to tune the Random Walk Metropolis-Hastings algorithm often requires a large amount of additional likelihood evaluations.

Koopman and Durbin (2000) propose a version of the KF in which they do not treat observations as vectors but consider each element of the observation vector as a new observation. Durbin and Koopman (2012, Chapter 6.4.4) show that this univariate treatment of multivariate observation vectors (UKF) requires fewer arithmetic operations than the regular KF, especially when the number of observed time series is large. Further, the UKF has proven particularly helpful when dealing with diffuse initialization problems.

Using the generic SSM of Chib and Ramamurthy (2010) – a simulation model with ten observable time series and five state variables – to compare the ASKF with the UKF, we find that the former eventually will outperform the latter, provided that the convergence process of the states' variance matrix lasts for at least 50 periods. Additionally, we use the model transformation by Jungbacker and Koopman (2014) to collapse the dimension of the observation vector, finding that, in this case, the ASKF becomes profitable after about 75 periods. The ASKF needs some periods to acclimatize because it requires determining the equilibrium variance matrix of the model's states prior to the actual recursion. However, since the convergence speed of the states' variance matrix typically cannot be determined ex-ante and the likelihood evaluation is usually relatively cheap in cases where the convergence process lasts only for a couple of periods, we consider the ASKF a valid option to evaluate the likelihood of SSMs, where the number of observed time series exceeds the number of states.

If, on the other hand, the number of states is significantly larger than the number of observable variables, as is often the case for structural DSGE models, the techniques mentioned above become less valuable. For this reason, Herbst (2015) suggests using the Chandrasekhar recursion (CR) developed by Morf (1974) and Morf et al. (1974) when estimating medium to large-scale DSGE models. Compared to the regular Kalman recursion, this algorithm replaces the Riccati difference equation (RDE), typically used to update the state variance matrix by another set of difference equations. When the number of state variables is significantly larger than the dimension of the observation vector, this set of „Chandrasekhar-type" difference equations can be shown to require fewer arithmetic operations than the original algorithm. We compare FORTRAN and MATLAB® implementations of the CR and the ASKF using the DSGE model introduced by Smets and Wouters (2007) as a benchmark. Even considering a variant of the Smets and Wouters (2007) model, in which all model variables are considered to be states, which is favorable for the CR, the FORTRAN implementation of the ASKF is almost twice as fast as the FORTRAN implementation of the CR. The ASKF performs even better in MATLAB®, being about three times quicker than the CR. Compared to the regular KF and the UKF, we find that the ASKF reduces the computational burden by 60 to 80 percent, depending on whether we consider all model variables as states or not.

The remainder of the paper reads as follows. The following section revisits some basic concepts necessary for the derivation of the ASKF. In Section 2.3, we will outline the basic idea of the ASKF and present an efficient algorithm to compute the log-likelihood of linear and time-invariant SSMs. Furthermore, we compare the additive and multiplicative operations of the regular KF and the ASKF for each additional observation and discuss the latter's implementation. In the subsequent section, we apply the ASKF to the generic SSM by Chib and Ramamurthy (2010) and the DSGE model introduced by Smets and Wouters (2007) and compare it in terms of speed and accuracy to the regular KF, the UKF, and the CR. The last section concludes the paper.

2.2 State-space models and the Kalman-Filter

In the following, we revisit some basic concepts and tools relevant throughout this paper. First, we introduce the class of linear and time-invariant state-space models (SSMs) and a textbook

version of the Kalman filter (KF). Then we analyze the asymptotic properties of the filter and the concept of a steady-state Kalman filter (SKF). Finally, we introduce the augmented Kalman filter (AKF), which will form the foundation for deriving the augmented steady-state Kalman filter (ASKF) in the subsequent section.

2.2.1 State-space representation

As a general framework for our analysis, let us assume we have the following time-invariant, linear, and Gaussian SSM:[4]

$$\mathbf{y}_t = \mathbf{h} + \mathbf{H} \cdot \mathbf{w}_t + \mathbf{u}_t, \qquad \mathbf{u}_t \sim \mathrm{N}(\mathbf{0}, \mathbf{R}), \qquad \forall t = 1, 2, \ldots, N \tag{2.2.1a}$$

$$\mathbf{w}_t = \mathbf{F} \cdot \mathbf{w}_{t-1} + \mathbf{v}_t, \qquad \mathbf{v}_t \sim \mathrm{N}(\mathbf{0}, \mathbf{Q}), \qquad \mathbf{w}_0 \sim \mathrm{N}(\boldsymbol{\mu}_0, \mathbf{C}_0), \qquad \forall t = 1, 2, \ldots, N \tag{2.2.1b}$$

where $\mathbf{y}_t \in \mathbb{R}^{n_y}$ and $\mathbf{w}_t \in \mathbb{R}^{n_w}$ are vectors containing the observed data and the potentially unobserved states at time t. The system matrices $\mathbf{F} \in \mathbb{R}^{n_w \times n_w}$, $\mathbf{H} \in \mathbb{R}^{n_y \times n_w}$, $\mathbf{Q} \in \mathbb{R}^{n_w \times n_w}$, $\mathbf{R} \in \mathbb{R}^{n_y \times n_y}$, and the vector $\mathbf{h} \in \mathbb{R}^{n_y}$ may be functions of a potentially uncertain vector $\boldsymbol{\theta}$ of time-invariant deep parameters. The normally distributed disturbances $\mathbf{u}_t \in \mathbb{R}^{n_y}$ and $\mathbf{v}_t \in \mathbb{R}^{n_w}$ are assumed to be serially independent and uncorrelated with each other, i.e.,

$$\mathrm{E}[\mathbf{u}_i \mathbf{u}_j^T] = \begin{cases} \mathbf{R}, & i = j, \\ \mathbf{0}, & i \neq j. \end{cases}, \quad \mathrm{E}[\mathbf{v}_i \mathbf{v}_j^T] = \begin{cases} \mathbf{Q}, & i = j, \\ \mathbf{0}, & i \neq j. \end{cases}, \quad \mathrm{E}[\mathbf{u}_i \mathbf{v}_j^T] = \mathbf{0}, \quad \forall\ i,\ j = 1, 2, \ldots, N.$$

Furthermore, they shall be uncorrelated to the initial state vector $\mathbf{w}_0$, so that

$$\mathrm{E}[\mathbf{u}_t (\mathbf{w}_0 - \boldsymbol{\mu}_0)^T] = \mathrm{E}[\mathbf{v}_t (\mathbf{w}_0 - \boldsymbol{\mu}_0)^T] = \mathbf{0}, \qquad \forall t = 1, 2, \ldots, N.$$

If all eigenvalues of the matrix $\mathbf{F}$ lie within the unit circle, we will call (2.2.1) a stationary SSM. Throughout this paper, we will use the SSM (2.2.1) as a flexible and general framework for the derivation and analysis of the ASKF. However, in some situations it will be convenient to consider the special case of the SSM (2.2.1) without the measurement error $\mathbf{u}_t$, i.e., $\mathbf{u}_t = \mathbf{0},\ \forall t = 1, 2, \ldots, N$ and $\mathbf{R} = \mathbf{0}$, resulting in

$$\mathbf{y}_t = \mathbf{h} + \mathbf{H} \cdot \mathbf{w}_t, \qquad \forall t = 1, 2, \ldots, N \tag{2.2.2a}$$

$$\mathbf{w}_t = \mathbf{F} \cdot \mathbf{w}_{t-1} + \mathbf{v}_t, \qquad \mathbf{v}_t \sim \mathrm{N}(\mathbf{0}, \mathbf{Q}), \qquad \mathbf{w}_0 \sim \mathrm{N}(\boldsymbol{\mu}_0, \mathbf{C}_0), \qquad \forall t = 1, 2, \ldots, N \tag{2.2.2b}$$

Further, we will assume the system matrices $\mathbf{H}$, $\mathbf{F}$, and $\mathbf{Q}$ of SSM (2.2.2) to take the form

$$\mathbf{H} = \begin{pmatrix} \mathbf{H}_z & \mathbf{H}_x \end{pmatrix}, \tag{2.2.2c}$$

$$\mathbf{F} = \begin{pmatrix} \mathbf{F}_z \\ \mathbf{F}_x \end{pmatrix}, \tag{2.2.2d}$$

$$\mathbf{Q} = \begin{pmatrix} \mathbf{Q}_z & \mathbf{0} \\ \mathbf{0} & \mathbf{0} \end{pmatrix}, \tag{2.2.2e}$$

and that the quantities $\mathbf{w}_t$ and $\mathbf{v}_t$ define as

$$\mathbf{w}_t := \begin{pmatrix} \mathbf{z}_t^T & \mathbf{x}_t^T \end{pmatrix}^T, \qquad \mathbf{v}_t := \begin{pmatrix} \mathbf{v}_{t,z}^T & \mathbf{0} \end{pmatrix}^T, \qquad \forall\ t = 1, 2, \ldots, N,$$

[4] We refer to Durbin and Koopman (2012, Chapter 4) for a textbook treatment of the KF with respect to SSMs, where the system matrices are allowed to change over time. However, note that most (log-) linearized DSGE and a variety of other time series models can be represented in terms of a time-invariant SSM.

where $\mathbf{x}_t \in \mathbb{R}^{n_x}$ represents the vector of the predetermined states already known from period $t-1$. In contrast, the vector $\mathbf{z}_t \in \mathbb{R}^{n_z}$ collects the exogenous states of the model, whose realization is affected by the stochastic innovations vector $\mathbf{v}_{t,z} \in \mathbb{R}^{n_z}$. The framework described by SSM (2.2.2) will meet the design requirements of a large number (log-) linearized DSGE models, such as the model introduced by Smets and Wouters (2007).

2.2.2 The Kalman filter

Both Bayesian and frequentist estimation techniques often require the evaluation of the likelihood function. A suitable tool for this purpose is the KF. Since the SSM (2.2.1) is Gaussian, for a given initialization $(\boldsymbol{\mu}_0, \mathbf{C}_0)$ and a set of observations $\mathbf{Y}_N = \{\mathbf{y}_1, \mathbf{y}_2, \dots, \mathbf{y}_N\}$ generated by SSM (2.2.1), the KF represents a recursive algorithm to compute the mean vectors — $\mathbf{w}_{t|t-1} := \mathrm{E}[\mathbf{w}_t|\mathbf{Y}_{t-1}]$ and $\boldsymbol{\mu}_t := \mathrm{E}[\mathbf{w}_t|\mathbf{Y}_t]$ — and variance matrices — $\mathbf{P}_{t|t-1} := \mathrm{Var}[\mathbf{w}_t|\mathbf{Y}_{t-1}]$ and $\mathbf{C}_t := \mathrm{Var}[\mathbf{w}_t|\mathbf{Y}_t]$ — of $\mathbf{w}_t$ given $\mathbf{Y}_{t-1}$ and $\mathbf{w}_t$ given $\mathbf{Y}_t$, respectively, for all periods $t = 1, 2, \dots, N$. If we define

$$\mathbf{K}_t := \mathbf{P}_{t|t-1}\mathbf{H}^T \left[\mathbf{H}\mathbf{P}_{t|t-1}\mathbf{H}^T + \mathbf{R}\right]^{-1}, \qquad \forall t = 1, 2, \dots, N, \tag{2.2.3}$$

and let $\mathbf{e}_t := \mathbf{y}_t - \mathbf{h} - \mathbf{H}\mathbf{w}_{t|t-1}$ and $\mathbf{U}_t := \mathbf{H}\mathbf{P}_{t|t-1}\mathbf{H}^T + \mathbf{R}$ denote the forecast error of $\mathbf{y}_t$ given $\mathbf{Y}_{t-1}$ and its corresponding variance matrix, respectively, we receive the Kalman recursion for $t = 1, 2, \dots, N$ as

$$\begin{aligned}
\mathbf{w}_{t|t-1} &= \mathbf{F}\,\boldsymbol{\mu}_{t-1}, & &(2.2.4a) & \mathbf{P}_{t|t-1} &= \mathbf{F}\,\mathbf{C}_{t-1}\,\mathbf{F}^T + \mathbf{Q}, & &(2.2.4b)\\
\mathbf{e}_t &= \mathbf{y}_t^{(\mathbf{h})} - \mathbf{H}\,\mathbf{w}_{t|t-1}, & &(2.2.4c) & \mathbf{U}_t &= \mathbf{H}\,\mathbf{P}_{t|t-1}\,\mathbf{H}^T + \mathbf{R}, & &(2.2.4d)\\
\boldsymbol{\mu}_t &= \mathbf{w}_{t|t-1} + \mathbf{K}_t\,\mathbf{e}_t, & &(2.2.4e) & \mathbf{C}_t &= \mathbf{P}_{t|t-1} - \mathbf{K}_t\,\mathbf{H}\,\mathbf{P}_{t|t-1}, & &(2.2.4f)
\end{aligned}$$

where $\mathbf{y}_t^{(\mathbf{h})} := \mathbf{y}_t - \mathbf{h}$ for all $t = 1, 2, \dots, N$. A detailed derivation of recursion (2.2.4) is provided in Appendix 2.A. Throughout this paper we will follow Lütkepohl (2007) and refer to the matrix $\mathbf{K}_t$ as the so-called Kalman gain.[5]

To avoid confusion, note that alternatively to the initialization $(\boldsymbol{\mu}_0, \mathbf{C}_0)$ the KF may also be initialized at $(\mathbf{w}_{1|0}, \mathbf{P}_{1|0})$ with $\mathbf{w}_1 \sim \mathrm{N}(\mathbf{w}_{1|0}, \mathbf{P}_{1|0})$. In this case the state equation (2.2.1b) for $t = 1$ becomes redundant so that the corresponding SSM reduces to

$$\begin{aligned}
&\mathbf{y}_t = \mathbf{h} + \mathbf{H}\cdot\mathbf{w}_t + \mathbf{u}_t, \quad \mathbf{u}_t \sim \mathrm{N}(\mathbf{0}, \mathbf{R}), && \forall t = 1, 2, \dots, N, && (2.2.5a)\\
&\mathbf{w}_t = \mathbf{F}\cdot\mathbf{w}_{t-1} + \mathbf{v}_t, \quad \mathbf{v}_t \sim \mathrm{N}(\mathbf{0}, \mathbf{Q}), \quad \mathbf{w}_1|\mathbf{Y}_0 \sim \mathrm{N}(\mathbf{w}_{1|0}, \mathbf{P}_{1|0}), && \forall t = 2, 3, \dots, N. && (2.2.5b)
\end{aligned}$$

The Kalman recursion for the SSM (2.2.5) is identical to recursion (2.2.4), apart from the fact that in $t = 1$ steps (2.2.4a) and (2.2.4b) are redundant, since $\mathbf{w}_{1|0}$ and $\mathbf{P}_{1|0}$ are already known. Thus, if we choose $\mathbf{w}_{1|0} = \mathbf{F}\boldsymbol{\mu}_0$ and $\mathbf{P}_{1|0} = \mathbf{F}\mathbf{C}_0\mathbf{F}^T + \mathbf{Q}$, the quantities computed by the KF are the same as the ones computed for the SSM (2.2.1). Although the Kalman filter is often derived based on the alternative SSM (2.2.5) (see e.g., Hamilton (1994, pp. 372-408), Durbin and Koopman (2012) or DeJong and Dave (2011)), hereafter we will focus on the SSM (2.2.1) presented at the beginning of this subsection, since it is more convenient for the derivation of the ASKF in Section 2.3.

As an important by-product the KF provides a possibility to evaluate the likelihood function of the SSM (2.2.1) for a given set of parameters $\boldsymbol{\theta}$ and a given initialization $(\boldsymbol{\mu}_0, \mathbf{C}_0)$. To see this, note that $\mathbf{y}_t$ given $\mathbf{Y}_{t-1}$ is normally distributed for all $t = 1, 2, \dots, N$, with corresponding mean

[5] Note that some authors, e.g., Hamilton (1994) and Durbin and Koopman (2012), define the Kalman gain as $\mathbf{K}_t := \mathbf{F}\mathbf{P}_{t|t-1}\mathbf{H}^T \left[\mathbf{H}\mathbf{P}_{t|t-1}\mathbf{H}^T\right]^{-1}$. In this case the Kalman gain defines the gain matrix with respect to $\mathbf{w}_{t+1}$ given $\mathbf{Y}_t$, while in the current paper it is treated as the gain matrix with respect to $\mathbf{w}_t$ given $\mathbf{Y}_t$.

vector $\mathbf{h}+\mathbf{H}\mathbf{w}_{t|t-1}$ and variance matrix $\mathbf{U}_t$. Hence using the forecast-error decomposition the log-density of $\mathbf{Y}_N$ yields:

$$\log\left(f_{\mathbf{Y}_N}\right) = -\frac{n_y\, N}{2}\, \log(2\pi)\, -\frac{1}{2}\sum_{t=1}^{N}\log|\mathbf{U}_t|\, -\frac{1}{2}\sum_{t=1}^{N}\mathbf{e}_t^T\, \mathbf{U}_t^{-1}\, \mathbf{e}_t. \tag{2.2.6}$$

It is well-known (see e.g., Durbin and Koopman (2012, pp. 185)) that under quite general regularity conditions the distribution of the maximum-likelihood estimator for the deep parameters $\boldsymbol{\theta}$, defined by

$$\hat{\boldsymbol{\theta}} := \arg\max_{\boldsymbol{\theta}} \log\left(f_{\mathbf{Y}_N}\right),$$

is for large N approximately normally distributed with mean vector $\hat{\boldsymbol{\theta}}$ and variance matrix

$$\widehat{\mathrm{Var}}\left[\hat{\boldsymbol{\theta}}\right] = \left[\frac{\partial \log\left(f_{\mathbf{Y}_N}\right)}{\partial\boldsymbol{\theta}\;\partial\boldsymbol{\theta}^T}\right]^{-1}.$$

For a more detailed treatment of the asymptotic properties of the maximum-likelihood estimator, see e.g Hamilton (1994) and Harvey (1990a).

Taking the Bayesian perspective the density $f_{\mathbf{Y}_N}$ for a given parameter vector $\boldsymbol{\theta}$ is also important, since it is required to generate draws from posterior distribution $f_{\boldsymbol{\theta}|\mathbf{Y}_N} \propto f_{\mathbf{Y}_N|\boldsymbol{\theta}} \cdot f_{\boldsymbol{\theta}}$.

Note that the quantities of the KF, and therefore the log-likelihood defined by (2.2.6), are conditional on the distribution of the initial state vector $\mathbf{w}_0$, which itself is determined by $(\boldsymbol{\mu}_0, \mathbf{C}_0)$. The probably most common initialization strategy for stationary SSMs, is to specify $\boldsymbol{\mu}_0$ and $\mathbf{C}_0$ as the unconditional mean vector $\boldsymbol{\mu}$ and the unconditional variance matrix $\mathbf{C}$ of the state vector $\mathbf{w}_t$ (see e.g., Hamilton (1994, pp. 378) or Durbin and Koopman (2012, pp. 123,137-138)). These are obtainable from the state equation (2.2.1b) as

$$\boldsymbol{\mu} = \mathbf{0} \tag{2.2.7a}$$

and as the positive semi-definite matrix $\mathbf{C}$ solving the discrete Lyapunov equation

$$\mathbf{0} = \mathbf{F}\mathbf{C}\mathbf{F}^T + \mathbf{Q} - \mathbf{C}. \tag{2.2.7b}$$

This means that $\boldsymbol{\mu}_0$ and $\mathbf{C}_0$ are determined by $\mathbf{F}$ and $\mathbf{Q}$, which in turn are determined by the vector of deep parameters $\boldsymbol{\theta}$. Consequently, using this initialization (2.2.6) represents the exact or unconditional log-likelihood of the model.

2.2.3 The steady-state Kalman filter

Within the class of time-invariant and linear SSMs, it is a well-known feature of the KF that under certain circumstances the sequences $\{\mathbf{C}_t\}_{t=1}^N$ and $\{\mathbf{P}_{t|t-1}\}_{t=1}^N$ converge towards fixed matrices. In this case we call the KF asymptotically time-invariant. To establish conditions for an asymptotically time-invariant filter, first note that in a time-invariant SSM like (2.2.1), the sequences $\{\mathbf{C}_t\}_{t=1}^N$ and $\{\mathbf{P}_{t|t-1}\}_{t=1}^N$, obtained by the Kalman recursion (2.2.4) do not depend on the data itself. This becomes obvious if we use (2.2.4b), (2.2.4d), and (2.2.4f) to obtain the law of motion of the sequence $\{\mathbf{C}_t\}_{t=1}^N$ as

$$\mathbf{C}_t = \mathbf{F}\mathbf{C}_{t-1}\mathbf{F}^T + \mathbf{Q} - \left(\mathbf{F}\mathbf{C}_{t-1}\bar{\mathbf{H}}^T + \bar{\mathbf{G}}\right)\left[\bar{\mathbf{H}}\mathbf{C}_{t-1}\bar{\mathbf{H}}^T + \bar{\mathbf{R}}\right]^{-1}\left(\bar{\mathbf{H}}\mathbf{C}_{t-1}\mathbf{F}^T + \bar{\mathbf{G}}^T\right), \tag{2.2.8a}$$

with $\bar{\mathbf{H}} := \mathbf{HF}$, $\bar{\mathbf{G}} := \mathbf{QH}^T$ and $\bar{\mathbf{R}} := \mathbf{HQH}^T + \mathbf{R}$. Analogously, we can also obtain the law of motion of the sequence $\{\mathbf{P}_{t|t-1}\}_{t=1}^N$ as

$$\mathbf{P}_{t+1|t} = \mathbf{FP}_{t|t-1}\mathbf{F}^T - \mathbf{FP}_{t|t-1}\mathbf{H}^T \left[\mathbf{HP}_{t|t-1}\mathbf{H}^T + \mathbf{R}\right]^{-1} \mathbf{HP}_{t|t-1}\mathbf{F}^T + \mathbf{Q}. \tag{2.2.8b}$$

Furthermore, both (2.2.8a) and (2.2.8b) belong to the class of Riccati difference equations (RDEs), which convergence properties have been intensively studied by the literature (see e.g., Caines and Mayne (1970), Chan et al. (1984), de Souza et al. (1986) or De Nicolao and Gevers (1992)). In what follows, we give a brief summary of their results by establishing some well-known sufficient conditions under which the sequences $\{\mathbf{C}_t\}_{t=1}^N$ and $\{\mathbf{P}_{t|t-1}\}_{t=1}^N$ converge against fixed matrices.[6]

We shall introduce some basic notions in advance: First, we call non-negative definite matrices $\mathbf{C}_+$ and $\mathbf{P}_+$ solutions of RDEs (2.2.8a) and (2.2.8b), respectively, if they satisfy the discrete algebraic Riccati equations (DAREs)

$$\mathbf{C}_+ = \mathbf{FC}_+\mathbf{F}^T + \mathbf{Q} - \left(\mathbf{FC}_+\bar{\mathbf{H}}^T + \bar{\mathbf{G}}\right)\left[\bar{\mathbf{H}}\mathbf{C}_+\bar{\mathbf{H}}^T + \bar{\mathbf{R}}\right]^{-1}\left(\bar{\mathbf{H}}\mathbf{C}_+\mathbf{F}^T + \bar{\mathbf{G}}^T\right), \tag{2.2.9a}$$

$$\mathbf{P}_+ = \mathbf{FP}_+\mathbf{F}^T - \mathbf{FP}_+\mathbf{H}^T \left[\mathbf{HP}_+\mathbf{H}^T + \mathbf{R}\right]^{-1} \mathbf{HP}_+\mathbf{F}^T + \mathbf{Q}, \tag{2.2.9b}$$

corresponding to (2.2.8a) and (2.2.8b), respectively. Furthermore, if $\mathbf{C}_+$ and $\mathbf{P}_+ = \mathbf{FC}_+\mathbf{F}^T + \mathbf{Q}$ are solutions to RDE (2.2.8a) and (2.2.8b), respectively, we call them stabilizing / strong solutions, if and only if all eigenvalues of the matrix

$$\tilde{\mathbf{F}} = \mathbf{F}\left(\mathbf{I} - \mathbf{P}_+\mathbf{H}^T\left[\mathbf{HP}_+\mathbf{H}^T + \mathbf{R}\right]^{-1}\mathbf{H}\right) \tag{2.2.10}$$

are inside / inside or on the unit circle.[7] Consequently, every stabilizing solution is also a strong solution, while a strong solution is not necessarily also a stabilizing solution. Further, we may show that RDEs such as (2.2.8a) or (2.2.8b) have at most one (and therefore unique) strong solution (see e.g., de Souza et al., 1986).

Using this terminology we may establish three sufficient conditions under which the KF becomes asymptotically time-invariant:

Proposition 2.2.1. Suppose $\mathbf{C}_0 \in \mathbb{R}^{n_w \times n_w}$ is an arbitrary, but symmetric and positive-definite matrix. Then in case of SSM (2.2.1) the sequences $\{\mathbf{C}_t\}_{t=1}^N$ and $\{\mathbf{P}_{t|t-1}\}_{t=1}^N$ converge towards fixed matrices $\mathbf{C}_+$ and $\mathbf{P}_+$, i.e.

$$\lim_{N\to\infty}\{\mathbf{C}_t\}_{t=1}^N = \mathbf{C}_+ \qquad \text{and} \qquad \lim_{N\to\infty}\{\mathbf{P}_{t|t-1}\}_{t=1}^N = \mathbf{P}_+,$$

if at least one of the following statements is true:

(i) The matrix $\mathbf{R}$ is non-singular and all eigenvalues of the matrix $\mathbf{F}$ are inside the unit-circle. In this case $\mathbf{C}_+$ and $\mathbf{P}_+$ are stabilizing solutions of the RDEs (2.2.8a) and (2.2.8b), respectively.

(ii) The matrix $\bar{\mathbf{R}}$ is non-singular and all eigenvalues of the matrix $\bar{\mathbf{F}} = \mathbf{F} - \bar{\mathbf{G}}\bar{\mathbf{R}}^{-1}\bar{\mathbf{H}}$ are inside the unit-circle. In this case $\mathbf{C}_+$ and $\mathbf{P}_+$ are stabilizing solutions of the RDEs (2.2.8a) and (2.2.8b), respectively.

[6] For a more general discussion on the convergence of time-invariant RDEs see Appendix 2.B.

[7] Note that some authors, e.g., Bini et al. (2012); Chiang et al. (2010), use the term almost stabilizing solution as synomym for a strong solution.

(iii) The matrix $\mathbf{C}_0$ satisfies the discrete Lyapunov equation

$$\mathbf{0} = \mathbf{F}\mathbf{C}_0\mathbf{F}^T + \mathbf{Q} - \mathbf{C}_0$$

and the all eigenvalues of the matrix $\mathbf{F}$ are inside the unit-circle. In this case $\mathbf{C}_+$ and $\mathbf{P}_+$ are strong solutions of the RDEs (2.2.8a) and (2.2.8b), respectively. Moreover, we may state that the matrices $\mathbf{C}_0 - \mathbf{C}_+$ and $\mathbf{P}_{1|0} - \mathbf{P}_+$ are positive-semi-definite.

We postpone the formal proof of Proposition 2.2.1 to Appendix 2.B. From statement (i) of Proposition 2.2.1 follows that for all SSMs relying on a stationary process for $\mathbf{w}_t$ the KF becomes asymptotically time-invariant if the variance matrix of the measurement error $\mathbf{u}_t$ is non-singular. These assumptions are often met, for example, in the context of dynamic factor models (see e.g., Stock and Watson, 2016). There are however situations where $\mathbf{R}$ might be singular, but $\bar{\mathbf{R}}$ has full rank. This is often the case in the DSGE context (see e.g., Chari et al., 2007), as measurement errors are often omitted in these models. In this case we may use statement (ii) of Proposition 2.2.1, to investigate the convergence of (2.2.8a). If neither the conditions of statement (i) nor the conditions of statement (ii) are satisfied, statement (iii) will at least ensure that for any stationary SSM, both the matrix sequences, $\{\mathbf{C}_t\}_{t=1}^N$ and $\{\mathbf{P}_{t|t-1}\}_{t=1}^N$, converge to an equilibrium, provided they are initialized at the unconditional variance matrix $\mathbf{C}$ of the state vector.

As mentioned before, all three statements of Proposition 2.2.1 provide sufficient conditions for the convergence of the matrix sequences $\{\mathbf{C}_t\}_{t=1}^N$ and $\{\mathbf{P}_{t|t-1}\}_{t=1}^N$. However, statements (i) and (ii) of Proposition 2.2.1 imply that $\mathbf{C}_+$ and $\mathbf{P}_+$ are stabilizing solutions of the RDEs (2.2.8a) and (2.2.8b), while statement (iii) guarantees only convergence to a strong solution. Note that convergence to a stabilizing solution has the major advantage that we may use standard methods, such as the Schur algorithm (Bini et al., 2012, Chapter 3.2), the Newton algorithm (Bini et al., 2012, Chapter 3.3) or the doubling algorithm (Anderson and Moore, 1979, Chapter 6.7), to numerically solve (2.2.9a) for its stabilizing solution. Although there are iterative algorithms for determining a strong solution, such as the structured doubling algorithm described by Bini et al. (2012, Chapter 5), these algorithms are potentially less efficient from a computational point of view (see e.g., Chiang et al., 2010).

One of the advantages of an asymptotically time-invariant filter is that at a certain period τ, when $\mathbf{C}_\tau$ has converged sufficiently close to $\mathbf{C}_+$, i.e., $\mathbf{C}_\tau \approx \mathbf{C}_{\tau-1}$, the Kalman recursion (2.2.4) for $\boldsymbol{\mu}_t$ might be replaced by

$$\boldsymbol{\mu}_{t,+} = \mathbf{K}_+ \, \mathbf{y}_t^{(\mathrm{h})} + \mathbf{J}_+ \, \boldsymbol{\mu}_{t-1,+}, \qquad \forall \; t = \tau+1, \tau+2, \ldots, N, \tag{2.2.11a}$$

with

$$\mathbf{P}_+ = \mathbf{F}\mathbf{C}_+\mathbf{F}^T + \mathbf{Q}, \tag{2.2.11b}$$
$$\mathbf{U}_+ = \mathbf{H}\mathbf{P}_+\mathbf{H}^T + \mathbf{R}, \tag{2.2.11c}$$
$$\mathbf{K}_+ = \mathbf{P}_+\mathbf{H}^T \, \mathbf{U}_+^{-1}, \tag{2.2.11d}$$
$$\mathbf{J}_+ = (\mathbf{I} - \mathbf{K}_+\mathbf{H})\,\mathbf{F}. \tag{2.2.11e}$$

This usually reduces the computational burden significantly, since (2.2.11) does not involve the computationally expensive steps (2.2.4b), (2.2.4d) and (2.2.4f) of the original recursion. Furthermore, from (2.2.4a) and (2.2.4c) follows that the quantities $\mathbf{e}_t$ and $\mathbf{w}_{t|t-1}$ for $t = \tau+1, \tau+2, \ldots, N$ may be received in vectorized form as

$$\begin{pmatrix} \mathbf{w}_{\tau+1|\tau,+} & \cdots & \mathbf{w}_{N|N-1,+} \end{pmatrix} = \mathbf{F}\begin{pmatrix} \boldsymbol{\mu}_{\tau,+} & \cdots & \boldsymbol{\mu}_{N-1,+} \end{pmatrix}, \tag{2.2.11f}$$
$$\begin{pmatrix} \mathbf{e}_{\tau+1,+} & \cdots & \mathbf{e}_{N,+} \end{pmatrix} = \begin{pmatrix} \mathbf{y}_{\tau+1}^{(\mathrm{h})} & \cdots & \mathbf{y}_N^{(\mathrm{h})} \end{pmatrix} - \bar{\mathbf{H}}\begin{pmatrix} \boldsymbol{\mu}_{\tau,+} & \cdots & \boldsymbol{\mu}_{N-1,+} \end{pmatrix}, \tag{2.2.11g}$$

Throughout this paper, we will refer to the time-invariant filter described by (2.2.11) as the SKF. A detailed derivation of (2.2.11) is given in Appendix 2.C.

Note that Hansen and Sargent (2013, pp. 160) suggest to initialize the KF at the stabilizing solution of (2.2.8a) or (2.2.8b), respectively, i.e., $\boldsymbol{\mu}_0 = \boldsymbol{\mu}_{0,+}$ and $\mathbf{C}_0 = \mathbf{C}_+$.[8] This initialization is often used in the context of maximum-likelihood estimation, since despite the fact that the log-likelihood calculated on the basis of this initialization usually does not reflect the exact or unconditional log-likelihood, the determined maximum-likelihood estimator may (under certain preconditions, see e.g., Harvey, 1990b, pp. 119, 129) have the same large-sample properties as the unconditional maximum-likelihood estimator. Although, the maximum-likelihood estimators based on an initialization different from the exact or unconditional initialization is in generally less efficient, the *steady-state* initialization has the advantage that the resulting log-likelihood can be computed using the quicker SKF (2.2.11) with $\tau = 0$. Furthermore, given $\mathbf{C}_0 = \mathbf{C}_+$ we can rewrite (2.2.6) in a more compact way:

$$\log\left(f_{\mathbf{Y}_N}\right)_+ = -\frac{1}{2}\Big[n_y\ N\ \log(2\pi)\ + N\ \log|\mathbf{U}_+| + \operatorname{tr}\left(\mathbf{e}_{1:N,+}^T\ \mathbf{U}_+^{-1}\ \mathbf{e}_{1:N,+}\right)\Big], \tag{2.2.12}$$

where $\mathbf{e}_{1:N,+} := \begin{pmatrix}\mathbf{e}_{1,+} & \cdots & \mathbf{e}_{N,+}\end{pmatrix}$.

2.2.4 The augmented Kalman filter

There may be situations where we want to investigate how the initial state vector (or some components of it) affects the quantities obtained by the KF. For instance, consider a SSM with several non-stationary states. A typical approach to initialize such a model is to consider the non-stationary elements of state vector as diffuse, which means that their variance will tend towards infinity. In such situations, it might be worth considering another variant of the KF, which goes back to influential work by de Jong (1988, 1991). In what follows, we briefly describe a version of what Durbin and Koopman (2012) call the augmented Kalman filter (AKF).[9]

Let us assume that $\bar{\mathbf{w}}_0 \in \mathbb{R}^{n_{\bar{w}}}$ and $\mathbf{d} \in \mathbb{R}^{n_d}$ with $n_{\bar{w}}, n_{\mathbf{d}} \leq n_w$ are two independent random vectors, such that we may write the initial state vector as

$$\mathbf{w}_0 = \mathbf{a}_w + \mathbf{A}_w\ \bar{\mathbf{w}}_0 + \mathbf{A}_d\ \mathbf{d}, \qquad \bar{\mathbf{w}}_0 \sim \mathrm{N}(\bar{\boldsymbol{\mu}}_0, \bar{\mathbf{C}}_0), \qquad \mathbf{d} \sim \mathrm{N}(\boldsymbol{\delta}_0, \mathbf{D}_0), \tag{2.2.13}$$

where $\mathbf{a}_w \in \mathbb{R}^{n_w}$, $\mathbf{A}_w \in \mathbb{R}^{n_w \times n_{\bar{w}}}$ and $\mathbf{A}_d \in \mathbb{R}^{n_w \times n_p}$. Note that (2.2.13) implies that $\mathbf{w}_0$ has the mean vector $\boldsymbol{\mu}_0 = \mathbf{a}_w + \mathbf{A}_w\bar{\boldsymbol{\mu}}_0 + \mathbf{A}_d\boldsymbol{\delta}_0$ and the variance matrix $\mathbf{C}_0 = \mathbf{A}_w\bar{\mathbf{C}}_0\mathbf{A}_w^T + \mathbf{A}_d\mathbf{D}_0\mathbf{A}_d^T$. By choosing $\mathbf{a}_w$, $\mathbf{A}_w$ and $\mathbf{A}_d$ appropriately, we may use (2.2.13) to decompose $\mathbf{w}_0$ into multiple components of interest. Durbin and Koopman (2012), for instance, choose $\mathbf{a}_w$, $\mathbf{A}_{\mathbf{w}}$ and $\mathbf{A}_{\mathbf{d}}$, such that $\mathbf{a}_w$ represents the fixed (and observable) elements, $\bar{\mathbf{w}}_0$ the stationary elements, and $\mathbf{d}$ the diffuse elements of $\mathbf{w}_0$.

Now suppose, we specified $\mathbf{w}_0$ according to (2.2.13) and want to examine how the distribution of the random vector $\mathbf{d}$ affects the quantities $\boldsymbol{\mu}_t$ and $\mathbf{C}_t$ of the KF. As we show in Appendix 2.D, denoting the time t quantities generated by the Kalman recursion (2.2.4) initialized at $(\tilde{\boldsymbol{\mu}}_0, \tilde{\mathbf{C}}_0)$, with

$$\tilde{\boldsymbol{\mu}}_0 = \mathbf{a}_w + \mathbf{A}_w\ \bar{\boldsymbol{\mu}}_0, \tag{2.2.14a}$$

$$\tilde{\mathbf{C}}_0 = \mathbf{A}_w\ \bar{\mathbf{C}}_0\ \mathbf{A}_w^T, \tag{2.2.14b}$$

[8] Note that in this context $\boldsymbol{\mu}_{0,+}$ is usually chosen to be unconditional mean vector $\boldsymbol{\mu} = \mathbf{0}$.

[9] A similar treatments of the AKF with respect to the alternative state-space representation (2.2.5) are given by Durbin and Koopman (2012, Chapter 5.7).

by $\tilde{\boldsymbol{\mu}}_t$, $\tilde{\mathbf{C}}_t$, $\tilde{\mathbf{w}}_{t|t-1}$, $\tilde{\mathbf{P}}_{t|t-1}$, $\tilde{\mathbf{e}}_t$, $\tilde{\mathbf{U}}_t$ and $\tilde{\mathbf{K}}_t$, we may express $\boldsymbol{\mu}_t$ and $\mathbf{C}_t$ as

$$\boldsymbol{\mu}_t = \tilde{\boldsymbol{\mu}}_t + \mathbf{M}_t\mathbf{A}_d \left(\mathbf{D}_0^{-1} + \mathbf{A}_d^T \mathbf{S}_t \mathbf{A}_d\right)^{-1}\left(\mathbf{D}_0^{-1}\boldsymbol{\delta}_0 + \mathbf{A}_d^T \mathbf{s}_t\right), \qquad \forall\ t = 1,2,\dots,N, \tag{2.2.15a}$$

$$\mathbf{C}_t = \tilde{\mathbf{C}}_t + \mathbf{M}_t\mathbf{A}_d \left(\mathbf{D}_0^{-1} + \mathbf{A}_d^T \mathbf{S}_t \mathbf{A}_d\right)^{-1}\mathbf{A}_d^T\mathbf{M}_t^T, \qquad \forall\ t = 1,2,\dots,N, \tag{2.2.15b}$$

where we may obtain $\mathbf{s}_t$, $\mathbf{S}_t$ and $\mathbf{M}_t$ recursively as

$$\mathbf{s}_t = \mathbf{s}_{t-1} + (\mathbf{H}\mathbf{F}\mathbf{M}_{t-1})^T \tilde{\mathbf{U}}_t^{-1}\tilde{\mathbf{e}}_t, \qquad \forall\ t = 1,2,\dots,N, \tag{2.2.15c}$$

$$\mathbf{S}_t = \mathbf{S}_{t-1} + (\mathbf{H}\mathbf{F}\mathbf{M}_{t-1})^T \tilde{\mathbf{U}}_t^{-1}(\mathbf{H}\mathbf{F}\mathbf{M}_{t-1}), \qquad \forall\ t = 1,2,\dots,N, \tag{2.2.15d}$$

$$\mathbf{M}_t = \left(\mathbf{I} - \tilde{\mathbf{K}}_t\mathbf{H}\right)\mathbf{F}\,\mathbf{M}_{t-1}, \qquad \forall\ t = 1,2,\dots,N, \tag{2.2.15e}$$

with $\mathbf{s}_0 = \mathbf{0}$, $\mathbf{S}_0 = \mathbf{0}$ and $\mathbf{M}_0 = \mathbf{I}$. Furthermore, we may write the log-density of $\mathbf{Y}_N$ as

$$\begin{aligned}\log(f_{\mathbf{Y}_N}) = \log\left(f_{\mathbf{Y}_N|\mathbf{d}=\mathbf{0}}\right) - \frac{1}{2}\log|\mathbf{I} + \mathbf{D}_0\,\mathbf{A}_d^T\,\mathbf{S}_N\,\mathbf{A}_d| - \frac{1}{2}\boldsymbol{\delta}_0^T\mathbf{D}_0^{-1}\boldsymbol{\delta}_0 \\ + \frac{1}{2}(\mathbf{D}_0^{-1}\boldsymbol{\delta}_0 + \mathbf{A}_d^T\,\mathbf{s}_N)^T(\mathbf{D}_0^{-1} + \mathbf{A}_d^T\,\mathbf{S}_N\,\mathbf{A}_d)^{-1}(\mathbf{D}_0^{-1}\boldsymbol{\delta}_0 + \mathbf{A}_d^T\,\mathbf{s}_N),\end{aligned} \tag{2.2.16}$$

where $\log\left(f_{\mathbf{Y}_N|\mathbf{d}=\mathbf{0}}\right)$ represents the log-density of $\mathbf{Y}_N$ given $\mathbf{d} = \mathbf{0}$.[10] Thus, using the AKF (2.2.15) we can directly examine the effect of $\boldsymbol{\delta}_0$ and $\mathbf{D}_0$ on $\boldsymbol{\mu}_t$, $\mathbf{C}_t$ and $\log(f_{\mathbf{Y}_N})$ from (2.2.15a), (2.2.15b), and (2.2.16). This allows us to study the special cases in which parts of $\mathbf{w}_0$ are considered to be fixed (i.e., $\mathbf{D}_0 \to \mathbf{0}$) or diffuse (i.e., $\mathbf{D}_0 \to \infty$). In Appendix 2.D we provide a digression on how to incorporate initialization strategies for non-stationary SSMs within the AKF (2.2.15).

2.3 Augmented steady-state Kalman filter

Equipped with the concepts introduced in the previous section, we now turn our attention to the derivation of the ASKF. For this purpose, we will first outline the basic idea of an ASKF and obtain a general algorithm to evaluate the likelihood function of a linear and time-invariant SSM. We show that compared to the standard KF this algorithm lowers the computational burden associated with each additional observation. Finally, we provide conditions for applicability of the ASKF which we show are satisfied for all stationary SSMs. Further, we show that for the SSM (2.2.2) with $n_y = n_z$ the algorithm can be additionally optimized, since in this case there is an analytical solution to RDE (2.2.8a).

2.3.1 Basic idea

Suppose we want to evaluate the log-density $\log(f_{\mathbf{Y}_N})$ of the SSM (2.2.1) for a given initialization $(\boldsymbol{\mu}_0, \mathbf{C}_0)$. Furthermore, suppose that the RDE (2.2.8a) has a solution $\mathbf{C}_+$ such that $\mathbf{C}_0 - \mathbf{C}_+$ is a positive semi-definite matrix.

As mentioned earlier, we can determine the $\log(f_{\mathbf{Y}_N})$ for this initialization using the KF (2.2.4) and equation (2.2.6). However, we could also employ the AKF (2.2.15) along with equation (2.2.16) to determine $\log(f_{\mathbf{Y}_N})$. To do so, we need to specify the model (2.2.13) for the initial

[10] Note that the recursion for $\mathbf{s}_t$, $\mathbf{S}_t$ and $\mathbf{M}_t$ can be incorporated in the Kalman recursion used to compute $\tilde{\boldsymbol{\mu}}_t$, $\tilde{\mathbf{C}}_t$, $\tilde{\mathbf{w}}_{t|t-1}$, $\tilde{\mathbf{P}}_{t|t-1}$, $\tilde{\mathbf{e}}_t$, $\tilde{\mathbf{U}}_t$ and $\tilde{\mathbf{K}}_t$. A detailed derivation of equations (2.2.15)-(2.2.16) and how these steps can be incorporated in the Kalman recursion (2.2.4) is provided in Appendix 2.D. A similar treatment of the AKF with respect to the alternative state-space representation (2.2.5) is given by Durbin and Koopman (2012, pp. 141-146).

state vector $\mathbf{w}_0$ such that

$$\boldsymbol{\mu}_0 = \mathbf{a}_w + \mathbf{A}_w\, \bar{\boldsymbol{\mu}}_0 + \mathbf{A}_d\, \boldsymbol{\delta}_0, \tag{2.3.1a}$$
$$\mathbf{C}_0 = \mathbf{A}_w\, \bar{\mathbf{C}}_0\, \mathbf{A}_w^T + \mathbf{A}_d\, \mathbf{D}_0\, \mathbf{A}_d^T, \tag{2.3.1b}$$

ensuring that $\mathbf{w}_0 \sim \mathrm{N}(\boldsymbol{\mu}_0, \mathbf{C}_0)$. There are several possible specifications of (2.2.13) which satisfy (2.3.1a) and (2.3.1b). The basic idea of the ASKF is to choose the model (2.2.13) for the initial state vector $\mathbf{w}_0$ in a way that makes the Kalman recursion, on which the AKF is based, time-invariant. To do so, we will specify (2.2.13) as follows: First, we will set

$$\mathbf{a}_w = \mathbf{0}, \tag{2.3.2a}$$
$$\mathbf{A}_w = \mathbf{I}, \tag{2.3.2b}$$
$$\bar{\boldsymbol{\mu}}_0 = \boldsymbol{\mu}_0, \tag{2.3.2c}$$
$$\bar{\mathbf{C}}_0 = \mathbf{C}_+, \tag{2.3.2d}$$

so that from (2.2.14a) and (2.2.14b) follows $\tilde{\boldsymbol{\mu}}_0 = \boldsymbol{\mu}_0$ and $\tilde{\mathbf{C}}_0 = \mathbf{C}_+$, respectively. Second, in order to satisfy (2.3.1a) and (2.3.1b), we set

$$\boldsymbol{\delta}_0 = \mathbf{0}, \tag{2.3.2e}$$
$$\mathbf{D}_0 = \mathbf{I}, \tag{2.3.2f}$$

and choose $\mathbf{A}_d$ such that

$$\mathbf{A}_d \mathbf{A}_d^T = \mathbf{C}_0 - \mathbf{C}_+. \tag{2.3.2g}$$

Hence, the fully specified version of (2.2.13) yields

$$\mathbf{w}_0 = \bar{\mathbf{w}}_0 + \mathbf{A}_\mathbf{d}\, \mathbf{d}, \qquad \bar{\mathbf{w}}_0 \sim \mathrm{N}(\boldsymbol{\mu}_0, \mathbf{C}_+), \qquad \mathbf{d} \sim \mathrm{N}(\mathbf{0}, \mathbf{I}). \tag{2.3.3}$$

In the current paper, we use the singular value decomposition of $\mathbf{C}_0 - \mathbf{C}_+$ to obtain $\mathbf{A}_d$. However, note that in the cases where $\mathbf{C}_0 - \mathbf{C}_+$ is non-singular, one might also set $\mathbf{A}_d = \mathbf{I}$ and $\mathbf{D}_0 = \mathbf{C}_0 - \mathbf{C}_+$. In either way, we need to ensure that $\mathbf{D}_0$ is positive definite.

Specifying (2.2.13) this way, the quantities $\tilde{\boldsymbol{\mu}}_t$, $\tilde{\mathbf{C}}_t$, $\tilde{\mathbf{w}}_{t|t-1}$, $\tilde{\mathbf{P}}_{t|t-1}$, $\tilde{\mathbf{e}}_t$, $\tilde{\mathbf{U}}_t$ and $\tilde{\mathbf{K}}_t$ corresponding to the KF (2.2.4) initialized at $(\tilde{\boldsymbol{\mu}}_0, \tilde{\mathbf{C}}_0)$ become

$$\tilde{\boldsymbol{\mu}}_t = \boldsymbol{\mu}_{t,+}, \qquad \tilde{\mathbf{w}}_{t|t-1} = \mathbf{w}_{t|t-1,+}, \qquad \tilde{\mathbf{e}}_t = \mathbf{e}_{t,+},$$
$$\tilde{\mathbf{C}}_t = \mathbf{C}_+, \qquad \tilde{\mathbf{P}}_{t|t-1} = \mathbf{P}_+, \qquad \tilde{\mathbf{U}}_t = \mathbf{U}_+, \qquad \tilde{\mathbf{K}}_t = \mathbf{K}_+, \quad \forall\ t = 1, 2, \ldots, N,$$

where $\boldsymbol{\mu}_{t,+}$, $\mathbf{C}_+$, $\mathbf{w}_{t|t-1,+}$, $\mathbf{P}_+$, $\mathbf{e}_{t,+}$, $\mathbf{U}_+$ and $\mathbf{K}_+$ are the quantities computed by the SKF based on the initialization $(\boldsymbol{\mu}_{0,+}, \mathbf{C}_+)$, with $\boldsymbol{\mu}_{0,+} = \boldsymbol{\mu}_0$. This reduces the computational burden of the AKF in two ways: First, instead of the regular KF we may use the faster SKF to compute the quantities $\tilde{\boldsymbol{\mu}}_t$, $\tilde{\mathbf{C}}_t$, $\tilde{\mathbf{w}}_{t|t-1}$, $\tilde{\mathbf{P}}_{t|t-1}$, $\tilde{\mathbf{e}}_t$, $\tilde{\mathbf{U}}_t$, $\tilde{\mathbf{K}}_t$ and $\log\left(f_{\mathbf{Y}_N|\mathbf{d}=\mathbf{0}}\right)$. Second, we can simplify the recursion (2.2.15c)-(2.2.15e), since the expression $\left(\mathbf{I} - \tilde{\mathbf{K}}_t \mathbf{H}\right)\mathbf{F}$ becomes time-invariant and identically to $\mathbf{J}_+$. Thus, the quantity $\mathbf{M}_t$ reduces to

$$\mathbf{M}_t = \mathbf{J}_+^t, \qquad \forall\ t = 0, 1, \ldots, N. \tag{2.3.4}$$

2.3.2 Likelihood evaluation

Furthermore, suppose our interest lies exclusively in the evaluation of the log-density $\log\left(f_{\mathbf{Y}_N}\right)$. If we specify (2.2.13) according to (2.3.2), we can simplify (2.2.16) to

$$\log(f_{\mathbf{Y}_N}) = \log\left(f_{\mathbf{Y}_N}\right)_+ - \frac{1}{2}\log|\mathbf{I} + \mathbf{A}_d^T\ \mathbf{S}_N\ \mathbf{A}_d| + \frac{1}{2}\mathbf{s}_N^T\ \mathbf{A}_d\ (\mathbf{I} + \mathbf{A}_d^T\ \mathbf{S}_N\ \mathbf{A}_d)^{-1}\ \mathbf{A}_d^T\ \mathbf{s}_N, \tag{2.3.5}$$

where $\log\left(f_{\mathbf{Y}_N}\right)_+ = \log\left(f_{\mathbf{Y}_N|\mathbf{d}=\mathbf{0}}\right)$ represents the log-density obtained from the SKF based on the initialization $(\boldsymbol{\mu}_{0,+}, \mathbf{C}_+)$, with $\boldsymbol{\mu}_{0,+} = \boldsymbol{\mu}_0$. Hence, the log-density $\log\left(f_{\mathbf{Y}_N}\right)$ is fully determined by $\log\left(f_{\mathbf{Y}_N}\right)_+$, $\mathbf{s}_N$, $\mathbf{S}_N$, and $\mathbf{A}_d$.

It turns out that we may further optimize the computation of $\mathbf{s}_N$, $\mathbf{S}_N$, and $\log\left(f_{\mathbf{Y}_N}\right)_+$, in terms of the required arithmetic operations. To do so, let us define

$$\mathbf{b}_t := \mathbf{V}^T\mathbf{e}_{t,+}, \qquad \forall\ t = 1, 2, \ldots, N, \tag{2.3.6a}$$

$$\mathbf{B}_t := \left(\mathbf{J}_+^t\right)^T\ \bar{\mathbf{H}}^T\ \mathbf{V}, \qquad \forall\ t = 0, 1, \ldots, N-1, \tag{2.3.6b}$$

with $\mathbf{V}$ satisfying $\mathbf{U}_+^{-1} = \mathbf{V}\mathbf{V}^T$, so that we may obtain $\mathbf{s}_N$ and $\mathbf{S}_N$ as

$$\mathbf{s}_N = \mathbf{B}_{0:N-1}\ \mathrm{vec}\left(\mathbf{b}_{1:N}\right), \tag{2.3.7a}$$

$$\mathbf{S}_N = \mathbf{B}_{0:N-1}\ \mathbf{B}_{0:N-1}^T, \tag{2.3.7b}$$

with $\mathbf{B}_{0:N-1} := \left(\mathbf{B}_0, \cdots, \mathbf{B}_{N-1}\right)$ and $\mathbf{b}_{1:N} := \left(\mathbf{b}_1, \cdots, \mathbf{b}_N\right)$. It follows from (2.3.6) that $\mathbf{b}_{1:N}$ yields

$$\mathbf{b}_{1:N} = \mathbf{V}^T\mathbf{e}_{1:N,+}, \tag{2.3.8}$$

and that $\mathbf{B}_{0:N-1}$ is recursively defined by

$$\mathbf{B}_t := \mathbf{J}_+^T\ \mathbf{B}_{t-1} \qquad \forall\ t = 1, 2, \ldots, N-1, \tag{2.3.9}$$

with $\mathbf{B}_0 = \bar{\mathbf{H}}^T\ \mathbf{V}$. Hence, using (2.3.8) to rewrite (2.2.12) as

$$\log\left(f_{\mathbf{Y}_N}\right)_+ = -\frac{1}{2}\left[n_y\ N\ \log(2\pi)\ + N\ \log|\mathbf{U}_+| + \mathrm{tr}\left(\mathbf{b}_{1:N}\ \mathbf{b}_{1:N}^T\right)\right], \tag{2.3.10}$$

the log-density $\log\left(f_{\mathbf{Y}_N}\right)_+$ is obtainable by performing the steps displayed in Algorithm 3.1.

The ASKF described in Algorithm 3.1 has several advantages compared to the regular KF, where the probably most important is that, although the initial setup (Steps (1)-(3)) of the filter is more expansive, it requires fewer arithmetic operations for each additional observation, so that the recursive part of the algorithm is more efficient. To see this, suppose we implement the KF and the ASKF using standard matrix multiplication, ignoring the advantages which may arise from the symmetrical nature of variance matrices. For this case, Table 2.1 lists the number of additional additive and multiplicative operations that result if we increase the number of observations from N to $N+1$. It turns out that the ASKF saves $n_y^2 + n_w(n_w^2 - 1) + n_w(n_w - 1) + n_w(n_w-1)^2 + 2n_y(n_y-1)(n_w-1)$ additive and $2n_w^3 + n_y + n_y^2(n_w-1) + n_y(n_y-1)n_w$ multiplicative operations for each additional observation. Further, and almost more importantly, the ASKF does not require the repeated computation of the inverse and the determinant of the $n_y \times n_y$ matrix $\mathbf{U}_t$. Finally, the ASKF offers more room for parallelization since only the computation of $\boldsymbol{\mu}_{t,+}$ and $\mathbf{B}_t$ are strictly sequential.

Algorithm 3.1: Using the ASKF to compute $\log\left(f_{\mathbf{Y}_N}\right)$ for the SSM (2.2.1)

Input : $\boldsymbol{\mu}_0$, $\mathbf{C}_0$ and $\mathbf{C}_+$, where $\mathbf{C}_0 - \mathbf{C}_+$ is positive semi-definite;

Execute : Steps (1)-(7);

(1) Choose $\mathbf{a}_w$, $\mathbf{A}_w$, $\bar{\boldsymbol{\mu}}_0$, $\bar{\mathbf{C}}_0$, $\boldsymbol{\delta}_0$, $\mathbf{D}_0$, and $\mathbf{A}_d$ according to (2.3.2);

(2) Obtain $\mathbf{P}_+$, $\mathbf{U}_+$, $\mathbf{K}_+$ and $\mathbf{J}_+$ from (2.2.11b)-(2.2.11e);

(3) Obtain $\mathbf{V}$ such that $\mathbf{U}_+^{-1} = \mathbf{V}\mathbf{V}^T$ and set $\mathbf{B}_0 = \bar{\mathbf{H}}^T\,\mathbf{V}$;

(4) **for** $t = 1$ **to** $N-1$ **do**

  Obtain $\boldsymbol{\mu}_{t,+}$ (with $\boldsymbol{\mu}_{0,+} = \boldsymbol{\mu}_0$) and $\mathbf{B}_t$ from (2.2.11a) and (2.3.9);

(5) Obtain $\mathbf{e}_{1:N,+}$ and $\mathbf{b}_{1:N}$ from (2.2.11g) and (2.3.8);

(6) Obtain $\mathbf{s}_N$, $\mathbf{S}_N$ and $\log\left(f_{\mathbf{Y}_N}\right)_+$ from (2.3.7a), (2.3.7b) and (2.3.10);

(7) Obtain $\log\left(f_{\mathbf{Y}_N}\right)$ from (2.3.5);

Output : $\log\left(f_{\mathbf{Y}_N}\right)$;

2.3.3 Requirements to apply the augmented steady-state Kalman filter

To apply Algorithm 3.1 to the SSM (2.2.1) for a given initialization $(\boldsymbol{\mu}_0, \mathbf{C}_0)$, we need to satisfy the following assumptions:

Assumption 2.3.1. We assume that

(i) there is a solution $\mathbf{C}_+$ to the RDE (2.2.8a),

(ii) such that the matrix $\mathbf{C}_0 - \mathbf{C}_+$ is positive semi-definite.

While Assumption 2.3.1(i) is needed to use the SKF at all, Assumption 2.3.1(ii) is necessary to satisfy (2.3.1b), since $\mathbf{D}_0$ is positive-definite by definition, so that $\mathbf{A}_d\mathbf{D}_0\mathbf{A}_d^T$ must be at least positive-semi-definite. Although it is not necessary in theory, in practice, it is advisable to ensure that $\mathbf{C}_+$ represents a strong solution of RDE (2.2.8a). Otherwise the matrix $\mathbf{J}_+$ possesses explosive eigenvalues, making Algorithm 1 numerically unstable.[11]

Stationary state-space models: To check how restrictive the conditions of Assumption 2.3.1 are, let us first consider the class of stationary SSMs. Thus, we consider models where all the eigenvalues of the transition matrix $\mathbf{F}$ lie within the unit circle, or in other words where $\mathbf{F}$ is stable. Thus, from Corollary 2.2.1(iii), we know that for stationary SSMs, the preconditions for the usage of the ASKF will be satisfied, provided we use the unconditional variance of $\mathbf{w}_t$ to initialize the SSM (2.2.1), i.e., $\mathbf{C}_0 = \mathbf{C}$. To obtain $\mathbf{C}_+$, which in this case is a strong solution to (2.2.8a), we could use an iterative algorithm, such as the structured doubling algorithm described by Bini et al. (2012, Chapter 5). It is convenient to consider two special cases where $\mathbf{C}_+$ we may obtain in a different manner.

[11] Note that we show in Appendix 2.B and 2.C that the matrices $\tilde{\mathbf{F}}$ and $\mathbf{J}_+$ share the same set of eigenvalues.

Table 2.1: Computational expanse of an additional observation

augmented steady-state Kalman filter			
Eqn.	Additional Matrix Operations	Multiplications	Additions
(2.2.11a)	$(n_w \times n_y)[(n_y \times 1)-(n_y \times 1)]+(n_w \times n_w)(n_w \times 1)$	$n_y n_w + n_w^2$	$n_y n_w + n_w^2 + n_y - n_w$
(2.3.9)	$(n_w \times n_w)(n_w \times n_y)$	$n_y n_w^2$	$n_y n_w^2 - n_y n_w$
(2.2.11g)	$(n_y \times 1)-(n_y \times n_w)(n_w \times 1)$	$n_y n_w$	$n_y n_w$
(2.3.8)	$(n_y \times n_y)(n_y \times 1)$	n_y^2	$n_y^2 - n_y$
(2.3.7a)	$(n_w \times 1)+(n_w \times n_y)(n_y \times 1)$	$n_y n_w$	$n_y n_w$
(2.3.7b)	$(n_w \times n_w)+(n_w \times n_y)(n_y \times n_w)$	$n_y n_w^2$	$n_y n_w^2$
(2.3.10)	$(n_y \times n_y)+(n_y \times 1)(1 \times n_y)$	n_y^2	n_y^2
m_{ASKF}	$2n_y^2 + n_w^2 + 2n_y n_w^2 + 3n_y n_w$		
a_{ASKF}	$2n_y^2 + n_w^2 - n_w + 2n_y n_w^2 + 2n_y n_w$		
Kalman filter			
Eqn.	Additional Matrix Operations	Multiplications	Additions
(2.2.4a)	$(n_w \times n_w)(n_w \times 1)$	n_w^2	$n_w^2 - n_w$
(2.2.4b)	$(n_w \times n_w)(n_w \times n_w)(n_w \times n_w)+(n_w \times n_w)$	$2n_w^3$	$2n_w^3 - n_w^2$
(2.2.4c)	$(n_y \times 1)-(n_y \times 1)-(n_y \times n_w)(n_w \times 1)$	$n_y n_w$	$n_y n_w + 2n_y - n_w$
(2.2.4d)	$(n_y \times n_w)(n_w \times n_w)(n_w \times n_y)+(n_y \times n_y)$	$n_y n_w^2 + n_y^2 n_w$	$n_y n_w^2 + n_y^2 n_w - n_y n_w$
(2.2.3)	$(n_w \times n_y)(n_y \times n_y)$	$n_y^2 n_w$	$n_y^2 n_w - n_y n_w$
(2.2.4e)	$(n_w \times 1)+(n_w \times n_y)(n_y \times 1)$	$n_y n_w$	$n_y n_w$
(2.2.4f)	$(n_w \times n_w)-(n_w \times n_y)(n_y \times n_w)$	$n_y n_w^2$	$n_y n_w^2$
(2.2.6)	$(1 \times 1)+(1 \times n_y)(n_y \times n_y)(n_y \times 1)$	$n_y^2 + n_y$	n_y^2
m_{KF}	$2n_w^3 + n_y^2 + n_w^2 + n_y + 2n_y^2 n_w + 2n_y n_w^2 + 2n_y n_w$		
a_{KF}	$2n_w^3 + n_y^2 + 2n_y - 2n_w + 2n_y^2 n_w + 2n_y n_w^2$		
Comparison			
$m_{KF} - m_{ASKF}$	$2n_w^3 + n_y + n_y^2(n_w - 1) + n_y(n_y - 1)n_w$		
$a_{KF} - a_{ASKF}$	$n_y^2 + n_w(n_w^2 - 1) + n_w(n_w - 1) + n_w(n_w - 1)^2 + 2n_y(n_y - 1)(n_w - 1)$		

We count $nm(l-1)$ additive and nml multiplicative operations for product of a $m \times l$ and a $l \times n$ matrix. Further, nm additive operations are counted for the sum/difference of two $m \times n$ matrices. The a_{KF} and a_{ASKF} denote the number additive operations of the corresponding filter, while m_{KF} and m_{ASKF} denote their required number of multiplicative operations.

Case 1: If we consider a stationary SSM, where the variance matrix $\mathbf{R}$ of the measurement error is positive-definite, it follows from Corollary 2.2.1(i) that the RDE (2.2.8a) converges to a stabilizing solution $\mathbf{C}_+$ for any positive-definite initialization $\mathbf{C}_0$. Furthermore, $\mathbf{C}_+$ can be considered the only non-negative-definite solution of the RDE (2.2.8a).[12] Thus, using the unconditional initialization, i.e., $\mathbf{C}_0 = \mathbf{C}$, we may apply the classic techniques discussed in the previous section to obtain the stabilizing solution $\mathbf{C}_+$ of RDE (2.2.8a). The same argumentation applies to stationary SSMs, where $\overline{\mathbf{R}}$ is positive-definite and where $\overline{\mathbf{F}}$ is stable.
Case 2: Now, let us consider SSMs of the form (2.2.2), where the number of observable variables n_y equals the number of exogenous states variables n_z. In the following Proposition, we will show that in this case, we may obtain $\mathbf{C}_+ = \mathbf{0}$ as a solution to the RDE (2.2.8a) if the matrix $\mathbf{H}_z$ is non-singular.

Proposition 2.3.1. Suppose there is a SSM of the form described by (2.2.2) where

(i) the number of observable variables n_y equals the number of (state-) disturbances n_z,

(ii) and where the matrix $\mathbf{H}_z$ is non-singular.

Then $\mathbf{C}_+ := \mathbf{0}$ is a solution to the RDE (2.2.8a).

Proof:
To prove that $\mathbf{C}_+ := \mathbf{0}$ is a solution to the RDE (2.2.8a), it is sufficient to show that $\mathbf{C}_+ := \mathbf{0}$

[12] This follows from Proposition 2.B.1(ii) in Appendix 2.B.

satisfies the DARE

$$\mathbf{C}_+ = \bar{\mathbf{F}}\mathbf{C}_+\bar{\mathbf{F}}^T + \bar{\mathbf{Q}} - \bar{\mathbf{F}}\mathbf{C}_+\bar{\mathbf{H}}^T \left[\bar{\mathbf{H}}\mathbf{C}_+\bar{\mathbf{H}}^T + \bar{\mathbf{R}}\right]^{-1} \bar{\mathbf{H}}\mathbf{C}_+\bar{\mathbf{F}}^T. \tag{2.3.11}$$

with $\bar{\mathbf{F}} := \mathbf{F} - \bar{\mathbf{G}}\bar{\mathbf{R}}^{-1}\bar{\mathbf{H}}$ and $\bar{\mathbf{Q}} := \mathbf{Q} - \bar{\mathbf{G}}\bar{\mathbf{R}}^{-1}\bar{\mathbf{G}}^T$, which, due to Lemma 2.B.1 in Appendix 2.B, is equivalent to the DARE (2.2.9a) corresponding to the RDE (2.2.8a). To see that $\mathbf{C}_+ := \mathbf{0}$ is a solution to (2.3.11), note that for the SSM (2.2.2)

$$\bar{\mathbf{R}} = \mathbf{H}\mathbf{Q}\mathbf{H}^T = \begin{pmatrix}\mathbf{H}_z & \mathbf{H}_x\end{pmatrix}\begin{pmatrix}\mathbf{Q}_z & \mathbf{0}\\ \mathbf{0} & \mathbf{0}\end{pmatrix}\begin{pmatrix}\mathbf{H}_z^T\\ \mathbf{H}_x^T\end{pmatrix} = \begin{pmatrix}\mathbf{H}_z\mathbf{Q}_z & \mathbf{0}\end{pmatrix}\begin{pmatrix}\mathbf{H}_z^T\\ \mathbf{H}_x^T\end{pmatrix} = \mathbf{H}_z\mathbf{Q}_z\mathbf{H}_z^T.$$

Thus, from the definition of $\bar{\mathbf{Q}}$ follows that

$$\begin{aligned}
\bar{\mathbf{Q}} &= \mathbf{Q} - \bar{\mathbf{G}}\bar{\mathbf{R}}^{-1}\bar{\mathbf{G}}^T = \mathbf{Q} - \mathbf{Q}\mathbf{H}^T\left(\mathbf{H}_z\mathbf{Q}_z\mathbf{H}_z^T\right)^{-1}\mathbf{H}\mathbf{Q}\\
&= \begin{pmatrix}\mathbf{Q}_z & \mathbf{0}\\ \mathbf{0} & \mathbf{0}\end{pmatrix} - \begin{pmatrix}\mathbf{Q}_z & \mathbf{0}\\ \mathbf{0} & \mathbf{0}\end{pmatrix}\begin{pmatrix}\mathbf{H}_z^T\\ \mathbf{H}_x^T\end{pmatrix}\left(\mathbf{H}_z\,\mathbf{Q}_z\,\mathbf{H}_z^T\right)^{-1}\begin{pmatrix}\mathbf{H}_z & \mathbf{H}_x\end{pmatrix}\begin{pmatrix}\mathbf{Q}_z & \mathbf{0}\\ \mathbf{0} & \mathbf{0}\end{pmatrix}\\
&= \begin{pmatrix}\mathbf{Q}_z & \mathbf{0}\\ \mathbf{0} & \mathbf{0}\end{pmatrix} - \begin{pmatrix}\mathbf{Q}_z\mathbf{H}_z^T\\ \mathbf{0}\end{pmatrix}(\mathbf{H}_z^T)^{-1}\,\mathbf{Q}_z^{-1}\,\mathbf{H}_z^{-1}\begin{pmatrix}\mathbf{H}_z\mathbf{Q}_z & \mathbf{0}\end{pmatrix}\\
&= \begin{pmatrix}\mathbf{Q}_z & \mathbf{0}\\ \mathbf{0} & \mathbf{0}\end{pmatrix} - \begin{pmatrix}\mathbf{Q}_z\\ \mathbf{0}\end{pmatrix}\mathbf{Q}_z^{-1}\begin{pmatrix}\mathbf{Q}_z & \mathbf{0}\end{pmatrix}\\
&= \begin{pmatrix}\mathbf{Q}_z & \mathbf{0}\\ \mathbf{0} & \mathbf{0}\end{pmatrix} - \begin{pmatrix}\mathbf{Q}_z & \mathbf{0}\\ \mathbf{0} & \mathbf{0}\end{pmatrix} = \mathbf{0}.
\end{aligned}$$

This, however, means that (2.3.11) simplifies to

$$\mathbf{C}_+ = \bar{\mathbf{F}}\mathbf{C}_+\bar{\mathbf{F}}^T - \bar{\mathbf{F}}\mathbf{C}_+\bar{\mathbf{H}}^T \left[\bar{\mathbf{H}}\mathbf{C}_+\bar{\mathbf{H}}^T + \bar{\mathbf{R}}\right]^{-1} \bar{\mathbf{H}}\mathbf{C}_+\bar{\mathbf{F}}^T,$$

which is clearly satisfied if we set $\mathbf{C}_+ = \mathbf{0}$.

□

This result is convenient since $\mathbf{C}_+ = \mathbf{0}$ satisfies Assumption 2.3.1(ii) for any positive semi-definite $\mathbf{C}_0$.[13] This means for $n_y = n_z = \text{rk}(\mathbf{H}_z)$, we do not even have to obtain $\mathbf{C}_+$ numerically and may use Algorithm 3.1 to compute $\log\left(f_{\mathbf{Y}_N}\right)$ for an arbitrary initialization $(\boldsymbol{\mu}_0, \mathbf{C}_0)$.

At this point, it is appropriate to discuss why most DSGE models without measurement errors will meet the preconditions of Proposition 2.3.1. To see this, first, consider the scenario where $n_y > n_z$. This, in general, will lead to a model that is unable to match the data.[14] Consequently, we will have to include an appropriate number of measurement disturbances into our SSM. However, adding zeros to the corresponding entries in the transitions matrix $\mathbf{F}$ we may treat these measurement disturbances as state disturbances and get yet a SSM without measurement error satisfying condition (i) of Proposition 2.3.1. Thus $n_y > n_z$ is less of a problem. Now consider the opposite case where $n_y < n_z$, which usually implies that our model can replicate the data with more than one set of state disturbances. Admittedly this does not necessarily pose a problem in estimating the model using the common KF (2.2.4). However, in this case, it is often possible to include additional observable data series to increase the information used to estimate the model's parameters. This is especially true in the DSGE context since the observation vector $\mathbf{y}_t$ often reflects only a fraction of the potentially observable variables for these models.

Assuming $n_z = n_y$ holds, we will usually find that condition (ii) of Proposition 2.3.1 is also satisfied. To see this, note that there are only two possible scenarios where the model might

[13] As mentioned before, in practice, we might have to check if $\mathbf{C}_+ = \mathbf{0}$ represents a strong solution.

[14] We exclude the trivial case with redundant observations that are linear combinations of the remaining set of data.

not satisfy condition (ii) of Proposition 2.3.1: In the first scenario, we have the trivial case with $\text{rk}(\mathbf{H}_z) \leq \text{rk}(\mathbf{H}) < n_y$, indicating that a fraction of the observations vector $\mathbf{y}_t$ can be written as a linear combination of the remaining set of observations in $\mathbf{y}_t$ and thus contains redundant information. More interesting is the second scenario, where $\text{rk}(\mathbf{H}_z) < \text{rk}(\mathbf{H}) = n_y$. In this case, a fraction of $\mathbf{y}_t$ contains information that, from the model's perspective, was already determined in the previous period $t-1$. To see this, note that we can reorder the observations vector $\mathbf{y}_t$ so that we can write

$$\mathbf{y}_t = \begin{bmatrix} \mathbf{y}_t^{(1)} \\ \mathbf{y}_t^{(2)} \end{bmatrix} = \begin{bmatrix} \mathbf{H}_x^{(1)} \\ \mathbf{H}_x^{(2)} \end{bmatrix} \mathbf{x}_t + \begin{bmatrix} \mathbf{H}_z^{(1)} \\ \mathbf{H}_z^{(2)} \end{bmatrix} \mathbf{z}_t \tag{2.3.12}$$

with $\text{rk}(\mathbf{H}_z^{(1)}) = \text{rk}(\mathbf{H}_z)$. This, however, means there is a matrix $\boldsymbol{\Gamma}$ satisfying

$$\mathbf{H}_z^{(2)} = \boldsymbol{\Gamma}\, \mathbf{H}_z^{(1)},$$

and we can rewrite (2.3.12) to

$$\underbrace{\begin{bmatrix} \mathbf{y}_t^{(1)} \\ \mathbf{y}_t^{(2)} \end{bmatrix} - \begin{bmatrix} \mathbf{0} \\ \boldsymbol{\Gamma} \end{bmatrix} \mathbf{y}_t^{(1)}}_{:=\tilde{\mathbf{y}}_t = \begin{bmatrix} \tilde{\mathbf{y}}_t^{(1)} \\ \tilde{\mathbf{y}}_t^{(2)} \end{bmatrix}} = \underbrace{\begin{bmatrix} \mathbf{H}_x^{(1)} \\ \mathbf{H}_x^{(2)} - \boldsymbol{\Gamma}\, \mathbf{H}_x^{(1)} \end{bmatrix}}_{:=\tilde{\mathbf{H}}_x} \mathbf{x}_t + \underbrace{\begin{bmatrix} \mathbf{H}_z^{(1)} \\ \mathbf{0} \end{bmatrix}}_{:=\tilde{\mathbf{H}}_z} \mathbf{z}_t. \tag{2.3.13}$$

It becomes obvious from (2.3.13) that $\tilde{\mathbf{y}}_t^{(2)}$, which is the lower part of the transformed observations vector $\tilde{\mathbf{y}}_t$, only depends on $\mathbf{x}_t$, which was determined in the previous period $t-1$. Hence information on $\tilde{\mathbf{y}}_t^{(2)}$, from the model's perspective, is already available in $t-1$. A possible solution to this problem might be to replace $\tilde{\mathbf{y}}_t^{(2)}$ with $\tilde{\tilde{\mathbf{y}}}_t^{(2)} := \tilde{\mathbf{y}}_{t+1}^{(2)}$. However, in summary, we can state that a singular $\mathbf{H}_z$ matrix in most cases is due to a misspecified observations vector $\mathbf{y}_t$.

Non-stationary state-space models: In cases where the initial state vector $\mathbf{w}_0$ contains non-stationary elements, there is typically no stabilizing solution to the RDE (2.2.8a), and it remains unclear if we can meet the preconditions of Assumption 2.3.1. However, this does not mean that Algorithm 3.1 is impractical for non-stationary SSMs. To see this, remember that it follows from Proposition 2.3.1 that for the SSM (2.2.2) with $n_y = n_z = \text{rk}(\mathbf{H}_z)$, there is a solution $\mathbf{C}_+ = \mathbf{0}$ satisfying Assumption 2.3.1. This can be seen as an advantage compared to the CR discussed by Herbst (2015), which strictly requires the transition matrix $\mathbf{F}$ to be stable.

2.4 Application

In this section, we illustrate the usage of the ASKF and compare it in terms of speed and performance to three competitors. As a benchmark algorithm, we use the regular KF (2.2.4), representing one of the most basic versions of the filter. The second competitor is a version of the Chandrasekhar recursion (CR) developed by Morf (1974) and Morf et al. (1974). Compared to the regular KF, this algorithm replaces the RDE (2.2.8a) or (2.2.8b), respectively, with another set of difference equations. Herbst (2015) points out that this set of „Chandrasekhar-type" difference equations requires fewer arithmetic operations than the regular KF, if the number of states n_w is large compared to the dimension n_y of the observation vector $\mathbf{y}_t$. Therefore, Herbst (2015) suggests using the CR when estimating medium to large-scale DSGE models since these models typically possess a large number of state variables and only a handful of observable variables. The implementation of the CR follows the procedure described by Herbst (2015). As the last competitor, we choose a version of the KF based on the univariate treatment of

multivariate observation vectors (UKF) by Koopman and Durbin (2000). To briefly recapitulate the basic idea of this method, suppose that H_i represents the ith row of the matrix $\mathbf{H}$ and that $y_{t,i}$, $u_{t,i}$, and h_i denote the ith element of the vectors $\mathbf{y}_t$, $\mathbf{u}_t$, and $\mathbf{h}$, respectively. Under the assumption that $\mathbf{R}$ is a diagonal matrix, with $\mathbf{R} = \text{diag}\left(R_1^2, \dots, R_{n_y}^2\right)$, Koopman and Durbin (2000) suggest replacing the multivariate measurement equation (2.2.1a) with its univariate equivalent

$$y_{t,i} = h_i + H_i \cdot \mathbf{w}_{t,i} + u_{t,i}, \qquad u_{t,i} \sim \text{N}(0, R_i^2) \qquad \forall i = 1, 2, \dots, n_y, \ \forall t = 1, 2, \dots, N, \tag{2.4.1a}$$

where $\mathbf{w}_{t,i-1} = \mathbf{w}_t$ for all $i = 1, 2, \dots, n_y$.[15] Subsequently, the corresponding version of the state equation yields

$$\mathbf{w}_{t,i} = \begin{cases} \mathbf{F} \cdot \mathbf{w}_{t-1,n_y} + \mathbf{v}_t, & i = 1, \\ \mathbf{w}_{t,i-1}, & i = 2, 3, \dots, n_y, \end{cases}, \qquad \forall t = 1, 2, \dots, N. \tag{2.4.1b}$$

Note that (2.4.1) can be interpreted as an univariate SSM with n_w states and $N \cdot n_y$ observations, whose log-likelihood function is obtainable employing the KF.[16] Durbin and Koopman (2012, Chapter 6.4.4) show that compared to the multivariate treatment, this univariate approach can significantly reduce the number of arithmetic operations. This is especially true for models where n_y is large since the UKF avoids the inversion of the $n_y \times n_y$ matrix $\mathbf{U}_t$. Instead, the UKF will compute n_y times the inverse of a scalar. For a textbook treatment of the UKF and its implementation, we refer to Durbin and Koopman (2012, Chapter 6.4)

To compare the four filters, we use two frameworks: First, we analyze the generic SSM by Chib and Ramamurthy (2010) as an example of a classic stationary SSM with measurement error. This simulation model essentially represents the SSM (2.2.1) with $n_y = 10$ observation variables and $n_w = 5$ state variables, where 60 of the parameters are estimated while treating the remaining parameters as fixed. We use the same (arbitrary) chosen set of data generating parameters as Chib and Ramamurthy (2010). While this generic SSM has no particular economic interpretation, it is an example of a SSM where the number of observable time series ($n_y = 10$) exceeds the number of unobserved states ($n_w = 5$). Therefore, we will also consider the model transformation suggested by Jungbacker and Koopman (2014), which collapses the initially 10×1 observation vector into a new 5×1 observation vector.[17]

Second, we consider the medium-scale DSGE model introduced by Smets and Wouters (2007)

[15] Note that the UKF is not restricted to cases where $\mathbf{R}$ is a diagonal matrix (see e.g., Durbin and Koopman, 2012, Chapter 6.4.3).

[16] At this point it should be mentioned that the system matrices of (2.4.1) depend on the index i. To deal with this the Kalman recursion (2.2.4) must be slightly adjusted.

[17] Briefly summarized, the idea behind this procedure is to find matrices $\mathbf{A}^* \in \mathbb{R}^{n_w \times n_w}$ and $\mathbf{A}^+ \in \mathbb{R}^{n_y - n_w \times n_w}$ to linearly transform $\mathbf{y}_t$ to

$$\begin{pmatrix} \mathbf{y}_t^* \\ \mathbf{y}_t^+ \end{pmatrix} := \begin{pmatrix} \mathbf{A}^* \\ \mathbf{A}^+ \end{pmatrix} \mathbf{y}_t,$$

such that we may write the transformed measurement equation as

$$\begin{pmatrix} \mathbf{y}_t^* \\ \mathbf{y}_t^+ \end{pmatrix} = \begin{pmatrix} \mathbf{h}^* \\ \mathbf{h}^+ \end{pmatrix} + \begin{pmatrix} \mathbf{H}^* \\ \mathbf{0} \end{pmatrix} \mathbf{w}_t + \begin{pmatrix} \mathbf{u}_t^* \\ \mathbf{u}_t^+ \end{pmatrix}, \qquad \begin{pmatrix} \mathbf{u}_t^* \\ \mathbf{u}_t^+ \end{pmatrix} \sim \text{N}\left(\begin{pmatrix} \mathbf{0} \\ \mathbf{0} \end{pmatrix}, \begin{pmatrix} \mathbf{R}_t^* & \mathbf{0} \\ \mathbf{0} & \mathbf{R}_t^+ \end{pmatrix} \right), \qquad \forall t = 1, 2, \dots, N.$$

Thus, the collapsed measurement equations yields

$$\mathbf{y}_t^* = \mathbf{h}^* + \mathbf{H}^* \ \mathbf{w}_t + \mathbf{u}_t^*, \qquad \mathbf{u}_t^* \sim \text{N}(\mathbf{0}, \mathbf{R}_t^*), \qquad \forall t = 1, 2, \dots, N.$$

The vector $\mathbf{y}_t^+ = \mathbf{h}^+ + \mathbf{u}_t^+$ with $\mathbf{u}_t^+ \sim \text{N}(\mathbf{0}, \mathbf{R}_t^+)$, however, is independent of $\mathbf{w}_t$ and $\mathbf{u}_t^*$ and can therefore be treated separately. For a textbook treatment we refer to Durbin and Koopman (2012, Chapter 6.5).

as an example for a SSM without measurement error, where we may use Proposition 2.3.1 to obtain $\mathbf{C}_+$. Since both the generic SSM by Chib and Ramamurthy (2010) as well as the model by Smets and Wouters (2007) represent stationary models, we use the unconditional initialization strategy to obtain $(\boldsymbol{\mu}_0, \mathbf{C}_0)$.

To obtain the steady-state variance matrix $\mathbf{C}_+$ in the case of the generic SSM by Chib and Ramamurthy (2010), we will use the Schur algorithm described by Bini et al. (2012, Chapter 3) to solve the DARE (2.2.9a) corresponding to RDE (2.2.8a). We use the same algorithm to solve the discrete Lyapunov equation (2.2.7b) for the unconditional variance matrix $\mathbf{C}$ of the state vector $\mathbf{w}_t$.

All computations in this section were coded in MATLAB® 2019a or FORTRAN (using the Intel® IFORT compiler) and executed on a Window 10 64-bit machine with a 3.60 GHz Intel® Core™i7-7700 CPU and 32 GB of RAM. Further, it is worth mentioning that the FORTRAN code makes extensive use of the BLAS and LAPACK routines, such as `dsymm` or `dsryk`, that come with Intel®'s Math Kernel Library to exploit the symmetric nature of variance matrices wherever possible.

To compare the different filters, we consider a Bayesian setup and use the tailored randomized block Metropolis-Hastings (TaRBMH) sampler to generate 11000 draws from the posterior distribution $f_{\boldsymbol{\theta}|\mathbf{Y}_t} \propto f_{\mathbf{Y}_t|\boldsymbol{\theta}} \times f_{\boldsymbol{\theta}}$, where we discard the first 1000 draws as burn-ins. Subsequently, we compare the speed and accuracy of each filter by recomputing each of the 10000 remaining parameter sets using the regular KF as the benchmark.

In a nutshell, we may summarize the TaRBMH sampler by Chib and Ramamurthy (2010) as follows: With each draw from the posterior distribution, we partition the parameter vector $\boldsymbol{\theta}$ into multiple blocks. Thereby, both the number of blocks and the allocation of the parameters into the blocks are random. The parameters of each block are then sequentially updated by a Metropolis-Hastings step, where we draw the proposals from a multivariate student-t density with ν degrees of freedom. To parameterize the proposal density, we follow Chib and Ramamurthy (2010) and detect the conditional posterior mode (with respect to the block-parameters) by means of simulated annealing based on a linear cooling schedule. The proposal density's mean vector and scaling matrix then reflect the conditional posterior mode and the corresponding Hessian matrix.

The tuning parameters of the TaRBMH sampler and the corresponding simulated annealing algorithm (see Table 2.2) used to specify the proposal density are identical to the setup by Chib and Ramamurthy (2010).

Table 2.2: TaRBMH and simulated annealing settings

TaRBMH			
Parameter	Description	GSSM[a]	SW07[b]
p_B	Probability for a new block	0.15	0.15
M	Number of draws	10000	10000
n_0	Number of burn-ins	1000	1000
ν	Degrees of freedom of the proposal density[a]	15	10
Simulated annealing with linear cooling schedule			
t_0	Initial temperature	5	5
a	Cooling constant	0.4	0.4
K	Number of stages in cooling schedule	8	4
b	Stage expansion factor	8	6
s	Scaling factor for new proposals	0.02	0.02

[a] GSSM: The generic SSM introduced by Chib and Ramamurthy (2010).
[b] SW07: The DSGE model introduced by Smets and Wouters (2007).

2.4.1 Generic state-space model

We may express the generic SSM by Chib and Ramamurthy (2010) in terms of the SSM (2.2.1) by defining the system matrices $\mathbf{h}$, $\mathbf{H}$, $\mathbf{F}$, $\mathbf{Q}$, and $\mathbf{R}$ as

$$\mathbf{h} = \begin{pmatrix} h_1 \\ \vdots \\ h_{10} \end{pmatrix} \in \mathbb{R}^{10\times 1}, \qquad \mathbf{H} = \begin{pmatrix} 1 & H_{2,1} & & \cdots & H_{10,1} \\ & \ddots & \ddots & & \vdots \\ & & 1 & H_{6,5} & \cdots & H_{10,5} \end{pmatrix}^T \in \mathbb{R}^{10\times 5},$$

$$\mathbf{F} = \operatorname{diag}(F_{1,1}, \ldots, F_{5,5}) \in \mathbb{R}^{5\times 5}, \qquad \mathbf{Q} = \mathbf{I} \in \mathbb{R}^{5\times 5}, \quad \mathbf{R} = \operatorname{diag}(e^{\sigma_1^2}, \ldots, e^{\sigma_{10}^2}) \in \mathbb{R}^{10\times 10}.$$

Further, the vector

$$\boldsymbol{\theta} = \begin{pmatrix} F_{1,1} & \ldots & F_{5,5} & h_1 & \ldots & h_{10} & H_{2,1} & \ldots & H_{10,5} & \sigma_1^2 & \ldots & \sigma_{10}^2 \end{pmatrix}^T$$

collects the 60 uncertain parameters of the model. To estimate the model, we follow Chib and Ramamurthy (2010) and simulate a set of 200 observations using the data generating parameters presented in Table 2.3. In choosing the prior distributions $f_{\boldsymbol{\theta}}$ of the uncertain parameters displayed in Table 2.3, we once again follow Chib and Ramamurthy (2010). We report the estimation results for each of the four filters in Table 2.4. The whole estimation procedure requires about 46 million likelihood evaluations.[18]

Table 2.5 shows the time needed by each filter to reevaluate the log-densities $f_{\mathbf{Y}_t|\boldsymbol{\theta}}$ and $f_{\boldsymbol{\theta}}$ for all 10000 draws from the posterior distribution. To get an intuition for the numerical accuracy of each filter, Table 2.5 also provides the l^2-Norm of the deviations between the log-likelihood computed with a particular filter and the log-likelihood evaluated using the regular KF.

For MATLAB® implementation of the full model, we see that, in comparison to the regular KF or the UKF, the ASKF requires less than half of the time. In FORTRAN, the ASKF reduces the computational burden, even more, requiring only about 12 percent and 33 percent of the time compared to the KF and UKF, respectively. Unsurprisingly, the slowest filter for both implementations is the CR. In line with the results of Herbst (2015), we find that the CR becomes inefficient compared to the regular KF when $n_y \geq n_w$.

The lower part of Table 2.5 displays the results obtained when using the technique described by Jungbacker and Koopman (2014) to collapse the observations vector to the dimension of the state vector. Except for the ASKF, this model transformation significantly reduces the computational burden of all filters. However, the ASKF remains the fastest filter in both the MATLAB® and the FORTRAN implementation.

Overall, the FORTRAN implementation of the generic SSM by Chib and Ramamurthy (2010) seems to be twice as fast as its MATLAB® counterpart. The numerical deviation of the filters compared to the standard KF are similar, with the CR being closest to the KF.

At this point, we have to mention that all results considered so far were under the hypothesis that the convergence process from $\mathbf{C}_0$ to $\mathbf{C}_+$ stretches over the complete observation interval ($N = 200$). However, in practice, there might be some period τ where $\mathbf{C}_\tau$ has converged sufficiently close to $\mathbf{C}_+$ so that we can switch from the filter at hand to the SKF described in (2.2.11). Thus, if the convergence process lasts only a few periods, it could be that the additional effort to solve the RDE (2.2.8a) for $\mathbf{C}_+$ outweighs the efficiency gains from the more efficient recursive part of the ASKF. To get an intuition of how many periods are necessary so that the ASKF outperforms the other filters in terms of speed, depending on the number of observations N, Figure 2.1 displays the computation time of each of the filters relative to the computation time of the KF.

[18] A large part of these likelihood evaluations stem from the repeated numerical evaluation of the conditional Hessian matrix, which is required to specify the proposal density of a random block.

As expected, Figure 2.1 shows that for a low number of observations ($N < 10$), the ASKF is outperformed by the other filters but becomes faster as N rises. For the MATLAB® implementation of the full model, the ASKF becomes the fastest option to compute the log-likelihood in cases where the convergence process takes more than 25 periods, while in FORTRAN, it takes the ASKF about 50 periods to outperform the UKF. When using the collapsed model, where the efficiency gains from the ASKF are smaller, in both MATLAB® and the FORTRAN implementation, it takes about 75 periods for the ASKF to become the fastest option.

Since, depending on the model's parameter values, the convergence speed of the matrix sequence $\{\mathbf{C}_t\}_{t=1}^{N}$ may vary, in practice, it is often impossible to determine ex-ante in which period a switch to SKF is possible. Thus, using the ASKF to evaluate the log-likelihood is probably not a bad choice, especially considering that in cases where we may switch early to the SKF, the choice of the filter might become secondary for the overall time needed to evaluate the log-likelihood.

Table 2.3: Data generating parameters and prior density – Generic state-space model

Parameter	Data generating parameters					Prior[a]				
$h_1,\dots,h_5$	0.20	1.40	1.80	0.10	0.90	0.50 (5.00)	0.50 (5.00)	0.50 (5.00)	0.50 (5.00)	0.50 (5.00)
$h_6,\dots,h_{10}$	1.00	2.00	0.10	2.20	1.50	0.50 (5.00)	0.50 (5.00)	0.50 (5.00)	0.50 (5.00)	0.50 (5.00)
$H_{2,1}$	0.50					0.00 (5.00)				
$H_{3,1},H_{3,2}$	0.60	0.00				0.00 (5.00)	0.00 (5.00)			
$H_{4,1},\dots,H_{4,3}$	0.00	0.20	−0.10			0.00 (5.00)	0.00 (5.00)	0.00 (5.00)		
$H_{5,1},\dots,H_{5,4}$	−0.20	0.00	−0.70	0.00		0.00 (5.00)	0.00 (5.00)	0.00 (5.00)	0.00 (5.00)	
$H_{6,1},\dots,H_{6,5}$	0.00	0.00	−0.40	−0.50	0.00	0.00 (5.00)	0.00 (5.00)	0.00 (5.00)	0.00 (5.00)	0.00 (5.00)
$H_{7,1},\dots,H_{7,5}$	0.30	0.20	0.00	0.00	−0.30	0.00 (5.00)	0.00 (5.00)	0.00 (5.00)	0.00 (5.00)	0.00 (5.00)
$H_{8,1},\dots,H_{8,5}$	−0.50	0.00	0.00	0.60	0.00	0.00 (5.00)	0.00 (5.00)	0.00 (5.00)	0.00 (5.00)	0.00 (5.00)
$H_{9,1},\dots,H_{9,5}$	0.00	−0.50	0.30	−0.10	0.00	0.00 (5.00)	0.00 (5.00)	0.00 (5.00)	0.00 (5.00)	0.00 (5.00)
$H_{10,1},\dots,H_{10,5}$	0.00	0.00	0.20	0.00	−0.40	0.00 (5.00)	0.00 (5.00)	0.00 (5.00)	0.00 (5.00)	0.00 (5.00)
$F_{1,1},\dots,F_{5,5}$	0.80	0.20	0.75	0.60	0.10					
$\sigma_1^2,\dots,\sigma_5^2$	log(1.00)	log(0.30)	log(1.00)	log(0.20)	log(0.60)	−1.00 (1.00)	−1.00 (1.00)	−1.00 (1.00)	−1.00 (1.00)	−1.00 (1.00)
$\sigma_6^2,\dots,\sigma_{10}^2$	log(0.50)	log(1.00)	log(1.00)	log(0.75)	log(0.60)	−1.00 (1.00)	−1.00 (1.00)	−1.00 (1.00)	−1.00 (1.00)	−1.00 (1.00)

[a] All parameters are normally distributed. The first parameter denotes the prior mean, while the second parameter (in parentheses) denotes the prior variance.

2.4.2 Smets and Wouters model

The model introduced by Smets and Wouters (2003, 2007) is at the core of most medium- to large-scale DSGE models used to analyze monetary policy. To put it in the words of Herbst and Schorfheide (2016, pp. 12): „By now, the SW model has become one of the workhorse models in the DSGE model literature and in central banks around the world."

Among other features, the model includes sticky prices and wages, investment adjustment costs, habit formation, and variable capital utilization. In what follows, we use the Smets and

Table 2.4: Estimation results – Generic state-space model

θ	Mean				5 percent quantile				95 percent quantile			
	KF	CR	UKF	ASKF	KF	CR	UKF	ASKF	KF	CR	UKF	ASKF
$F_{1,1}$	0.74	0.74	0.74	0.74	0.64	0.64	0.64	0.64	0.84	0.83	0.84	0.84
$F_{2,2}$	0.36	0.36	0.36	0.36	0.19	0.19	0.19	0.19	0.53	0.53	0.53	0.53
$F_{3,3}$	0.70	0.70	0.70	0.70	0.58	0.58	0.58	0.58	0.81	0.81	0.81	0.81
$F_{4,4}$	0.41	0.41	0.42	0.42	0.27	0.27	0.28	0.28	0.55	0.56	0.56	0.56
$F_{5,5}$	0.06	0.06	0.06	0.06	−0.15	−0.15	−0.15	−0.15	0.28	0.27	0.27	0.28
h_1	0.15	0.16	0.14	0.15	−0.40	−0.38	−0.43	−0.41	0.69	0.68	0.70	0.71
h_2	1.20	1.21	1.20	1.20	0.88	0.88	0.86	0.87	1.51	1.52	1.53	1.52
h_3	1.65	1.68	1.64	1.66	1.11	1.04	1.02	1.06	2.25	2.30	2.26	2.27
h_4	0.22	0.22	0.22	0.21	−0.06	−0.07	−0.06	−0.06	0.49	0.50	0.50	0.48
h_5	0.89	0.88	0.90	0.89	0.52	0.48	0.51	0.50	1.27	1.30	1.29	1.26
h_6	0.94	0.94	0.95	0.95	0.72	0.71	0.71	0.72	1.17	1.17	1.18	1.18
h_7	1.90	1.90	1.90	1.90	1.67	1.66	1.67	1.67	2.12	2.12	2.12	2.12
h_8	0.33	0.32	0.33	0.32	0.07	0.07	0.07	0.06	0.57	0.59	0.59	0.57
h_9	2.10	2.10	2.10	2.10	1.89	1.88	1.88	1.89	2.32	2.32	2.32	2.32
h_{10}	1.50	1.50	1.50	1.50	1.36	1.35	1.35	1.36	1.64	1.65	1.65	1.65
$H_{2,1}$	0.44	0.44	0.44	0.44	0.28	0.29	0.29	0.28	0.60	0.60	0.60	0.60
$H_{3,1}$	0.69	0.69	0.70	0.69	0.46	0.46	0.47	0.46	0.92	0.93	0.93	0.92
$H_{4,1}$	0.14	0.14	0.14	0.13	−0.02	−0.03	−0.05	−0.04	0.31	0.31	0.31	0.30
$H_{5,1}$	−0.30	−0.30	−0.31	−0.30	−0.48	−0.50	−0.50	−0.49	−0.11	−0.11	−0.12	−0.12
$H_{6,1}$	−0.08	−0.08	−0.08	−0.08	−0.22	−0.21	−0.22	−0.21	0.05	0.06	0.06	0.06
$H_{7,1}$	0.31	0.31	0.31	0.31	0.20	0.20	0.20	0.20	0.42	0.42	0.43	0.42
$H_{8,1}$	−0.27	−0.28	−0.28	−0.28	−0.42	−0.43	−0.43	−0.43	−0.13	−0.13	−0.12	−0.13
$H_{9,1}$	0.07	0.07	0.07	0.08	−0.06	−0.05	−0.05	−0.05	0.20	0.20	0.20	0.20
$H_{10,1}$	0.03	0.03	0.03	0.03	−0.06	−0.06	−0.06	−0.06	0.13	0.13	0.13	0.13
$H_{3,2}$	−0.06	−0.06	−0.06	−0.05	−0.32	−0.33	−0.33	−0.33	0.20	0.22	0.21	0.22
$H_{4,2}$	0.21	0.21	0.21	0.22	−0.00	−0.01	−0.01	0.00	0.44	0.44	0.45	0.46
$H_{5,2}$	−0.00	−0.00	−0.00	−0.01	−0.26	−0.28	−0.27	−0.28	0.25	0.26	0.26	0.26
$H_{6,2}$	0.18	0.18	0.18	0.17	0.01	0.00	−0.01	−0.00	0.36	0.35	0.36	0.35
$H_{7,2}$	0.14	0.14	0.14	0.14	−0.04	−0.04	−0.04	−0.04	0.31	0.32	0.31	0.31
$H_{8,2}$	−0.05	−0.05	−0.05	−0.05	−0.26	−0.26	−0.26	−0.25	0.16	0.15	0.16	0.16
$H_{9,2}$	−0.57	−0.57	−0.57	−0.57	−0.75	−0.75	−0.75	−0.75	−0.39	−0.39	−0.39	−0.39
$H_{10,2}$	−0.11	−0.10	−0.11	−0.10	−0.25	−0.25	−0.25	−0.25	0.03	0.04	0.04	0.04
$H_{4,3}$	−0.21	−0.20	−0.20	−0.19	−0.39	−0.39	−0.39	−0.39	−0.01	−0.01	−0.02	−0.00
$H_{5,3}$	−0.63	−0.63	−0.63	−0.63	−0.80	−0.80	−0.80	−0.81	−0.46	−0.46	−0.46	−0.46
$H_{6,3}$	−0.34	−0.34	−0.34	−0.35	−0.48	−0.47	−0.47	−0.49	−0.22	−0.21	−0.21	−0.22
$H_{7,3}$	−0.11	−0.11	−0.11	−0.11	−0.23	−0.24	−0.24	−0.23	0.01	0.01	0.01	0.01
$H_{8,3}$	−0.14	−0.14	−0.14	−0.14	−0.30	−0.30	−0.30	−0.30	0.03	0.03	0.02	0.03
$H_{9,3}$	0.28	0.28	0.28	0.28	0.17	0.17	0.17	0.17	0.39	0.39	0.39	0.39
$H_{10,3}$	0.17	0.17	0.17	0.17	0.08	0.07	0.07	0.07	0.27	0.27	0.26	0.27
$H_{5,4}$	0.09	0.08	0.09	0.09	−0.12	−0.11	−0.11	−0.11	0.28	0.28	0.28	0.29
$H_{6,4}$	−0.58	−0.58	−0.58	−0.58	−0.70	−0.70	−0.70	−0.70	−0.47	−0.46	−0.47	−0.47
$H_{7,4}$	−0.00	0.00	0.00	0.00	−0.14	−0.13	−0.14	−0.13	0.14	0.14	0.14	0.14
$H_{8,4}$	0.61	0.61	0.61	0.61	0.47	0.47	0.47	0.47	0.76	0.76	0.76	0.76
$H_{9,4}$	−0.11	−0.11	−0.11	−0.11	−0.23	−0.23	−0.23	−0.23	0.01	0.01	0.01	0.01
$H_{10,4}$	−0.01	−0.01	−0.01	−0.01	−0.13	−0.12	−0.12	−0.12	0.10	0.10	0.10	0.10
$H_{6,5}$	0.19	0.19	0.19	0.19	0.05	0.05	0.05	0.05	0.33	0.33	0.33	0.33
$H_{7,5}$	−0.41	−0.42	−0.42	−0.42	−0.61	−0.61	−0.61	−0.61	−0.23	−0.23	−0.23	−0.23
$H_{8,5}$	−0.03	−0.02	−0.03	−0.02	−0.22	−0.21	−0.22	−0.21	0.16	0.17	0.16	0.17
$H_{9,5}$	−0.18	−0.18	−0.18	−0.18	−0.34	−0.33	−0.34	−0.34	−0.02	−0.02	−0.02	−0.02
$H_{10,5}$	−0.49	−0.49	−0.49	−0.49	−0.64	−0.65	−0.65	−0.65	−0.34	−0.34	−0.34	−0.34
σ_1^2	0.08	0.09	0.09	0.08	−0.23	−0.23	−0.23	−0.24	0.39	0.40	0.40	0.38
σ_2^2	−0.69	−0.70	−0.70	−0.68	−1.31	−1.34	−1.30	−1.28	−0.21	−0.22	−0.22	−0.21
σ_3^2	−0.34	−0.35	−0.35	−0.34	−0.81	−0.83	−0.82	−0.81	0.07	0.05	0.05	0.07
σ_4^2	−1.44	−1.45	−1.43	−1.44	−2.30	−2.31	−2.24	−2.29	−0.81	−0.81	−0.80	−0.80
σ_5^2	−0.15	−0.14	−0.15	−0.15	−0.58	−0.57	−0.56	−0.56	0.20	0.21	0.21	0.21
σ_6^2	−0.97	−0.96	−0.97	−0.97	−1.29	−1.28	−1.29	−1.29	−0.68	−0.68	−0.69	−0.68
σ_7^2	−0.10	−0.10	−0.10	−0.10	−0.33	−0.34	−0.33	−0.34	0.12	0.12	0.11	0.12
σ_8^2	0.07	0.07	0.07	0.07	−0.13	−0.13	−0.13	−0.13	0.27	0.28	0.28	0.27
σ_9^2	−0.48	−0.48	−0.48	−0.49	−0.75	−0.75	−0.75	−0.76	−0.23	−0.23	−0.24	−0.24
σ_{10}^2	−0.72	−0.73	−0.72	−0.73	−1.00	−1.02	−1.01	−0.99	−0.47	−0.48	−0.48	−0.49

Wouters (2007) model, which is a slightly adjusted version of the original model described by Smets and Wouters (2003). The model consists of 62 equations in 35 endogenous variables, 20 predetermined, and 7 endogenous state variables. We give a complete description of the model's implementation in Appendix 2.E. To fit the model to the data, we follow Smets and Wouters (2007) and use quarterly time series of the log difference of real GDP, the log difference of real consumption, the log difference of real investment, and the log difference of real wages,

Table 2.5: Speed comparison – Generic state-space model

Full	MATLAB®				FORTRAN			
$n_y = 10,\ n_w = 5$	KF	CR	UKF	ASKF	KF	CR	UKF	ASKF
Elapsed time:	$43s$	$82s$	$35s$	$17s$	$17s$	$19s$	$6s$	$2s$
l^2-Norm:	-	$2.1e^{-09}$	$2.2e^{-09}$	$2.1e^{-09}$	-	$0.5e^{-10}$	$0.6e^{-09}$	$0.2e^{-09}$

Collapsed	MATLAB®				FORTRAN			
$n_y = 5,\ n_w = 5$	KF	CR	UKF	ASKF	KF	CR	UKF	ASKF
Elapsed time:	$32s$	$46s$	$22s$	$16s$	$9s$	$9s$	$4s$	$2s$
l^2-Norm:	-	$1.1e^{-09}$	$1.2e^{-09}$	$1.1e^{-09}$	-	$0.3e^{-10}$	$0.2e^{-09}$	$0.1e^{-09}$

Figure 2.1: Speed comparison – Generic state-space model

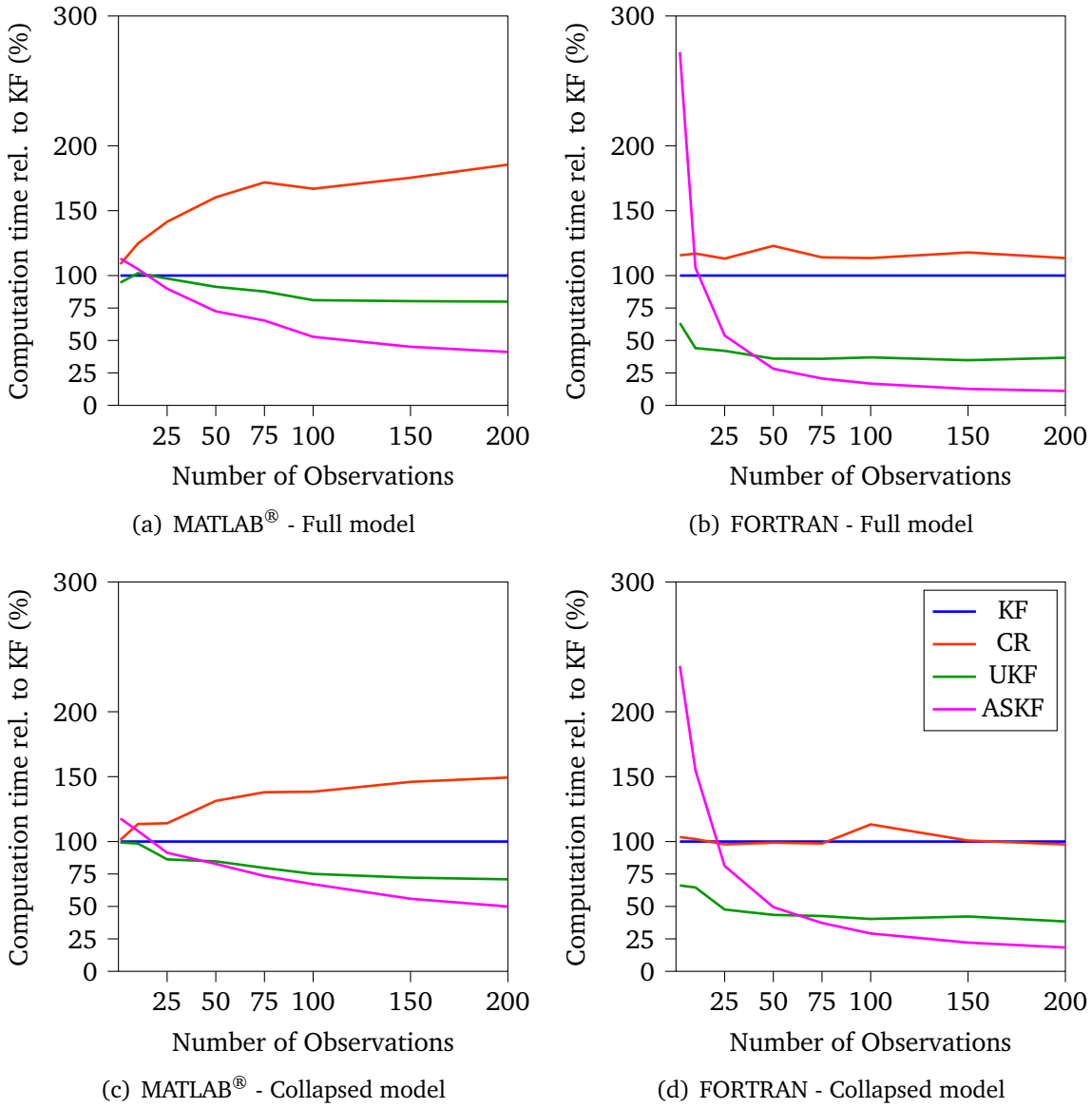

(a) MATLAB® - Full model

(b) FORTRAN - Full model

(c) MATLAB® - Collapsed model

(d) FORTRAN - Collapsed model

the log of hours worked, the log difference of GDP deflator, and the federal funds rate for the U.S. from 1966 : 1 to 2004 : 4.

To obtain the model's linear policy function, we use the general Schur decomposition in the

manner of Klein (2000). We then transform the solved model into a SSM without a measurement error. We consider two different state-space representations of the model: (i) A reduced SSM with $n_y = 7$ and $n_w = 27$, including only the predetermined and endogenous state variables in the state vector, and (ii) the full SSM with $n_y = 7$ and $n_w = 62$, treating all of the model's variables as state variables.[19] Further, as shown in Appendix 2.E, the log-linearized model satisfies the preconditions of Proposition 2.3.1, and thus we may obtain the solution of the RDE (2.2.8a) as $\mathbf{C}_+ = \mathbf{0}$.

To estimate the model, we use the same prior densities as Smets and Wouters (2007). In Table 2.6, we report these prior densities together with the estimation results of the four different filters. All results of Table 2.6 refer to the reduced SSM and were computed in MATLAB®. Again, the posterior statistics obtained by the different filters are similar. Each filter requires about 15 million likelihood evaluations to generate the 10000 draws from the posterior distribution. The filters also perform similarly in terms of the percentages of failed tries, where the particular algorithm could not evaluate the objective function.

The most significant differences between the filters occur in the total time required to estimate the model. The ASKF is about one-third faster than the standard KF and reduces the overall estimation time by more than 11 hours. Moreover, compared to the UKF, which represents the second fastest option in this setup, the ASKF is still 6 hours ahead. This is despite the fact that the evaluation of the log-likelihood now also includes the computation of the policy function so that the actual filtering process only accounts for a part of the total evaluation time. Surprisingly, the CR performs even slower than the KF, which leads to the conclusion that in the reduced version of the Smets and Wouters model, n_w is too small compared to n_y for the CR to be efficient.

Table 2.7 shows the results of the reevaluation of the 10000 draws from the posterior distribution. In addition to the time required for the actual filtering process, we also report the times required to compute the policy function, the unconditional initialization, and the prior density. Considering the reduced model, we again see that the ASKF significantly reduces the computational time required in both MATLAB® and FORTRAN. In MATLAB®, the ASKF reduces the actual filtering time compared to the KF, the CR, and the UKF by about 73, 79, and 60 percent, respectively. In FORTRAN, the computation time is reduced by 82 and 69 percent, respectively, compared to the KF and the UKF. Compared to its MATLAB® implementation, the CR performs better in FORTRAN. Nevertheless, compared to the ASKF, the computational burden is almost four times higher.

The lower part of Table 2.7 displays the results of the speed comparison in case we include all 62 variables of the Smets and Wouters model as states in the SSM. The main difference in this setup is the performance of the CR, which is now about twice as fast as the KF and UKF, respectively, in both MATLAB® and FORTRAN. The CR also gets closest to the ASKF in terms of speed, but it is still three times faster in MATLAB® and almost twice as fast in FORTRAN.

In all four implementations considered in Table 2.7, the ASKF reduces the portion of the actual filtering process on the total computing time to less than one-fifth. Furthermore, it is worth mentioning that in the case of the Smets and Wouters model, the performance of the ASKF is also less dependent on the convergence speed of the matrix sequence $\{\mathbf{C}_t\}_{t=1}^N$, since due to Proposition 2.3.1, we do not have to determine $\mathbf{C}_+$ numerically.

[19] Note that using the full SSM will result in a singular unconditional variance matrix $\mathbf{C}$ of the state vector $\mathbf{w}_t$, since in this case $\mathbf{w}_t$ contains redundant states.

Table 2.6: Prior and estimation results – Smets and Wouters model

θ	Prior			Posterior											
				Mean				5 percent quantile				95 percent quantile			
	Density[a]	Mean	Std. Dev.	KF	CR	UKF	ASKF	KF	CR	UKF	ASKF	KF	CR	UKF	ASKF
φ	Normal	4.000	1.500	5.60	5.47	5.54	5.48	3.63	3.40	3.60	3.40	8.04	7.91	7.93	7.98
σ_c	Normal	1.500	0.375	1.33	1.32	1.31	1.33	1.11	1.09	1.10	1.11	1.59	1.57	1.56	1.59
h	Beta	0.700	0.100	0.72	0.72	0.72	0.71	0.63	0.63	0.64	0.62	0.79	0.80	0.80	0.80
ξ_w	Beta	0.500	0.100	0.70	0.69	0.70	0.69	0.57	0.57	0.57	0.57	0.81	0.80	0.82	0.80
σ_l	Normal	2.000	0.750	1.83	1.84	1.85	1.79	0.82	0.79	0.84	0.77	3.13	3.15	3.08	3.05
ξ_p	Beta	0.500	0.100	0.64	0.63	0.64	0.64	0.54	0.54	0.55	0.54	0.75	0.73	0.75	0.74
ι_w	Beta	0.500	0.150	0.59	0.58	0.58	0.58	0.34	0.34	0.36	0.33	0.80	0.82	0.80	0.80
ι_p	Beta	0.500	0.150	0.24	0.25	0.24	0.25	0.10	0.11	0.10	0.11	0.41	0.44	0.42	0.42
ψ	Beta	0.500	0.150	0.56	0.57	0.56	0.56	0.34	0.35	0.36	0.35	0.77	0.77	0.75	0.76
Φ	Normal	1.250	0.125	1.60	1.60	1.60	1.60	1.46	1.46	1.46	1.46	1.75	1.74	1.74	1.75
r_π	Normal	1.500	0.250	2.03	2.05	2.03	2.06	1.71	1.75	1.72	1.73	2.39	2.38	2.37	2.40
ρ	Beta	0.750	0.100	0.80	0.80	0.80	0.80	0.75	0.75	0.75	0.75	0.84	0.84	0.84	0.85
r_y	Normal	0.125	0.050	0.08	0.08	0.08	0.09	0.05	0.05	0.05	0.05	0.13	0.13	0.13	0.13
$r_{\Delta y}$	Normal	0.125	0.050	0.22	0.22	0.22	0.22	0.17	0.17	0.17	0.17	0.27	0.27	0.27	0.27
$\bar{\pi}$	Gamma	0.625	0.100	0.71	0.70	0.71	0.71	0.51	0.52	0.52	0.52	0.91	0.91	0.91	0.91
$\bar{\beta}$	Gamma	0.250	0.100	0.16	0.16	0.17	0.16	0.07	0.07	0.08	0.07	0.28	0.27	0.27	0.27
$\bar{l}$	Normal	0.000	2.000	0.73	0.84	0.84	0.74	−1.87	−1.60	−1.71	−1.77	3.30	3.29	3.22	3.31
$\bar{\gamma}$	Normal	0.400	0.100	0.42	0.42	0.42	0.42	0.39	0.38	0.39	0.39	0.45	0.45	0.45	0.45
α	Normal	0.300	0.050	0.19	0.19	0.19	0.19	0.16	0.16	0.16	0.16	0.22	0.22	0.22	0.22
ρ_a	Beta	0.500	0.200	0.96	0.96	0.96	0.96	0.93	0.94	0.93	0.94	0.98	0.98	0.98	0.98
ρ_b	Beta	0.500	0.200	0.24	0.25	0.24	0.26	0.08	0.09	0.08	0.08	0.48	0.45	0.46	0.51
ρ_g	Beta	0.500	0.200	0.98	0.98	0.98	0.98	0.96	0.96	0.96	0.96	0.99	0.99	0.99	0.99
ρ_i	Beta	0.500	0.200	0.71	0.72	0.72	0.71	0.60	0.60	0.61	0.60	0.82	0.83	0.83	0.82
ρ_r	Beta	0.500	0.200	0.16	0.16	0.16	0.16	0.06	0.06	0.06	0.05	0.29	0.29	0.28	0.28
ρ_p	Beta	0.500	0.200	0.90	0.90	0.89	0.90	0.79	0.80	0.78	0.79	0.97	0.97	0.97	0.98
ρ_w	Beta	0.500	0.200	0.97	0.97	0.97	0.97	0.94	0.95	0.94	0.94	0.99	0.99	0.99	0.99
μ_p	Beta	0.500	0.200	0.69	0.70	0.68	0.70	0.45	0.46	0.45	0.49	0.84	0.87	0.85	0.86
μ_w	Beta	0.500	0.200	0.85	0.85	0.84	0.84	0.72	0.71	0.70	0.70	0.94	0.94	0.93	0.94
ρ_{ga}	Beta	0.500	0.250	0.52	0.52	0.51	0.52	0.34	0.35	0.34	0.34	0.69	0.69	0.69	0.69
σ_a	Inv. Gamma	0.100	2.000	0.46	0.46	0.46	0.46	0.41	0.41	0.41	0.41	0.51	0.51	0.51	0.51
σ_b	Inv. Gamma	0.100	2.000	0.24	0.24	0.24	0.23	0.18	0.19	0.19	0.18	0.28	0.28	0.29	0.28
σ_g	Inv. Gamma	0.100	2.000	0.53	0.53	0.53	0.53	0.48	0.48	0.48	0.48	0.58	0.59	0.59	0.59
σ_i	Inv. Gamma	0.100	2.000	0.45	0.45	0.45	0.45	0.37	0.37	0.36	0.37	0.54	0.55	0.54	0.56
σ_r	Inv. Gamma	0.100	2.000	0.25	0.25	0.25	0.25	0.22	0.22	0.22	0.22	0.28	0.28	0.28	0.28
σ_p	Inv. Gamma	0.100	2.000	0.14	0.14	0.14	0.14	0.11	0.11	0.11	0.11	0.17	0.17	0.17	0.17
σ_w	Inv. Gamma	0.100	2.000	0.25	0.25	0.25	0.25	0.21	0.21	0.21	0.21	0.29	0.29	0.29	0.29

	KF	CR	UKF	ASKF
Overall - Estimation time:	35h 05m 23s	38h 43m 02s	30h 11m 23s	23h 46m 24s
Value of Ojc.Fct at Posterior Mode:[b]	−858.14	−858.26	−857.97	−856.63
Number of likelihood evaluations:	15174679	15173491	15193695	15190701
Percentage of failed evaluations:	0.49	0.50	0.47	0.49
Acceptance rate (in %):	49.86	50.12	49.77	49.85

[a] Inv. Gamma denotes the Inverse Gamma type-1 distribution.
[b] Refers to the highest value of the object function for all 10000 draws.

Table 2.7: Speed comparison – Smets and Wouters model

Reduced	MATLAB®				FORTRAN			
$n_y = 7,\ n_w = 27$	KF	CR	UKF	ASKF	KF	CR	UKF	ASKF
Filtering time:	37s	47s	25s	10s	22s	15s	13s	4s
l^2-Norm:	-	$3.0e^{-08}$	$3.0e^{-09}$	$1.2e^{-10}$	-	$0.8e^{-07}$	$0.1e^{-08}$	$0.2e^{-09}$
Policy function			17s				33s	
Initialization			18s				18s	
Prior density			13s				0s	

Full	MATLAB®				FORTRAN			
$n_y = 7,\ n_w = 62$	KF	CR	UKF	ASKF	KF	CR	UKF	ASKF
Filtering time:	101s	57s	92s	18s	79s	28s	65s	15s
l^2-Norm:	-	$1.8e^{-08}$	$2.1e^{-09}$	$2.2e^{-09}$	-	$0.9e^{-08}$	$0.9e^{-09}$	$0.4e^{-09}$
Policy function			18s				33s	
Initialization			74s				71s	
Prior density			13s				0s	

2.5 Conclusion

The objective of this paper was to propose the ASKF as an efficient algorithm to evaluate the likelihood of linear and time-invariant SSMs. The results concerning the performance of the ASKF are promising. It performs well regardless of whether the number of observable time series n_y outweighs the number of states n_z or vice versa. The basis for its efficiency is the – compared to the regular KF – faster recursive part of the ASKF, reducing the cost per additional observation. The ultimate performance of the ASKF is mainly determined by two factors: The length of the filtering period and the time needed to determine the equilibrium variance matrix of the model's states, where the former is determined by the number of observations N of the available data set and the required periods τ until it might be possible to switch to the SKF. The larger the filtering period, the less the additional computational effort to solve RDE (2.2.8a) for $\mathbf{C}_+$ will weigh compared to the total filtering time. Furthermore, as we show in Proposition 2.3.1, for many DSGE models, such as the model introduced by Smets and Wouters (2007), it is not even necessary to solve RDE (2.2.8a) numerically, since for SSMs of the form (2.2.2) with $n_y = n_z = \text{rk}(\mathbf{H}_z)$ an analytic solution for $\mathbf{C}_+$ is available. This feature makes the ASKF for these kinds of model even more attractive.

Acknowledgment

I am grateful to my Ph.D. advisor Prof. Alfred Maußner for initial ideas and ensuing discussions. I also thank Prof. Burkhard Heer, Dr. Daniel Fehrle, Dr. Christopher Heiberger and Vasilij Konysev for valuable comments.

Bibliography

AN, S. AND F. SCHORFHEIDE (2007): "Bayesian Analysis of DSGE Models," *Econometric Reviews*, 26, 113–172.

ANDERSON, B. AND J. MOORE (1979): *Optimal Filtering*, Information and System Sciences Series, Englewood Cliffs, NJ: Prentice-Hall.

ANDREASEN, M. M. (2010): "How to Maximize the Likelihood Function for a DSGE Model," *Comput. Econ.*, 35, 127–154.

BINI, D. A., B. IANNAZZO, AND B. MEINI (2012): *Numerical Solution of Algebraic Riccati Equations*, Philadelphia, PA: Society for Industrial and Applied Mathematics.

CAINES, P. E. AND D. Q. MAYNE (1970): "On the Discrete Time Matrix Riccati Equation of Optimal Control," *International Journal of Control*, 12, 785–794.

CHAN, S., G. GOODWIN, AND K. SIN (1984): "Convergence Properties of the Riccati Difference Equation in Optimal Filtering of Nonstabilizable Systems," *IEEE Transactions on Automatic Control*, 29, 110–118.

CHARI, V. V., P. J. KEHOE, AND E. R. MCGRATTAN (2007): "Business Cycle Accounting," *Econometrica*, 75, 781–836.

CHIANG, C.-Y., H.-Y. FAN, AND W.-W. LIN (2010): "A Structured Doubling Algorithm for Discrete-Time Algebraic Riccati Equations with Singular Control Weighting Matrices," *Taiwanese Journal of Mathematics*, 14, 933–954.

CHIB, S. AND S. RAMAMURTHY (2010): "Tailored Randomized Block MCMC Methods with Application to DSGE Models," *Journal of Econometrics*, 155, 19–38.

CHRISTIANO, L., M. EICHENBAUM, AND C. EVANS (2005): "Nominal Rigidities and the Dynamic Effects of a Shock to Monetary Policy," *Journal of Political Economy*, 113, 1–45.

DE JONG, P. (1988): "The Likelihood for a State Space Model," *Biometrika*, 75, 165–169.

——— (1991): "The Diffuse Kalman Filter," *The Annals of Statistics*, 19, 1073–1083.

DE NICOLAO, G. AND M. GEVERS (1992): "Difference and Differential Riccati Equations: A Note on the Convergence to the Strong Solution," *IEEE Transactions on Automatic Control*, 37, 1055–1057.

DE SOUZA, C., M. GEVERS, AND G. GOODWIN (1986): "Riccati Equations in Optimal Filtering of Nonstabilizable Systems Having Singular State Transition Matrices," *IEEE Transactions on Automatic Control*, 31, 831–838.

DEJONG, D. N. AND C. DAVE (2011): *Structural Macroeconometrics: Second Edition*, Princeton, NJ: Princeton University Press.

DRYGALLA, A., O. HOLTEMÖLLER, AND K. KIESEL (2020): "The Effects of Fiscal Policy in an Estimated DSGE Model – The Case of the German Stimulus Packages during the Great Recession," *Macroeconomic Dynamics*, 24, 1315–1345.

DURBIN, J. AND S. J. KOOPMAN (2012): *Time Series Analysis by State Space Methods: Second Edition*, Oxford Statistical Science Series, Oxford, UK: Oxford University Press.

GADATSCH, N., K. HAUZENBERGER, AND N. STÄHLER (2016): "Fiscal Policy during the Crisis: A Look on Germany and the Euro Area with GEAR," *Economic Modelling*, 52, 997–1016.

GU, G. (2012): *Discrete-Time Linear Systems: Theory and Design with Applications*, New York, NY: Springer.

HAMILTON, J. D. (1994): *Time Series Analysis*, Princeton, NJ: Princeton University Press.

HANSEN, G. D. (1985): "Indivisible Labor and the Business Cycle," *Journal of Monetary Economics*, 16, 309–327.

HANSEN, L. P. AND T. J. SARGENT (2013): *Recursive Models of Dynamic Linear Economies*, Princeton, NJ: Princeton University Press.

HARVEY, A. C. (1990a): *The Econometric Analysis of Time Series, 2nd Edition*, MIT Press Books, Cambridge, MA: The MIT Press.

——— (1990b): *Forecasting, Structural Time Series Models and the Kalman Filter*, Cambridge, UK: Cambridge University Press.

HERBST, E. (2015): "Using the "Chandrasekhar Recursions" for Likelihood Evaluation of DSGE Models," *Comput. Econ.*, 45, 693–705.

HERBST, E. AND F. SCHORFHEIDE (2014): "Sequential Monte Carlo Sampling for DSGE Models," *Journal of Applied Econometrics*, 29, 1073–1098.

HERBST, E. P. AND F. SCHORFHEIDE (2016): *Bayesian Estimation of DSGE Models*, Princeton, NJ: Princeton University Press.

IRELAND, P. N. (2004): "A Method for Taking Models to the Data," *Journal of Economic Dynamics and Control*, 28, 1205–1226.

JUNGBACKER, B. AND S. J. KOOPMAN (2014): "Likelihood-Based Dynamic Factor Analysis for Measurement and Forecasting," *The Econometrics Journal*, 18, C1–C21.

KING, R. G., C. I. PLOSSER, AND S. T. REBELO (1988): "Production, Growth and Business Cycles: I. The Basic Neoclassical Model," *Journal of Monetary Economics*, 21, 195–232.

KLEIN, P. (2000): "Using the Generalized Schur Form to Solve a Multivariate Linear Rational Expectations Model," *Journal of Economic Dynamics and Control*, 24, 1405–1423.

KOOPMAN, S. J. AND J. DURBIN (2000): "Fast Filtering and Smoothing for Multivariate State Space Models," *Journal of Time Series Analysis*, 21, 281–296.

LEEPER, E. M., M. PLANTE, AND N. TRAUM (2010): "Dynamics of Fiscal Financing in the United States," *Journal of Econometrics*, 156, 304–321.

LÜTKEPOHL, H. (2007): *New Introduction to Multiple Time Series Analysis*, Berlin / Heidelberg, Germany: Springer.

MORF, M. (1974): "Fast Algorithms for Multivariable Systems." Ph.D. thesis, Stanford University, Stanford, CA.

MORF, M., G. SIDHU, AND T. KAILATH (1974): "Some New Algorithms for Recursive Estimation in Constant, Linear, Discrete-Time Systems," *IEEE Transactions on Automatic Control*, 19, 315–323.

ROSENBERG, B. (1973): "Random Coefficients Models: The Analysis of a Cross Section of Time Series by Stochastically Convergent Parameter Regression," in *Annals of Economic and Social Measurement, Volume 2, number 4*, ed. by S. V. Berg, NBER, 399–428.

SEARLE, S. R. AND A. I. KHURI (2017): *Matrix Algebra Useful for Statistics*, Wiley Series in Probability and Statistics, Hoboken, NJ: Wiley.

SMETS, F. AND R. WOUTERS (2003): "An Estimated Dynamic Stochastic General Equilibrium Model of the Euro Area," *Journal of the European Economic Association*, 1, 1123–1175.

——— (2007): "Shocks and Frictions in US Business Cycles: A Bayesian DSGE Approach," *American Economic Review*, 97, 586–606.

STOCK, J. AND M. WATSON (2016): "Chapter 8 - Dynamic Factor Models, Factor-Augmented Vector Autoregressions, and Structural Vector Autoregressions in Macroeconomics," in *Handbook of Macroeconomics*, ed. by J. B. Taylor and H. Uhlig, Elsevier, vol. 2, 415–525.

ŠUSTEK, R. (2011): "Monetary Business Cycle Accounting," *Review of Economic Dynamics*, 14, 592–612.

Appendix

The Appendix of this paper is structured as follows: The first section contains the formal derivation of the standard Kalman filter (KF) and, in particular, of the difference equations that determine the sequence $\{\mathbf{C}_t\}_{t=1}^N$ of the states' conditional variance matrix. In Section 2.B, we establish the formal foundation to address the question under which conditions the sequence $\{\mathbf{C}_t\}_{t=1}^N$ converges to a long-run equilibrium. Given this long-term equilibrium, we derive the set of equations determining the steady-state Kalman filter (SKF) in Section 2.C. In Section 2.D, we provide the formal derivation of the augmented Kalman filter (AKF), which, together with the SKF, builds the basis of the augmented steady-state Kalman filter (ASKF) proposed in this paper. The last section of the Appendix outlines the implementation of the dynamic stochastic general equilibrium (DSGE) model by Smets and Wouters (2007) that we employ as an application in this paper.

2.A Derivation of the Kalman filter

This appendix contains the formal derivation of the Kalman recursion (2.2.4) with respect to the state-space model (SSM) (2.2.1), where for the most part, we will follow the textbook treatments by Durbin and Koopman (2012, Chapter 4) and Harvey (1990b, Chapter 3). For convenience, let us restate the linear, time-invariant, and Gaussian SSM (2.2.1) introduced in Section 2.2:

$$\begin{aligned}
&\mathbf{y}_t = \mathbf{h} + \mathbf{H}\cdot\mathbf{w}_t + \mathbf{u}_t, && \mathbf{u}_t \sim \mathrm{N}(\mathbf{0},\mathbf{R}), && && \forall t = 1,2,\ldots,N\\
&\mathbf{w}_t = \mathbf{F}\cdot\mathbf{w}_{t-1} + \mathbf{v}_t, && \mathbf{v}_t \sim \mathrm{N}(\mathbf{0},\mathbf{Q}), && \mathbf{w}_0 \sim \mathrm{N}(\boldsymbol{\mu}_\mathbf{0},\mathbf{C}_0), && \forall t = 1,2,\ldots,N
\end{aligned}$$

with

$$\mathrm{E}[\mathbf{u}_i\mathbf{u}_j^T] = \begin{cases}\mathbf{R}, & i=j,\\ \mathbf{0}, & i\neq j.\end{cases}, \quad \mathrm{E}[\mathbf{v}_i\mathbf{v}_j^T] = \begin{cases}\mathbf{Q}, & i=j,\\ \mathbf{0}, & i\neq j.\end{cases}, \quad \mathrm{E}[\mathbf{u}_i\mathbf{v}_j^T] = \mathbf{0}, \quad \forall\ i,\ j = 1,2,\ldots,N,$$

and

$$\mathrm{E}[\mathbf{u}_t(\mathbf{w}_0-\boldsymbol{\mu}_\mathbf{0})^T] = \mathbf{0}, \qquad \mathrm{E}[\mathbf{v}_t(\mathbf{w}_0-\boldsymbol{\mu}_\mathbf{0})^T] = \mathbf{0}, \qquad \forall t = 1,2,\ldots,N.$$

Before turning to the derivation of recursion (2.2.4), it is appropriate to discuss some implications arising from the assumptions made regarding the SSM (2.2.1), which are essential for the subsequent derivation of the Kalman recursion. First, since $\mathbf{y}_{t-1}$ is a linear combination of $\mathbf{u}_1,\ldots,\mathbf{u}_{t-1}$, $\mathbf{v}_1,\ldots,\mathbf{v}_{t-1}$, and $\mathbf{w}_0$, and since $\mathbf{v}_t$ is independent of $\mathbf{u}_1,\ldots,\mathbf{u}_{t-1}$, $\mathbf{v}_1,\ldots,\mathbf{v}_{t-1}$ and $\mathbf{w}_0$, it is straightforward that $\mathbf{v}_t$ is independent of $\mathbf{Y}_{t-1} = \{\mathbf{y}_1,\mathbf{y}_2,\ldots,\mathbf{y}_N\}$, i.e., $\mathbf{v}_t$ given $\mathbf{Y}_{t-1}$ equals $\mathbf{v}_t$. Second, since the initial state vector $\mathbf{w}_0$ and the disturbances $\mathbf{u}_1,\ldots,\mathbf{u}_N$, $\mathbf{v}_1,\ldots,\mathbf{v}_N$ are normally distributed, it follows from the linearity of equations (2.2.1a) and (2.2.1b) that $\mathbf{w}_1,\ldots,\mathbf{w}_N$ and $\mathbf{y}_1,\ldots,\mathbf{y}_N$ are normally distributed as well. Consequently, $\mathbf{w}_t$ and $\mathbf{y}_t$ given $\mathbf{Y}_{t-1}$

as well as $\mathbf{w}_t$ given $\mathbf{Y}_t$ are also normally distributed for $t = 1, 2, \ldots, N$. This directly follows from a well-known Lemma about the conditional distribution of jointly normally distributed random vectors.

Lemma 2.A.1. Suppose the random vectors $\mathbf{x} \in \mathbb{R}^n$ and $\mathbf{y} \in \mathbb{R}^m$ are jointly normally distributed with mean vector and variance matrix:

$$\mathrm{E}\begin{pmatrix} \mathbf{x} \\ \mathbf{y} \end{pmatrix} = \begin{pmatrix} \boldsymbol{\mu}_\mathbf{x} \\ \boldsymbol{\mu}_\mathbf{y} \end{pmatrix} \quad \text{and} \quad \mathrm{Var}\begin{pmatrix} \mathbf{x} \\ \mathbf{y} \end{pmatrix} = \begin{pmatrix} \boldsymbol{\Sigma}_{\mathbf{xx}} & \boldsymbol{\Sigma}_{\mathbf{xy}} \\ \boldsymbol{\Sigma}_{\mathbf{yx}} & \boldsymbol{\Sigma}_{\mathbf{yy}} \end{pmatrix},$$

where $\boldsymbol{\Sigma}_{\mathbf{yy}}$ has rank m. Then the conditional distribution of $\mathbf{x}$ given $\mathbf{y}$ is normal with mean vector and variance matrix:

$$\mathrm{E}[\mathbf{x}|\mathbf{y}] = \boldsymbol{\mu}_\mathbf{x} + \boldsymbol{\Sigma}_{\mathbf{xy}}\boldsymbol{\Sigma}_{\mathbf{yy}}^{-1}(\mathbf{y} - \boldsymbol{\mu}_\mathbf{y}) \quad \text{and} \quad \mathrm{Var}[\mathbf{x}|\mathbf{y}] = \boldsymbol{\Sigma}_{\mathbf{xx}} - \boldsymbol{\Sigma}_{\mathbf{xy}}\boldsymbol{\Sigma}_{\mathbf{yy}}^{-1}\boldsymbol{\Sigma}_{\mathbf{xy}}{}^T.$$

Proof:
See Durbin and Koopman (2012, pp. 77-78).

□

Lemma 2.A.1 is also a fundamental element of the Kalman filter (KF) in the context of a linear SSM with normally distributed disturbances. Starting in $t = 1$, for each period $t = 1, 2, \ldots, N$ the KF performs two steps:

Prediction step: First we use equation (2.2.1b) to obtain the mean vector

$$\begin{aligned} \mathbf{w}_{t|t-1} &= \mathrm{E}[\mathbf{w}_t|\mathbf{Y}_{t-1}] \\ &= \mathrm{E}[\mathbf{F}\,\mathbf{w}_{t-1} + \mathbf{v}_t|\mathbf{Y}_{t-1}] \\ &= \mathbf{F}\;\mathrm{E}[\mathbf{w}_{t-1}|\mathbf{Y}_{t-1}] + \mathrm{E}[\mathbf{v}_t|\mathbf{Y}_{t-1}] \\ &= \mathbf{F}\,\boldsymbol{\mu}_{t-1}, \end{aligned} \tag{2.A.1}$$

and variance matrix

$$\begin{aligned} \mathbf{P}_{t|t-1} &= \mathrm{Var}[\mathbf{w}_t|\mathbf{Y}_{t-1}] \\ &= \mathrm{Var}[\mathbf{F}\,\mathbf{w}_{t-1} + \mathbf{v}_t|\mathbf{Y}_{t-1}] \\ &= \mathbf{F}\;\mathrm{Var}[\mathbf{w}_{t-1}|\mathbf{Y}_{t-1}]\;\mathbf{F}^T + \mathrm{Var}[\mathbf{v}_t|\mathbf{Y}_{t-1}] \\ &= \mathbf{F}\,\mathbf{C}_{t-1}\,\mathbf{F}^T + \mathbf{Q}, \end{aligned} \tag{2.A.2}$$

of $\mathbf{w}_t$ given $\mathbf{Y}_{t-1}$, where $\boldsymbol{\mu}_{t-1}$ and $\mathbf{C}_{t-1}$ are known from a previous iteration or in case of $t = 1$ directly through the initialization $(\boldsymbol{\mu}_0, \mathbf{C}_0)$.

Updating step: In this second step, we use Lemma 2.A.1 and the new information derived from $\mathbf{y}_t$ to compute $\boldsymbol{\mu}_t = \mathrm{E}[\mathbf{w}_t|\mathbf{Y}_t]$ and $\mathbf{C}_t = \mathrm{Var}[\mathbf{w}_t|\mathbf{Y}_t]$. Note that given $\mathbf{Y}_{t-1}$, the random vector

$$\begin{pmatrix} \mathbf{w}_t \\ \mathbf{y}_t \end{pmatrix} = \begin{pmatrix} \mathbf{w}_t \\ \mathbf{h} + \mathbf{H}\mathbf{w}_t + \mathbf{u}_t \end{pmatrix} = \begin{pmatrix} \mathbf{0} \\ \mathbf{h} \end{pmatrix} + \begin{pmatrix} \mathbf{I} & \mathbf{0} \\ \mathbf{H} & \mathbf{I} \end{pmatrix} \begin{pmatrix} \mathbf{w}_t \\ \mathbf{u}_t \end{pmatrix}$$

is jointly normally distributed since it is linear in $\mathbf{w}_t$ given $\mathbf{Y}_{t-1}$ and $\mathbf{u}_t$. Thus $\mathbf{w}_t$ given $\mathbf{Y}_{t-1}$ and $\mathbf{y}_t$ given $\mathbf{Y}_{t-1}$ are jointly normally distributed with mean vector and variance matrix:

$$\mathrm{E}\left(\begin{pmatrix} \mathbf{w}_t \\ \mathbf{y}_t \end{pmatrix} \middle| \mathbf{Y}_{t-1}\right) = \begin{pmatrix} \mathbf{w}_{t|t-1} \\ \mathbf{h} + \mathbf{H}\mathbf{w}_{t|t-1} \end{pmatrix} \quad \text{and} \quad \mathrm{Var}\left(\begin{pmatrix} \mathbf{w}_t \\ \mathbf{y}_t \end{pmatrix} \middle| \mathbf{Y}_{t-1}\right) = \begin{pmatrix} \mathbf{P}_{t|t-1} & \mathbf{X}_t \\ \mathbf{X}_t^T & \mathbf{U}_t \end{pmatrix}.$$

with

$$\begin{aligned}
\mathbf{U}_t := \mathrm{Var}[\mathbf{y}_t|\mathbf{Y}_{t-1}] &= \mathrm{Var}[\mathbf{h}+\mathbf{H}\,\mathbf{w}_t+\mathbf{u}_t|\mathbf{Y}_{t-1}] \\
&= \mathbf{H}\ \mathrm{Var}[\mathbf{w}_t|\mathbf{Y}_{t-1}]\ \mathbf{H}^T+\mathrm{Var}[\mathbf{u}_t|\mathbf{Y}_{t-1}] \\
&= \mathbf{H}\,\mathbf{P}_{t|t-1}\,\mathbf{H}^T+\mathbf{R}, \\
\mathbf{X}_t := \mathrm{Cov}[\mathbf{w}_t,\mathbf{y}_t|\mathbf{Y}_{t-1}] &= \mathrm{E}\Big[(\mathbf{w}_t-\mathrm{E}[\mathbf{w}_t|\mathbf{Y}_{t-1}])\,(\mathbf{y}_t-\mathrm{E}[\mathbf{y}_t|\mathbf{Y}_{t-1}])^T\,\Big|\mathbf{Y}_{t-1}\Big] \\
&= \mathrm{E}\Big[\big(\mathbf{w}_t-\mathbf{w}_{t|t-1}\big)\,(\mathbf{h}+\mathbf{H}\mathbf{w}_t+\mathbf{u}_t-\mathrm{E}[\mathbf{h}+\mathbf{H}\mathbf{w}_t+\mathbf{u}_t|\mathbf{Y}_{t-1}])^T\,\Big|\mathbf{Y}_{t-1}\Big] \\
&= \mathrm{E}\Big[\big(\mathbf{w}_t-\mathbf{w}_{t|t-1}\big)\big(\mathbf{w}_t-\mathbf{w}_{t|t-1}\big)^T\,\Big|\mathbf{Y}_{t-1}\Big]\mathbf{H}^T+\mathrm{E}\Big[\big(\mathbf{w}_t-\mathbf{w}_{t|t-1}\big)\,\mathbf{u}_t^T\Big|\mathbf{Y}_{t-1}\Big] \\
&= \mathrm{Var}[\mathbf{w}_t|\mathbf{Y}_{t-1}]\mathbf{H}^T+\mathrm{Cov}[\mathbf{w}_t,\mathbf{u}_t|\mathbf{Y}_{t-1}] \\
&= \mathbf{P}_{t|t-1}\,\mathbf{H}^T.
\end{aligned}$$

Hence, the mean vector $\boldsymbol{\mu}_t$ and the variance matrix $\mathbf{C}_t$ of $\mathbf{w}_t$ given $\mathbf{Y}_t$ follow directly from Lemma 2.A.1 as

$$\begin{aligned}
\boldsymbol{\mu}_t &= \mathrm{E}[\mathbf{w}_t|\mathbf{Y}_t] = \mathrm{E}[\mathbf{w}_t|\mathbf{y}_t,\mathbf{Y}_{t-1}] \\
&= \mathbf{w}_{t|t-1}+\mathbf{X}_t\ \mathbf{U}_t^{-1}\,(\mathbf{y}_t-\mathrm{E}[\mathbf{y}_t|\mathbf{Y}_{t-1}]) \\
&= \mathbf{w}_{t|t-1}+\mathbf{P}_{t|t-1}\mathbf{H}^T\ \Big[\mathbf{H}\mathbf{P}_{t|t-1}\mathbf{H}^T+\mathbf{R}\Big]^{-1}\big(\mathbf{y}_t-\mathbf{h}-\mathbf{H}\mathbf{w}_{t|t-1}\big) \qquad \text{(2.A.3)} \\
\mathbf{C}_t &= \mathrm{Var}[\mathbf{w}_t|\mathbf{Y}_t] = \mathrm{Var}[\mathbf{w}_t|\mathbf{y}_t,\mathbf{Y}_{t-1}] \\
&= \mathbf{P}_{t|t-1}-\mathbf{X}_t\ \mathbf{U}_t^{-1}\ \mathbf{X}_t^T \\
&= \mathbf{P}_{t|t-1}-\mathbf{P}_{t|t-1}\mathbf{H}^T\ \Big[\mathbf{H}\mathbf{P}_{t|t-1}\mathbf{H}^T+\mathbf{R}\Big]^{-1}\ \mathbf{H}\mathbf{P}_{t|t-1}. \qquad \text{(2.A.4)}
\end{aligned}$$

If we define $\mathbf{K}_t$ for all $t=1,2,\ldots,N$ as in (2.2.3) and replace $\mathbf{y}_t-\mathbf{h}$ with $\mathbf{y}_t^{(\mathbf{h})}$, the Kalman recursion (2.2.4) follows directly from (2.A.1) – (2.A.4).

2.B Convergence properties of the Riccati difference equation

The purpose of this appendix is to give the reader a general idea under which conditions the Riccati difference equations (RDEs)

$$\begin{aligned}
\mathbf{C}_t &= \mathbf{F}\mathbf{C}_{t-1}\mathbf{F}^T+\mathbf{Q}-\big(\mathbf{F}\mathbf{C}_{t-1}\bar{\mathbf{H}}^T+\bar{\mathbf{G}}\big)\big[\bar{\mathbf{H}}\mathbf{C}_{t-1}\bar{\mathbf{H}}^T+\bar{\mathbf{R}}\big]^{-1}\big(\bar{\mathbf{H}}\mathbf{C}_{t-1}\mathbf{F}^T+\bar{\mathbf{G}}^T\big), \\
\mathbf{P}_{t+1|t} &= \mathbf{F}\mathbf{P}_{t|t-1}\mathbf{F}^T-\mathbf{F}\mathbf{P}_{t|t-1}\mathbf{H}^T\ \big[\mathbf{H}\mathbf{P}_{t|t-1}\mathbf{H}^T+\mathbf{R}\big]^{-1}\mathbf{H}\mathbf{P}_{t|t-1}\mathbf{F}^T+\mathbf{Q},
\end{aligned}$$

with $\bar{\mathbf{H}} := \mathbf{H}\mathbf{F}$, $\bar{\mathbf{G}} := \mathbf{Q}\mathbf{H}^T$, and $\bar{\mathbf{R}} := \mathbf{H}\mathbf{Q}\mathbf{H}^T+\mathbf{R}$, described by equations (2.2.8a) and (2.2.8b), have a fixed-point and for which initialization they converge to this fixed-point. To this end, the first part of this appendix deals with cases where either the matrix $\mathbf{R}$ or at least the matrix $\bar{\mathbf{R}}$ is non-singular, drawing from the convergence results provided by de Souza et al. (1986).[20] Since the results of de Souza et al. (1986) are fairly general, we shall also discuss some more frequently consulted conditions — namely *stability*, *observability* and *reachability*, *detectability* and *stabilizability* — sufficient for convergence of RDEs, such as (2.2.8a) or (2.2.8b). The second part of this appendix contains the formal proof of Proposition 2.2.1.

[20] Note that the non-singularity of $\mathbf{R}$ implies that $\bar{\mathbf{R}}$ must be also non-singular.

2.B.1 Results by de Souza et al. (1986)

De Souza et al. (1986) provide some general convergence results related to (ordinary) RDEs of the form

$$\boldsymbol{\Sigma}_t = \mathbf{F}\boldsymbol{\Sigma}_{t-1}\mathbf{F}^T - \mathbf{F}\boldsymbol{\Sigma}_{t-1}\mathbf{H}^T \left[\mathbf{H}\boldsymbol{\Sigma}_{t-1}\mathbf{H}^T + \mathbf{R}\right]^{-1} \mathbf{H}\boldsymbol{\Sigma}_{t-1}\mathbf{F}^T + \mathbf{Q}, \quad \forall t = 1,2,\dots,N, \tag{2.B.1}$$

with $\mathbf{F} \in \mathbb{R}^{n\times n}$, $\mathbf{H} \in \mathbb{R}^{m\times n}$, $\mathbf{Q} \in \mathbb{R}^{n\times n}$, and $\mathbf{R} \in \mathbb{R}^{m\times m}$. Further, they assume that $\mathbf{Q}$ and $\mathbf{R}$ are symmetric matrices with $\mathbf{Q} = \mathbf{D}\mathbf{D}^T \geq \mathbf{0}$, $\mathbf{D} \in \mathbb{R}^{n\times n}$ and $\mathbf{R} > \mathbf{0}$.[21] Thus, their results are directly transferable to RDE (2.2.8b) if the variance matrix $\mathbf{R}$ of the measurement error $\mathbf{u}_t$ is non-singular. On the other hand, if $\mathbf{R}$ is singular, we can use their results to study the convergence properties of RDE (2.2.8a), which is sometimes called a generalized RDE, provided at least $\bar{\mathbf{R}}$ is non-singular. To do so, we can transform the general RDE (2.2.8a) into an ordinary RDE of the form (2.B.1) using the following lemma:

Lemma 2.B.1. Suppose the matrices $\mathbf{F} \in \mathbb{R}^{n\times n}$, $\bar{\mathbf{H}} \in \mathbb{R}^{m\times n}$ and $\bar{\mathbf{G}} \in \mathbb{R}^{n\times m}$, as well as the variances matrices $\mathbf{Q} \in \mathbb{R}^{n\times n}$ and $\bar{\mathbf{R}} \in \mathbb{R}^{m\times m}$ with $\bar{\mathbf{R}} > \mathbf{0}$ refer to the generalized RDE

$$\bar{\boldsymbol{\Sigma}}_t = \mathbf{F}\bar{\boldsymbol{\Sigma}}_{t-1}\mathbf{F}^T + \mathbf{Q} - \left(\mathbf{F}\bar{\boldsymbol{\Sigma}}_{t-1}\bar{\mathbf{H}}^T + \bar{\mathbf{G}}\right)\left[\bar{\mathbf{H}}\bar{\boldsymbol{\Sigma}}_{t-1}\bar{\mathbf{H}}^T + \bar{\mathbf{R}}\right]^{-1}\left(\bar{\mathbf{H}}\bar{\boldsymbol{\Sigma}}_{t-1}\mathbf{F}^T + \bar{\mathbf{G}}^T\right), \tag{2.B.2}$$

that generates the matrix sequence $\{\bar{\boldsymbol{\Sigma}}_t\}_{t=0}^N$ with a variance matrix $\bar{\boldsymbol{\Sigma}}_0 \geq \mathbf{0}$. Then the RDE

$$\bar{\boldsymbol{\Sigma}}_t = \bar{\mathbf{F}}\bar{\boldsymbol{\Sigma}}_{t-1}\bar{\mathbf{F}}^T + \bar{\mathbf{Q}} - \bar{\mathbf{F}}\bar{\boldsymbol{\Sigma}}_{t-1}\bar{\mathbf{H}}^T\left[\bar{\mathbf{H}}\bar{\boldsymbol{\Sigma}}_{t-1}\bar{\mathbf{H}}^T + \bar{\mathbf{R}}\right]^{-1}\bar{\mathbf{H}}\bar{\boldsymbol{\Sigma}}_{t-1}\bar{\mathbf{F}}^T,$$

with $\bar{\mathbf{F}} := \mathbf{F} - \bar{\mathbf{G}}\bar{\mathbf{R}}^{-1}\bar{\mathbf{H}}$ and $\bar{\mathbf{Q}} := \mathbf{Q} - \bar{\mathbf{G}}\bar{\mathbf{R}}^{-1}\bar{\mathbf{G}}^T$, is equivalent to (2.B.2).

Proof:
The statement follows from the fact that we may rewrite the right-hand side of (2.B.2) to

$$\begin{aligned}
&\mathbf{F}\bar{\boldsymbol{\Sigma}}_{t-1}\mathbf{F}^T + \mathbf{Q} - \left(\mathbf{F}\bar{\boldsymbol{\Sigma}}_{t-1}\bar{\mathbf{H}}^T + \bar{\mathbf{G}}\right)\left[\bar{\mathbf{H}}\bar{\boldsymbol{\Sigma}}_{t-1}\bar{\mathbf{H}}^T + \bar{\mathbf{R}}\right]^{-1}\left(\bar{\mathbf{H}}\bar{\boldsymbol{\Sigma}}_{t-1}\mathbf{F}^T + \bar{\mathbf{G}}^T\right)\\
&= \left(\bar{\mathbf{F}} + \bar{\mathbf{G}}\bar{\mathbf{R}}^{-1}\bar{\mathbf{H}}\right)\bar{\boldsymbol{\Sigma}}_{t-1}\left(\bar{\mathbf{F}} + \bar{\mathbf{G}}\bar{\mathbf{R}}^{-1}\bar{\mathbf{H}}\right)^T + \bar{\mathbf{Q}} + \bar{\mathbf{G}}\bar{\mathbf{R}}^{-1}\bar{\mathbf{G}}^T\\
&\quad - \left[\left(\bar{\mathbf{F}} + \bar{\mathbf{G}}\bar{\mathbf{R}}^{-1}\bar{\mathbf{H}}\right)\bar{\boldsymbol{\Sigma}}_{t-1}\bar{\mathbf{H}}^T + \bar{\mathbf{G}}\right]\left[\bar{\mathbf{H}}\bar{\boldsymbol{\Sigma}}_{t-1}\bar{\mathbf{H}}^T + \bar{\mathbf{R}}\right]^{-1}\left[\bar{\mathbf{H}}\bar{\boldsymbol{\Sigma}}_{t-1}\left(\bar{\mathbf{F}} + \bar{\mathbf{G}}\bar{\mathbf{R}}^{-1}\bar{\mathbf{H}}\right)^T + \bar{\mathbf{G}}^T\right]\\
&= \bar{\mathbf{F}}\bar{\boldsymbol{\Sigma}}_{t-1}\bar{\mathbf{F}}^T + \bar{\mathbf{F}}\bar{\boldsymbol{\Sigma}}_{t-1}\bar{\mathbf{H}}^T\bar{\mathbf{R}}^{-1}\bar{\mathbf{G}}^T + \bar{\mathbf{G}}\bar{\mathbf{R}}^{-1}\bar{\mathbf{H}}\bar{\boldsymbol{\Sigma}}_{t-1}\bar{\mathbf{F}}^T + \bar{\mathbf{G}}\bar{\mathbf{R}}^{-1}\bar{\mathbf{H}}\bar{\boldsymbol{\Sigma}}_{t-1}\bar{\mathbf{H}}^T\bar{\mathbf{R}}^{-1}\bar{\mathbf{G}}^T + \bar{\mathbf{Q}} + \bar{\mathbf{G}}\bar{\mathbf{R}}^{-1}\bar{\mathbf{G}}^T\\
&\quad - \left[\bar{\mathbf{F}}\bar{\boldsymbol{\Sigma}}_{t-1}\bar{\mathbf{H}}^T + \bar{\mathbf{G}}\bar{\mathbf{R}}^{-1}\bar{\mathbf{H}}\bar{\boldsymbol{\Sigma}}_{t-1}\bar{\mathbf{H}}^T + \bar{\mathbf{G}}\right]\left[\bar{\mathbf{H}}\bar{\boldsymbol{\Sigma}}_{t-1}\bar{\mathbf{H}}^T + \bar{\mathbf{R}}\right]^{-1}\left[\bar{\mathbf{H}}\bar{\boldsymbol{\Sigma}}_{t-1}\bar{\mathbf{F}}^T + \bar{\mathbf{H}}\bar{\boldsymbol{\Sigma}}_{t-1}\bar{\mathbf{H}}^T\bar{\mathbf{R}}^{-1}\bar{\mathbf{G}}^T + \bar{\mathbf{G}}^T\right]\\
&= \bar{\mathbf{F}}\bar{\boldsymbol{\Sigma}}_{t-1}\bar{\mathbf{F}}^T + \bar{\mathbf{Q}} - \bar{\mathbf{F}}\bar{\boldsymbol{\Sigma}}_{t-1}\bar{\mathbf{H}}^T\left[\bar{\mathbf{H}}\bar{\boldsymbol{\Sigma}}_{t-1}\bar{\mathbf{H}}^T + \bar{\mathbf{R}}\right]^{-1}\bar{\mathbf{H}}\bar{\boldsymbol{\Sigma}}_{t-1}\bar{\mathbf{F}}^T\\
&\quad + \bar{\mathbf{F}}\bar{\boldsymbol{\Sigma}}_{t-1}\bar{\mathbf{H}}^T\bar{\mathbf{R}}^{-1}\bar{\mathbf{G}}^T + \bar{\mathbf{G}}\bar{\mathbf{R}}^{-1}\bar{\mathbf{H}}\bar{\boldsymbol{\Sigma}}_{t-1}\bar{\mathbf{F}}^T + \bar{\mathbf{G}}\bar{\mathbf{R}}^{-1}\bar{\mathbf{H}}\bar{\boldsymbol{\Sigma}}_{t-1}\bar{\mathbf{H}}^T\bar{\mathbf{R}}^{-1}\bar{\mathbf{G}}^T + \bar{\mathbf{G}}\bar{\mathbf{R}}^{-1}\bar{\mathbf{G}}^T\\
&\quad - \bar{\mathbf{F}}\bar{\boldsymbol{\Sigma}}_{t-1}\bar{\mathbf{H}}^T\left[\bar{\mathbf{H}}\bar{\boldsymbol{\Sigma}}_{t-1}\bar{\mathbf{H}}^T + \bar{\mathbf{R}}\right]^{-1}\left[\bar{\mathbf{H}}\bar{\boldsymbol{\Sigma}}_{t-1}\bar{\mathbf{H}}^T\bar{\mathbf{R}}^{-1}\bar{\mathbf{G}}^T + \bar{\mathbf{G}}^T\right]\\
&\quad - \left[\bar{\mathbf{G}}\bar{\mathbf{R}}^{-1}\bar{\mathbf{H}}\bar{\boldsymbol{\Sigma}}_{t-1}\bar{\mathbf{H}}^T + \bar{\mathbf{G}}\right]\left[\bar{\mathbf{H}}\bar{\boldsymbol{\Sigma}}_{t-1}\bar{\mathbf{H}}^T + \bar{\mathbf{R}}\right]^{-1}\bar{\mathbf{H}}\bar{\boldsymbol{\Sigma}}_{t-1}\bar{\mathbf{F}}^T\\
&\quad - \left[\bar{\mathbf{G}}\bar{\mathbf{R}}^{-1}\bar{\mathbf{H}}\bar{\boldsymbol{\Sigma}}_{t-1}\bar{\mathbf{H}}^T + \bar{\mathbf{G}}\right]\left[\bar{\mathbf{H}}\bar{\boldsymbol{\Sigma}}_{t-1}\bar{\mathbf{H}}^T + \bar{\mathbf{R}}\right]^{-1}\left[\bar{\mathbf{H}}\bar{\boldsymbol{\Sigma}}_{t-1}\bar{\mathbf{H}}^T\bar{\mathbf{R}}^{-1}\bar{\mathbf{G}}^T + \bar{\mathbf{G}}^T\right]\\
&= \bar{\mathbf{F}}\bar{\boldsymbol{\Sigma}}_{t-1}\bar{\mathbf{F}}^T + \bar{\mathbf{Q}} - \bar{\mathbf{F}}\bar{\boldsymbol{\Sigma}}_{t-1}\bar{\mathbf{H}}^T\left[\bar{\mathbf{H}}\bar{\boldsymbol{\Sigma}}_{t-1}\bar{\mathbf{H}}^T + \bar{\mathbf{R}}\right]^{-1}\bar{\mathbf{H}}\bar{\boldsymbol{\Sigma}}_{t-1}\bar{\mathbf{F}}^T\\
&\quad + \bar{\mathbf{F}}\bar{\boldsymbol{\Sigma}}_{t-1}\bar{\mathbf{H}}^T\bar{\mathbf{R}}^{-1}\bar{\mathbf{G}}^T + \bar{\mathbf{G}}\bar{\mathbf{R}}^{-1}\bar{\mathbf{H}}\bar{\boldsymbol{\Sigma}}_{t-1}\bar{\mathbf{F}}^T + \bar{\mathbf{G}}\bar{\mathbf{R}}^{-1}\left[\bar{\mathbf{H}}\bar{\boldsymbol{\Sigma}}_{t-1}\bar{\mathbf{H}}^T + \bar{\mathbf{R}}\right]\bar{\mathbf{R}}^{-1}\bar{\mathbf{G}}^T\\
&\quad - \bar{\mathbf{F}}\bar{\boldsymbol{\Sigma}}_{t-1}\bar{\mathbf{H}}^T\left[\bar{\mathbf{H}}\bar{\boldsymbol{\Sigma}}_{t-1}\bar{\mathbf{H}}^T + \bar{\mathbf{R}}\right]^{-1}\left[\bar{\mathbf{H}}\bar{\boldsymbol{\Sigma}}_{t-1}\bar{\mathbf{H}}^T + \bar{\mathbf{R}}\right]\bar{\mathbf{R}}^{-1}\bar{\mathbf{G}}^T\\
&\quad - \bar{\mathbf{G}}\bar{\mathbf{R}}^{-1}\left[\bar{\mathbf{H}}\bar{\boldsymbol{\Sigma}}_{t-1}\bar{\mathbf{H}}^T + \bar{\mathbf{R}}\right]\left[\bar{\mathbf{H}}\bar{\boldsymbol{\Sigma}}_{t-1}\bar{\mathbf{H}}^T + \bar{\mathbf{R}}\right]^{-1}\bar{\mathbf{H}}\bar{\boldsymbol{\Sigma}}_{t-1}\bar{\mathbf{F}}^T\\
&\quad - \bar{\mathbf{G}}\bar{\mathbf{R}}^{-1}\left[\bar{\mathbf{H}}\bar{\boldsymbol{\Sigma}}_{t-1}\bar{\mathbf{H}}^T + \bar{\mathbf{R}}\right]\left[\bar{\mathbf{H}}\bar{\boldsymbol{\Sigma}}_{t-1}\bar{\mathbf{H}}^T + \bar{\mathbf{R}}\right]^{-1}\left[\bar{\mathbf{H}}\bar{\boldsymbol{\Sigma}}_{t-1}\bar{\mathbf{H}}^T + \bar{\mathbf{R}}\right]\bar{\mathbf{R}}^{-1}\bar{\mathbf{G}}^T
\end{aligned}$$

[21] Note that the notation $\mathbf{A} > 0$ (or $\mathbf{A} \geq 0$) means that the matrix $\mathbf{A}$ is positive-definite (or positive-semi-definite).

$$
\begin{aligned}
&= \bar{\mathbf{F}}\bar{\mathbf{\Sigma}}_{t-1}\bar{\mathbf{F}}^T + \bar{\mathbf{Q}} - \bar{\mathbf{F}}\bar{\mathbf{\Sigma}}_{t-1}\bar{\mathbf{H}}^T \left[\bar{\mathbf{H}}\bar{\mathbf{\Sigma}}_{t-1}\bar{\mathbf{H}}^T + \bar{\mathbf{R}}\right]^{-1} \bar{\mathbf{H}}\bar{\mathbf{\Sigma}}_{t-1}\bar{\mathbf{F}}^T \\
&\quad + \bar{\mathbf{F}}\bar{\mathbf{\Sigma}}_{t-1}\bar{\mathbf{H}}^T\bar{\mathbf{R}}^{-1}\bar{\mathbf{G}}^T + \bar{\mathbf{G}}\bar{\mathbf{R}}^{-1}\bar{\mathbf{H}}\bar{\mathbf{\Sigma}}_{t-1}\bar{\mathbf{F}}^T + \bar{\mathbf{G}}\bar{\mathbf{R}}^{-1}\left[\bar{\mathbf{H}}\bar{\mathbf{\Sigma}}_{t-1}\bar{\mathbf{H}}^T + \bar{\mathbf{R}}\right]\bar{\mathbf{R}}^{-1}\bar{\mathbf{G}}^T \\
&\quad - \bar{\mathbf{F}}\bar{\mathbf{\Sigma}}_{t-1}\bar{\mathbf{H}}^T\bar{\mathbf{R}}^{-1}\bar{\mathbf{G}}^T - \bar{\mathbf{G}}\bar{\mathbf{R}}^{-1}\bar{\mathbf{H}}\bar{\mathbf{\Sigma}}_{t-1}\bar{\mathbf{F}}^T - \bar{\mathbf{G}}\bar{\mathbf{R}}^{-1}\left[\bar{\mathbf{H}}\bar{\mathbf{\Sigma}}_{t-1}\bar{\mathbf{H}}^T + \bar{\mathbf{R}}\right]\bar{\mathbf{R}}^{-1}\bar{\mathbf{G}}^T \\
&= \bar{\mathbf{F}}\bar{\mathbf{\Sigma}}_{t-1}\bar{\mathbf{F}}^T + \bar{\mathbf{Q}} - \bar{\mathbf{F}}\bar{\mathbf{\Sigma}}_{t-1}\bar{\mathbf{H}}^T \left[\bar{\mathbf{H}}\bar{\mathbf{\Sigma}}_{t-1}\bar{\mathbf{H}}^T + \bar{\mathbf{R}}\right]^{-1} \bar{\mathbf{H}}\bar{\mathbf{\Sigma}}_{t-1}\bar{\mathbf{F}}^T.
\end{aligned}
$$

□

Stabilizing and strong solutions: Note that if the RDE (2.B.1) converges to a fixed matrix $\mathbf{\Sigma}$, we may state that $\mathbf{\Sigma}$ is a solution to the discrete algebraic Riccati equation (DARE)

$$\mathbf{\Sigma} = \mathbf{F}\mathbf{\Sigma}\mathbf{F}^T - \mathbf{F}\mathbf{\Sigma}\mathbf{H}^T \left[\mathbf{H}\mathbf{\Sigma}\mathbf{H}^T + \mathbf{R}\right]^{-1} \mathbf{H}\mathbf{\Sigma}\mathbf{F}^T + \mathbf{Q}. \tag{2.B.3}$$

We call (2.B.3) the DARE corresponding to the RDE (2.B.1). Considering the convergence of (2.B.1), two types of solutions to the DARE (2.B.3) are of particular importance.

Definition 2.B.1. Suppose the matrices $\mathbf{F} \in \mathbb{R}^{n\times n}$, $\mathbf{H} \in \mathbb{R}^{m\times n}$, $\mathbf{Q} \in \mathbb{R}^{n\times n}$ and $\mathbf{R} \in \mathbb{R}^{m\times m}$ refer to the RDE (2.B.1) that generates the matrix sequence $\{\mathbf{\Sigma}_t\}_{t=0}^N$ with a variance matrix $\mathbf{\Sigma}_0 \geq \mathbf{0}$. Further suppose that (2.B.3) is the DARE corresponding to the RDE (2.B.1), then a real symmetric matrix $\mathbf{\Sigma} \geq \mathbf{0}$ satisfying the DARE (2.B.3) is called a **stabilizing / strong** solution, if and only if the eigenvalues of the matrix

$$\tilde{\mathbf{F}} = \mathbf{F}\left(\mathbf{I} - \mathbf{\Sigma}\mathbf{H}^T \left[\mathbf{H}\mathbf{\Sigma}\mathbf{H}^T + \mathbf{R}\right]^{-1} \mathbf{H}\right)$$

are **inside / inside or on** the unit circle.[22]

As we will see, (2.B.1) often converges towards its strong (stabilizing) solution, provided this solution exists. Furthermore, to show that the DAREs

$$\mathbf{C}_+ = \mathbf{F}\mathbf{C}_+\mathbf{F}^T + \mathbf{Q} - \left(\mathbf{F}\mathbf{C}_+\bar{\mathbf{H}}^T + \bar{\mathbf{G}}\right)\left[\bar{\mathbf{H}}\mathbf{C}_+\bar{\mathbf{H}}^T + \bar{\mathbf{R}}\right]^{-1}\left(\bar{\mathbf{H}}\mathbf{C}_+\mathbf{F}^T + \bar{\mathbf{G}}^T\right), \tag{2.B.4}$$

$$\mathbf{P}_+ = \mathbf{F}\mathbf{P}_+\mathbf{F}^T - \mathbf{F}\mathbf{P}_+\mathbf{H}^T \left[\mathbf{H}\mathbf{P}_+\mathbf{H}^T + \mathbf{R}\right]^{-1} \mathbf{H}\mathbf{P}_+\mathbf{F}^T + \mathbf{Q}, \tag{2.B.5}$$

corresponding to the RDEs (2.2.8a) and (2.2.8b) have strong (stabilizing) solutions, it is sufficient to show that one of the DAREs (2.B.4) and (2.B.5) has a strong (stabilizing) solution. To see this we propose the following Lemma:

Lemma 2.B.2. The matrix $\mathbf{C}_+$ is a **stabilizing / strong** solution to (2.B.4), if and only if $\mathbf{P}_+$ is a **strong / stabilizing** solution to (2.B.5).

Proof:
From Definition 2.B.1 follows that $\mathbf{P}_+$ is a **stabilizing / strong** solution to (2.B.5), if and only if the eigenvalues of the matrix

$$\tilde{\mathbf{F}}_{\mathbf{P}_+} = \mathbf{F}\left(\mathbf{I} - \mathbf{P}_+\mathbf{H}^T \left[\mathbf{H}\mathbf{P}_+\mathbf{H}^T + \mathbf{R}\right]^{-1} \mathbf{H}\right)$$

are **inside / inside or on** the unit circle. Analogously, using Lemma 2.B.1 we may state that $\mathbf{C}_+$ is a **stabilizing / strong** solution to (2.B.4), if and only if the eigenvalues of the matrix

$$\tilde{\mathbf{F}}_{\mathbf{C}_+} = \bar{\mathbf{F}}\left(\mathbf{I} - \mathbf{C}_+\bar{\mathbf{H}}^T \left[\bar{\mathbf{H}}\mathbf{C}_+\bar{\mathbf{H}}^T + \bar{\mathbf{R}}\right]^{-1} \bar{\mathbf{H}}\right)$$

[22] This definition is taken from Chan et al. (1984) and de Souza et al. (1986).

are **inside / inside or on** the unit circle. Thus, to prove the claim of Lemma 2.B.2 we will show that $\tilde{\mathbf{F}}_{\mathbf{P}_+}$ and $\tilde{\mathbf{F}}_{\mathbf{C}_+}$ share the same set of eigenvalues. To see this, note that using the definitions of $\bar{\mathbf{F}}$, $\bar{\mathbf{H}}$, and $\bar{\mathbf{R}}$ as well as (2.2.4b), we may write

$$
\begin{aligned}
\tilde{\mathbf{F}}_{\mathbf{C}_+} &= \bar{\mathbf{F}}\left(\mathbf{I}-\mathbf{C}_+\bar{\mathbf{H}}^T\left[\bar{\mathbf{H}}\mathbf{C}_+\bar{\mathbf{H}}^T+\bar{\mathbf{R}}\right]^{-1}\bar{\mathbf{H}}\right)\\
&= \left(\mathbf{F}-\bar{\mathbf{G}}\bar{\mathbf{R}}^{-1}\bar{\mathbf{H}}\right)\left(\mathbf{I}-\mathbf{C}_+\mathbf{F}^T\mathbf{H}^T\left[\mathbf{H}\mathbf{F}\mathbf{C}_+\mathbf{F}^T\mathbf{H}^T+\mathbf{H}\mathbf{Q}\mathbf{H}^T+\mathbf{R}\right]^{-1}\mathbf{H}\mathbf{F}\right)\\
&= \left(\mathbf{F}-\mathbf{Q}\mathbf{H}^T\left[\mathbf{H}\mathbf{Q}\mathbf{H}^T+\mathbf{R}\right]^{-1}\mathbf{H}\mathbf{F}\right)\left(\mathbf{I}-\mathbf{C}_+\mathbf{F}^T\mathbf{H}^T\left[\mathbf{H}\mathbf{F}\mathbf{C}_+\mathbf{F}^T\mathbf{H}^T+\mathbf{H}\mathbf{Q}\mathbf{H}^T+\mathbf{R}\right]^{-1}\mathbf{H}\mathbf{F}\right)\\
&= \left(\mathbf{F}-\mathbf{Q}\mathbf{H}^T\left[\mathbf{H}\mathbf{Q}\mathbf{H}^T+\mathbf{R}\right]^{-1}\mathbf{H}\mathbf{F}\right)\left(\mathbf{I}-\mathbf{C}_+\mathbf{F}^T\mathbf{H}^T\left[\mathbf{H}\mathbf{P}_+\mathbf{H}^T+\mathbf{R}\right]^{-1}\mathbf{H}\mathbf{F}\right)\\
&= \left(\mathbf{I}-\mathbf{Q}\mathbf{H}^T\left[\mathbf{H}\mathbf{Q}\mathbf{H}^T+\mathbf{R}\right]^{-1}\mathbf{H}\right)\left(\mathbf{F}-\mathbf{F}\mathbf{C}_+\mathbf{F}^T\mathbf{H}^T\left[\mathbf{H}\mathbf{P}_+\mathbf{H}^T+\mathbf{R}\right]^{-1}\mathbf{H}\mathbf{F}\right)\\
&= \left(\mathbf{I}-\mathbf{Q}\mathbf{H}^T\left[\mathbf{H}\mathbf{Q}\mathbf{H}^T+\mathbf{R}\right]^{-1}\mathbf{H}\right)\left(\mathbf{F}-\mathbf{P}_+\mathbf{H}^T\left[\mathbf{H}\mathbf{P}_+\mathbf{H}^T+\mathbf{R}\right]^{-1}\mathbf{H}\mathbf{F}+\mathbf{Q}\mathbf{H}^T\left[\mathbf{H}\mathbf{P}_+\mathbf{H}^T+\mathbf{R}\right]^{-1}\mathbf{H}\mathbf{F}\right)\\
&= \mathbf{F}-\mathbf{P}_+\mathbf{H}^T\left[\mathbf{H}\mathbf{P}_+\mathbf{H}^T+\mathbf{R}\right]^{-1}\mathbf{H}\mathbf{F}+\mathbf{Q}\mathbf{H}^T\left[\mathbf{H}\mathbf{P}_+\mathbf{H}^T+\mathbf{R}\right]^{-1}\mathbf{H}\mathbf{F}-\mathbf{Q}\mathbf{H}^T\left[\mathbf{H}\mathbf{Q}\mathbf{H}^T+\mathbf{R}\right]^{-1}\mathbf{H}\mathbf{F}\\
&\quad+\mathbf{Q}\mathbf{H}^T\left[\mathbf{H}\mathbf{Q}\mathbf{H}^T+\mathbf{R}\right]^{-1}\mathbf{H}\mathbf{P}_+\mathbf{H}^T\left[\mathbf{H}\mathbf{P}_+\mathbf{H}^T+\mathbf{R}\right]^{-1}\mathbf{H}\mathbf{F}\\
&\quad-\mathbf{Q}\mathbf{H}^T\left[\mathbf{H}\mathbf{Q}\mathbf{H}^T+\mathbf{R}\right]^{-1}\mathbf{H}\mathbf{Q}\mathbf{H}^T\left[\mathbf{H}\mathbf{P}_+\mathbf{H}^T+\mathbf{R}\right]^{-1}\mathbf{H}\mathbf{F}\\
&= \mathbf{F}-\mathbf{P}_+\mathbf{H}^T\left[\mathbf{H}\mathbf{P}_+\mathbf{H}^T+\mathbf{R}\right]^{-1}\mathbf{H}\mathbf{F}+\mathbf{Q}\mathbf{H}^T\left[\mathbf{H}\mathbf{P}_+\mathbf{H}^T+\mathbf{R}\right]^{-1}\mathbf{H}\mathbf{F}-\mathbf{Q}\mathbf{H}^T\left[\mathbf{H}\mathbf{Q}\mathbf{H}^T+\mathbf{R}\right]^{-1}\mathbf{H}\mathbf{F}\\
&\quad+\mathbf{Q}\mathbf{H}^T\left[\mathbf{H}\mathbf{Q}\mathbf{H}^T+\mathbf{R}\right]^{-1}\mathbf{H}\mathbf{P}_+\mathbf{H}^T\left[\mathbf{H}\mathbf{P}_+\mathbf{H}^T+\mathbf{R}\right]^{-1}\mathbf{H}\mathbf{F}\\
&\quad-\mathbf{Q}\mathbf{H}^T\left[\mathbf{H}\mathbf{Q}\mathbf{H}^T+\mathbf{R}\right]^{-1}\mathbf{R}\left[\mathbf{H}\mathbf{P}_+\mathbf{H}^T+\mathbf{R}\right]^{-1}\mathbf{H}\mathbf{F}\\
&\quad+\mathbf{Q}\mathbf{H}^T\left[\mathbf{H}\mathbf{Q}\mathbf{H}^T+\mathbf{R}\right]^{-1}\mathbf{R}\left[\mathbf{H}\mathbf{P}_+\mathbf{H}^T+\mathbf{R}\right]^{-1}\mathbf{H}\mathbf{F}\\
&= \mathbf{F}-\mathbf{P}_+\mathbf{H}^T\left[\mathbf{H}\mathbf{P}_+\mathbf{H}^T+\mathbf{R}\right]^{-1}\mathbf{H}\mathbf{F}+\mathbf{Q}\mathbf{H}^T\left[\mathbf{H}\mathbf{P}_+\mathbf{H}^T+\mathbf{R}\right]^{-1}\mathbf{H}\mathbf{F}-\mathbf{Q}\mathbf{H}^T\left[\mathbf{H}\mathbf{Q}\mathbf{H}^T+\mathbf{R}\right]^{-1}\mathbf{H}\mathbf{F}\\
&\quad+\mathbf{Q}\mathbf{H}^T\left[\mathbf{H}\mathbf{Q}\mathbf{H}^T+\mathbf{R}\right]^{-1}\left[\mathbf{H}\mathbf{P}_+\mathbf{H}^T+\mathbf{R}\right]\left[\mathbf{H}\mathbf{P}_+\mathbf{H}^T+\mathbf{R}\right]^{-1}\mathbf{H}\mathbf{F}\\
&\quad-\mathbf{Q}\mathbf{H}^T\left[\mathbf{H}\mathbf{Q}\mathbf{H}^T+\mathbf{R}\right]^{-1}\left[\mathbf{H}\mathbf{Q}\mathbf{H}^T+\mathbf{R}\right]\left[\mathbf{H}\mathbf{P}_+\mathbf{H}^T+\mathbf{R}\right]^{-1}\mathbf{H}\mathbf{F}\\
&= \mathbf{F}-\mathbf{P}_+\mathbf{H}^T\left[\mathbf{H}\mathbf{P}_+\mathbf{H}^T+\mathbf{R}\right]^{-1}\mathbf{H}\mathbf{F}+\mathbf{Q}\mathbf{H}^T\left[\mathbf{H}\mathbf{P}_+\mathbf{H}^T+\mathbf{R}\right]^{-1}\mathbf{H}\mathbf{F}-\mathbf{Q}\mathbf{H}^T\left[\mathbf{H}\mathbf{Q}\mathbf{H}^T+\mathbf{R}\right]^{-1}\mathbf{H}\mathbf{F}\\
&\quad+\mathbf{Q}\mathbf{H}^T\left[\mathbf{H}\mathbf{Q}\mathbf{H}^T+\mathbf{R}\right]^{-1}\mathbf{H}\mathbf{F}-\mathbf{Q}\mathbf{H}^T\left[\mathbf{H}\mathbf{P}_+\mathbf{H}^T+\mathbf{R}\right]^{-1}\mathbf{H}\mathbf{F}\\
&= \mathbf{F}-\mathbf{P}_+\mathbf{H}^T\left[\mathbf{H}\mathbf{P}_+\mathbf{H}^T+\mathbf{R}\right]^{-1}\mathbf{H}\mathbf{F}\\
&= \left(\mathbf{I}-\mathbf{P}_+\mathbf{H}^T\left[\mathbf{H}\mathbf{P}_+\mathbf{H}^T+\mathbf{R}\right]^{-1}\mathbf{H}\right)\mathbf{F}
\end{aligned}
$$

Since $\mathbf{F}$ and $\left(\mathbf{I}-\mathbf{P}_+\mathbf{H}^T\left[\mathbf{H}\mathbf{P}_+\mathbf{H}^T+\mathbf{R}\right]^{-1}\mathbf{H}\right)$ are both square matrices, the matrix $\tilde{\mathbf{F}}_{\mathbf{C}_+}$ must have the same set of eigenvalues as the matrix $\tilde{\mathbf{F}}_{\mathbf{P}_+}$.[23] This completes the proof.

□

Some concepts of linear systems theory: To eventually obtain conditions under which RDE (2.B.1) converges to a fixed matrix $\boldsymbol{\Sigma}$, we introduce the concepts of stability, observability, and reachability from linear system theory:[24]

Definition 2.B.2. Suppose the matrices $\mathbf{F}\in\mathbb{R}^{n\times n}$, $\mathbf{H}\in\mathbb{R}^{m\times n}$, $\mathbf{R}\in\mathbb{R}^{m\times m}$ and $\mathbf{Q}\in\mathbb{R}^{n\times n}$, with $\mathbf{Q}=\mathbf{D}\mathbf{D}^T$, $\mathbf{D}\in\mathbb{R}^{n\times n}$, refer to the RDE (2.B.1) that generates the matrix sequence $\{\boldsymbol{\Sigma}_t\}_{t=0}^N$ with a

[23] Note that from $\mathbf{A},\mathbf{B}\in\mathbb{R}^{n\times n}$ follows that the matrices $\mathbf{C}=\mathbf{A}\mathbf{B}$ and $\mathbf{D}=\mathbf{B}\mathbf{A}$ share the same set of eigenvalues. See e.g. Theorem 6.12 by Searle and Khuri (2017, pp. 140).

[24] See also (Gu, 2012, Chapter 3).

variance matrix $\mathbf{\Sigma}_0 \geq \mathbf{0}$. Further suppose that (2.B.3) is the DARE corresponding to the RDE (2.B.1), then

(i) The matrix $\mathbf{F}$ is called stable, if and only if for any eigenvalue λ of the matrix $\mathbf{F}$ it holds that

$$|\lambda| < 1.$$

(ii) The pair $(\mathbf{H}, \mathbf{F})$ is called observable, if and only if

$$\operatorname{rk}\begin{pmatrix}\mathbf{H}^T & \mathbf{F}^T\,\mathbf{H}^T & \cdots & (\mathbf{F}^T)^{n-1}\,\mathbf{H}^T\end{pmatrix} = n.$$

(iii) The pair $(\mathbf{F}, \mathbf{D})$ is called reachable, if and only if

$$\operatorname{rk}\begin{pmatrix}\mathbf{D} & \mathbf{F}\,\mathbf{D} & \cdots & \mathbf{F}^{n-1}\,\mathbf{D}\end{pmatrix} = n.$$

With respect to the SSM (2.2.1), a stable transition matrix $\mathbf{F}$ ensures that $\mathbf{w}_t$ follows a stationary process so that the unforced system

$$\mathbf{w}_t = \mathbf{F}\mathbf{w}_{t-1}, \quad \mathbf{w}_0 \neq 0,$$

is asymptotically stable, i.e., $\lim_{t\to\infty} \mathbf{w}_t = \mathbf{0}$. Observability and reachability are dual concepts, i.e., for an observable pair $(\mathbf{H}, \mathbf{F})$, we may claim that the pair $(\mathbf{F}^T, \mathbf{H}^T)$ is reachable and vice versa. Observability of the pair $(\mathbf{H}, \mathbf{F})$ can also be understood in the sense that, in the case of an unforced system

$$\mathbf{y}_t = \mathbf{H}\mathbf{w}_t, \quad \mathbf{w}_t = \mathbf{F}\mathbf{w}_{t-1},$$

there is some $l \in \mathbb{N}$, such that the initial state vector $\mathbf{w}_0$ may be obtained from $\{\mathbf{y}_t\}_{t=1}^{l}$ (see Gu, 2012, pp. 70). Reachability of the pair $(\mathbf{F}, \mathbf{D})$, on the other hand, can be interpreted in the sense that there is a bounded control input $\{\mathbf{v}_t\}_{t=1}^{l}$, $l \in \mathbb{N}$, so that the system

$$\mathbf{w}_t = \mathbf{F}\mathbf{w}_{t-1} + \mathbf{D}\mathbf{v}_t,$$

can reach a state $\mathbf{w}^*$, i.e., $\mathbf{w}_l = \mathbf{w}^*$, for a given initial state $\mathbf{w}_0$ (see Gu, 2012, pp. 75). As we will see, observability and reachability are sufficient conditions for (2.B.1) to converge to a stabilizing solution for $\mathbf{\Sigma}_0 > \mathbf{0}$. However, since especially the assumption of reachability does not hold for a variety of econometric models,[25] somewhat weaker concepts than observability and reachablility are detectability and stabilizability:

Definition 2.B.3. Suppose the matrices $\mathbf{F} \in \mathbb{R}^{n\times n}$, $\mathbf{H} \in \mathbb{R}^{m\times n}$, $\mathbf{R} \in \mathbb{R}^{m\times m}$ and $\mathbf{Q} \in \mathbb{R}^{n\times n}$, with $\mathbf{Q} = \mathbf{D}\mathbf{D}^T$, $\mathbf{D} \in \mathbb{R}^{n\times n}$, refer to the RDE (2.B.1) that generates the matrix sequence $\{\mathbf{\Sigma}_t\}_{t=0}^{N}$ with a variance matrix $\mathbf{\Sigma}_0 \geq \mathbf{0}$. Further suppose that (2.B.3) is the DARE corresponding to the RDE (2.B.1), then

(i) The pair $(\mathbf{H}, \mathbf{F})$ is called detectable, if for any eigenvalue λ of the matrix $\mathbf{F}$ with $|\lambda| \geq 1$, there does not exist a n-dimensional eigenvector $\mathbf{q} \neq \mathbf{0}$ such that

$$\mathbf{F}\mathbf{q} = \lambda\mathbf{q}, \quad \mathbf{H}\mathbf{q} = \mathbf{0}.$$

[25] See e.g. Harvey (1990b, pp. 118) who illustrates that a non-invertible moving average process of order one will always be observable, but never be reachable.

(ii) The pair $(\mathbf{F}, \mathbf{D})$ is called stabilizable, if for any eigenvalue λ of the matrix $\mathbf{F}^T$ with $|\lambda| \geq 1$, there does not exist a n-dimensional eigenvector $\mathbf{q} \neq \mathbf{0}$ such that

$$\mathbf{F}^T \mathbf{q} = \lambda \mathbf{q}, \quad \mathbf{D}^T \mathbf{q} = \mathbf{0}.$$

(iii) Further an eigenvalue λ of the matrix $\mathbf{F}$ is said to be $(\mathbf{F}, \mathbf{D})$-unreachable (of rank p) if and only if there exists a set of (p) n-dimensional generalized eigenvectors $\mathbf{q}_i \neq 0$ with $i = 1, \ldots, p$ and $\mathbf{q}_0 = 0$ such that

$$\mathbf{F}^T \mathbf{q}_i = \lambda \mathbf{q}_i + \mathbf{q}_{i-1}, \quad \mathbf{D}^T \mathbf{q}_i = 0.$$

In the following lemma, we postulate some well-known links from detectability and stabilizability to the concepts in Definition 2.B.2:

Lemma 2.B.3. Suppose the matrices $\mathbf{F} \in \mathbb{R}^{n \times n}$, $\mathbf{H} \in \mathbb{R}^{m \times n}$, $\mathbf{R} \in \mathbb{R}^{m \times m}$ and $\mathbf{Q} \in \mathbb{R}^{n \times n}$, with $\mathbf{Q} = \mathbf{D}\mathbf{D}^T$, $\mathbf{D} \in \mathbb{R}^{n \times n}$, refer to the RDE (2.B.1) that generates the matrix sequence $\{\mathbf{\Sigma}_t\}_{t=0}^N$ with a variance matrix $\mathbf{\Sigma}_0 \geq \mathbf{0}$. Further suppose that (2.B.3) is the DARE corresponding to the RDE (2.B.1), then we may state that:

(i) If the matrix $\mathbf{F}$ is stable, then the pair $(\mathbf{H}, \mathbf{F})$ is detectable.

(ii) If the matrix $\mathbf{F}$ is stable, then the pair $(\mathbf{F}, \mathbf{D})$ is stabilizable.

(iii) If the pair $(\mathbf{H}, \mathbf{F})$ is observable it is also detectable.

(iv) If the pair $(\mathbf{F}, \mathbf{D})$ is reachable it is also stabilizable.

(v) The pair $(\mathbf{F}, \mathbf{D})$ is stabilizable, if and only if the matrix $\mathbf{F}$ has no $(\mathbf{F}, \mathbf{D})$-unreachable eigenvalues on or outside the unit circle, i.e. $\lambda \leq 1$.

(vi) The pair is $(\mathbf{F}, \mathbf{D})$ is reachable, if and only if the matrix $\mathbf{F}$ has no $(\mathbf{F}, \mathbf{D})$-unreachable eigenvalues.

Proof:

(i) Note that the stability of $\mathbf{F}$ implies that there are no eigenvalues λ of the matrix $\mathbf{F}$ with $|\lambda| \geq 1$. Consequently, for all eigenvalues with $|\lambda| \geq 1$ (where there are none), there does not exist an n-dimensional vector $\mathbf{q} \neq \mathbf{0}$ such that

$$\mathbf{F}\mathbf{q} = \lambda \mathbf{q}, \quad \mathbf{H}\mathbf{q} = \mathbf{0}.$$

(ii) Note that the stability of $\mathbf{F}$ implies that there are no eigenvalues λ of the matrix $\mathbf{F}^T$ with $|\lambda| \geq 1$. Consequently, for all eigenvalues with $|\lambda| \geq 1$ (where there are none), there does not exist an n-dimensional vector $\mathbf{q} \neq \mathbf{0}$ such that

$$\mathbf{F}^T \mathbf{q} = \lambda \mathbf{q}, \quad \mathbf{D}^T \mathbf{q} = \mathbf{0}.$$

(iii) The statement follows from the fact that observability of the pair $(\mathbf{H}, \mathbf{F})$ implies that the matrix $\mathbf{F}$ has no eigenvector $\mathbf{q}$ (corresponding to an eigenvalue λ) such that

$$\mathbf{F}\mathbf{q} = \lambda \mathbf{q}, \quad \mathbf{H}\mathbf{q} = \mathbf{0}.$$

This is true, since otherwise we could write

$$\begin{aligned}\mathbf{q}^T \begin{pmatrix}\mathbf{H}^T & \mathbf{F}^T\mathbf{H}^T & \cdots & (\mathbf{F}^T)^{n-1}\mathbf{H}^T\end{pmatrix} &= \begin{pmatrix}\mathbf{q}^T\mathbf{H}^T & \mathbf{q}^T\mathbf{F}^T\mathbf{H}^T & \cdots & \mathbf{q}^T(\mathbf{F}^T)^{n-1}\mathbf{H}^T\end{pmatrix} \\ &= \begin{pmatrix}(\mathbf{H}\mathbf{q})^T & (\mathbf{H}\mathbf{F}\mathbf{q})^T & \cdots & (\mathbf{H}\mathbf{F}^{n-1}\mathbf{q})^T\end{pmatrix} \\ &= \begin{pmatrix}(\mathbf{H}\mathbf{q})^T & \lambda(\mathbf{H}\mathbf{q})^T & \cdots & \lambda^{n-1}(\mathbf{H}\mathbf{q})^T\end{pmatrix} \\ &= \begin{pmatrix}\mathbf{0} & \mathbf{0} & \cdots & \mathbf{0}\end{pmatrix} \\ &= \mathbf{0},\end{aligned}$$

so that

$$\mathrm{rk}\begin{pmatrix}\mathbf{H}^T & \mathbf{F}^T\mathbf{H}^T & \cdots & (\mathbf{F}^T)^{n-1}\mathbf{H}^T\end{pmatrix} < n.$$

(iv) The statement follows from the fact that reachability of the pair $(\mathbf{F}, \mathbf{D})$ implies that the matrix $\mathbf{F}^T$ has no eigenvector $\mathbf{q}$ (corresponding to an eigenvalue λ) such that

$$\mathbf{F}^T\mathbf{q} = \lambda\mathbf{q}, \quad \mathbf{D}^T\mathbf{q} = \mathbf{0}.$$

This is true, since otherwise we could write

$$\begin{aligned}\mathbf{q}^T \begin{pmatrix}\mathbf{D} & \mathbf{F}\mathbf{D} & \cdots & \mathbf{F}^{n-1}\mathbf{D}\end{pmatrix} &= \begin{pmatrix}\mathbf{q}^T\mathbf{D} & \mathbf{q}^T\mathbf{F}\mathbf{D} & \cdots & \mathbf{q}^T\mathbf{F}^{n-1}\mathbf{H}\end{pmatrix} \\ &= \begin{pmatrix}(\mathbf{D}^T\mathbf{q})^T & (\mathbf{D}^T\mathbf{F}^T\mathbf{q})^T & \cdots & (\mathbf{D}^T(\mathbf{F}^T)^{n-1}\mathbf{q})^T\end{pmatrix} \\ &= \begin{pmatrix}(\mathbf{D}^T\mathbf{q})^T & \lambda(\mathbf{D}^T\mathbf{q})^T & \cdots & \lambda^{n-1}(\mathbf{D}^T\mathbf{q})^T\end{pmatrix} \\ &= \begin{pmatrix}\mathbf{0} & \mathbf{0} & \cdots & \mathbf{0}\end{pmatrix} \\ &= \mathbf{0},\end{aligned}$$

so that

$$\mathrm{rk}\begin{pmatrix}\mathbf{D} & \mathbf{F}\mathbf{D} & \cdots & \mathbf{F}^{n-1}\mathbf{D}\end{pmatrix} < n.$$

(v) Follows directly from Definition 2.B.3 (ii)-(iii).

(vi) Follows from Theorem 3.10. Gu (2012, pp. 77).

□

Roughly speaking, we may describe **detectability / stabilizability** as the claim that all parts, or more precisely all eigenvalues of the transition matrix $\mathbf{F}$, are either $(\mathbf{H}, \mathbf{F})$ **observable** / $(\mathbf{F}, \mathbf{D})$ **reachable** or stable. Please note that some authors, e.g., Harvey (1990b, pp. 115), use the related concept of Controllability instead of the concept of Reachability. For more details on linear systems theory, we refer the reader to Gu (2012, Chapter 3) as well as Anderson and Moore (1979, Appendix C).

Some general convergence results: Finally, we collect the main results on the convergence of the RDE (2.B.1) provided by de Souza et al. (1986) in the following Proposition:

Proposition 2.B.1. Suppose the matrices $\mathbf{F} \in \mathbb{R}^{n\times n}$, $\mathbf{H} \in \mathbb{R}^{m\times n}$, $\mathbf{R} \in \mathbb{R}^{m\times m}$ and $\mathbf{Q} \in \mathbb{R}^{n\times n}$, with $\mathbf{Q} = \mathbf{D}\mathbf{D}^T$, $\mathbf{D} \in \mathbb{R}^{n\times n}$, refer to the RDE (2.B.1) that generates the matrix sequence $\{\mathbf{\Sigma}_t\}_{t=0}^N$ with a variance matrix $\mathbf{\Sigma}_0 \geq \mathbf{0}$. Further suppose that (2.B.3) is the DARE corresponding to the RDE (2.B.1), then

(i) The strong solution $\mathbf{\Sigma}_s$ of the DARE (2.B.3) exists and is unique if and only if $(\mathbf{H}, \mathbf{F})$ is detectable. Furthermore, subject to $(\mathbf{\Sigma}_0 - \mathbf{\Sigma}_s) \geq \mathbf{0}$, the RDE (2.B.1) converges to the strong solution (i.e. $\lim_{t\to\infty} \mathbf{\Sigma}_t = \mathbf{\Sigma}_s$).

(ii) The strong solution $\boldsymbol{\Sigma}_s$ is the only non-negative definite solution of the DARE (2.B.3) if and only if $(\mathbf{H}, \mathbf{F})$ is detectable and $\mathbf{F}$ has no $(\mathbf{F}, \mathbf{D})$-unreachable eigenvalues outside the unit circle.

(iii) The strong solution $\boldsymbol{\Sigma}_s$ is a stabilizing solution of the DARE (2.B.3) if and only if $(\mathbf{H}, \mathbf{F})$ is detectable and $\mathbf{F}$ has no $(\mathbf{F}, \mathbf{D})$-unreachable eigenvalues on the unit circle. Furthermore, subject to $\boldsymbol{\Sigma}_0 > \mathbf{0}$, the RDE (2.B.1) converges to the strong and stabilizing solution $\boldsymbol{\Sigma}_s$.

Proof:

(i) See de Souza et al. (1986, Theorem 3.2-A and theorem 4.2).

(ii) See de Souza et al. (1986, Theorem 3.2-B).

(iii) See de Souza et al. (1986, Theorem 3.2-C and theorem 4.1).

□

From Proposition 2.B.1(i)-(iii) and Lemma 2.B.3(v) follows the well-known result that the RDE (2.B.1) converges to a stabilizing solution if the pair $(\mathbf{H}, \mathbf{F})$ is detectable while the pair $(\mathbf{F}, \mathbf{D})$ is stabilizable. Furthermore, it follows from Lemma 2.B.3(i)-(iii) that the same holds true if $\mathbf{F}$ is stable and/or if the pair $(\mathbf{H}, \mathbf{F})$ is observable while the pair $(\mathbf{F}, \mathbf{D})$ is reachable. However, Proposition 2.B.1(i) also allows to investigate the existence and convergence to a strong solution.

2.B.2 Proof of Proposition 2.2.1

To prove claims (i) and (ii) of Proposition 2.2.1, we will consult the results of Proposition 2.B.1 and Lemmas 2.B.1, 2.B.2 and 2.B.3, while the proof of claim (iii) basis on Proposition 13.1 by (Hamilton, 1994, pp. 390) and Lemma 2.B.2.

Statement (i): To prove the claim (i), we first consider the sequence $\{\mathbf{P}_{t|t-1}\}_{t=1}^N$ determined by the (ordinary) RDE (2.2.8b). Since $\mathbf{R}$ is a non-singular matrix by assumption, we may use the results by de Souza et al. (1986) to analyze the convergence behavior of $\{\mathbf{P}_{t|t-1}\}_{t=1}^N$. Using the fact that the matrix $\mathbf{F}$ is stable by assumption, it follows from Lemma 2.B.3 (i), (ii), and (v) that $(\mathbf{H}, \mathbf{F})$ is detectable and $\mathbf{F}$ has no $(\mathbf{F}, \mathbf{D})$-unreachable eigenvalues on (or outside) the unit circle. Thus, the claim related to the sequence $\{\mathbf{P}_{t|t-1}\}_{t=1}^N$ follows directly from the „if “ part of Proposition 2.B.1 (iii). The claim related to the sequence $\{\mathbf{C}_t\}_{t=1}^N$ then follows directly from Lemma 2.B.2 and the „only if“ part of Proposition 2.B.1 (iii).

Statement (ii): To prove the claim (ii), we first consider the sequence $\{\mathbf{C}_t\}_{t=1}^N$ determined by the (general) RDE (2.2.8a). Since $\bar{\mathbf{R}}$ is a non-singular matrix by assumption, we may use Lemma 2.B.1 to transform (2.2.8a) into the (ordinary) RDE

$$\mathbf{C}_t = \bar{\mathbf{F}}\mathbf{C}_{t-1}\bar{\mathbf{F}}^T + \bar{\mathbf{Q}} - \bar{\mathbf{F}}\mathbf{C}_{t-1}\bar{\mathbf{H}}^T\left[\bar{\mathbf{H}}\mathbf{C}_{t-1}\bar{\mathbf{H}}^T + \bar{\mathbf{R}}\right]^{-1}\bar{\mathbf{H}}\mathbf{C}_{t-1}\bar{\mathbf{F}}^T, \tag{2.B.6}$$

with $\bar{\mathbf{F}} := \mathbf{F} - \bar{\mathbf{G}}\bar{\mathbf{R}}^{-1}\bar{\mathbf{H}}$ and $\bar{\mathbf{Q}} := \mathbf{Q} - \bar{\mathbf{G}}\bar{\mathbf{R}}^{-1}\bar{\mathbf{G}}^T$. Based on (2.B.6), we may use the results by de Souza et al. (1986) to analyze the convergence behavior of $\{\mathbf{C}_t\}_{t=1}^N$. Using the fact that the matrix $\bar{\mathbf{F}}$ is stable by assumption, it follows from Lemma 2.B.3 (i), (ii), and (v) that $(\mathbf{H}, \mathbf{F})$ is detectable and $\bar{\mathbf{F}}$ has no $(\bar{\mathbf{F}}, \bar{\mathbf{D}})$-unreachable eigenvalues on (or outside) the unit circle. Thus, the claim related to the sequence $\{\mathbf{C}_t\}_{t=1}^N$ follows directly from the „if “ part of Proposition 2.B.1 (iii). The claim related to the sequence $\{\mathbf{P}_{t|t-1}\}_{t=1}^N$ then follows directly from Lemma 2.B.2 and the „only if “ part of Proposition 2.B.1 (iii).

Statement (iii)**:** Hamilton (1994, Chapter 13) shows that using the unconditional initialization, the sequence $\{\mathbf{P}_{t|t-1}\}_{t=1}^{N}$ is non-increasing, i.e., $\mathbf{P}_{t|t-1}-\mathbf{P}_{t+1|t}$ is positive semi-definite for all $t=1,\dots,N-1$, and converges to a strong solution $\mathbf{P}_+$, with $\mathbf{P}_{1|0}-\mathbf{P}_+ = \mathbf{C}_0-\mathbf{P}_+ \geq \mathbf{0}$.[26] Furthermore, it follows from (2.2.3) and (2.2.4f) that

$$\mathbf{P}_+ - \mathbf{C}_+ = \mathbf{P}_+\mathbf{H}^T\left(\mathbf{H}\mathbf{P}_+\mathbf{H}^T+\mathbf{R}\right)^{-1}\left(\mathbf{H}\mathbf{P}_+\mathbf{H}^T+\mathbf{R}\right)\left(\mathbf{H}\mathbf{P}_+\mathbf{H}^T+\mathbf{R}\right)^{-1}\mathbf{H}\mathbf{P}_+ \geq \mathbf{0}$$

so that

$$\mathbf{C}_0-\mathbf{C}_+ \geq \mathbf{C}_0-\mathbf{P}_+ = \mathbf{P}_{1|0}-\mathbf{P}_+ \geq \mathbf{0}.$$

Since we know from Lemma 2.B.2 that $\mathbf{C}_+$ is a strong solution of RDE (2.2.8a), the claim related to the sequence $\{\mathbf{C}_t\}_{t=1}^{N}$ follows directly from Proposition 2.B.1 (i).

□

2.C Derivation of the steady-state Kalman filter

In this appendix, we provide the formal derivation of the steady-state Kalman filter (SKF) (2.2.11) and the steady-state log-likelihood (2.2.12). To do so, note that if we initialize the KF at $(\boldsymbol{\mu}_{0,+},\mathbf{C}_+)$, where $\mathbf{C}_+$ is a solution to (2.B.4), $\mathbf{C}_t=\mathbf{C}_+$ for all $t=1,2,\dots,N$. Furthermore, the quantities $\mathbf{P}_{t|t-1}$, $\mathbf{U}_t$, and $\mathbf{K}_t$ become time-invariant, too. If we denote their steady-state equivalents as $\mathbf{P}_+$, $\mathbf{U}_+$, and $\mathbf{K}_+$, it follows directly from (2.2.4b), (2.2.4d), and (2.2.3) that

$$\mathbf{P}_+ = \mathbf{F}\mathbf{C}_+\mathbf{F}^T+\mathbf{Q}, \qquad \mathbf{U}_+ = \mathbf{H}\mathbf{P}_+\mathbf{H}^T+\mathbf{R}, \qquad \mathbf{K}_+ = \mathbf{P}_+\mathbf{H}^T\,\mathbf{U}_+^{-1}.$$

Since, in this case, the updating steps (2.2.4b),(2.2.4d), and (2.2.4f) of the Kalman recursion (2.2.4), and the updating of the gain matrix (2.2.3), become redundant, the Kalman recursion (2.2.4) for $t=1,2,\dots,N$ reduces to

$$\mathbf{w}_{t|t-1,+} = \mathbf{F}\boldsymbol{\mu}_{t-1,+}, \tag{2.C.1a}$$
$$\mathbf{e}_{t,+} = \mathbf{y}_t^{(\mathrm{h})} - \mathbf{H}\mathbf{w}_{t|t-1,+}, \tag{2.C.1b}$$
$$\boldsymbol{\mu}_{t,+} = \mathbf{w}_{t|t-1,+} + \mathbf{K}_+\mathbf{e}_{t,+}. \tag{2.C.1c}$$

Defining

$$\mathbf{J}_+ := (\mathbf{I}-\mathbf{K}_+\mathbf{H})\,\mathbf{F},$$

we can use equations (2.C.1a) to (2.C.1c) to determine the law of motion for $\boldsymbol{\mu}_{t,+}$ as

$$\begin{aligned}\boldsymbol{\mu}_{t,+} &= \mathbf{w}_{t|t-1,+} + \mathbf{K}_+\mathbf{e}_{t,+}\\ &= \mathbf{w}_{t|t-1,+} + \mathbf{K}_+\left(\mathbf{y}_t^{(\mathrm{h})} - \mathbf{H}\mathbf{w}_{t|t-1,+}\right)\\ &= \mathbf{F}\boldsymbol{\mu}_{t-1,+} + \mathbf{K}_+\left(\mathbf{y}_t^{(\mathrm{h})} - \mathbf{H}\mathbf{F}\boldsymbol{\mu}_{t-1,+}\right)\\ &= \mathbf{K}_+\,\mathbf{y}_t^{(\mathrm{h})} + (\mathbf{I}-\mathbf{K}_+\mathbf{H})\,\mathbf{F}\,\boldsymbol{\mu}_{t-1,+}\\ &= \mathbf{K}_+\,\mathbf{y}_t^{(\mathrm{h})} + \mathbf{J}_+\,\boldsymbol{\mu}_{t-1,+}, \qquad \forall t=1,2,\dots,N.\end{aligned} \tag{2.C.2}$$

This means we can use (2.C.2) to determine $\boldsymbol{\mu}_{t,+}$ for $t=0,1,\dots,N-1$ recursively. It follows directly from equations (2.C.1b) and (2.C.1c) that the quantities $\mathbf{w}_{t|t-1}$ and $\mathbf{e}_t$ for $t=1,2,\dots,N$

[26] Note that from $\mathbf{C}_0=\mathbf{F}\,\mathbf{C}_0\mathbf{F}^T+\mathbf{Q}$ and (2.2.4b) follows that $\mathbf{P}_{1|0}=\mathbf{F}\,\mathbf{C}_0\mathbf{F}^T+\mathbf{Q}=\mathbf{C}_0$.

are then determined by

$$\begin{pmatrix}\mathbf{w}_{1|0,+} & \cdots & \mathbf{w}_{N|N-1,+}\end{pmatrix} = \mathbf{F}\begin{pmatrix}\boldsymbol{\mu}_{0,+} & \cdots & \boldsymbol{\mu}_{N-1,+}\end{pmatrix}, \tag{2.C.3}$$

$$\begin{aligned}\begin{pmatrix}\mathbf{e}_{1,+} & \cdots & \mathbf{e}_{N,+}\end{pmatrix} &= \begin{pmatrix}\mathbf{y}_1^{(\mathrm{h})} & \cdots & \mathbf{y}_N^{(\mathrm{h})}\end{pmatrix} - \mathbf{H}\begin{pmatrix}\mathbf{w}_{1|0,+} & \cdots & \mathbf{w}_{N|N-1,+}\end{pmatrix} \\ &= \begin{pmatrix}\mathbf{y}_1^{(\mathrm{h})} & \cdots & \mathbf{y}_N^{(\mathrm{h})}\end{pmatrix} - \mathbf{HF}\begin{pmatrix}\boldsymbol{\mu}_{0,+} & \cdots & \boldsymbol{\mu}_{N-1,+}\end{pmatrix}.\end{aligned} \tag{2.C.4}$$

Note that we can also simplify the log-likelihood conditional to the initialization $(\boldsymbol{\mu}_{0,+}, \mathbf{C}_+)$, since in this case $\mathbf{U}_t = \mathbf{U}_+$ for all $t = 1,\dots,N$. Hence, we can define the log-likelihood computed based on the SKF as

$$\begin{aligned}\log\left(f_{\mathbf{Y}_N}\right)_+ &= -\frac{1}{2}\left(n_y\ N\ \log(2\pi)\ + \sum_{t=1}^{N}\log|\mathbf{U}_+|\ + \sum_{t=1}^{N}\mathbf{e}_{t,+}^T\ \mathbf{U}_+^{-1}\ \mathbf{e}_{t,+}\right) \\ &= -\frac{1}{2}\left(n_y\ N\ \log(2\pi)\ + N\ \log|\mathbf{U}_+|\right) - \frac{1}{2}\sum_{t=1}^{N}\mathrm{tr}\left(\mathbf{e}_{t,+}^T\ \mathbf{U}_+^{-1}\ \mathbf{e}_{t,+}\right) \\ &= -\frac{1}{2}\left(n_y\ N\ \log(2\pi)\ + N\ \log|\mathbf{U}_+|\right) - \frac{1}{2}\sum_{t=1}^{N}\mathrm{tr}\left(\mathbf{U}_+^{-1}\ \mathbf{e}_{t,+}\mathbf{e}_{t,+}^T\right) \\ &= -\frac{1}{2}\left(n_y\ N\ \log(2\pi)\ + N\ \log|\mathbf{U}_+|\right) - \frac{1}{2}\mathrm{tr}\left(\sum_{t=1}^{N}\mathbf{U}_+^{-1}\ \mathbf{e}_{t,+}\mathbf{e}_{t,+}^T\right) \\ &= -\frac{1}{2}\left(n_y\ N\ \log(2\pi)\ + N\ \log|\mathbf{U}_+|\right) - \frac{1}{2}\mathrm{tr}\left(\mathbf{U}_+^{-1}\ \sum_{t=1}^{N}\mathbf{e}_{t,+}\mathbf{e}_{t,+}^T\right) \\ &= -\frac{1}{2}\left[n_y\ N\ \log(2\pi)\ + N\ \log|\mathbf{U}_+| + \mathrm{tr}\left(\mathbf{U}_+^{-1}\begin{pmatrix}\mathbf{e}_{1,+} & \cdots & \mathbf{e}_{N,+}\end{pmatrix}\begin{pmatrix}\mathbf{e}_{1,+} & \cdots & \mathbf{e}_{N,+}\end{pmatrix}^T\right)\right] \\ &= -\frac{1}{2}\left[n_y\ N\ \log(2\pi)\ + N\ \log|\mathbf{U}_+| + \mathrm{tr}\left(\mathbf{U}_+^{-1}\ \mathbf{e}_{1:N,+}\mathbf{e}_{1:N,+}^T\right)\right], \\ &= -\frac{1}{2}\left[n_y\ N\ \log(2\pi)\ + N\ \log|\mathbf{U}_+| + \mathrm{tr}\left(\mathbf{e}_{1:N,+}^T\ \mathbf{U}_+^{-1}\ \mathbf{e}_{1:N,+}\right)\right],\end{aligned} \tag{2.C.5}$$

with $\mathbf{e}_{1:N,+} := \begin{pmatrix}\mathbf{e}_{1,+} & \cdots & \mathbf{e}_{N,+}\end{pmatrix}$.

Further, note that since $\mathbf{J}_+ = \tilde{\mathbf{F}}_{\mathbf{C}_+}$, we may analyze its eigenvalues to check if $\mathbf{C}_+$ is a strong / stabilizing solution to RDE (2.2.8a).

2.D Derivation of the augmented Kalman filter

The first part of this appendix contains the formal derivation of the augmented Kalman filter (AKF) (2.2.15) and the log-density $\log\left(f_{\mathbf{Y}_N}\right)$ given in (2.2.16). In the second part, we provide a brief digression on how initialization strategies for non-stationary SSMs, such as the *fixed-but-unknown* or the *diffuse* initialization, can be incorporated within the AKF (2.2.15). In the last part of this appendix, we show how to incorporate the additional steps of the AKF into the KF (2.2.4).

2.D.1 The augmented Kalman filter

Note that the derivation of the AKF given here in large parts follows the arguments of Durbin and Koopman (2012, Chapter 5.7). However, we shall derive the AKF with respect to SSM (2.2.1), while the elaborations of Durbin and Koopman (2012) are based on the alternative state-space representation (2.2.5).

For convenience, let us restate the model for the initial state vector from equation (2.2.13):

$$\mathbf{w}_0 = \mathbf{a}_w + \mathbf{A}_\mathbf{w}\,\bar{\mathbf{w}}_0 + \mathbf{A}_\mathbf{d}\,\mathbf{d}, \qquad \bar{\mathbf{w}}_0 \sim \mathrm{N}(\bar{\boldsymbol{\mu}}_0, \bar{\mathbf{C}}_0), \qquad \mathbf{d} \sim \mathrm{N}(\boldsymbol{\delta}_0, \mathbf{D}_0),$$

Further, we denoted the time t quantities generated by the Kalman recursion (2.2.4) initialized at $(\tilde{\boldsymbol{\mu}}_0, \tilde{\mathbf{C}}_0)$, with $\tilde{\boldsymbol{\mu}}_0 = \mathbf{a}_w + \mathbf{A}_\mathbf{w}\bar{\boldsymbol{\mu}}_0$ and $\tilde{\mathbf{C}}_0 = \mathbf{A}_\mathbf{w}\bar{\mathbf{C}}_0\mathbf{A}_\mathbf{w}^T$, by $\tilde{\boldsymbol{\mu}}_t$, $\tilde{\mathbf{C}}_t$, $\tilde{\mathbf{w}}_{t|t-1}$, $\tilde{\mathbf{P}}_{t|t-1}$, $\tilde{\mathbf{e}}_t$, $\tilde{\mathbf{U}}_t$, and $\tilde{\mathbf{K}}_t$. In the following derivation of the AKF (2.2.15a)-(2.2.15e)

$$\begin{aligned}
\boldsymbol{\mu}_t &= \tilde{\boldsymbol{\mu}}_t + \mathbf{M}_t\mathbf{A}_d\,\left(\mathbf{D}_0^{-1} + \mathbf{A}_\mathbf{d}^T\,\mathbf{S}_t\,\mathbf{A}_\mathbf{d}\right)^{-1}\left(\mathbf{D}_0^{-1}\boldsymbol{\delta}_0 + \mathbf{A}_\mathbf{d}^T\,\mathbf{s}_t\right), && \forall\ t = 1,2,\ldots,N,\\
\mathbf{C}_t &= \tilde{\mathbf{C}}_t + \mathbf{M}_t\mathbf{A}_d\left(\mathbf{D}_0^{-1} + \mathbf{A}_\mathbf{d}^T\,\mathbf{S}_t\,\mathbf{A}_\mathbf{d}\right)^{-1}\mathbf{A}_d^T\mathbf{M}_t^T, && \forall\ t = 1,2,\ldots,N,\\
\mathbf{s}_t &= \mathbf{s}_{t-1} + (\mathbf{HFM}_{t-1})^T\,\tilde{\mathbf{U}}_t^{-1}\,\tilde{\mathbf{e}}_t, && \mathbf{s}_0 = \mathbf{0},\ \forall\ t = 1,2,\ldots,N,\\
\mathbf{S}_t &= \mathbf{S}_{t-1} + (\mathbf{HFM}_{t-1})^T\,\tilde{\mathbf{U}}_t^{-1}\,(\mathbf{HFM}_{t-1}), && \mathbf{S}_0 = \mathbf{0},\ \forall\ t = 1,2,\ldots,N,\\
\mathbf{M}_t &= \left(\mathbf{I} - \tilde{\mathbf{K}}_t\mathbf{H}\right)\mathbf{F}\,\mathbf{M}_{t-1}, && \mathbf{M}_0 = \mathbf{I},\ \forall\ t = 1,2,\ldots,N,
\end{aligned}$$

and especially of the log-density

$$\begin{aligned}
\log(f_{\mathbf{Y}_N}) = \log\left(f_{\mathbf{Y}_N|\mathbf{d}=\mathbf{0}}\right) &- \frac{1}{2}\log|\mathbf{I} + \mathbf{D}_0\,\mathbf{A}_\mathbf{d}^T\,\mathbf{S}_N\,\mathbf{A}_\mathbf{d}| - \frac{1}{2}\boldsymbol{\delta}_0^T\mathbf{D}_\mathbf{0}^{-1}\boldsymbol{\delta}_0\\
&+ \frac{1}{2}(\mathbf{D}_0^{-1}\boldsymbol{\delta}_0 + \mathbf{A}_\mathbf{d}^T\,\mathbf{s}_N)^T(\mathbf{D}_0^{-1} + \mathbf{A}_\mathbf{d}^T\,\mathbf{S}_N\,\mathbf{A}_\mathbf{d})^{-1}(\mathbf{D}_0^{-1}\boldsymbol{\delta}_0 + \mathbf{A}_\mathbf{d}^T\,\mathbf{s}_N),
\end{aligned}$$

given in (2.2.16), the Bayes theorem will play a key role as it allows us to decompose the log-density $\log(f_{\mathbf{Y}_N})$ into

$$\begin{aligned}
\log\left(f_{\mathbf{Y}_N}\right) &= \log\left(\frac{f_{\mathbf{Y}_N|\mathbf{d}}\cdot f_\mathbf{d}}{f_{\mathbf{d}|\mathbf{Y}_N}}\right)\\
&= \log(f_\mathbf{d}) + \log\left(f_{\mathbf{Y}_N|\mathbf{d}}\right) - \log\left(f_{\mathbf{d}|\mathbf{Y}_N}\right).
\end{aligned} \tag{2.D.1}$$

While for given $\boldsymbol{\delta}_0$ and $\mathbf{D}_0$, the log-density $\log(f_\mathbf{d})$ is fully specified, we need to obtain $\log\left(f_{\mathbf{Y}_N|\mathbf{d}}\right)$ and $\log\left(f_{\mathbf{d}|\mathbf{Y}_N}\right)$ to determine $\log\left(f_{\mathbf{Y}_N}\right)$ from the right-hand side of (2.D.1). Therefore, in the first step, we will show that we can express the log-density $\log(f_{\mathbf{Y}_N|\mathbf{d}})$ as a function of $\log(f_{\mathbf{Y}_N|\mathbf{d}=\mathbf{0}})$, $\mathbf{d}$, $\mathbf{A}_d$, $\mathbf{s}_N$, and $\mathbf{S}_N$, where a crucial preliminary result will be the observation that the quantities $\boldsymbol{\mu}_t$, $\mathbf{w}_{t|t-1}$, and $\mathbf{e}_t$ of the KF are linear functions of $\boldsymbol{\mu}_0$. This observation is due to Rosenberg (1973) and forms the basis for the so-called fixed-but-unknown initialization discussed later in this appendix. Eventually, we will receive (2.2.15) and (2.2.16) using a fixed-point smoothing algorithm to obtain $\log\left(f_{\mathbf{d}|\mathbf{Y}_N}\right)$.

Linearity of $\boldsymbol{\mu}_t$, $\mathbf{w}_{t|t-1}$, and $\mathbf{e}_t$ in $\boldsymbol{\mu}_0$: In the following lemma, we will show that the quantities $\boldsymbol{\mu}_t$, $\mathbf{w}_{t|t-1}$, and $\mathbf{e}_t$ of the KF are linear in $\boldsymbol{\mu}_0$, while the quantities $\mathbf{C}_t$, $\mathbf{P}_{t|t-1}$, and $\mathbf{U}_t$ are independent of $\boldsymbol{\mu}_0$:

Lemma 2.D.1. Suppose for the SSM (2.2.1) the time t quantities generated by the Kalman recursion (2.2.4) initialized at $(\tilde{\boldsymbol{\mu}}_0, \mathbf{C}_0)$ are denoted by $\tilde{\boldsymbol{\mu}}_t$, $\tilde{\mathbf{C}}_t$, $\tilde{\mathbf{w}}_{t|t-1}$, $\tilde{\mathbf{P}}_{t|t-1}$, $\tilde{\mathbf{e}}_t$, $\tilde{\mathbf{U}}_t$ and $\tilde{\mathbf{K}}_t$. Further suppose $\boldsymbol{\mu}_t$, $\mathbf{C}_t$, $\mathbf{w}_{t|t-1}$, $\mathbf{P}_{t|t-1}$, $\mathbf{e}_t$, $\mathbf{U}_t$ and $\mathbf{K}_t$ denote the time t quantities generated by the Kalman recursion (2.2.4) initialized at $(\boldsymbol{\mu}_0, \mathbf{C}_0)$, then we can state that

$$\mathbf{C}_t = \tilde{\mathbf{C}}_t, \qquad \mathbf{P}_{t|t-1} = \tilde{\mathbf{P}}_{t|t-1}, \qquad \mathbf{U}_t = \tilde{\mathbf{U}}_t, \qquad \mathbf{K}_t = \tilde{\mathbf{K}}_t,$$

and that

$$\boldsymbol{\mu}_t = \tilde{\boldsymbol{\mu}}_t + \mathbf{M}_t\,\boldsymbol{\Delta}_0, \qquad \mathbf{w}_{t|t-1} = \tilde{\mathbf{w}}_{t|t-1} + \mathbf{FM}_{t-1}\,\boldsymbol{\Delta}_0, \qquad \mathbf{e}_t = \tilde{\mathbf{e}}_t - \mathbf{HFM}_{t-1}\,\boldsymbol{\Delta}_0,$$

with

$$\boldsymbol{\Delta}_0 = \boldsymbol{\mu}_0 - \tilde{\boldsymbol{\mu}}_0, \qquad \mathbf{M}_s = \prod_{j=1}^{s} \mathbf{J}_{s-j+1}, \qquad \mathbf{J}_t = (\mathbf{I} - \mathbf{K}_t\mathbf{H})\,\mathbf{F}, \qquad \forall s = 0,1,\ldots,N,$$

for all $t = 1,2,\ldots,N$.

Proof:
Defining $\mathbf{J}_t := (\mathbf{I} - \mathbf{K}_t\mathbf{H})\,\mathbf{F}$ we can use equation (2.2.4a), (2.2.4c) and (2.2.4e) to obtain the law of motion for $\boldsymbol{\mu}_t$ as

$$\begin{aligned}
\boldsymbol{\mu}_t &= \mathbf{w}_{t|t-1} + \mathbf{K}_t\mathbf{e}_t \\
&= \mathbf{w}_{t|t-1} + \mathbf{K}_t\left(\mathbf{y}_t - \mathbf{h} - \mathbf{H}\,\mathbf{w}_{t|t-1}\right) \\
&= \mathbf{w}_{t|t-1} + \mathbf{K}_t\left(\mathbf{y}_t - \mathbf{h}\right) - \mathbf{K}_t\mathbf{H}\,\mathbf{w}_{t|t-1} \\
&= (\mathbf{I} - \mathbf{K}_t\mathbf{H})\,\mathbf{w}_{t|t-1} + \mathbf{K}_t\ \left(\mathbf{y}_t - \mathbf{h}\right) \\
&= (\mathbf{I} - \mathbf{K}_t\mathbf{H})\,\mathbf{F}\ \boldsymbol{\mu}_{t-1} + \mathbf{K}_t\ \left(\mathbf{y}_t - \mathbf{h}\right) \\
&= \mathbf{J}_t\ \boldsymbol{\mu}_{t-1} + \mathbf{K}_t\ \left(\mathbf{y}_t - \mathbf{h}\right), \qquad \forall t = 1,2,\ldots,N. \qquad \text{(2.D.2)}
\end{aligned}$$

Note that it follows from equations (2.2.3), (2.2.4b), (2.2.4d) and (2.2.4f), that the sequences $\{\mathbf{K}_t\}_{t=1}^N$, $\{\mathbf{P}_{t|t-1}\}_{t=1}^N$, $\{\mathbf{U}_t\}_{t=1}^N$ and $\{\mathbf{C}_t\}_{t=0}^N$ referring to the initialization $(\boldsymbol{\mu}_0, \mathbf{C}_0)$ do not depend on $\boldsymbol{\mu}_0$ and therefore are identical to the sequences $\{\tilde{\mathbf{K}}_t\}_{t=1}^N$, $\{\tilde{\mathbf{P}}_{t|t-1}\}_{t=1}^N$, $\{\tilde{\mathbf{U}}_t\}_{t=1}^N$ and $\{\tilde{\mathbf{C}}_t\}_{t=0}^N$ referring to the initialization $(\tilde{\boldsymbol{\mu}}_0, \mathbf{C}_0)$. Consequently, we can state that law of motion for $\tilde{\boldsymbol{\mu}}_t$ similar to (2.D.2) is given by

$$\tilde{\boldsymbol{\mu}}_t = \mathbf{J}_t\ \tilde{\boldsymbol{\mu}}_{t-1} + \mathbf{K}_t\ \left(\mathbf{y}_t - \mathbf{h}\right), \qquad \forall t = 1,2,\ldots,N. \qquad \text{(2.D.3)}$$

Moreover, defining $\boldsymbol{\Delta}_t = \boldsymbol{\mu}_t - \tilde{\boldsymbol{\mu}}_t$ for all $t = 0,1,\ldots,N$, we may use (2.D.2) and (2.D.3) to write

$$\begin{aligned}
\boldsymbol{\Delta}_t &= \mathbf{J}_t\ \boldsymbol{\Delta}_{t-1} \\
&= \mathbf{J}_t \cdot \mathbf{J}_{t-1}\ \boldsymbol{\Delta}_{t-2} \\
&\ \ \vdots \\
&= \mathbf{J}_t \cdot \mathbf{J}_{t-1} \cdot \ldots \cdot \mathbf{J}_1\ \boldsymbol{\Delta}_0 \\
&= \left(\prod_{j=1}^{t} \mathbf{J}_{t-j+1}\right) \boldsymbol{\Delta}_0 \\
&= \mathbf{M}_t\ \boldsymbol{\Delta}_0, \qquad \forall t = 0,1,\ldots,N, \qquad \text{(2.D.4)}
\end{aligned}$$

with

$$\mathbf{M}_t := \prod_{j=1}^{t} \mathbf{J}_{t-j+1}, \qquad \forall t = 0,1,\ldots,N.$$

Note that from the definition of the $\prod(\cdot)$ operator follows that $\mathbf{M}_0 = \prod_{j=1}^{0} \mathbf{J}_{j+1} = \mathbf{I}$. The statement of Lemma 2.D.1 then follows directly from (2.D.4), (2.2.4a) and (2.2.4b):

$$\begin{aligned}
\boldsymbol{\mu}_t &= \tilde{\boldsymbol{\mu}}_t + \mathbf{M}_t\ \boldsymbol{\Delta}_0, \qquad \forall t = 0,1,\ldots,N, \qquad \text{(2.D.5)} \\
\mathbf{w}_{t|t-1} &= \mathbf{F}\ \boldsymbol{\mu}_{t-1} \\
&= \mathbf{F}\ \tilde{\boldsymbol{\mu}}_{t-1} + \mathbf{F}\mathbf{M}_{t-1}\ \boldsymbol{\Delta}_0 \\
&= \tilde{\mathbf{w}}_{t|t-1} + \mathbf{F}\mathbf{M}_{t-1}\ \boldsymbol{\Delta}_0, \qquad \forall t = 1,2,\ldots,N, \qquad \text{(2.D.6)} \\
\mathbf{e}_t &= \mathbf{y}_t - \mathbf{h} - \mathbf{H}\mathbf{w}_{t|t-1}
\end{aligned}$$

$$
\begin{aligned}
&= \mathbf{y}_t - \mathbf{h} - \mathbf{H}\left(\tilde{\mathbf{w}}_{t|t-1} + \mathbf{F}\mathbf{M}_{t-1}\,\boldsymbol{\Delta}_0\right) \\
&= \mathbf{y}_t - \mathbf{h} - \mathbf{H}\tilde{\mathbf{w}}_{t|t-1} - \mathbf{H}\mathbf{F}\mathbf{M}_{t-1}\,\boldsymbol{\Delta}_0 \\
&= \tilde{\mathbf{e}}_t - \mathbf{H}\mathbf{F}\mathbf{M}_{t-1}\,\boldsymbol{\Delta}_0, \qquad\qquad \forall t = 1,2,\ldots,N. \qquad\qquad (2.D.7)
\end{aligned}
$$

□

As mentioned before, this observation, closely connected to the so-called fixed-but-unknown initialization, where we treat the elements of $\mathbf{d}$ as fixed parameters that we may estimate via maximum-likelihood, is due to Rosenberg (1973).

Obtaining $\log(f_{\mathbf{Y}_N|\mathbf{d}})$ as a function of $\log(f_{\mathbf{Y}_N|\mathbf{d}=\mathbf{0}})$, $\mathbf{d}$, $\mathbf{A}_d$, $\mathbf{s}_N$, and $\mathbf{S}_N$: In the following Proposition, we use Lemma 2.D.1 to obtain the analytical maximum-likelihood estimator for $\mathbf{d}$ and show that we may rewrite $\log(f_{\mathbf{Y}_N|\mathbf{d}})$ as a function of $\log(f_{\mathbf{Y}_N|\mathbf{d}=\mathbf{0}})$, $\mathbf{d}$, $\mathbf{A}_d$, $\mathbf{s}_N$, and $\mathbf{S}_N$:

Proposition 2.D.1. Suppose the initial state vector $\mathbf{w}_0$ can be written as

$$
\mathbf{w}_0 = \mathbf{a}_w + \mathbf{A}_\mathbf{w}\,\bar{\mathbf{w}}_0 + \mathbf{A}_\mathbf{d}\,\mathbf{d}, \qquad \bar{\mathbf{w}}_0 \sim \mathrm{N}(\bar{\boldsymbol{\mu}}_0, \bar{\mathbf{C}}_0), \qquad \mathbf{d} \sim \mathrm{N}(\boldsymbol{\delta}_0, \mathbf{D}_0),
$$

where $\bar{\mathbf{w}}_0 \in \mathbb{R}^{n_{\bar{w}}}$, $n_{\bar{w}} \leq n_w$ and $\mathbf{d} \in \mathbb{R}^{n_d}$, $n_d \leq n_w$ represent two independent random vectors. Suppose for SSM (2.2.1) the time t quantities generated by the Kalman recursion (2.2.4) initialized at $(\tilde{\boldsymbol{\mu}}_0, \tilde{\mathbf{C}}_0)$, with $\tilde{\boldsymbol{\mu}}_0 = \mathbf{a}_w + \mathbf{A}_\mathbf{w}\bar{\boldsymbol{\mu}}_0$ and $\tilde{\mathbf{C}}_0 = \mathbf{A}_\mathbf{w}\bar{\mathbf{C}}_0\mathbf{A}_\mathbf{w}^T$, are denoted by $\tilde{\boldsymbol{\mu}}_t$, $\tilde{\mathbf{C}}_t$, $\tilde{\mathbf{w}}_{t|t-1}$, $\tilde{\mathbf{P}}_{t|t-1}$, $\tilde{\mathbf{e}}_t$, $\tilde{\mathbf{U}}_t$ and $\tilde{\mathbf{K}}_t$. Then for the SSM (2.2.1) the conditional log-density of $\mathbf{Y}_N$ given $\mathbf{d}$ may be written as

$$
\log\left(f_{\mathbf{Y}_N|\mathbf{d}}\right) = \log\left(f_{\mathbf{Y}_N|\mathbf{d}=\mathbf{0}}\right) + \mathbf{d}^T\,\mathbf{A}_\mathbf{d}^T\,\mathbf{s}_N - \frac{1}{2}\,\mathbf{d}^T\,\mathbf{A}_\mathbf{d}^T\,\mathbf{S}_N\,\mathbf{A}_\mathbf{d}\,\mathbf{d},
$$

with

$$
\mathbf{s}_t = \sum_{i=1}^{N} \mathbf{E}_i^T \tilde{\mathbf{U}}_i^{-1}\,\tilde{\mathbf{e}}_i, \qquad \mathbf{S}_t = \sum_{i=1}^{N} \mathbf{E}_i^T \tilde{\mathbf{U}}_i^{-1} \mathbf{E}_i
$$

$$
\mathbf{E}_t = \mathbf{H}\mathbf{F}\mathbf{M}_{t-1}, \qquad \mathbf{M}_{t-1} = \prod_{j=1}^{t-1} \mathbf{J}_{t-j}, \qquad \mathbf{J}_t = \left(\mathbf{I} - \tilde{\mathbf{K}}_t\mathbf{H}\right)\mathbf{F}, \qquad \forall t = 1,2,\ldots,N.
$$

Further, the maximum-likelihood estimator of $\mathbf{d}$ for a given sample $\mathbf{Y}_N$ yields

$$
\hat{\mathbf{d}} = \arg\max_{\mathbf{d}} \log\left(f_{\mathbf{Y}_N|\mathbf{d}}\right) = \left(\mathbf{A}_\mathbf{d}^T\,\mathbf{S}_N\,\mathbf{A}_\mathbf{d}\right)^{-1}\,\mathbf{A}_\mathbf{d}^T\,\mathbf{s}_N,
$$

with

$$
\widehat{\mathrm{Var}}[\hat{\mathbf{d}}] = -\left(\frac{\partial^2 \log\left(f_{\mathbf{Y}_N|\mathbf{d}}\right)}{\partial\mathbf{d}\,\partial\mathbf{d}^T}\right)^{-1} = \left(\mathbf{A}_\mathbf{d}^T\,\mathbf{S}_N\,\mathbf{A}_\mathbf{d}\right)^{-1}.
$$

Proof:
Note that we may write the mean vector and the variance matrix of $\mathbf{w}_0$ given $\mathbf{d}$ as

$$
\boldsymbol{\mu}_{0|\mathbf{d}} := \mathrm{E}[\mathbf{w}_0|\mathbf{d}] = \tilde{\boldsymbol{\mu}}_0 + \bar{\mathbf{d}}, \qquad \mathbf{C}_{0|\mathbf{d}} := \mathrm{Var}[\mathbf{w}_0|\mathbf{d}] = \tilde{\mathbf{C}}_0,
$$

with $\bar{\mathbf{d}} = \mathbf{A}_\mathbf{d}\,\mathbf{d}$. Suppose for SSM (2.2.1) the time t quantities generated by the Kalman recursion (2.2.4) initialized at $(\boldsymbol{\mu}_{0|\mathbf{d}}, \mathbf{C}_{0|\mathbf{d}})$ are denoted by $\boldsymbol{\mu}_{t|\mathbf{d}}$, $\mathbf{C}_{t|\mathbf{d}}$, $\mathbf{w}_{t|t-1,\mathbf{d}}$, $\mathbf{P}_{t|t-1,\mathbf{d}}$, $\mathbf{e}_{t|\mathbf{d}}$, $\mathbf{U}_{t|\mathbf{d}}$ and $\mathbf{K}_{t|\mathbf{d}}$. Then the conditional log-density of $\mathbf{Y}_N$ given $\mathbf{d}$ follows from (2.2.6) as

$$
\log\left(f_{\mathbf{Y}_N|\mathbf{d}}\right) = -\frac{N\,n_y}{2}\,\log(2\pi) - \frac{1}{2}\sum_{t=1}^{N}\log\left|\mathbf{U}_{t|\mathbf{d}}\right| - \frac{1}{2}\sum_{t=1}^{N}\mathbf{e}_{t|\mathbf{d}}^T\,\mathbf{U}_{t|\mathbf{d}}^{-1}\,\mathbf{e}_{t|\mathbf{d}}.
$$

Hence, using Lemma 2.D.1 we may write

$$\log\left(f_{\mathbf{Y}_N|\mathbf{d}}\right) = -\frac{N\ n_y}{2}\ \log(2\pi)\ -\frac{1}{2}\ \sum_{t=1}^{N}\log\left|\tilde{\mathbf{U}}_t\right| - \frac{1}{2}\ \sum_{t=1}^{N}\left(\tilde{\mathbf{e}}_t - \mathbf{E}_t\ \bar{\mathbf{d}}\right)^T\ \tilde{\mathbf{U}}_t^{-1}\left(\tilde{\mathbf{e}}_t - \mathbf{E}_t\ \bar{\mathbf{d}}\right). \quad \text{(2.D.8)}$$

The first part of the proof is completed by rewriting the (2.D.8) to

$$\begin{aligned}
\log\left(f_{\mathbf{Y}_N|\mathbf{d}}\right) &= -\frac{N\ n_y}{2}\ \log(2\pi)\ -\frac{1}{2}\ \sum_{t=1}^{N}\log\left|\tilde{\mathbf{U}}_t\right| - \frac{1}{2}\ \sum_{t=1}^{N}\left(\tilde{\mathbf{e}}_t - \mathbf{E}_t\ \bar{\mathbf{d}}\right)^T\ \tilde{\mathbf{U}}_t^{-1}\left(\tilde{\mathbf{e}}_t - \mathbf{E}_t\ \bar{\mathbf{d}}\right) \\
&= \underbrace{-\frac{N\ n_y}{2}\ \log(2\pi)\ -\frac{1}{2}\sum_{t=1}^{N}\log\left|\tilde{\mathbf{U}}_t\right|\ -\frac{1}{2}\left(\sum_{t=1}^{N}\tilde{\mathbf{e}}_t^T\ \tilde{\mathbf{U}}_t^{-1}\ \tilde{\mathbf{e}}_t\right)}_{=\log\left(f_{\mathbf{Y}_N|\mathbf{d}=\mathbf{0}}\right)} \\
&\quad + \frac{1}{2}\left(\sum_{t=1}^{N}\tilde{\mathbf{e}}_t^T\ \tilde{\mathbf{U}}_t^{-1}\ \mathbf{E}_t\ \bar{\mathbf{d}}\right) + \frac{1}{2}\left(\sum_{t=1}^{N}\bar{\mathbf{d}}^T\ \mathbf{E}_t^T\ \tilde{\mathbf{U}}_t^{-1}\ \tilde{\mathbf{e}}_t\right) - \frac{1}{2}\left(\sum_{t=1}^{N}\bar{\mathbf{d}}^T\ \mathbf{E}_t^T\ \tilde{\mathbf{U}}_t^{-1}\ \mathbf{E}_t\ \bar{\mathbf{d}}\right) \\
&= \log\left(f_{\mathbf{Y}_N|\mathbf{d}=\mathbf{0}}\right) \\
&\quad + \frac{1}{2}\left(\sum_{t=1}^{N}\tilde{\mathbf{e}}_t^T\ \tilde{\mathbf{U}}_t^{-1}\ \mathbf{E}_t\right)\bar{\mathbf{d}} + \frac{1}{2}\bar{\mathbf{d}}^T\left(\sum_{t=1}^{N}\mathbf{E}_t^T\ \tilde{\mathbf{U}}_t^{-1}\ \tilde{\mathbf{e}}_t\right) - \frac{1}{2}\bar{\mathbf{d}}^T\left(\sum_{t=1}^{N}\mathbf{E}_t^T\ \tilde{\mathbf{U}}_t^{-1}\ \mathbf{E}_t\right)\bar{\mathbf{d}} \\
&= \log\left(f_{\mathbf{Y}_N|\mathbf{d}=\mathbf{0}}\right)\ \underbrace{+\frac{1}{2}\mathbf{s}_N^T\bar{\mathbf{d}} + \frac{1}{2}\bar{\mathbf{d}}^T\ \mathbf{s}_N}_{=\bar{\mathbf{d}}^T\mathbf{s}_N,\ \text{since}\ \left(\bar{\mathbf{d}}^T\mathbf{s}_N\right)\in\mathbb{R}^{1\times 1}.}\ -\frac{1}{2}\bar{\mathbf{d}}^T\ \mathbf{S}_N\ \bar{\mathbf{d}} \\
&= \log\left(f_{\mathbf{Y}_N|\mathbf{d}=\mathbf{0}}\right)\ + \bar{\mathbf{d}}^T\mathbf{s}_N - \frac{1}{2}\bar{\mathbf{d}}^T\ \mathbf{S}_N\ \bar{\mathbf{d}} \\
&= \log\left(f_{\mathbf{Y}_N|\mathbf{d}=\mathbf{0}}\right)\ + \mathbf{d}^T\mathbf{A}_\mathbf{d}^T\ \mathbf{s}_N - \frac{1}{2}\ \mathbf{d}^T\ \mathbf{A}_\mathbf{d}^T\ \mathbf{S}_N\ \mathbf{A}\ \mathbf{d}. \qquad \text{(2.D.9)}
\end{aligned}$$

Since $\mathbf{s}_N$, $\mathbf{S}_N$, $\mathbf{A}_\mathbf{d}$ and $\log\left(f_{\mathbf{Y}_N|\mathbf{d}=\mathbf{0}}\right)$ do not depend on $\mathbf{d}$, using matrix differentiating rules (see e.g. Lütkepohl (2007, pp. 664-671)) the first and second order derivatives of $\log\left(f_{\mathbf{Y}_N|\mathbf{d}}\right)$ with respect to $\mathbf{d}$ yield

$$\frac{\partial\log\left(f_{\mathbf{Y}_N|\mathbf{d}}\right)}{\partial\mathbf{d}} = \mathbf{A}_\mathbf{d}^T\ \mathbf{s}_N - \mathbf{A}_\mathbf{d}^T\ \mathbf{S}_N\ \mathbf{A}_\mathbf{d}\ \mathbf{d}, \qquad \text{(2.D.10a)} \qquad \frac{\partial\log\left(f_{\mathbf{Y}_N|\mathbf{d}}\right)}{\partial\mathbf{d}\ \partial\mathbf{d}^T} = -\mathbf{A}_\mathbf{d}^T\ \mathbf{S}_N\ \mathbf{A}_\mathbf{d}. \qquad \text{(2.D.10b)}$$

If the matrix $\mathbf{A}_\mathbf{d}^T\ \mathbf{S}_N\ \mathbf{A}_\mathbf{d}$ has full rank, equating (2.D.10a) to zero yields the maximum-likelihood estimator for $\mathbf{d}$ given $(\mathbf{Y}_N)$

$$\hat{\mathbf{d}} = \arg\max_{\mathbf{d}}\log\left(f_{\mathbf{Y}_N|\mathbf{d}}\right) = \left(\mathbf{A}_\mathbf{d}^T\ \mathbf{S}_N\ \mathbf{A}_\mathbf{d}\right)^{-1}\ \mathbf{A}_\mathbf{d}^T\ \mathbf{s}_N,$$

with

$$\widehat{\text{Var}}[\hat{\mathbf{d}}] = -\left(\frac{\partial^2\log\left(f_{\mathbf{Y}_N|\mathbf{d}}\right)}{\partial\mathbf{d}\ \partial\mathbf{d}^T}\right)^{-1} = \left(\mathbf{A}_\mathbf{d}^T\ \mathbf{S}_N\ \mathbf{A}_\mathbf{d}\right)^{-1}.$$

□

Derivation of (2.2.15) and (2.2.16): Using the results of Lemma 2.D.1 and Proposition 2.D.1, we may ultimately obtain the formulas of the AKF (2.2.15) and the log-density $\log(f_{\mathbf{Y}_N})$ given in (2.2.16). Therefore, let us establish the following Proposition:

Proposition 2.D.2. Suppose the initial state vector $\mathbf{w}_0$ can be written as

$$\mathbf{w}_0 = \mathbf{a}_w + \mathbf{A_w}\,\bar{\mathbf{w}}_0 + \mathbf{A_d}\,\mathbf{d}, \qquad \bar{\mathbf{w}}_0 \sim \mathrm{N}(\bar{\boldsymbol{\mu}}_0, \bar{\mathbf{C}}_0), \qquad \mathbf{d} \sim \mathrm{N}(\boldsymbol{\delta}_0, \mathbf{D}_0),$$

where $\bar{\mathbf{w}}_0 \in \mathbb{R}^{n_{\bar{w}}}$, $n_{\bar{w}} \leq n_w$ and $\mathbf{d} \in \mathbb{R}^{n_d}$, $n_d \leq n_w$ represent two independent random vectors. Suppose for SSM (2.2.1) the time t quantities generated by the Kalman recursion (2.2.4) initialized at $(\tilde{\boldsymbol{\mu}}_0, \tilde{\mathbf{C}}_0)$, with $\tilde{\boldsymbol{\mu}}_0 = \mathbf{a}_w + \mathbf{A_w}\bar{\boldsymbol{\mu}}_0$ and $\tilde{\mathbf{C}}_0 = \mathbf{A_w}\bar{\mathbf{C}}_0\mathbf{A_w}^T$, are denoted by $\tilde{\boldsymbol{\mu}}_t$, $\tilde{\mathbf{C}}_t$, $\tilde{\mathbf{w}}_{t|t-1}$, $\tilde{\mathbf{P}}_{t|t-1}$, $\tilde{\mathbf{e}}_t$, $\tilde{\mathbf{U}}_t$ and $\tilde{\mathbf{K}}_t$. Suppose the variance matrix $\mathbf{D}_0$ is positive definite. Then for the SSM (2.2.1) the conditional distributions of $\mathbf{d}$ and $\mathbf{w}_t$ given $\mathbf{Y}_t$ are Gaussian with mean vectors

$$\begin{aligned}
\boldsymbol{\delta}_t &:= \mathrm{E}[\mathbf{d}|\mathbf{Y}_t] = \left(\mathbf{D}_0^{-1} + \mathbf{A_d}^T\,\mathbf{S}_t\,\mathbf{A_d}\right)^{-1}\left(\mathbf{D}_0^{-1}\boldsymbol{\delta}_0 + \mathbf{A_d}^T\,\mathbf{s}_t\right),\\
\boldsymbol{\mu}_t &:= \mathrm{E}[\mathbf{w}_t|\mathbf{Y}_t] = \tilde{\boldsymbol{\mu}}_t + \mathbf{M}_t\mathbf{A}_d\,\boldsymbol{\delta}_t,
\end{aligned}$$

and variance matrices:

$$\begin{aligned}
\mathbf{D}_t &:= \mathrm{Var}[\mathbf{d}|\mathbf{Y}_t] = \left(\mathbf{D}_0^{-1} + \mathbf{A_d}^T\,\mathbf{S}_t\,\mathbf{A_d}\right)^{-1},\\
\mathbf{C}_t &:= \mathrm{Var}[\mathbf{w}_t|\mathbf{Y}_t] = \tilde{\mathbf{C}}_t + \mathbf{M}_t\mathbf{A}_d\mathbf{D}_t\mathbf{A}_d^T\mathbf{M}_t^T,
\end{aligned}$$

where

$$\mathbf{s}_t = \sum_{i=1}^{t}\mathbf{E}_i^T\tilde{\mathbf{U}}_i^{-1}\,\tilde{\mathbf{e}}_i, \qquad \mathbf{S}_t = \sum_{i=1}^{t}\mathbf{E}_i^T\tilde{\mathbf{U}}_i^{-1}\mathbf{E}_i \qquad \text{and}$$

$$\mathbf{E}_t = \mathbf{HFM}_{t-1}, \qquad \mathbf{M}_{t-1} = \prod_{j=1}^{t-1}\mathbf{J}_{t-j}, \quad \mathbf{J}_t = \left(\mathbf{I} - \tilde{\mathbf{K}}_t\mathbf{H}\right)\mathbf{F}, \quad \forall t = 1, 2, \ldots, N.$$

Further, the log-density of $\mathbf{Y}_N$ may be written as

$$\begin{aligned}
\log(f_{\mathbf{Y}_N}) = \log\left(f_{\mathbf{Y}_N|\mathbf{d}=\mathbf{0}}\right) - \frac{1}{2}\log|\mathbf{I} + \mathbf{D}_0\,\mathbf{A_d}^T\,\mathbf{S}_N\,\mathbf{A_d}| - \frac{1}{2}\boldsymbol{\delta}_0^T\mathbf{D}_0^{-1}\boldsymbol{\delta}_0\\
+ \frac{1}{2}(\mathbf{D}_0^{-1}\boldsymbol{\delta}_0 + \mathbf{A_d}^T\,\mathbf{s}_N)^T(\mathbf{D}_0^{-1} + \mathbf{A_d}^T\,\mathbf{S}_N\,\mathbf{A_d})^{-1}(\mathbf{D}_0^{-1}\boldsymbol{\delta}_0 + \mathbf{A_d}^T\,\mathbf{s}_N).
\end{aligned}$$

Proof:
From Lemma 2.A.1 and the linearity of the SSM (2.2.1) follows that $\mathbf{d}$ given $\mathbf{Y}_t$ is normally distributed with the corresponding log-density

$$\log\left(f_{\mathbf{d}|\mathbf{Y}_t}\right) = -\frac{n_d}{2}\log(2\pi)\; - \frac{1}{2}\log|\mathbf{D}_t|\; - \frac{1}{2}(\mathbf{d} - \boldsymbol{\delta}_t)^T\;\mathbf{D}_t^{-1}\;(\mathbf{d} - \boldsymbol{\delta}_t), \tag{2.D.11}$$

where $\boldsymbol{\delta}_t := \mathrm{E}[\mathbf{d}|\mathbf{Y}_t]$ and $\mathbf{D}_t := \mathrm{Var}[\mathbf{d}|\mathbf{Y}_t]$ denote mean vector and the variance matrix of $\mathbf{d}$ given $\mathbf{Y}_t$. Since $\mathbf{d}$ given $\mathbf{Y}_t$ is normally distributed, the mode and the mean of $\log\left(f_{\mathbf{d}|\mathbf{Y}_t}\right)$ coincide and we can write

$$\boldsymbol{\delta}_t = \arg\max_{\mathbf{d}}\;\log\left(f_{\mathbf{d}|\mathbf{Y}_t}\right).$$

Additionally from (2.D.11) and matrix differentiating rules (see e.g. Lütkepohl (2007, pp. 664-671)) follows that the Hessian matrix of $\log\left(f_{\mathbf{d}|\mathbf{Y}_t}\right)$ with respect to $\mathbf{d}$ is

$$\frac{\partial^2\log\left(f_{\mathbf{d}|\mathbf{Y}_t}\right)}{\partial\mathbf{d}\,\partial\mathbf{d}^T} = \frac{\partial}{\partial\mathbf{d}}\left(-\frac{1}{2}\frac{\partial\,(\mathbf{d} - \boldsymbol{\delta}_t)^T\;\mathbf{D}_t^{-1}\;(\mathbf{d} - \boldsymbol{\delta}_t)}{\partial\mathbf{d}^T}\right)$$

$$
\begin{aligned}
&= \frac{\partial}{\partial \mathbf{d}} \left(-\frac{1}{2} \frac{\partial \left(\boldsymbol{\delta}_t - \mathbf{d}\right)^T \mathbf{D}_t^{-1} \left(\boldsymbol{\delta}_t - \mathbf{d}\right)}{\partial \mathbf{d}^T} \right) \\
&= \frac{\partial}{\partial \mathbf{d}} \left(-\frac{1}{2} \left(-2 \left(\boldsymbol{\delta}_t - \mathbf{d}\right)^T \mathbf{D}_t^{-1} \right) \right) \\
&= \frac{\partial}{\partial \mathbf{d}} \left(\left(\boldsymbol{\delta}_t - \mathbf{d}\right)^T \mathbf{D}_t^{-1} \right) \\
&= -\mathbf{D}_t^{-1},
\end{aligned}
$$

and the variance matrix $\mathbf{D}_t$ yields

$$
\mathbf{D}_t = -\left(\frac{\partial^2 \log\left(f_{\mathbf{d}|\mathbf{Y}_t}\right)}{\partial \mathbf{d}\, \partial \mathbf{d}^T} \right)^{-1}. \tag{2.D.12}
$$

Hence, to prove the first part of Proposition 2.D.2 we need to obtain the first and second order derivatives of $\log\left(f_{\mathbf{d}|\mathbf{Y}_t}\right)$ with respect to $\mathbf{d}$. To do so, we first use the Bayes Theorem to rewrite $\log\left(f_{\mathbf{d}|\mathbf{Y}_t}\right)$ as

$$
\begin{aligned}
\log\left(f_{\mathbf{d}|\mathbf{Y}_t}\right) &= \log\left(\frac{f_{\mathbf{Y}_t|\mathbf{d}} \cdot f_{\mathbf{d}}}{f_{\mathbf{Y}_t}} \right) \\
&= \log(f_{\mathbf{d}}) + \log\left(f_{\mathbf{Y}_t|\mathbf{d}}\right) - \log\left(f_{\mathbf{Y}_t}\right).
\end{aligned} \tag{2.D.13}
$$

Note that the first term on the right-hand side of (2.D.13) is the log-density of $\mathbf{d}$, which yields

$$
\log(f_{\mathbf{d}}) = -\frac{n_d}{2} \log(2\pi) \; - \frac{1}{2} \log|\mathbf{D}_0| \; - \frac{1}{2} (\mathbf{d} - \boldsymbol{\delta}_0)^T \; \mathbf{D}_0^{-1} \; (\mathbf{d} - \boldsymbol{\delta}_0). \tag{2.D.14}
$$

Differentiating equation (2.D.14) with respect to $\mathbf{d}$ we get

$$
\begin{aligned}
\frac{\partial \log(f_{\mathbf{d}})}{\partial \mathbf{d}} &= -\frac{1}{2} \frac{\partial}{\partial \mathbf{d}} \left((\mathbf{d} - \boldsymbol{\delta}_0)^T \; \mathbf{D}_0^{-1} \; (\mathbf{d} - \boldsymbol{\delta}_0) \right) \\
&= -\frac{1}{2} \frac{\partial}{\partial \mathbf{d}} \left((\boldsymbol{\delta}_0 - \mathbf{d})^T \; \mathbf{D}_0^{-1} \; (\boldsymbol{\delta}_0 - \mathbf{d}) \right) \\
&= -\frac{1}{2} \left(-2\mathbf{D}_0^{-1} (\boldsymbol{\delta}_0 - \mathbf{d}) \right) \\
&= \mathbf{D}_0^{-1} (\boldsymbol{\delta}_0 - \mathbf{d}) \\
&= \mathbf{D}_0^{-1} \boldsymbol{\delta}_0 - \mathbf{D}_0^{-1} \mathbf{d}.
\end{aligned} \tag{2.D.15}
$$

Furthermore, we already obtained the first order derivatives of the conditional log-likelihood $\log\left(f_{\mathbf{Y}_t|\mathbf{d}}\right)$ with respect to $\mathbf{d}$ in equation (2.D.10a). Finally, we get the first order derivatives of $\log\left(f_{\mathbf{Y}_t}\right)$ with respect to $\mathbf{d}$ as

$$
\frac{\partial \log\left(f_{\mathbf{Y}_t}\right)}{\partial \mathbf{d}} = 0, \tag{2.D.16}
$$

since we can obtain $\log\left(f_{\mathbf{Y}_t}\right)$ without knowledge of $\mathbf{d}$ from equation (2.2.6) by initializing the Kalman recursion (2.2.4) at $\left(\boldsymbol{\mu}_0, \mathbf{C}_0\right)$ with $\boldsymbol{\mu}_0 = \mathbf{a}_w + \mathbf{A}_w \, \bar{\boldsymbol{\mu}}_0 + \mathbf{A}_d \, \boldsymbol{\delta}_0$ and $\mathbf{C}_0 = \mathbf{A}_w \, \bar{\mathbf{C}}_0 \, \mathbf{A}_w^T + \mathbf{A}_d \, \mathbf{D}_0 \, \mathbf{A}_d^T$. Hence, from equations (2.D.10a), (2.D.13), (2.D.15) and (2.D.16) we receive

$$
\frac{\partial \log\left(f_{\mathbf{d}|\mathbf{Y}_t}\right)}{\partial \mathbf{d}} = \frac{\partial \log(f_{\mathbf{d}})}{\partial \mathbf{d}} + \frac{\partial \log\left(f_{\mathbf{Y}_t|\mathbf{d}}\right)}{\partial \mathbf{d}} - \frac{\partial \log\left(f_{\mathbf{Y}_t}\right)}{\partial \mathbf{d}}
$$

$$
\begin{aligned}
&= \mathbf{D}_0^{-1}\boldsymbol{\delta}_0 - \mathbf{D}_0^{-1}\mathbf{d} + \mathbf{A}_\mathbf{d}^T\,\mathbf{s}_t - \mathbf{A}_\mathbf{d}^T\,\mathbf{S}_t\,\mathbf{A}_\mathbf{d}\,\mathbf{d} \\
&= \mathbf{D}_0^{-1}\boldsymbol{\delta}_0 + \mathbf{A}_\mathbf{d}^T\,\mathbf{s}_t - \left(\mathbf{D}_0^{-1} + \mathbf{A}_\mathbf{d}^T\,\mathbf{S}_t\,\mathbf{A}_\mathbf{d}\right)\mathbf{d},
\end{aligned} \tag{2.D.17}
$$

and the mean vector $\boldsymbol{\delta}_t$ of $\mathbf{d}$ given $\mathbf{Y}_t$ is obtained as

$$
\begin{aligned}
\boldsymbol{\delta}_t &= \arg\max_{\mathbf{d}}\ \log\left(f_{\mathbf{d}|\mathbf{Y}_t}\right) \\
&= \left(\mathbf{D}_0^{-1} + \mathbf{A}_\mathbf{d}^T\,\mathbf{S}_t\,\mathbf{A}_\mathbf{d}\right)^{-1}\left(\mathbf{D}_0^{-1}\boldsymbol{\delta}_0 + \mathbf{A}_\mathbf{d}^T\,\mathbf{s}_t\right),
\end{aligned}
$$

by equating (2.D.17) to zero and solving with respect to $\mathbf{d}$. To obtain $\mathbf{D}_t$, we compute the Hessian of $\log\left(f_{\mathbf{d}|\mathbf{Y}_t}\right)$ with respect to $\mathbf{d}$ by differentiating (2.D.17) with respect to $\mathbf{d}^T$, which results in

$$
\frac{\partial \log\left(f_{\mathbf{d}|\mathbf{Y}_t}\right)}{\partial \mathbf{d}\,\partial \mathbf{d}^T} = -\left(\mathbf{D}_0^{-1} + \mathbf{A}_\mathbf{d}^T\,\mathbf{S}_t\,\mathbf{A}_\mathbf{d}\right). \tag{2.D.18}
$$

Thus, due to (2.D.12), the variance matrix $\mathbf{D}_t$ of $\mathbf{d}$ given $\mathbf{Y}_t$ equals

$$
\mathbf{D}_t = -\left(\frac{\partial^2 \log\left(f_{\mathbf{d}|\mathbf{Y}_t}\right)}{\partial \mathbf{d}\,\partial \mathbf{d}^T}\right)^{-1} = \left(\mathbf{D}_0^{-1} + \mathbf{A}_\mathbf{d}^T\,\mathbf{S}_t\,\mathbf{A}_\mathbf{d}\right)^{-1}.
$$

Moreover, we can state that $\begin{pmatrix}\mathbf{d}\\ \mathbf{w}_t\end{pmatrix}$ given $\mathbf{Y}_t$ is normally distributed with mean vector

$$
\mathrm{E}\left(\begin{matrix}\mathbf{d}\\ \mathbf{w}_t\end{matrix}\,\middle|\,\mathbf{Y}_t\right) = \begin{pmatrix}\boldsymbol{\delta}_t\\ \tilde{\boldsymbol{\mu}}_t + \mathbf{M}_t\mathbf{A}_d\,\boldsymbol{\delta}_t\end{pmatrix} \tag{2.D.19}
$$

and variance matrix

$$
\mathrm{Var}\left(\begin{matrix}\mathbf{d}\\ \mathbf{w}_t\end{matrix}\,\middle|\,\mathbf{Y}_t\right) = \begin{pmatrix}\mathbf{D}_t & \mathbf{D}_t\mathbf{A}_d^T\mathbf{M}_t^T\\ \mathbf{M}_t\mathbf{A}_d\mathbf{D}_t & \tilde{\mathbf{C}}_t + \mathbf{M}_t\mathbf{A}_d\mathbf{D}_t\mathbf{A}_d^T\mathbf{M}_t^T\end{pmatrix}. \tag{2.D.20}
$$

This may be seen from the fact that we can write the joint density function of $\mathbf{d}$ and $\mathbf{w}_t$ given $\mathbf{Y}_t$ as

$$
\begin{aligned}
f_{\mathbf{d},\mathbf{w}_t|\mathbf{Y}_t} =& f_{\mathbf{d}|\mathbf{Y}_t}\cdot f_{\mathbf{w}_t|\mathbf{d},\mathbf{Y}_t} \\
=& (2\pi)^{-\frac{n_p}{2}}\ |\mathbf{D}_t|^{-\frac{1}{2}}\ \exp\left(-\frac{1}{2}(\mathbf{d}-\boldsymbol{\delta}_t)^T\ \mathbf{D}_t^{-1}\ (\mathbf{d}-\boldsymbol{\delta}_t)\right) \\
&\times (2\pi)^{-\frac{n_w}{2}}\ \left|\tilde{\mathbf{C}}_t\right|^{-\frac{1}{2}}\ \exp\left(-\frac{1}{2}\left(\mathbf{w}_t - \tilde{\boldsymbol{\mu}}_t - \mathbf{M}_t\mathbf{A}_d\mathbf{d}\right)^T\ \tilde{\mathbf{C}}_t^{-1}\ \left(\mathbf{w}_t - \tilde{\boldsymbol{\mu}}_t - \mathbf{M}_t\mathbf{A}_d\mathbf{d}\right)\right) \\
=& (2\pi)^{-\frac{n_p+n_w}{2}}\left|\begin{pmatrix}\mathbf{D}_t & \mathbf{0}\\ \mathbf{0} & \tilde{\mathbf{C}}_t\end{pmatrix}\right|^{-\frac{1}{2}} \\
&\times \exp\left[-\frac{1}{2}\begin{pmatrix}\mathbf{d}-\boldsymbol{\delta}_t\\ \mathbf{w}_t - \tilde{\boldsymbol{\mu}}_t - \mathbf{M}_t\mathbf{A}_d\mathbf{d}\end{pmatrix}^T\begin{pmatrix}\mathbf{D}_t^{-1} & \mathbf{0}\\ \mathbf{0} & \tilde{\mathbf{C}}_t^{-1}\end{pmatrix}\begin{pmatrix}\mathbf{d}-\boldsymbol{\delta}_t\\ \mathbf{w}_t - \tilde{\boldsymbol{\mu}}_t - \mathbf{M}_t\mathbf{A}_d\mathbf{d}\end{pmatrix}\right] \\
=& (2\pi)^{-\frac{n_p+n_w}{2}}\left(\underbrace{\left|\begin{pmatrix}\mathbf{I} & \mathbf{0}\\ \mathbf{M}_t\mathbf{A}_d & \mathbf{I}\end{pmatrix}\right|}_{=1}\left|\begin{pmatrix}\mathbf{D}_t & \mathbf{0}\\ \mathbf{0} & \tilde{\mathbf{C}}_t\end{pmatrix}\right|\underbrace{\left|\begin{pmatrix}\mathbf{I} & \mathbf{A}_d^T\mathbf{M}_t^T\\ \mathbf{0} & \mathbf{I}\end{pmatrix}\right|}_{=1}\right)^{-\frac{1}{2}}
\end{aligned}
$$

$$
\begin{aligned}
&\times \exp\left[-\frac{1}{2}\begin{pmatrix} \mathbf{d}-\boldsymbol{\delta}_t \\ \mathbf{w}_t-\tilde{\boldsymbol{\mu}}_t-\mathbf{M}_t\mathbf{A}_d\mathbf{d}\end{pmatrix}^T \underbrace{\begin{pmatrix} \mathbf{I} & \mathbf{A}_d^T\mathbf{M}_t^T \\ \mathbf{0} & \mathbf{I}\end{pmatrix}\begin{pmatrix} \mathbf{I} & \mathbf{A}_d^T\mathbf{M}_t^T \\ \mathbf{0} & \mathbf{I}\end{pmatrix}^{-1}}_{=\mathbf{I}} \right. \\
&\qquad \left. \times \begin{pmatrix} \mathbf{D}_t & \mathbf{0} \\ \mathbf{0} & \tilde{\mathbf{C}}_t\end{pmatrix}^{-1} \underbrace{\begin{pmatrix} \mathbf{I} & \mathbf{0} \\ \mathbf{M}_t\mathbf{A}_d & \mathbf{I}\end{pmatrix}^{-1}\begin{pmatrix} \mathbf{I} & \mathbf{0} \\ \mathbf{M}_t\mathbf{A}_d & \mathbf{I}\end{pmatrix}}_{=\mathbf{I}} \begin{pmatrix} \mathbf{d}-\boldsymbol{\delta}_t \\ \mathbf{w}_t-\tilde{\boldsymbol{\mu}}_t-\mathbf{M}_t\mathbf{A}_d\mathbf{d}\end{pmatrix} \right] \\
=&(2\pi)^{-\frac{n_p+n_w}{2}} \left| \begin{pmatrix} \mathbf{I} & \mathbf{0} \\ \mathbf{M}_t\mathbf{A}_d & \mathbf{I}\end{pmatrix}\begin{pmatrix} \mathbf{D}_t & \mathbf{0} \\ \mathbf{0} & \tilde{\mathbf{C}}_t\end{pmatrix}\begin{pmatrix} \mathbf{I} & \mathbf{A}_d^T\mathbf{M}_t^T \\ \mathbf{0} & \mathbf{I}\end{pmatrix} \right|^{-\frac{1}{2}} \\
&\times \exp\left[-\frac{1}{2}\begin{pmatrix} \mathbf{d}-\boldsymbol{\delta}_t \\ \mathbf{M}_t\mathbf{A}_d\mathbf{d}-\mathbf{M}_t\mathbf{A}_d\boldsymbol{\delta}_t+\mathbf{w}_t-\tilde{\boldsymbol{\mu}}_t-\mathbf{M}_t\mathbf{A}_d\mathbf{d}\end{pmatrix}^T \right. \\
&\qquad \times \left(\begin{pmatrix} \mathbf{I} & \mathbf{0} \\ \mathbf{M}_t\mathbf{A}_d & \mathbf{I}\end{pmatrix}\begin{pmatrix} \mathbf{D}_t & \mathbf{0} \\ \mathbf{0} & \tilde{\mathbf{C}}_t\end{pmatrix}\begin{pmatrix} \mathbf{I} & \mathbf{A}_d^T\mathbf{M}_t^T \\ \mathbf{0} & \mathbf{I}\end{pmatrix} \right)^{-1} \\
&\qquad \left. \times \begin{pmatrix} \mathbf{d}-\boldsymbol{\delta}_t \\ \mathbf{M}_t\mathbf{A}_d\mathbf{d}-\mathbf{M}_t\mathbf{A}_d\boldsymbol{\delta}_t+\mathbf{w}_t-\tilde{\boldsymbol{\mu}}_t-\mathbf{M}_t\mathbf{A}_d\mathbf{d}\end{pmatrix} \right] \\
=&(2\pi)^{-\frac{n_p+n_w}{2}} \left| \begin{pmatrix} \mathbf{D}_t & \mathbf{D}_t\mathbf{A}_d^T\mathbf{M}_t^T \\ \mathbf{M}_t\mathbf{A}_d\mathbf{D}_t & \tilde{\mathbf{C}}_t+\mathbf{M}_t\mathbf{A}_d\mathbf{D}_t\mathbf{A}_d^T\mathbf{M}_t^T\end{pmatrix} \right|^{-\frac{1}{2}} \\
&\times \exp\left[-\frac{1}{2}\begin{pmatrix} \mathbf{d}-\boldsymbol{\delta}_t \\ \mathbf{w}_t-\left(\tilde{\boldsymbol{\mu}}_t+\mathbf{M}_t\mathbf{A}_d\boldsymbol{\delta}_t\right)\end{pmatrix}^T \begin{pmatrix} \mathbf{D}_t & \mathbf{D}_t\mathbf{A}_d^T\mathbf{M}_t^T \\ \mathbf{M}_t\mathbf{A}_d\mathbf{D}_t & \tilde{\mathbf{C}}_t+\mathbf{M}_t\mathbf{A}_d\mathbf{D}_t\mathbf{A}_d^T\mathbf{M}_t^T\end{pmatrix}^{-1} \right. \\
&\qquad \left. \times \begin{pmatrix} \mathbf{d}-\boldsymbol{\delta}_t \\ \mathbf{w}_t-\left(\tilde{\boldsymbol{\mu}}_t+\mathbf{M}_t\mathbf{A}_d\boldsymbol{\delta}_t\right)\end{pmatrix} \right].
\end{aligned}
$$

Consequently, it follows from (2.D.19) and (2.D.20) that $\mathbf{w}_t$ given $\mathbf{Y}_t$ is normally distributed with mean vector $\boldsymbol{\mu}_t$ and variance matrix $\mathbf{C}_t$ defined by

$$
\begin{aligned}
\boldsymbol{\mu}_t &:= \mathrm{E}[\mathbf{w}_t|\mathbf{Y}_t] = \tilde{\boldsymbol{\mu}}_t + \mathbf{M}_t\mathbf{A}_d\boldsymbol{\delta}_t, \\
\mathbf{C}_t &:= \mathrm{Var}[\mathbf{w}_t|\mathbf{Y}_t] = \tilde{\mathbf{C}}_t + \mathbf{M}_t\mathbf{A}_d\mathbf{D}_t\mathbf{A}_d^T\mathbf{M}_t^T.
\end{aligned}
$$

The claim about log-density of $\mathbf{Y}_N$ then follows directly from equations (2.D.9), (2.D.11), (2.D.13) and (2.D.14):

$$
\begin{aligned}
\log(f_{\mathbf{Y}_N}) &= \log(f_{\mathbf{Y}_N|\mathbf{d}}) + \log(f_{\mathbf{d}}) - \log(f_{\mathbf{d}|\mathbf{Y}_N}) \\
&= \underbrace{\log\left(f_{\mathbf{Y}_N|\mathbf{d}=\mathbf{0}}\right) + \mathbf{d}^T\,\mathbf{A}_{\mathbf{d}}^T\,\mathbf{s}_N\, - \frac{1}{2}\,\mathbf{d}^T\,\mathbf{A}_{\mathbf{d}}^T\,\mathbf{S}_N\,\mathbf{A}_{\mathbf{d}}\,\mathbf{d}}_{\log(f_{\mathbf{Y}_N|\mathbf{d}}),\text{ from (2.D.9).}} \\
&\quad \underbrace{-\frac{n_d}{2}\log(2\pi)\, -\frac{1}{2}\log|\mathbf{D}_0|\, -\frac{1}{2}(\mathbf{d}-\boldsymbol{\delta}_0)^T\,\mathbf{D}_0^{-1}\,(\mathbf{d}-\boldsymbol{\delta}_0)}_{=\log(f_{\mathbf{d}}),\text{ from (2.D.14).}} \\
&\quad \underbrace{-\left(-\frac{n_d}{2}\log(2\pi)\, -\frac{1}{2}\log|\mathbf{D}_N|\, -\frac{1}{2}(\mathbf{d}-\boldsymbol{\delta}_N)^T\,\mathbf{D}_N^{-1}\,(\mathbf{d}-\boldsymbol{\delta}_N)\right)}_{=\log(f_{\mathbf{d}|\mathbf{Y}_N}),\text{ from (2.D.11).}} \\
&= \log\left(f_{\mathbf{Y}_N|\mathbf{d}=\mathbf{0}}\right) - \frac{1}{2}\log|\mathbf{D}_0| + \frac{1}{2}\log|\mathbf{D}_N| + \mathbf{d}^T\,\mathbf{A}_{\mathbf{d}}^T\,\mathbf{s}_N\, - \frac{1}{2}\,\mathbf{d}^T\,\mathbf{A}_{\mathbf{d}}^T\,\mathbf{S}_N\,\mathbf{A}_{\mathbf{d}}\,\mathbf{d} \\
&\quad - \frac{1}{2}(\mathbf{d}-\boldsymbol{\delta}_0)^T\,\mathbf{D}_0^{-1}\,(\mathbf{d}-\boldsymbol{\delta}_0) \\
&\quad + \frac{1}{2}(\mathbf{d}-\boldsymbol{\delta}_N)^T\,\mathbf{D}_N^{-1}\,(\mathbf{d}-\boldsymbol{\delta}_N)
\end{aligned}
$$

$$
\begin{aligned}
&= \log\left(f_{\mathbf{Y}_N|\mathbf{d}=\mathbf{0}}\right) - \frac{1}{2}\left(\log|\mathbf{D}_0| - \log|\mathbf{D}_N|\right) + \mathbf{d}^T\,\mathbf{A}_\mathbf{d}^T\,\mathbf{s}_N\; - \frac{1}{2}\,\mathbf{d}^T\,\mathbf{A}_\mathbf{d}^T\,\mathbf{S}_N\,\mathbf{A}_\mathbf{d}\,\mathbf{d} \\
&\quad - \frac{1}{2}\mathbf{d}^T\mathbf{D}_0^{-1}\mathbf{d} \underbrace{+\frac{1}{2}\mathbf{d}^T\mathbf{D}_0^{-1}\boldsymbol{\delta}_0 + \frac{1}{2}\boldsymbol{\delta}_0^T\mathbf{D}_0^{-1}\mathbf{d}}_{=\mathbf{d}^T\left(\mathbf{D}_0^{-1}\boldsymbol{\delta}_0\right),\ \text{since}\ \left(\boldsymbol{\delta}_0^T\mathbf{D}_0^{-1}\mathbf{d}\right)\in\mathbb{R}.} - \frac{1}{2}\boldsymbol{\delta}_0^T\mathbf{D}_0^{-1}\boldsymbol{\delta}_0 \\
&\quad + \frac{1}{2}\mathbf{d}^T\mathbf{D}_N^{-1}\mathbf{d} \underbrace{-\frac{1}{2}\mathbf{d}^T\mathbf{D}_N^{-1}\boldsymbol{\delta}_N - \frac{1}{2}\boldsymbol{\delta}_N^T\mathbf{D}_N^{-1}\mathbf{d}}_{=-\mathbf{d}^T\left(\mathbf{D}_N^{-1}\boldsymbol{\delta}_N\right),\ \text{since}\ \left(\boldsymbol{\delta}_N^T\mathbf{D}_N^{-1}\mathbf{d}\right)\in\mathbb{R}.} + \frac{1}{2}\boldsymbol{\delta}_N^T\mathbf{D}_N^{-1}\boldsymbol{\delta}_N \\
&= \log\left(f_{\mathbf{Y}_N|\mathbf{d}=\mathbf{0}}\right) - \frac{1}{2}\log\left|\mathbf{D}_0\mathbf{D}_N^{-1}\right| - \frac{1}{2}\boldsymbol{\delta}_0^T\mathbf{D}_0^{-1}\boldsymbol{\delta}_0 + \frac{1}{2}\boldsymbol{\delta}_N^T\mathbf{D}_N^{-1}\boldsymbol{\delta}_N \\
&\quad - \frac{1}{2}\underbrace{\left(\mathbf{d}^T\,\mathbf{A}_\mathbf{d}^T\,\mathbf{S}_N\,\mathbf{A}_\mathbf{d}\,\mathbf{d} + \mathbf{d}^T\mathbf{D}_0^{-1}\mathbf{d}\right)}_{=\mathbf{d}^T\left(\mathbf{D}_0^{-1}+\mathbf{A}_\mathbf{d}^T\,\mathbf{S}_N\,\mathbf{A}_\mathbf{d}\right)\mathbf{d}} + \underbrace{\mathbf{d}^T\left(\mathbf{D}_0^{-1}\boldsymbol{\delta}_0\right) + \mathbf{d}^T\,\mathbf{A}_\mathbf{d}^T\,\mathbf{s}_N}_{=\mathbf{d}^T\left(\mathbf{D}_0^{-1}\boldsymbol{\delta}_0+\mathbf{A}_\mathbf{d}^T\,\mathbf{s}_N\right)} \\
&\quad + \frac{1}{2}\underbrace{\mathbf{d}^T\mathbf{D}_N^{-1}\mathbf{d}}_{=\mathbf{d}^T\left(\mathbf{D}_0^{-1}+\mathbf{A}_\mathbf{d}^T\,\mathbf{S}_N\,\mathbf{A}_\mathbf{d}\right)\mathbf{d}} - \underbrace{\mathbf{d}^T\left(\mathbf{D}_N^{-1}\boldsymbol{\delta}_N\right)}_{=\mathbf{d}^T\left(\mathbf{D}_0^{-1}\boldsymbol{\delta}_0+\mathbf{A}_\mathbf{d}^T\,\mathbf{s}_N\right)} \\
&= \log\left(f_{\mathbf{Y}_N|\mathbf{d}=\mathbf{0}}\right) - \frac{1}{2}\boldsymbol{\delta}_0^T\mathbf{D}_0^{-1}\boldsymbol{\delta}_0 \\
&\quad - \underbrace{\frac{1}{2}\log\left|\mathbf{D}_0\mathbf{D}_N^{-1}\right|}_{=-\frac{1}{2}\log\left|\mathbf{D}_0\left(\mathbf{D}_0^{-1}+\mathbf{A}_\mathbf{d}^T\,\mathbf{S}_N\,\mathbf{A}_\mathbf{d}\right)\right|} + \underbrace{\frac{1}{2}\boldsymbol{\delta}_N^T\mathbf{D}_N^{-1}\boldsymbol{\delta}_N}_{=\frac{1}{2}\left(\mathbf{D}_0^{-1}\boldsymbol{\delta}_0+\mathbf{A}_\mathbf{d}^T\,\mathbf{s}_N\right)^T\left(\mathbf{D}_0^{-1}+\mathbf{A}_\mathbf{d}^T\,\mathbf{S}_N\,\mathbf{A}_\mathbf{d}\right)^{-1}\left(\mathbf{D}_0^{-1}\boldsymbol{\delta}_0+\mathbf{A}_\mathbf{d}^T\,\mathbf{s}_N\right)} \\
&= \log\left(f_{\mathbf{Y}_N|\mathbf{d}=\mathbf{0}}\right) - \frac{1}{2}\log|\mathbf{I} + \mathbf{D}_0\,\mathbf{A}_\mathbf{d}^T\,\mathbf{S}_N\,\mathbf{A}_\mathbf{d}| - \frac{1}{2}\boldsymbol{\delta}_0^T\mathbf{D}_\mathbf{0}^{-1}\boldsymbol{\delta}_0 \\
&\quad + \frac{1}{2}(\mathbf{D}_0^{-1}\boldsymbol{\delta}_0 + \mathbf{A}_\mathbf{d}^T\,\mathbf{s}_N)^T(\mathbf{D}_0^{-1} + \mathbf{A}_\mathbf{d}^T\,\mathbf{S}_N\,\mathbf{A}_\mathbf{d})^{-1}(\mathbf{D}_0^{-1}\boldsymbol{\delta}_0 + \mathbf{A}_\mathbf{d}^T\,\mathbf{s}_N),
\end{aligned}
$$

which completes the proof.[27]

□

Note that (2.2.16) follows directly from the claims of Proposition 2.D.2, while we may obtain (2.2.15a) and (2.2.15b) by substituting $\boldsymbol{\delta}_t = \left(\mathbf{D}_0^{-1} + \mathbf{A}_\mathbf{d}^T\,\mathbf{S}_t\,\mathbf{A}_\mathbf{d}\right)^{-1}\left(\mathbf{D}_0^{-1}\boldsymbol{\delta}_0 + \mathbf{A}_\mathbf{d}^T\,\mathbf{s}_t\right)$ and $\mathbf{D}_t = \left(\mathbf{D}_0^{-1} + \mathbf{A}_\mathbf{d}^T\,\mathbf{S}_t\,\mathbf{A}_\mathbf{d}\right)^{-1}$ into $\boldsymbol{\mu}_t = \tilde{\boldsymbol{\mu}}_t + \mathbf{M}_t\mathbf{A}_d\,\boldsymbol{\delta}_t$ and $\mathbf{C}_t = \tilde{\mathbf{C}}_t + \mathbf{M}_t\mathbf{A}_d\mathbf{D}_t\mathbf{A}_d^T\mathbf{M}_t^T$, respectively. To derive the remaining formulas of the AKF, notice that defining the sequences $\{\mathbf{s}_t\}_{t=0}^N$, $\{\mathbf{M}_t\}_{t=0}^N$, and $\{\mathbf{S}_t\}_{t=0}^N$ as in Propositions 2.D.1 and 2.D.2 is equivalent to their recursive derivation given in (2.2.15c)-(2.2.15e). To see this, note that

$$
\begin{aligned}
\mathbf{s}_t &= \sum_{i=1}^{t}\mathbf{E}_i^T\tilde{\mathbf{U}}_i^{-1}\,\tilde{\mathbf{e}}_i \\
&= \sum_{i=1}^{t}(\mathbf{H}\mathbf{F}\mathbf{M}_{i-1})^T\tilde{\mathbf{U}}_i^{-1}\,\tilde{\mathbf{e}}_i \\
&= (\mathbf{H}\mathbf{F}\mathbf{M}_{t-1})^T\tilde{\mathbf{U}}_t^{-1}\,\tilde{\mathbf{e}}_t + \sum_{i=1}^{t-1}(\mathbf{H}\mathbf{F}\mathbf{M}_{i-1})^T\tilde{\mathbf{U}}_i^{-1}\,\tilde{\mathbf{e}}_i \\
&= \mathbf{s}_{t-1} + (\mathbf{H}\mathbf{F}\mathbf{M}_{t-1})^T\tilde{\mathbf{U}}_t^{-1}\,\tilde{\mathbf{e}}_t, \\
\mathbf{S}_t &= \sum_{i=1}^{t}\mathbf{E}_i^T\tilde{\mathbf{U}}_i^{-1}\,\mathbf{E}_i
\end{aligned}
$$

[27] Note that some arguments of this proof are taken from Durbin and Koopman (2012, pp. 141-144) and de Jong (1988).

$$
\begin{aligned}
&= \sum_{i=1}^{t} (\mathbf{HFM}_{i-1})^T \tilde{\mathbf{U}}_i^{-1} \, (\mathbf{HFM}_{i-1}) \\
&= (\mathbf{HFM}_{t-1})^T \tilde{\mathbf{U}}_t^{-1} \, (\mathbf{HFM}_{t-1}) + \sum_{i=1}^{t-1} (\mathbf{HFM}_{i-1})^T \tilde{\mathbf{U}}_i^{-1} \, (\mathbf{HFM}_{i-1}) \\
&= \mathbf{S}_{t-1} + (\mathbf{HFM}_{t-1})^T \tilde{\mathbf{U}}_t^{-1} \, (\mathbf{HFM}_{t-1}), \\
\mathbf{M}_t &= \prod_{\mathbf{j=1}}^{\mathbf{t}} \mathbf{J}_{t+1-j} \\
&= \mathbf{J}_t \, \mathbf{J}_{t-1} \, \ldots \, \mathbf{J}_1 \\
&= \mathbf{J}_t \, \prod_{\mathbf{j=1}}^{\mathbf{t-1}} \mathbf{J}_{t-j} \\
&= \mathbf{J}_t \, \mathbf{M}_{t-1} \\
&= \left(\mathbf{I} - \tilde{\mathbf{K}}_t \mathbf{H}\right) \mathbf{F} \, \mathbf{M}_{t-1}.
\end{aligned}
$$

Further, by definition of the $\sum(\cdot)$ and the $\prod(\cdot)$ operator, we get:

$$
\mathbf{s}_0 = \sum_{i=1}^{0} \mathbf{E}_i^T \tilde{\mathbf{U}}_i^{-1} \, \tilde{\mathbf{e}}_i = \mathbf{0}, \qquad \mathbf{S}_0 = \sum_{i=1}^{0} \mathbf{E}_i^T \tilde{\mathbf{U}}_i^{-1} \, \mathbf{E}_i = \mathbf{0}, \qquad \mathbf{M}_0 = \prod_{\mathbf{j=1}}^{0} \mathbf{J}_{1-j} = \mathbf{I}.
$$

2.D.2 Initialization strategies for non-stationary state-space models

In the following, we present two well-known strategies, namely the *fixed-but-unknown* and the *diffuse* initialization, to choose $(\boldsymbol{\mu}_0, \mathbf{C}_0)$ in the context of non-stationary SSMs.

Fixed-but-unknown initialization: Imagine the state vector $\mathbf{w}_t$ contains some non-stationary elements, which implies that the unconditional second moments of $\mathbf{w}_t$ do not exist; therefore an unconditional initialization is impossible. One way to handle non-stationary SSMs is to treat the non-stationary elements in $\mathbf{w}_0$ as fixed-but-unknown and estimate them via maximum-likelihood. We refer to this approach, which goes back to Rosenberg (1973), as the *fixed-but-unknown* initialization. As de Jong (1988) shows, we can easily apply the *fixed-but-unknown* initialization within the framework of the AKF. To see this, suppose that we may reorder the initial state vector $\mathbf{w}_0$ such that

$$
\mathbf{w}_0 = \begin{pmatrix} \mathbf{w}_0^{(1)} \\ \mathbf{w}_0^{(2)} \end{pmatrix} \sim \mathrm{N}\left(\begin{pmatrix} \boldsymbol{\mu}_0^{(1)} \\ \boldsymbol{\mu}_0^{(2)} \end{pmatrix}, \begin{pmatrix} \mathbf{C}_0^{(1)} & \mathbf{0} \\ \mathbf{0} & \mathbf{C}_0^{(2)} \end{pmatrix} \right), \quad \boldsymbol{\mu}_0^{(1)} = \boldsymbol{\mu}^{(1)}, \quad \mathbf{C}_0^{(1)} = \mathbf{C}^{(1)}, \quad \mathbf{C}_0^{(2)} = z\mathbf{I}, \tag{2.D.21}
$$

where $\mathbf{w}_0^{(1)}$ and $\mathbf{w}_0^{(2)}$ denote the stationary and non-stationary elements, respectively, and where $\boldsymbol{\mu}^{(1)}$ and $\mathbf{C}^{(1)}$ represent the unconditional mean vector and the unconditional variance matrix of $\mathbf{w}_t^{(1)}$. For an initial state vector $\mathbf{w}_0$ as defined in (2.D.21), we can consider the fixed-but-unknown initialization as the case where z tends to zero. We may also express $\mathbf{w}_0$, defined via (2.D.21) using (2.2.13) by setting

$$
\begin{aligned}
&\bar{\boldsymbol{\mu}}_0 = \mathbf{0}, && \bar{\mathbf{C}}_0 = \mathbf{C}_0^{(1)}, && \mathbf{a}_\mathbf{w} = \begin{pmatrix} \mathbf{0} \\ \mathbf{0} \end{pmatrix}, && \mathbf{A}_\mathbf{w} = \begin{pmatrix} \mathbf{I} \\ \mathbf{0} \end{pmatrix}, \\
&\boldsymbol{\delta}_0 = \boldsymbol{\mu}_0^{(2)} && \mathbf{D}_0 = \mathbf{C}_0^{(2)} = z\mathbf{I}, && \mathbf{A}_\mathbf{d} = \begin{pmatrix} \mathbf{0} \\ \mathbf{I} \end{pmatrix}.
\end{aligned}
$$

Hence, we can apply the AKF to the initial state vector $\mathbf{w}_0$ defined by (2.D.21). If we now let z tend to zero, i.e., $\mathbf{d} = \boldsymbol{\delta}_0$ and $\mathbf{D}_0 \to \mathbf{0}$, (2.2.15a) and (2.2.15b) become

$$\begin{aligned}
\boldsymbol{\mu}_{t|\mathbf{d}} &= \mathrm{E}[\mathbf{w}_t|\mathbf{Y}_t, \mathbf{d}] \\
&= \lim_{\mathbf{D}_0 \to \mathbf{0}} \boldsymbol{\mu}_t \\
&= \lim_{\mathbf{D}_0 \to \mathbf{0}} \tilde{\boldsymbol{\mu}}_t + \mathbf{M}_t \mathbf{A}_d \left(\mathbf{D}_0^{-1} + \mathbf{A}_\mathbf{d}^T \mathbf{S}_t \mathbf{A}_\mathbf{d}\right)^{-1} \left(\mathbf{D}_0^{-1} \boldsymbol{\delta}_0 + \mathbf{A}_\mathbf{d}^T \mathbf{s}_t\right) \\
&= \lim_{\mathbf{D}_0 \to \mathbf{0}} \tilde{\boldsymbol{\mu}}_t + \mathbf{M}_t \mathbf{A}_d \left(\mathbf{I} + \mathbf{D}_0 \mathbf{A}_\mathbf{d}^T \mathbf{S}_t \mathbf{A}_\mathbf{d}\right)^{-1} \mathbf{D}_0 \left(\mathbf{D}_0^{-1} \boldsymbol{\delta}_0 + \mathbf{A}_\mathbf{d}^T \mathbf{s}_t\right) \\
&= \lim_{\mathbf{D}_0 \to \mathbf{0}} \tilde{\boldsymbol{\mu}}_t + \mathbf{M}_t \mathbf{A}_d \left(\mathbf{I} + \mathbf{D}_0 \mathbf{A}_\mathbf{d}^T \mathbf{S}_t \mathbf{A}_\mathbf{d}\right)^{-1} \left(\boldsymbol{\delta}_0 + \mathbf{D}_0 \mathbf{A}_\mathbf{d}^T \mathbf{s}_t\right) \\
&= \tilde{\boldsymbol{\mu}}_t + \mathbf{M}_t \mathbf{A}_d \ (\mathbf{I})^{-1} \mathbf{d} \\
&= \tilde{\boldsymbol{\mu}}_t + \mathbf{M}_t \mathbf{A}_d \ \mathbf{d}, \qquad \forall\ t = 1, 2, \ldots, N, \qquad \text{(2.D.22a)} \\
\mathbf{C}_{t|\mathbf{d}} &= \mathrm{Var}[\mathbf{w}_t|\mathbf{Y}_t, \mathbf{d}] \\
&= \lim_{\mathbf{D}_0 \to \mathbf{0}} \mathbf{C}_t \\
&= \lim_{\mathbf{D}_0 \to \mathbf{0}} \tilde{\mathbf{C}}_t + \mathbf{M}_t \mathbf{A}_d \left(\mathbf{D}_0^{-1} + \mathbf{A}_\mathbf{d}^T \mathbf{S}_t \mathbf{A}_\mathbf{d}\right)^{-1} \mathbf{A}_d^T \mathbf{M}_t^T \\
&= \lim_{\mathbf{D}_0 \to \mathbf{0}} \tilde{\mathbf{C}}_t + \mathbf{M}_t \mathbf{A}_d \left(\mathbf{I} + \mathbf{D}_0 \mathbf{A}_\mathbf{d}^T \mathbf{S}_t \mathbf{A}_\mathbf{d}\right)^{-1} \mathbf{D}_0 \mathbf{A}_d^T \mathbf{M}_t^T \\
&= \tilde{\mathbf{C}}_t, \qquad \forall\ t = 1, 2, \ldots, N, \qquad \text{(2.D.22b)}
\end{aligned}$$

and the conditional log-density of $\mathbf{Y}_N$ given $\mathbf{d}$ follows from Proposition 2.D.1 as

$$\log\left(f_{\mathbf{Y}_N|\mathbf{d}}\right) = \log\left(f_{\mathbf{Y}_N|\mathbf{d}=\mathbf{0}}\right) + \mathbf{d}^T \mathbf{A}_\mathbf{d}^T \mathbf{s}_N - \frac{1}{2} \mathbf{d}^T \mathbf{A}_\mathbf{d}^T \mathbf{S}_N \mathbf{A}_\mathbf{d} \mathbf{d}. \qquad \text{(2.D.23)}$$

Further, if $\mathbf{A}_\mathbf{d}^T \mathbf{S}_N \mathbf{A}_\mathbf{d}$ is non-singular, we may obtain the maximum-likelihood estimator of $\mathbf{d}$ and its estimated variance matrix from Proposition 2.D.1 as

$$\hat{\mathbf{d}} = \left(\mathbf{A}_\mathbf{d}^T \mathbf{S}_N \mathbf{A}_\mathbf{d}\right)^{-1} \mathbf{A}_\mathbf{d}^T \mathbf{s}_N, \qquad \text{(2.D.24a)}$$

$$\widehat{\mathrm{Var}}[\hat{\mathbf{d}}] = \left(\mathbf{A}_\mathbf{d}^T \mathbf{S}_N \mathbf{A}_\mathbf{d}\right)^{-1}. \qquad \text{(2.D.24b)}$$

Hence, substituting $\mathbf{d}$ by $\hat{\mathbf{d}}$ in (2.D.23) yields

$$\begin{aligned}
\log\left(f_{\mathbf{Y}_N|\mathbf{d}=\hat{\mathbf{d}}}\right) &= \log\left(f_{\mathbf{Y}_N|\mathbf{d}=\mathbf{0}}\right) + \hat{\mathbf{d}}^T \mathbf{A}_\mathbf{d}^T \mathbf{s}_N - \frac{1}{2} \hat{\mathbf{d}}^T \mathbf{A}_\mathbf{d}^T \mathbf{S}_N \mathbf{A}_\mathbf{d} \hat{\mathbf{d}} \\
&= \log\left(f_{\mathbf{Y}_N|\mathbf{d}=\mathbf{0}}\right) + \left[\left(\mathbf{A}_\mathbf{d}^T \mathbf{S}_N \mathbf{A}_\mathbf{d}\right)^{-1} \mathbf{A}_\mathbf{d}^T \mathbf{s}_N\right]^T \mathbf{A}_\mathbf{d}^T \mathbf{s}_N \\
&\quad - \frac{1}{2} \left[\left(\mathbf{A}_\mathbf{d}^T \mathbf{S}_N \mathbf{A}_\mathbf{d}\right)^{-1} \mathbf{A}_\mathbf{d}^T \mathbf{s}_N\right]^T \mathbf{A}_\mathbf{d}^T \mathbf{S}_N \mathbf{A}_\mathbf{d} \left[\left(\mathbf{A}_\mathbf{d}^T \mathbf{S}_N \mathbf{A}_\mathbf{d}\right)^{-1} \mathbf{A}_\mathbf{d}^T \mathbf{s}_N\right] \\
&= \log\left(f_{\mathbf{Y}_N|\mathbf{d}=\mathbf{0}}\right) + \mathbf{s}_N^T \mathbf{A}_\mathbf{d} \left(\mathbf{A}_\mathbf{d}^T \mathbf{S}_N \mathbf{A}_\mathbf{d}\right)^{-1} \mathbf{A}_\mathbf{d}^T \mathbf{s}_N \\
&\quad - \frac{1}{2} \mathbf{s}_N^T \mathbf{A}_\mathbf{d} \left(\mathbf{A}_\mathbf{d}^T \mathbf{S}_N \mathbf{A}_\mathbf{d}\right)^{-1} \mathbf{A}_\mathbf{d}^T \mathbf{S}_N \mathbf{A}_\mathbf{d} \left(\mathbf{A}_\mathbf{d}^T \mathbf{S}_N \mathbf{A}_\mathbf{d}\right)^{-1} \mathbf{A}_\mathbf{d}^T \mathbf{s}_N \\
&= \log\left(f_{\mathbf{Y}_N|\mathbf{d}=\mathbf{0}}\right) + \mathbf{s}_N^T \mathbf{A}_\mathbf{d} \left(\mathbf{A}_\mathbf{d}^T \mathbf{S}_N \mathbf{A}_\mathbf{d}\right)^{-1} \mathbf{A}_\mathbf{d}^T \mathbf{s}_N - \frac{1}{2} \mathbf{s}_N^T \mathbf{A}_\mathbf{d} \left(\mathbf{A}_\mathbf{d}^T \mathbf{S}_N \mathbf{A}_\mathbf{d}\right)^{-1} \mathbf{A}_\mathbf{d}^T \mathbf{s}_N \\
&= \log\left(f_{\mathbf{Y}_N|\mathbf{d}=\mathbf{0}}\right) + \frac{1}{2} \mathbf{s}_N^T \mathbf{A}_\mathbf{d} \left(\mathbf{A}_\mathbf{d}^T \mathbf{S}_N \mathbf{A}_\mathbf{d}\right)^{-1} \mathbf{A}_\mathbf{d}^T \mathbf{s}_N, \qquad \text{(2.D.25)}
\end{aligned}$$

which is the log-density of $\mathbf{Y}_N$ concentrated with respect to $\mathbf{d}$. This means that if we want to evaluate the log-density of $\mathbf{Y}_N$ based on the *fixed-but-unknown* initialization for the non-stationary elements $\mathbf{w}_0^{(2)}$ of $\mathbf{w}_0$, we replace (2.2.6) with (2.D.25).

Diffuse initialization: A rather contrary approach to the *fixed-but-unknown* initialization is the so-called *diffuse* initialization, where we treat the non-stationary elements $\mathbf{w}_0^{(2)}$ of the initial state vector $\mathbf{w}_0$ as diffuse, i.e., $z \to \infty$ or equivalently $\mathbf{D}_0 \to \infty$. Thus, treating $\mathbf{w}_0^{(2)}$ as diffuse, (2.2.15a) and (2.2.15b) yield

$$\boldsymbol{\mu}_{t,z\to\infty} := \lim_{z\to\infty} \boldsymbol{\mu}_t = \tilde{\boldsymbol{\mu}}_t + \mathbf{M}_t \mathbf{A}_d \left(\mathbf{A}_\mathbf{d}^T \mathbf{S}_t \mathbf{A}_\mathbf{d}\right)^{-1} \left(\mathbf{A}_\mathbf{d}^T \mathbf{s}_t\right), \qquad \forall\ t = k, k+1, \ldots, N, \tag{2.D.26a}$$

$$\mathbf{C}_{t,z\to\infty} := \lim_{z\to\infty} \mathbf{C}_t = \tilde{\mathbf{C}}_t + \mathbf{M}_t \mathbf{A}_d \left(\mathbf{A}_\mathbf{d}^T \mathbf{S}_t \mathbf{A}_\mathbf{d}\right)^{-1} \mathbf{A}_d^T \mathbf{M}_t^T, \qquad \forall\ t = k, k+1, \ldots, N, \tag{2.D.26b}$$

where k is the first period where the matrix $\mathbf{A}_\mathbf{d}^T \mathbf{S}_t \mathbf{A}_\mathbf{d}$ becomes non-singular. Thus, although the initial state vector $\mathbf{w}_0$ in this case ($z \to \infty$) has an improper distribution, in the sense that it does not integrate to one, it has a proper distribution conditional on $\mathbf{Y}_k$. In practice, when dealing with non-stationary SSMs, we often use often only the first k observations to obtain $\boldsymbol{\mu}_{k,z\to\infty}$ and $\mathbf{C}_{k,z\to\infty}$. We then use the remaining observations to evaluate the log-likelihood based on the original Kalman recursion (2.2.4) initialized at $(\boldsymbol{\mu}_{k,z\to\infty}, \mathbf{C}_{k,z\to\infty})$. For more detailed treatments of the diffuse initialization using the AKF, we refer the reader to textbook treatments by Harvey (1990b) or Durbin and Koopman (2012).

2.D.3 Incorporating the augmented Kalman filter into the Kalman recursion

To compute the log-likelihood $\log\left(f_{\mathbf{Y}_N}\right)$ based on the AKF, one augments the standard Kalman recursion (2.2.4) initialized at $(\tilde{\boldsymbol{\mu}}_0, \tilde{\mathbf{C}}_0)$ so that for all $t = 1, 2, \ldots, N$, the quantity $\mathbf{M}_t$ can be computed in parallel. To do so, we define

$$\mathbf{W}_{t|t-1} := \mathbf{F}\mathbf{M}_{t-1}, \qquad ,\forall\ t = 1, 2, \ldots, N \tag{2.D.27}$$

so that we may compute $\mathbf{M}_t$ as

$$\begin{aligned}
\mathbf{M}_t &= \prod_{\mathbf{j=1}}^{\mathbf{t}} \mathbf{J}_{t-j+1} \\
&= \mathbf{J}_t \mathbf{M}_{t-1} \\
&= \left(\mathbf{I} - \tilde{\mathbf{K}}_t \mathbf{H}\right) \mathbf{F}\mathbf{M}_{t-1} \\
&= \left(\mathbf{I} - \tilde{\mathbf{K}}_t \mathbf{H}\right) \mathbf{W}_{t|t-1} \\
&= \mathbf{W}_{t|t-1} - \tilde{\mathbf{K}}_t \mathbf{H}\mathbf{W}_{t|t-1} \\
&= \mathbf{W}_{t|t-1} - \tilde{\mathbf{K}}_t \mathbf{E}_t \qquad ,\forall\ t = 1, 2, \ldots, N.
\end{aligned} \tag{2.D.28}$$

Based on (2.D.27) and (2.D.28), we get the augmented Kalman recursion by extending (2.2.4a), (2.2.4c), and (2.2.4e) from the standard Kalman recursion (2.2.4) initialized at $(\tilde{\boldsymbol{\mu}}_0, \tilde{\mathbf{C}}_0)$ to

$$\left(\tilde{\mathbf{w}}_{t|t-1} \quad \mathbf{W}_{t|t-1}\right) = \mathbf{F}\ \left(\tilde{\boldsymbol{\mu}}_{t-1} \quad \mathbf{M}_{t-1}\right), \tag{2.D.29a}$$

$$\left(\tilde{\mathbf{e}}_t \quad \mathbf{E}_t\right) = \left(\mathbf{y}_t^{(\mathbf{h})} \quad \mathbf{0}\right) - \mathbf{H}\ \left(\tilde{\mathbf{w}}_{t|t-1} \quad \mathbf{W}_{t|t-1}\right), \tag{2.D.29c}$$

$$\left(\tilde{\boldsymbol{\mu}}_t \quad \mathbf{M}_t\right) = \left(\tilde{\mathbf{w}}_{t|t-1} \quad \mathbf{W}_{t|t-1}\right) + \tilde{\mathbf{K}}_t\ \left(\tilde{\mathbf{e}}_t \quad \mathbf{E}_t\right), \tag{2.D.29e}$$

for all $t = 1, 2, \ldots, N$.

2.E Smets and Wouters model

The version of the dynamic stochastic general equilibrium (DSGE) model introduced by Smets and Wouters (2007) that we use in this paper reflects a slightly adjusted version of the original model that follows the Dynare implementation made available by Johannes Pfeifer.[28]

2.E.1 Stochastic process and residuals

The stochastic process driving the economy is given by

$$\begin{aligned}
\varepsilon_t^a &= \rho_a \varepsilon_{t-1}^a + \eta_t^a & \eta_t^a &\sim N(0,\sigma_a),\\
\varepsilon_t^b &= \rho_b \varepsilon_{t-1}^b + \eta_t^b & \eta_t^b &\sim N(0,\sigma_b),\\
\varepsilon_t^g &= \rho_g \varepsilon_{t-1}^g + \rho_{ga} \eta_t^a + \eta_t^g & \eta_t^g &\sim N(0,\sigma_g),\\
\varepsilon_t^i &= \rho_i \varepsilon_{t-1}^i + \eta_t^i & \eta_t^i &\sim N(0,\sigma_i),\\
\varepsilon_t^r &= \rho_r \varepsilon_{t-1}^r + \eta_t^r & \eta_t^r &\sim N(0,\sigma_r),\\
\varepsilon_t^p &= \rho_p \varepsilon_{t-1}^p - \mu_p \eta_{t-1}^p + \eta_t^p & \eta_t^p &\sim N(0,\sigma_p),\\
\varepsilon_t^w &= \rho_w \varepsilon_{t-1}^w - \mu_w \eta_{t-1}^w + \eta_t^w & \eta_t^w &\sim N(0,\sigma_w),
\end{aligned}$$

where ε_t^a, ε_t^b, ε_t^g, ε_t^i, ε_t^r, ε_t^p, and ε_t^w denote a productivity shock, a risk premium shock, an exogenous government spending shock, an investment-specific technology shock, a monetary policy shock, a price markup shock, and a wage markup shock, respectively. In two periods, we can write this stochastic process as

$$0 = \varepsilon_t^a - \eta_t^a - \rho_a L\left(\varepsilon_t^a\right), \tag{2.E.1}$$
$$0 = \varepsilon_t^b - \eta_t^b - \rho_b L\left(\varepsilon_t^b\right), \tag{2.E.2}$$
$$0 = \varepsilon_t^g - \eta_t^g - \eta_t^a \rho_{ga} - \rho_g L\left(\varepsilon_t^g\right), \tag{2.E.3}$$
$$0 = \varepsilon_t^i - \eta_t^i - \rho_i L\left(\varepsilon_t^i\right), \tag{2.E.4}$$
$$0 = \varepsilon_t^r - \eta_t^r - \rho_r L\left(\varepsilon_t^r\right), \tag{2.E.5}$$
$$0 = \varepsilon_t^p - \eta_t^p + L\left(\eta_t^p\right)\mu_p - \rho_p L\left(\varepsilon_t^p\right), \tag{2.E.6}$$
$$0 = \varepsilon_t^w - \eta_t^w + L\left(\eta_t^w\right)\mu_w - \rho_w L\left(\varepsilon_t^w\right), \tag{2.E.7}$$
$$0 = \mathbb{E}_t\left[\eta_{t+1}^a\right], \tag{2.E.8}$$
$$0 = \mathbb{E}_t\left[\eta_{t+1}^b\right], \tag{2.E.9}$$
$$0 = \mathbb{E}_t\left[\eta_{t+1}^g\right], \tag{2.E.10}$$
$$0 = \mathbb{E}_t\left[\eta_{t+1}^i\right], \tag{2.E.11}$$
$$0 = \mathbb{E}_t\left[\eta_{t+1}^r\right], \tag{2.E.12}$$
$$0 = \mathbb{E}_t\left[\eta_{t+1}^p\right], \tag{2.E.13}$$
$$0 = \mathbb{E}_t\left[\eta_{t+1}^w\right], \tag{2.E.14}$$

where $L(x_t)$ denotes the variable x_t lagged by one period, i.e, $L(x_t) = x_{t-1}$.

[28] Link: https://github.com/JohannesPfeifer/DSGE_mod/blob/master/Smets_Wouters_2007/Smets_Wouters_2007_45.mod

2.E.2 Economy with sticky prices and wages

At the core of the log-linearized version of the model are 13 equations

$$0 = y_t - \Phi\,\varepsilon_t^a - \alpha\,\Phi\,k_t^s + \Phi\,l_t\,(\alpha-1), \tag{2.E.15}$$

$$0 = k_t^s - L\,(k_t) - z_t, \tag{2.E.16}$$

$$0 = z_t + \frac{r_t^k\,(\psi-1)}{\psi}, \tag{2.E.17}$$

$$0 = \mu_{p_t} + \varepsilon_t^a - \alpha\,r_t^k + w_t\,(\alpha-1), \tag{2.E.18}$$

$$0 = k_t^s - l_t + r_t^k - w_t, \tag{2.E.19}$$

$$0 = y_t - \varepsilon_t^g - c_t\,c_y - i_t\,i_y - z_t\,z_y, \tag{2.E.20}$$

$$\begin{aligned} 0 = {} & r_t - \varepsilon_t^r - L\,(r_t)\,\rho + r_{\Delta y}\,L\,(y_t) - r_{\Delta y}\,L\left(y_t^f\right) - y_t\left(r_{\Delta y} - r_y\,(\rho-1)\right) \\ & + y_t^f\left(r_{\Delta y} - r_y\,(\rho-1)\right) + \pi_t\,r_\pi\,(\rho-1), \end{aligned} \tag{2.E.21}$$

$$0 = -i_{k,\gamma}\,\varepsilon_t^i\,\varphi\,\gamma^2 + k_t - i_t\,i_{k,\gamma} + L\,(k_t)\left(i_{k,\gamma}-1\right), \tag{2.E.22}$$

$$0 = i_t - \varepsilon_t^i - \frac{L\,(i_t)}{\bar\beta\,\gamma+1} - \frac{q_t}{\gamma^2\,\varphi\left(\bar\beta\,\gamma+1\right)} - \frac{\mathbb{E}_t\,[i_{t+1}]\,\bar\beta\,\gamma}{\bar\beta\,\gamma+1}, \tag{2.E.23}$$

$$0 = q_t - \mathbb{E}_t\,[\pi_{t+1}] + r_t - \frac{\mathbb{E}_t\left[r_{t+1}^k\right]r_{ss}^k}{r_{ss}^k-\delta+1} + \frac{\mathbb{E}_t\,[q_{t+1}]\,(\delta-1)}{r_{ss}^k-\delta+1} + \frac{\sigma_c\,\varepsilon_t^b\left(\frac{h}{\gamma}+1\right)}{\frac{h}{\gamma}-1}, \tag{2.E.24}$$

$$\begin{aligned} 0 = {} & c_t - \varepsilon_t^b - \frac{\mathbb{E}_t\,[c_{t+1}]}{\frac{h}{\gamma}+1} - \frac{L\,(c_t)\,h}{\gamma\left(\frac{h}{\gamma}+1\right)} + \frac{\mathbb{E}_t\,[\pi_{t+1}]\left(\frac{h}{\gamma}-1\right)}{\sigma_c\left(\frac{h}{\gamma}+1\right)} - \frac{r_t\left(\frac{h}{\gamma}-1\right)}{\sigma_c\left(\frac{h}{\gamma}+1\right)} \\ & + \frac{\mathbb{E}_t\,[l_{t+1}]\,wl_c\,(\sigma_c-1)}{\sigma_c\left(\frac{h}{\gamma}+1\right)} - \frac{l_t\,wl_c\,(\sigma_c-1)}{\sigma_c\left(\frac{h}{\gamma}+1\right)}, \end{aligned} \tag{2.E.25}$$

$$0 = \pi_t - \varepsilon_t^p - \frac{\iota_p\,L\,(\pi_t)}{\bar\beta\,\gamma\,\iota_p+1} - \frac{\mathbb{E}_t\,[\pi_{t+1}]\,\bar\beta\,\gamma}{\bar\beta\,\gamma\,\iota_p+1} - \frac{\mu_{p_t}\left(\bar\beta\,\gamma\,\xi_p-1\right)\left(\xi_p-1\right)}{\xi_p\left(\varepsilon_p\,(\Phi-1)+1\right)\left(\bar\beta\,\gamma\,\iota_p+1\right)}, \tag{2.E.26}$$

$$\begin{aligned} 0 = {} & w_t\left(\frac{\left(\bar\beta\,\gamma\,\xi_w-1\right)\left(\xi_w-1\right)}{\xi_w\left(\bar\beta\,\gamma+1\right)\left(\varepsilon_w\,(\lambda_w-1)+1\right)}+1\right) - \varepsilon_t^w - \frac{L\,(w_t)}{\bar\beta\,\gamma+1} - \frac{\iota_w\,L\,(\pi_t)}{\bar\beta\,\gamma+1} \\ & + \frac{\pi_t\left(\bar\beta\,\gamma\,\iota_w+1\right)}{\bar\beta\,\gamma+1} - \frac{\mathbb{E}_t\,[\pi_{t+1}]\,\bar\beta\,\gamma}{\bar\beta\,\gamma+1} - \frac{\mathbb{E}_t\,[w_{t+1}]\,\bar\beta\,\gamma}{\bar\beta\,\gamma+1} \\ & - \frac{l_t\,\sigma_l\left(\bar\beta\,\gamma\,\xi_w-1\right)\left(\xi_w-1\right)}{\xi_w\left(\bar\beta\,\gamma+1\right)\left(\varepsilon_w\,(\lambda_w-1)+1\right)} + \frac{c_t\left(\bar\beta\,\gamma\,\xi_w-1\right)\left(\xi_w-1\right)}{\xi_w\left(\bar\beta\,\gamma+1\right)\left(\frac{h}{\gamma}-1\right)\left(\varepsilon_w\,(\lambda_w-1)+1\right)} \\ & - \frac{L\,(c_t)\,h\left(\bar\beta\,\gamma\,\xi_w-1\right)\left(\xi_w-1\right)}{\gamma\,\xi_w\left(\bar\beta\,\gamma+1\right)\left(\frac{h}{\gamma}-1\right)\left(\varepsilon_w\,(\lambda_w-1)+1\right)}, \end{aligned} \tag{2.E.27}$$

in the 14 endogenous variables that describe an economy with sticky price and wage contracts: output y_t, consumption c_t, investment i_t, hours worked l_t, capital services k_t^s, capital stock k_t, real wage w_t, rental rate of capital r_t^k, capital utilization rate z_t, real value of existing capital stock q_t, inflation π_t, nominal interest rate r_t, gross price markup μ_{p_t}, and potential output y_t^f.

2.E.3 Economy with flexible prices and wages

To determine potential output y_t^f the model is augmented by the 11 equations

$$0 = y_t^f - \Phi\,\varepsilon_t^a - \alpha\,\Phi\,k_t^{s,f} + \Phi\,l_t^f\;(\alpha-1), \tag{2.E.28}$$
$$0 = k_t^{s,f} - L\left(k_t^f\right) - z_t^f, \tag{2.E.29}$$
$$0 = z_t^f + \frac{r_t^{kf}\;(\psi-1)}{\psi}, \tag{2.E.30}$$
$$0 = \varepsilon_t^a - \alpha\,r_t^{kf} + w_t^f\;(\alpha-1), \tag{2.E.31}$$
$$0 = k_t^{s,f} - l_t^f + r_t^{kf} - w_t^f, \tag{2.E.32}$$
$$0 = w_t^f + \frac{c_t^f}{\frac{h}{\gamma}-1} - l_t^f\,\sigma_l - \frac{L\left(c_t^f\right)h}{\gamma\left(\frac{h}{\gamma}-1\right)}, \tag{2.E.33}$$
$$0 = y_t^f - \varepsilon_t^g - c_y\,c_t^f - i_y\,i_t^f - z_y\,z_t^f, \tag{2.E.34}$$
$$0 = -i_{k,\gamma}\,\varepsilon_t^i\,\varphi\,\gamma^2 + k_t^f - i_{k,\gamma}\,i_t^f + L\left(k_t^f\right)\left(i_{k,\gamma}-1\right), \tag{2.E.35}$$
$$0 = i_t^f - \varepsilon_t^i - \frac{L\left(i_t^f\right)}{\bar\beta\,\gamma+1} - \frac{q_t^f}{\gamma^2\,\varphi\,\left(\bar\beta\,\gamma+1\right)} - \frac{\mathbb{E}_t\left[i_{t+1}^f\right]\bar\beta\,\gamma}{\bar\beta\,\gamma+1}, \tag{2.E.36}$$
$$0 = q_t^f + r_t^f - \frac{\mathbb{E}_t\left[r_{t+1}^{kf}\right]r_{ss}^k}{r_{ss}^k-\delta+1} + \frac{\mathbb{E}_t\left[q_{t+1}^f\right](\delta-1)}{r_{ss}^k-\delta+1} + \frac{\sigma_c\,\varepsilon_t^b\left(\frac{h}{\gamma}+1\right)}{\frac{h}{\gamma}-1}, \tag{2.E.37}$$
$$\begin{aligned}0 = {} & c_t^f - \varepsilon_t^b - \frac{\mathbb{E}_t\left[c_{t+1}^f\right]}{\frac{h}{\gamma}+1} - \frac{L\left(c_t^f\right)h}{\gamma\left(\frac{h}{\gamma}+1\right)} - \frac{r_t^f\left(\frac{h}{\gamma}-1\right)}{\sigma_c\left(\frac{h}{\gamma}+1\right)} \\ & + \frac{\mathbb{E}_t\left[l_{t+1}^f\right]wl_c\,(\sigma_c-1)}{\sigma_c\left(\frac{h}{\gamma}+1\right)} - \frac{l_t^f\,wl_c\,(\sigma_c-1)}{\sigma_c\left(\frac{h}{\gamma}+1\right)},\end{aligned} \tag{2.E.38}$$

in the variables y_t^f, c_t^f, i_t^f, l_t^f, $k_t^{s,f}$, k_t^f, w_t^f, $r_t^{k,f}$, z_t^f, q_t^f, and r_t^f, describing the corresponding economy with flexible prices and wages.

2.E.4 Law of motion of lagged variables

The motion of the model's 20 lagged and therefore predetermined variables is given by

$$0 = L\left(y_{t+1}\right) - y_t, \tag{2.E.39}$$
$$0 = L\left(c_{t+1}\right) - c_t, \tag{2.E.40}$$
$$0 = L\left(i_{t+1}\right) - i_t, \tag{2.E.41}$$
$$0 = L\left(k_{t+1}\right) - k_t, \tag{2.E.42}$$
$$0 = L\left(r_{t+1}\right) - r_t, \tag{2.E.43}$$
$$0 = L\left(w_{t+1}\right) - w_t, \tag{2.E.44}$$
$$0 = L\left(\pi_{t+1}\right) - \pi_t, \tag{2.E.45}$$
$$0 = L\left(\varepsilon_{t+1}^a\right) - \varepsilon_t^a, \tag{2.E.46}$$
$$0 = L\left(\varepsilon_{t+1}^b\right) - \varepsilon_t^b, \tag{2.E.47}$$
$$0 = L\left(\varepsilon_{t+1}^g\right) - \varepsilon_t^g, \tag{2.E.48}$$
$$0 = L\left(\varepsilon_{t+1}^i\right) - \varepsilon_t^i, \tag{2.E.49}$$

$$0 = L\left(\varepsilon_{t+1}^{r}\right) - \varepsilon_{t}^{r}, \tag{2.E.50}$$
$$0 = L\left(\varepsilon_{t+1}^{p}\right) - \varepsilon_{t}^{p}, \tag{2.E.51}$$
$$0 = L\left(\varepsilon_{t+1}^{w}\right) - \varepsilon_{t}^{w}, \tag{2.E.52}$$
$$0 = L\left(\eta_{t+1}^{p}\right) - \eta_{t}^{p}, \tag{2.E.53}$$
$$0 = L\left(\eta_{t+1}^{w}\right) - \eta_{t}^{w}, \tag{2.E.54}$$
$$0 = L\left(y_{t+1}^{f}\right) - y_{t}^{f}, \tag{2.E.55}$$
$$0 = L\left(c_{t+1}^{f}\right) - c_{t}^{f}, \tag{2.E.56}$$
$$0 = L\left(i_{t+1}^{f}\right) - i_{t}^{f}, \tag{2.E.57}$$
$$0 = L\left(k_{t+1}^{f}\right) - k_{t}^{f}. \tag{2.E.58}$$

2.E.5 Data and auxiliary variables

We fit the model to 7 quarterly time series of the log difference of per capita real GDP ($dlGDP_t$), the log difference of per capita real consumption ($dlCONS_t$), the log difference of per capita real investment ($dlINV_t$) and the log difference of per capita real wages ($dlWAGE_t$), log of per capita hours worked ($lHOURs_t/100$), the log difference of GDP deflator (dlP_t), and the federal funds rate ($FEDFUNDS_t$) for U.S. from 1966 to 2004. The series are displayed in Figure 2.2. To link the model's variables to the data we add 4 auxiliary variables $\bar{y}_t$, $\bar{c}_t$, $\bar{i}_t$, and $\bar{w}_t$ which are determined by

$$0 = \bar{y}_t + L\left(y_t\right) - y_t, \tag{2.E.59}$$
$$0 = \bar{c}_t + L\left(c_t\right) - c_t, \tag{2.E.60}$$
$$0 = \bar{i}_t + L\left(i_t\right) - i_t, \tag{2.E.61}$$
$$0 = \bar{w}_t + L\left(w_t\right) - w_t. \tag{2.E.62}$$

The link between the vector of observations $\mathbf{y}_t$ and the model's variables is then given by

$$\mathbf{y}_t = \begin{pmatrix} dlGDP_t \\ dlCONS_t \\ dlINV_t \\ dlWAGE_t \\ lHOURS_t \\ dlP_t \\ FEDFUNDS_t \end{pmatrix} = \begin{pmatrix} \bar{\gamma} \\ \bar{\gamma} \\ \bar{\gamma} \\ \bar{\gamma} \\ \bar{l} \\ \bar{\pi} \\ \bar{r} \end{pmatrix} + \begin{pmatrix} \bar{y}_t \\ \bar{c}_t \\ \bar{i}_t \\ \bar{w}_t \\ l_t \\ \pi_t \\ r_t \end{pmatrix}.$$

2.E.6 Policy function and BA-model

The economy described in equations (2.E.1)-(2.E.62) includes 62 variables: The 35 endogenous variables y_t, c_t, i_t, l_t, k_t^s, k_t, w_t, r_t^k, z_t, q_t, π_t, r_t, μ_{p_t}, y_t^f, c_t^f, i_t^f, l_t^f, $k_t^{s,f}$, k_t^f, w_t^f, $r_t^{k,f}$, z_t^f, q_t^f, r_t^f, $\bar{y}_t$, $\bar{c}_t$, $\bar{i}_t$, $\bar{w}_t$, ε_t^a, ε_t^b, ε_t^g, ε_t^i, ε_t^r, ε_t^p, and ε_t^w, the 20 predetermined states $L\left(y_t\right)$, $L\left(c_t\right)$, $L\left(i_t\right)$, $L\left(k_t\right)$, $L\left(r_t\right)$, $L\left(w_t\right)$, $L\left(\pi_t\right)$, $L\left(\varepsilon_t^a\right)$, $L\left(\varepsilon_t^b\right)$, $L\left(\varepsilon_t^g\right)$, $L\left(\varepsilon_t^i\right)$, $L\left(\varepsilon_t^r\right)$, $L\left(\varepsilon_t^p\right)$, $L\left(\varepsilon_t^w\right)$, $L\left(\eta_t^p\right)$, $L\left(\eta_t^w\right)$, $L\left(y_t^f\right)$, $L\left(c_t^f\right)$, $L\left(i_t^f\right)$, and $L\left(k_t^f\right)$, and the 7 exogenous state variables η_t^a, η_t^b, η_t^g, η_t^i, η_t^r, η_t^p, and η_t^w. To solve the model for its policy function we collect the endogenous variables in the vector $\mathbf{y}_t^{(m)}$, the predetermined states in the vector $\mathbf{x}_t^{(m)}$, and the exogenous states in the vector $\mathbf{z}_t^{(m)}$. Since equations (2.E.1)-(2.E.62) are linear in $\mathbf{x}_t^{(m)}$, $\mathbf{y}_t^{(m)}$, $\mathbf{z}_t^{(m)}$, $\mathbf{x}_{t+1}^{(m)}$, $\mathbb{E}_t\mathbf{y}_{t+1}^{(m)}$, and $\mathbb{E}_t\mathbf{z}_{t+1}^{(m)}$ they

Figure 2.2: Data – Smets and Wouters model

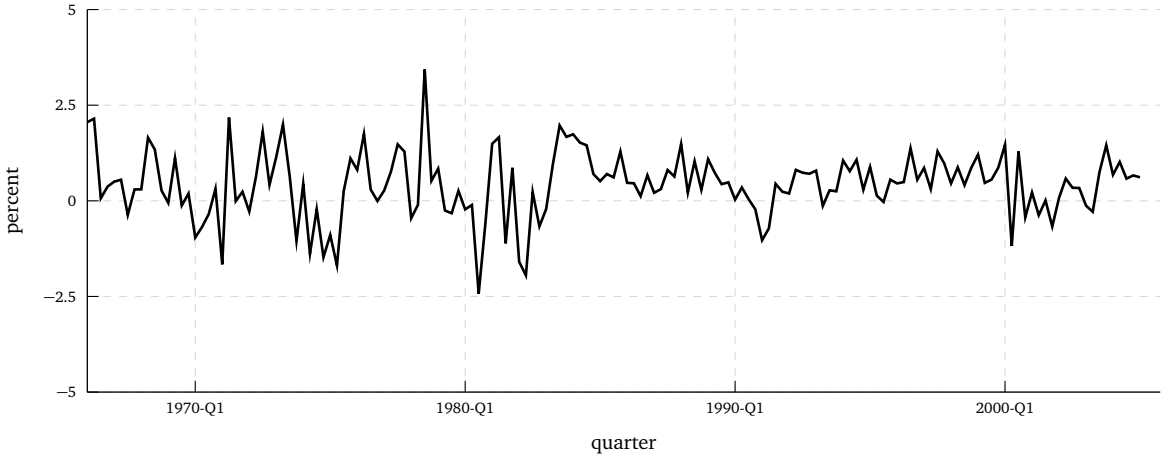

(a) Per Capita Real Output Growth – $dlGDP_t$

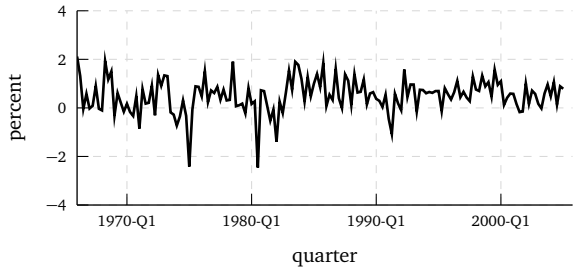

(b) Per Capita Real Consumption Growth – $dlCONS_t$

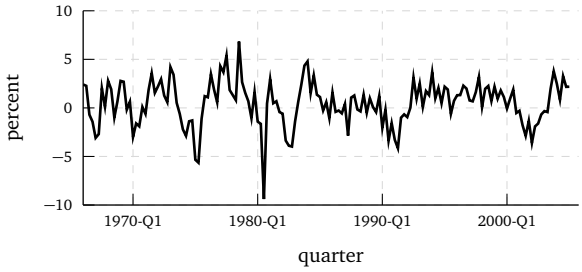

(c) Per Capita Real Investment Growth – $dlINV_t$

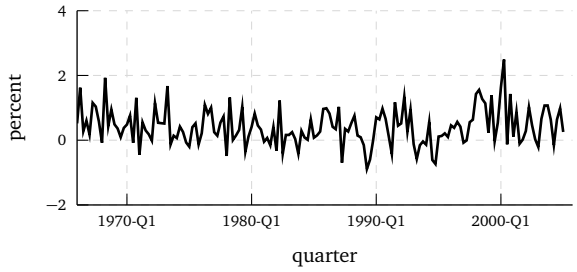

(d) Per Capita Real Wage Growth – $dlWAGE_t$

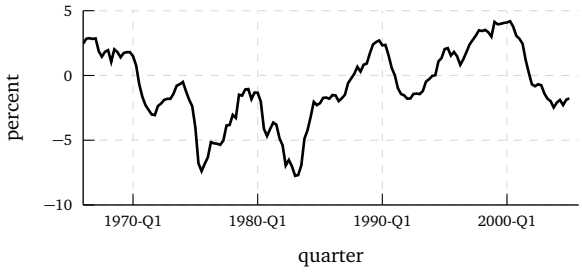

(e) Per Capita Hours Index – $lHOURS_t$

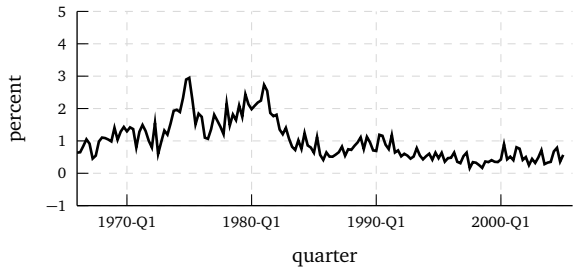

(f) Inflation – dlP_t

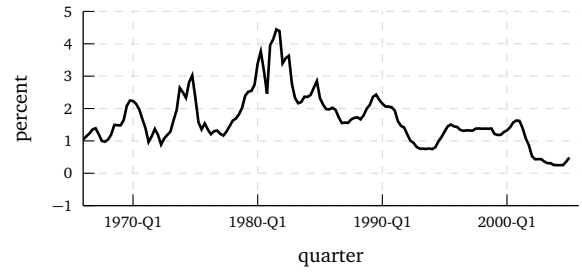

(g) Federal Funds Rate – $FEDFUNDS_t$

Notes: The data is adopted from the FORTRAN codes provided by Herbst (2015) and covers 1966:Q1 to 2004:Q4. The construction follows that of Smets and Wouters (2007) and is explained in detail by Herbst and Schorfheide (2016). **Source:** Herbst (2015).

may be rewritten as a rational expectations model of the form

$$B\,\mathbb{E}_t\begin{pmatrix}\mathbf{w}_{t+1}^{(m)}\\ \mathbf{y}_{t+1}^{(m)}\end{pmatrix}=A\begin{pmatrix}\mathbf{w}_{t}^{(m)}\\ \mathbf{y}_{t}^{(m)}\end{pmatrix},$$

where $\mathbf{w}_t^{(m)}=\begin{pmatrix}\mathbf{z}_t^{(m)} & \mathbf{x}_t^{(m)}\end{pmatrix}^T$. As shown by Klein (2000), this model can be solved using the generalized Schur decomposition. The resulting policy function takes the form:

$$\mathbf{x}_{t+1}^{(m)}=L_x^x\,\mathbf{x}_t^{(m)}+L_z^x\,\mathbf{z}_t^{(m)}, \tag{2.E.63a}$$
$$\mathbf{y}_{t}^{(m)}=L_x^y\,\mathbf{x}_t^{(m)}+L_z^y\,\mathbf{z}_t^{(m)}, \tag{2.E.63b}$$
$$\mathbf{z}_{t+1}^{(m)}=\boldsymbol{\eta}_{t+1}, \tag{2.E.63c}$$

where the vector $\boldsymbol{\eta}_t$ collects the residuals η_t^a, η_t^b, η_t^g, η_t^i, η_t^r, η_t^p, and η_t^w. Further, we denote $\tilde{L}_z^y$ and $\tilde{L}_x^y$ as the rows of L_x^y and L_z^y that correspond to the endogenous variables $\bar{y}_t$, $\bar{c}_t$, $\bar{i}_t$, $\bar{w}_t$, l_t, π_t, and r_t, so that

$$\mathbf{y}_t=\begin{pmatrix}\bar{\gamma} & \bar{\gamma} & \bar{\gamma} & \bar{\gamma} & \bar{l} & \bar{\pi} & \bar{r}\end{pmatrix}^T+\tilde{L}_x^y\,\mathbf{x}_t^{(m)}+\tilde{L}_z^y\,\mathbf{z}_t^{(m)}.$$

2.E.7 State-space representation

Using the policy function (2.E.63), we may rewrite the solved model in terms of the SSM (2.2.2) by defining $\mathbf{w}_t$, $\mathbf{v}_{t,z}$, $\mathbf{h}$, $\mathbf{H}$, $\mathbf{F}$ and $\mathbf{Q}$ as

$$\mathbf{v}_{t,z}=\begin{pmatrix}\eta_t^a & \eta_t^b & \eta_t^g & \eta_t^i & \eta_t^r & \eta_t^p & \eta_t^w\end{pmatrix}^T,\qquad \mathbf{w}_t=\mathbf{w}_t^{(m)},$$
$$\mathbf{h}=\begin{pmatrix}\bar{\gamma} & \bar{\gamma} & \bar{\gamma} & \bar{\gamma} & \bar{l} & \bar{\pi} & \bar{r}\end{pmatrix}^T,\qquad \mathbf{H}_z=\tilde{L}_z^y,\qquad \mathbf{H}_x=\tilde{L}_x^y,$$
$$\mathbf{Q}_z=\operatorname{diag}\left(\sigma_a^2,\sigma_b^2,\sigma_g^2,\sigma_i^2,\sigma_r^2,\sigma_p^2,\sigma_w^2\right),\qquad \mathbf{F}_z=\begin{pmatrix}\mathbf{0} & \mathbf{0}\end{pmatrix},\qquad \mathbf{F}_x=\begin{pmatrix}L_z^x & L_x^x\end{pmatrix}.$$

Consequently, the model satisfies the preconditions of Proposition 2.3.1, provided the matrix is $\tilde{L}_x^y$ is non-singular.

2.E.8 Parameters and steady-state

The model has 36 parameters to be estimated. The prior distributions of these parameters are displayed in Table 2.6. Further, the model contains the 5 fixed parameters:

$$\delta=0.03,\qquad \lambda_w=1.50,\qquad g_y=0.18,\qquad \varepsilon_p=10.00,\qquad \varepsilon_w=10.00.$$

as well as the 15 dependent parameters defined by

$$\pi^*=\frac{\bar{\pi}}{100}+1,$$
$$\gamma=\frac{\bar{\gamma}}{100}+1,$$
$$\beta=\frac{1}{\frac{\bar{\beta}}{100}+1},$$
$$\bar{r}=\frac{100\,\gamma^{\sigma_c}\,\pi^*}{\beta}-100,$$
$$\bar{\beta}=\frac{\beta}{\gamma^{\sigma_c}},$$

$$
\begin{aligned}
r_{ss}^{k} &= \delta + \frac{\gamma^{\sigma_c}}{\beta} - 1, \\
w_{ss} &= \frac{1}{\left(\frac{\alpha^{\alpha}(1-\alpha)^{1-\alpha}}{\Phi\, r_{ss}^{k\,\alpha}}\right)^{\frac{1}{\alpha-1}}}, \\
i_{k,\gamma} &= \frac{\delta - 1}{\gamma} + 1, \\
i_k &= \gamma\left(\frac{\delta - 1}{\gamma} + 1\right), \\
l_k &= -\frac{r_{ss}^{k}\,(\alpha - 1)}{\alpha\, w_{ss}}, \\
k_y &= \Phi\, l_k^{\,\alpha-1}, \\
i_y &= i_k\, k_y, \\
c_y &= 1 - i_k\, k_y - g_y, \\
z_y &= k_y\, r_{ss}^{k}, \\
wl_c &= -\frac{k_y\, r_{ss}^{k}\,(\alpha - 1)}{\alpha\, c_y\, \lambda_w}.
\end{aligned}
$$

Chapter 3

Business Cycle Accounting for the German Fiscal Stimulus Program during the Great Recession

— *Daniel Fehrle and Johannes Huber* —

3.1 Introduction

In response to the Great Recession in 2008 and 2009, the German government, like many others, launched an expansive fiscal stimulus program. This policy intervened on different markets by increasing transfers and government spending, decreasing tax rates and social contributions and expanding short-time work possibilities. Particularly noteworthy is the German cash for clunkers program, since this car subsidy affected one of Germany's core industries and was internationally incomparably large (5 Billion € or 0.2 percent of Gross Domestic Product (GDP)). Altogether, the program amounted to 82 billion € or 3.2 percent of GDP. These considerable expenditures raise the following questions: What are the consequences of these measures for macroeconomic markets and how effective was this program for aggregated output?

Such questions are difficult to answer, which is why fiscal stimuli might be the most controversially discussed anti-cyclical measures. To address them, there are basically two approaches (see e.g. Hebous (2011)): The first is to model a theoretical framework with deep structural equations, parameters, and shocks. An arbitrary number of shocks describes changes in fiscal policy, and impulse response functions as well as multipliers illustrate the consequences. Since the structure, the parametrization, and, at least partly, the parameter values ground on assumptions, the results are assumption-driven. The second approach bases on statistical models, in particular vector autoregressions (VARs). They are less theoretical and, in comparison to many of the former models, can be estimated with classical techniques. Unfortunately, in general it is impossible to distinguish between market distortions and the agent's responses to these distortions. This makes it rather impractical to study the effects of the various market interventions. Instead of selecting from these two approaches, we apply a third option, which we describe as kind of a middle course. By employing the business cycle accounting (BCA) approach as proposed by Chari et al. (2007) and revisited by Brinca et al. (2016), we investigate the impact of the Great Recession during 2008 and 2009 in Germany, its aftermath, the impact of monetary policy, and in particular, the effects of the German stimulus program.

The BCA framework is based on the benchmark real business cycle (RBC) model, which is extended by time-varying distortions in nearly every market, the so-called "prototype economy". Chari et al. (2007) interpret the origins of these market distortions as taxes, nominal and real frictions, changes in expectations, etc. and call them "wedges". In contrast to most medium or large scale dynamic stochastic general equilibrium (DSGE) models, the mechanisms underlying these distortions are not structural. They are parameterized like taxes, technology, or government spending and are driven by a reduced-form Markov process.[1] Commonly this process is specified

[1] Note that Chari et al. (2009) argue that also some of the shocks in medium or large scale DSGE models, i.e. New

by a VAR(1). Using time series data one can estimate the parameters of the VAR process and measure the values of the wedges. These measured wedges are fed back into the model one by one, to assess the contribution of each wedge to the business cycle. In a nutshell, BCA is the fully developed "...through the lens of a neoclassical model"-approach.[2] The slim theoretical framework and the applicability of classical estimation techniques, in this instance maximum-likelihood estimation (MLE), minimizes the number of assumptions required and thus the results are less assumption-driven. Nevertheless, one can distinguish between market distortions and the agents responses.

To increase the practicability of BCA in general and make it more suitable for the study of the German stimulus program in particular, we differ from Chari et al. (2007) in our "prototype-economy", in our estimation methodology, and in our mapping strategy.

Prototype-economy: We extend the benchmark model for the following reasons in three ways. First, the wedges include a long- and a short-run component. This allows to differentiate between growth and business cycle accounting. Since the German reunification, subaggregates of demand grew at different rates. Without growth accounting, the underlying stochastic process is non-stationary. Chari et al. (2007) set a common growth rate unfoundedly for all countries equal to 1.6 percent. Brinca et al. (2016) detrend in such a way that the average trend-adjusted log output of the economy under consideration is equal zero. The latter makes the estimation procedure more robust. Our approach can be seen as a further stage.[3] Second, we distinguish between government spending and net exports. This enables a government spending analysis and accounts for the fact that German industry is strongly depended on foreign trade. Third, we exclude durable consumption goods from aggregated investment in order to consider the cash for clunkers program separately. After all, the model includes the following wedges: *government consumption, durables, investment, labor, net exports, and efficiency*. Previous work already extends the benchmark model in various ways, e.g. Šustek (2011) includes an asset market and a monetary policy wedge.

Estimation: We estimate two structural parameters and all parameters of the VAR process using MLE, in sum 59, and identify the wedges with Kalman-smoothing. MLE in this context is difficult, e.g. Gerth and Otsu (2018) report unsolved problems concerning likelihood optimization and BCA.[4] As many others, they avoid the problem by switching to Bayesian estimation. As we argue, Bayesian methods are impracticable for BCA, because the reduced-form process is highly abstract and thus, it seems impossible to make any a-priori assumptions. Furthermore, Brinca et al. (2018) argue that weak identification associated with parameters of the VAR process is negligible in the context of BCA. Unfortunately, this does not hold for structural parameters. We introduce a reliable and quick procedure to locate the maximum of the likelihood function. Using this procedure, it is a feasible exercise to apply tools that help overcome problems of weak identification, namely plotting the likelihood contour, detecting the global maximum, and executing robustness checks, all with respect to the uncertain structural parameters.

The procedure can be summarized as follows: In advance, we make sure that all uncertain parameters are locally strictly identified according to the strategy of Iskrev (2010). Then, we maximize the likelihood function, which we receive from a Kalman recursion, assuming that the initial states are fixed and known in their long-run equilibrium. This initialization is

Keynesian models, are rather reduced-form than structural.

[2] This long-lasting approach was established by Solow (1957). To name but a few more recent applications: Kehoe and Prescott (2002), Ohanian (2010), Lu (2012), Cho and Doblas-Madrid (2013), Karabarbounis (2014) or Hansen and Ohanian (2016).

[3] Note that growth accounting is implicitly applied whenever different time series are detrended by univariate filters, such as the HP-filter, the Hamilton filter or the Baxton-King filter. DeJong and Dave (2011, Chapter 6.1) suggest a general procedure to estimate a common linear trend. Even by applying this strategy, the estimated process lacks stationarity here.

[4] Gerth and Otsu (2018) do not account for growth, which potentially explains the problem.

eventually equivalent to the procedure of Chari et al. (2007) but provides two advantages, i) the computation of the likelihood function is less time-consuming and, ii) there exists an analytical and unique solution for the maximizing conditional covariance matrix. Under fairly general conditions, the estimator obtained with this procedure retains the properties of a maximum-likelihood estimator, yet, it is less efficient than the maximum-likelihood estimator based on the commonly used unconditional likelihood. Thus, we use the first parameter estimation only as a guess for the actual estimation based on the more common, unconditional likelihood function. As mentioned, we complete the process by determining the wedges with Kalman-smoothing.
Mapping: Chari et al. (2007) map different types of structural frictions towards the reduced-form wedges, which they call "equivalent results". We map the particular measures of the fiscal stimulus program and monetary policy in a similar manner and analyze whether these interventions can explain counter-cyclical behavior. This follows Mulligan (2005) who initiates the study of policy interventions as reduced-form errors of RBC models, and Kersting (2008) who initiates the mapping of political measures, namely the 1980's U.K. labor market reforms, towards the wedges inside the BCA framework.

Our findings suggest that the crisis was mainly driven by the efficiency wedge, followed by the net exports and the investment wedge. The government consumption wedge and especially the durables wedge acted counter-cyclically. Furthermore, the labor wedge induced a fast recovery. The results are robust except for the investment wedge.

We attribute the counter-cyclicality of the durables wedge to the cash for clunkers program, which is equivalent to a durable good subsidy. Since the expenditures for government consumption were higher than for the cash for clunkers program and the effects were similar, subsidies for durable goods stimulated aggregated demand more efficiently. Mian and Sufi (2012) examine the U.S. cash for clunkers program as a representative of durables and investment subsidies using cross-section variation. They find that the program induced a large increase in car sales. Indeed, in their study, the positive effect vanishes within one year due to intertemporal substitution. In Germany, durable goods bust after the program, which suggest a similar substitution effect. However, our BCA analysis indicates that this is the transmission towards the trajectory of durables that would have occurred in the absence of the cash for clunkers program. In sum the program's effects are neither substituted entirely intra- nor intertemporally untill 2011-Q3. This is at odds with the results of a times-series analysis by Leuwer and Süssmuth (2018), who find large substitution effects. However, their work relies on the strong assumption that there were no substantial changes simultaneously to the car subsidy. Berger and Vavra (2015) investigates the households' responses to durables subsidies over the business cycle for the U.S. and find smaller effects in recessions, which is not at odds to our results, but make them more striking.

The labor market wedge induced recovery can be explained by expanded short-time work possibilities as they can decrease hiring frictions in the aftermath of recessions. Using the unemployment rate, Gehrke et al. (2019) argue that previous labor market reforms (so-called Hartz reforms) probably drove the labor market wedge induced recovery. Our method cannot distinguish between these explanations because both achieve equivalent results.

Similar interpretation problems concerning reduced-form shocks arise with measures of the stimulus program which we map towards the efficiency, investment, and net exports wedge. Since these wedges caused the crisis, pro-cyclical distortions exceed the effects of counter-cyclical fiscal stimulus and monetary policy measures in those markets. Hence, pro-cyclical wedges give no evidence for ineffective measures. Assuming that the fiscal stimulus program together with monetary policy were the only counter-cyclical distortions, counter-cyclical wedges give evidence for effective measures. Under this assumption, our results represent a lower bound for the impact of fiscal and monetary policy measures and the pro-cyclical distortions.

Existing BCA applications for the Great Recession in Germany by Brinca et al. (2016) and Gerth and Otsu (2018) suggest negligible effects of the investment wedge on the business cycle.

Both treat durables and other investment goods as a composite. We get similar results, feeding back both wedges at the same time into the model. In detail, the pro-cyclicality of the investment wedge and the counter-cyclicality of the durables wedge offset each other, which is why previous work potentially underrate the importance of the investment wedge and, as a consequence, equivalent financial frictions.

Drygalla et al. (2020) as well as Gadatsch et al. (2016) investigate the German fiscal stimulus program in medium-scale New-Keynesian DSGE models using Bayesian inference. They find positive but small effects on GDP and the latter finds negative effects in the aftermath of the crisis. However, neither of these studies account for durable consumption goods separately.

The remainder of the paper reads as follows. The next section sketches the German fiscal stimulus program and the monetary policy of the European Central Bank (ECB). Furthermore, we provide long-term series with focus on the crisis from 2008 till 2011 for the reunified German economy. Thereafter, we describe our version of a prototype economy. We map the single measures of the program to the wedges. In a next step, we present our calibration exercises and the estimation strategy. We show the results with a robustness and discussion section and then the paper concludes. Our Appendix presents the entire model as well as the source of our data and the corresponding manipulation.

3.2 The German case

3.2.1 The fiscal stimuli packages I and II in detail

The German fiscal stimulus program was composed of two packages. The first became effective at the end of 2008 and the second at the beginning of 2009 (Bundesgesetzblatt, 2008, 2009).

As Rosenberger (2013) describes, the first package amounted to 32 Billion € plus a loan program of 15 Billion €. The fiscal stimulus consisted of a one year's tax exemption on new cars, higher tax deductions by permitting the reducing-balance method and increasing child allowance, a lower employment insurance tax, as well as higher transfers for students and retirees.

The second stimulus package amounted to 50 Billion € plus both a loan and guarantee program of 100 Billion € and an increase of the German export credit guarantee program (Hermes cover) of about 2 Billion €. The package consisted of investments in public infrastructure, financial support for local and state authority spending, a subsidy on new cars at the amount of 2500 € per car and in total 5 Billion €, subsidies for private innovations as well as lower income taxes and social contributions. Short-time work possibilities and benefits were expanded, further training was supported, and the Federal Employment Agency increased the number of job agents.

Table 3.1 presents following calculations by the OECD (2009) for the stimulus program. The size of the fiscal stimulus program was on equal terms by reducing taxes and increasing transfers and spending. Transfers to households amounted to 0.3 percent of GDP, where the cash for clunkers composed two out of three. Extra government spending amounted to 0.8 percent of GDP. The fiscal packages amounted to 3.2 percent of GDP, excluding all measures which did not affected the national budget directly, e.g. the loan and guarantee program.

Table 3.1: Composition of the fiscal program in percent of GDP

Tax	Individuals	Social Contribution	Business	Total*
	-0.6	-0.7	-0.3	-1.6
Spending	Transfers to households	Transfers to business	Government spending**	Total***
	0.3	0.3	0.8	1.6

Notes: * Including consumption tax measures. ** Final consumption + investment *** Including transfers to sub-national government. **Source:** OECD (2009).

3.2.2 Monetary policy in the Great Recession

The monetary policy of the ECB also reacted to the recession. Figure 3.1 shows the minimum bid rate on main refinancing operations and the interest rate on deposit facilities declined in the aftermath of the declined inflation rate. The former declined from 4.25 percent in mid 2008 to 1 percent by mid 2009. Both interest rates have persisted since then.

Figure 3.1: Monetary policy and usage of the deposit facility

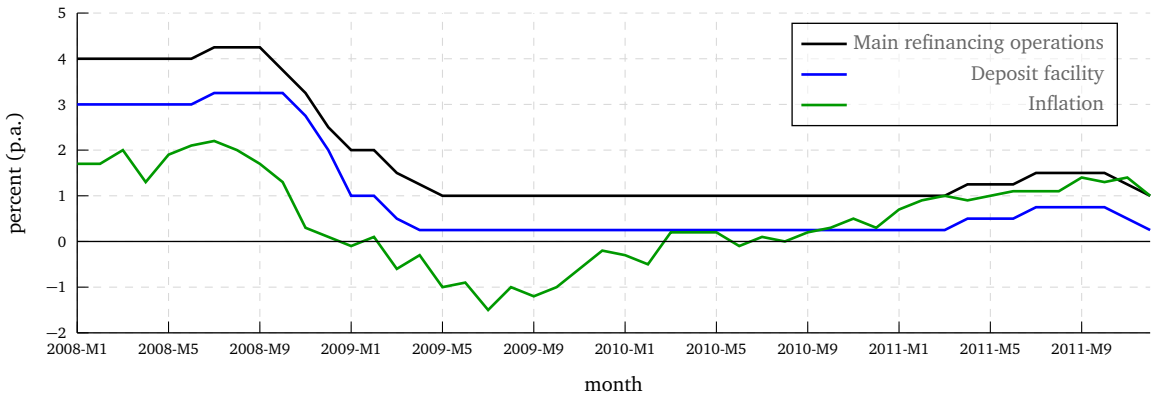

Besides the conventional interest rate policy, the ECB applied further tools of monetary policy. Here we give a short overview of the detailed reports of the European Central Bank (2010, 2011). In October 2008 the ECB switched from a variable-rate to a fixed-rate tender, eased collateral requirements and enhanced the provision of liquidity. The ECB's Governing Council prolonged these measures several times. It decided to purchase bonds issued in the Euro area in May 2009 and launched the Security Markets Program in June 2009. This program conducted interventions on public and private debt securities markets in the Euro area. Then, in March and May 2010, the Governing Council decided to switch back and forth between a variable- and a fixed-rate tender and to intervene once again on the Euro area public and private debt securities markets. The Council determined long-term refinance operations to provide liquidity in August and October 2010.

3.2.3 Stylized facts for the German economy

Table 3.2 presents average long-run shares of subaggregates of the reunified German economy (1991–2018). Private consumption expenditures account for 56 percent, whereby durables account for 6 percent and non-durables for the half of GDP. The share of investment is determined at 21 percent and of government consumption close to 19 percent. Net exports account for almost 4 percent.

Table 3.2: Long-run ratios in percent of GDP (1991–2018)

Description	$\overline{x_t/\text{GDP}_t}$
polynomial chaos expansion	56.05
Non-durables consumption	49.72
Durable consumption	06.33
Investment	21.32
Government consumption.	18.87
Net exports	03.76

Source: See Appendix 3.C, own calculations.

Figures 3.2 and 3.3 present the cyclical behavior of GDP, its subaggregates and hours worked. The time series are the relative deviations from the concerning linear trend. We choose a linear trend filter instead of the commonly used HP-filter to be consistent with our estimation strategy.[5]

We observe a boom-bust cycle in GDP at about the same time of the dot-com bubble. This cycle was followed by a recovery from 2005 till 2008, which ended in a heavy drop. This drop depicts the Great Recession. GDP recovered fast and has moved along the long-run trend since then.

Figure 3.2: Cyclical behavior of GDP

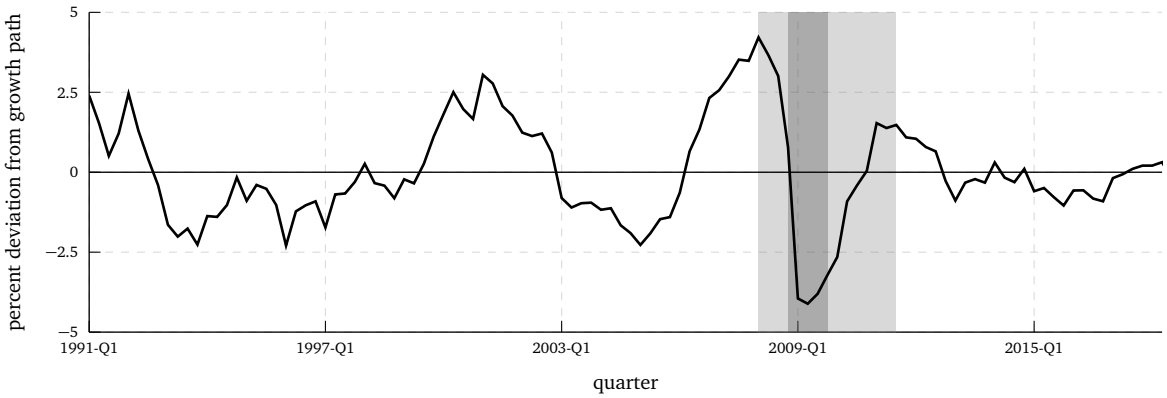

Notes: The data is presented as relative deviations from linear trend. The light gray area indicates the crisis from 2008-Q1 – 2011-Q3, the dark gray area indicates the main effective period of the fiscal stimulus program 2008-Q4 – 2009-Q4. **Source:** see Appendix 3.C, own calculations.

Panel (a) of Figure 3.3 shows that investment has co-moved with GDP, but with a higher volatility. Panel (b) displays two heavy short boom-bust-cycles of durables. The first peaked at the end of 2006, shortly after the announcement of a value-added tax (VAT) increase. This was followed by a bust at the beginning of 2007, when the increase took place. We observe the second peak at the same time as the German cash for clunkers program, which was also followed by a bust as the program expired. Government consumption was above its trend in the middle and late 1990's. It decreased at the beginning of the 2000's and increased from 2008 till 2010. Since 2010 it has fluctuated around its trend. Non-durable consumption was below its trend in the aftermath of the reunification, and was above the trend in the 2000's until the Great Recession and decreased slightly afterwards. Net exports relative to GDP decreased from

[5] Flor (2014) presents an overview of HP-filtered second moments of similar data.

1997 till 2001 from their trend, and increased sharply afterwards till 2003. From then on until the crisis they moved above the trend. Since the crisis they have fluctuated around the trend. In the medium-run, hours worked declined after the German reunification till 2005 and from then on they have increased. Hours worked have co-moved with GDP from 2000 onwards.

Figure 3.3: Cyclical behavior of different economic measures

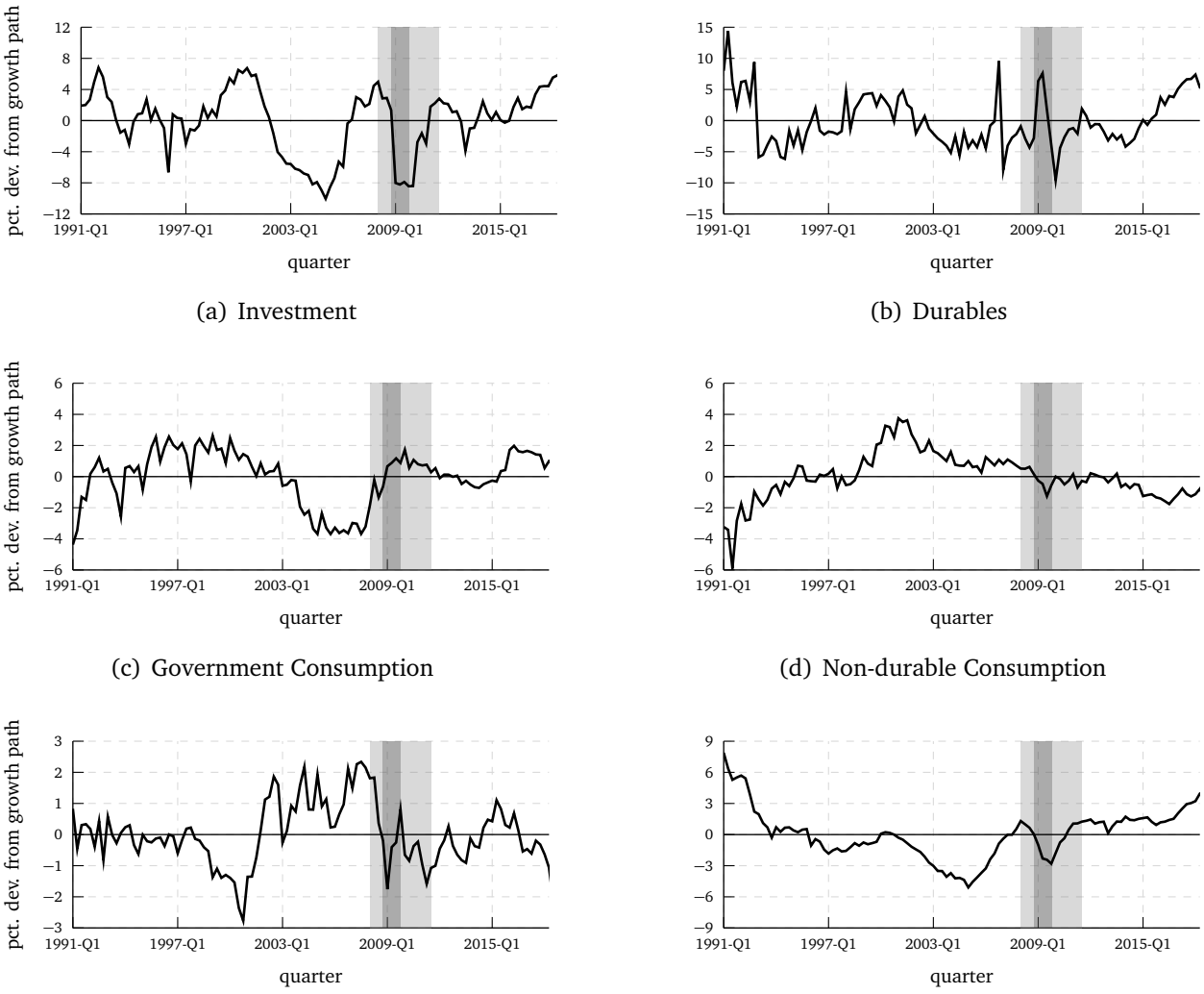

(a) Investment

(b) Durables

(c) Government Consumption

(d) Non-durable Consumption

(e) Net exports to GDP

(f) Hours

Notes: Despite hours worked, the data are presented as relative deviations from the corresponding linear trend. Hours worked is the relative deviation from the average. The light gray area indicates the crisis from 2008-Q1 – 2011-Q3, the dark gray area indicates the main effective period of the fiscal stimulus program 2008-Q4 – 2009-Q4.
Source: see Appendix 3.C, own calculations.

The light gray area in Figures 3.2 and 3.3 indicates the Great Recession. GDP, hours worked and investment decreased from the end of 2008 until the peak of the crisis in 2009-Q2 by 5 percentage points, 4 percentage points and 12 percentage points, respectively. Their recovery completed in 2011. Durables increased during the time of the car subsidy – indicated through the dark gray area – by 12 percentage points and decreased by 18 percentage points afterwards. Durables recovered at the end of 2010. Government consumption increased at the beginning of 2009 by 5 percentage points and remained till the end of 2011 by 4 percentage points above its trend. Non-durables were less than 2 percent below their trend at the end of 2009 and recovered fast.

3.3 Methods

3.3.1 The prototype economy

The prototype economy consists of an infinitely-lived household, a firm facing perfect competition, and a government which finances its expenditures by levying taxes on labor, durables, and investment. The model of Chari et al. (2007) is extended in three ways. First, we distinguish between government spending and net exports and second, exclude durables from aggregated investment goods. Both enable a deeper analysis of the stimulus program and the former allows to account for the strong export-dependency of the German economy. Third, wedges consist of a growth and a business cycle part. This allows separate procedures for growth and business cycle accounting and ensures stationarity of the stochastic process. The model also accounts for productive capital and durable consumption capital adjustment costs. Chang (2000) shows that adjustment costs for capital goods in the market and at home solves problems with excess volatility and negative co-movements, because adjustment costs lower the substitutability, which is why we model this structural friction explicitly. The model is written in per capita terms.

3.3.1.1 Model

The per period utility of the representative household is parameterized as follows

$$u(C_t, D_t, N_t) = \begin{cases} \phi \ln(C_t) + (1-\phi)\ln(K_{Dt}) + \psi \ln(1-N_t) & \text{for } \eta = 1, \\ \frac{\left(C_t^{\phi} \cdot K_{Dt}^{1-\phi} \cdot (1-N_t)^{\psi}\right)^{1-\eta} - 1}{1-\eta} & \text{for } \eta \neq 1, \end{cases} \tag{3.3.1}$$

where C_t denotes consumption of non-durable goods and N_t is the household's labor supply. The stock of durable consumption goods K_{Dt} accumulates according to

$$\gamma_n K_{Dt+1} = (1-\delta_D)K_{Dt} + D_t - \Theta_{Dt}\left(\frac{D_t}{K_{Dt}}\right)K_{Dt}, \; \Theta_{Dt}\left(\frac{D_t}{K_{Dt}}\right) = \frac{a_D}{2}\left(\frac{D_t}{K_{Dt}} - b_D\right)^2, \tag{3.3.2}$$

where γ_n denotes the population growth factor, D_t are investments in durable consumption goods, and b_D is the ratio of investment in durables to the stock of durables in the long run. The household maximizes its expected life-time-utility

$$U_t = \mathbb{E}_t \sum_{s=0}^{\infty} (\beta\gamma_n)^s u(C_{t+s}, K_{Dt+s}, N_{t+s}) \tag{3.3.3}$$

subject to the budget constraint

$$C_t + (1+\tau_{It})P_{It}I_t + (1+\tau_{Dt})P_{Dt}D_t \leq R_t K_{It} + (1-\tau_{Nt})W_t N_t + T_t - P_{Et}E_t, \tag{3.3.4}$$

where K_{It} denotes the productive capital stock (capital stock hereafter), I_t investment in capital, T_t lump-sum transfers, E_t net exports, R_t the rental rate on capital, and W_t the real wage. The tax rates τ_{Nt}, τ_{It} and τ_{Dt} are used to model wedges in the labor, investment and durables market. P_{Et}, P_{It} and P_{Dt} are the relative prices for net exports, investment, and durable goods and reflects the wedges' long-run element. The consumption good is the numeraire. The capital stock follows the law-of-motion

$$\gamma_n K_{It+1} = (1-\delta_I)K_{It} + I_t - \Theta_{It}\left(\frac{I_t}{K_{It}}\right)K_{It}, \; \Theta_{It}\left(\frac{I_t}{K_{It}}\right) = \frac{a_I}{2}\left(\frac{I_t}{K_{It}} - b_I\right)^2, \tag{3.3.5}$$

with b_I as the investment-to-capital ratio in the long run.

The representative firm produces its output good Y_t with the Cobb-Douglas technology

$$Y_t = K_{It}^{\alpha}(\gamma_z^t Z_t N_t)^{1-\alpha} \tag{3.3.6}$$

and faces perfect competition. The parameter γ_z denotes the growth factor of labor augmenting technical progress and Z_t the efficiency wedge.

The government expenditures G_t are exogenous and the government chooses lump-sum transfers T_t, so that its budget constraint

$$P_{Gt}G_t + T_t \leq \tau_{Nt}W_tN_t + \tau_{It}P_{It}I_t + \tau_{Dt}P_{Dt}D_t \tag{3.3.7}$$

always binds. Thereby, the resource constraint of the economy is

$$Y_t = C_t + P_{It}I_t + P_{Dt}D_t + P_{Gt}G_t + P_{Et}E_t. \tag{3.3.8}$$

Growth component: As already mentioned, the population grows with γ_n and technical progress with γ_z. Furthermore, the wedges evolve differently. The relative prices reflect this. In the long run $P_{Xt} \in \{P_{It}, P_{Dt}, P_{Gt}, P_{Et}\}$ evolves with $P_{Xt} = g_{P_X}P_{Xt-1}$. The ensuing trend growth factors of different variables X_t are described in Table 3.3. These variables are scaled by $x_t = \frac{X_t}{g_X^t}$ and are thus stationary variables.

Table 3.3: Growth factors

X_t	Y_t	C_t	W_t	T_t	I_t	K_{It}	R_t	D_t	K_{Dt}	G_t	E_t	γ_z	N_t	P_{Xt}
g_X	g_Y	g_Y	g_Y	g_Y	g_I	g_I	g_Y/g_I	g_D	g_D	g_G	g_E	$g_Y^{\frac{1}{1-\alpha}} g_I^{\frac{\alpha}{\alpha-1}}$	1	$g_{P_X} = \frac{g_Y}{g_X}$

Business cycle component: The VAR(1)-process

$$\mathbf{s_{t+1}} = \Pi \mathbf{s_t} + \epsilon_{\mathbf{t+1}},\ \epsilon_{\mathbf{t}} \sim \mathcal{N}(0, \Sigma), \tag{3.3.9}$$

drives the fluctuation of the model, where

$$\mathbf{s_t} = \begin{bmatrix} \ln(s_{At}) & s_{Nt} & s_{It} & s_{Dt} & s_{Et} & \ln(s_{Gt}) \end{bmatrix}^{\mathbf{T}},$$
$$\epsilon_{\mathbf{t}} = \begin{bmatrix} \epsilon_{At} & \epsilon_{Nt} & \epsilon_{It} & \epsilon_{Dt} & \epsilon_{Et} & \epsilon_{Gt} \end{bmatrix}^{\mathbf{T}}.$$

The stochastic process affects the wedges as follows

$$Z_t = A^* \cdot s_{At}, \qquad \tau_{Nt} = \tau_N^* + s_{Nt}, \qquad \tau_{It} = \tau_I^* + s_{It},$$
$$\tau_{Dt} = \tau_D^* + s_{Dt}, \qquad e_t = e^* + s_{Et}, \qquad g_t = g^* \cdot s_{Gt},$$

where A^*, τ_N^*, τ_I^*, τ_D^*, e^* and g^* are the corresponding steady-state component of the different distortions. Similar to Chari et al. (2007), we define the six wedges as follows: The efficiency wedge Z_t, the net export wedge e_t, the government spending wedge g_t, the labor wedge $1-\tau_{Nt}$, the investment wedge $\frac{1}{1+\tau_{It}}$, and the durables wedge $\frac{1}{1+\tau_{Dt}}$. The latter two are defined so that, similar to the labor market wedge, increases act like subsidies and decreases like taxes in comparison to the steady-state value. Since the cyclical component includes the steady-state component, detrended prices p_{Et}, p_{Gt}, p_{It}, p_{Dt} are normed to one. We present in Appendix 3.A the full dynamic equilibrium of the model with stationary variables.

Solution: To derive the model's decision rules, we use a linear perturbation method. In detail, we apply the method of undetermined coefficients as Uhlig (2001) and Christiano (2002) describe to solve the log-linearized model. The solved model then can be written as

$$\mathbf{y_t} = \mathbf{L_x^y} \cdot \mathbf{x_t} + \mathbf{L_s^y} \cdot \mathbf{s_t}, \tag{3.3.10}$$
$$\mathbf{c_t} = \mathbf{L_x^c} \cdot \mathbf{x_t} + \mathbf{L_s^c} \cdot \mathbf{s_t}, \tag{3.3.11}$$
$$\mathbf{x_{t+1}} = \mathbf{L_x^x} \cdot \mathbf{x_t} + \mathbf{L_s^x} \cdot \mathbf{s_t}, \tag{3.3.12}$$

where the matrices $\mathbf{L_x^{\cdot}}$ characterize the policy function of the deterministic part of the model's solution, while $\mathbf{L_s^{\cdot}}$ describe the policy function of the stochastic part. With $\hat{x}_t = \ln(x_t) - \ln(x)$ as the approximation of the relative deviation of a variable x_t from its steady state value x, the vector of observables is $\mathbf{y_t} = \left[\hat{y}_t \quad \hat{N}_t \quad \hat{i}_t \quad \hat{d}_t \quad \hat{g}_t \quad \widehat{\frac{e_t}{y_t}}\right]^{\mathbf{T}}$, while $\mathbf{c_t}$ denotes the vector of unobserved control variables and $\mathbf{x_t} = \left[\hat{k}_{It} \quad \hat{k}_{Dt}\right]^{\mathbf{T}}$ the vector of endogenous states.[6]

3.3.1.2 Mapping

Chari et al. (2007), Brinca et al. (2016), and various other authors map structural models into their prototype economy. Nutahara and Inaba (2012) apply BCA for misspecified wedges and find they are able to approximate the true wedges and the corresponding response of the agents adequately. We show first how to map the stimulus program to the prototype economy. Since the wedges' drivers are modeled as taxes, this is straightforward for most of the measures. Secondly, we reflect monetary policy.

Mapping the stimulus program

Government Wedge: We assign total government spending to the government spending wedge. These are mainly investments in infrastructure and financial support for local and state authority spending. Hence, the stimulus program increases the government wedge directly.

Durables Wedge: The two measures concerning new cars affect the durables wedge. For a given producer price, both measures reduce the absolute tax or the relative price of durables from the households perspective. Hence, they increase the durables wedge.

Investment Wedge: The first part of the stimulus program which affects the investment wedge are subsidies for investments in innovations. The second are increased tax deductions by allowing for a reducing-balance method. For given producer prices, absolute taxes or the relative price of investment decreases and thus the investment wedge increases.

Chari et al. (2007) show how to map financial frictions in terms of a financial accelerator and Brinca et al. (2016) show how to map financial frictions in terms of collateral constraints into a prototype economy with an investment wedge. The loan and guarantee program lowers financial frictions, in particular they mitigate the banks' collateral constraints. Following this, the loan and guarantee program also raises the investment wedge.

Labor Wedge: The stimulus program loweres income tax and social contribution, this increases the labor wedge in general.

Brinca et al. (2016) show the link between a prototype economy with efficiency and labor wedges and an economy with search and matching frictions. The mentioned labor market actions, e.g. expanded short-time work, reduce such frictions and thus, increase the labor market wedge. The effects should be delayed in time due to lower hiring frictions in the aftermath of the crisis.

Efficiency Wedge: Due to the labor market actions in the previous paragraph, the efficiency wedge increases also due to a better matching. Further, the expanded short-time work possibilities reduce labor hoarding, since the firm can both retain employees to lower future hiring

[6] The use of $\widehat{\frac{e_t}{y_t}}$ instead of $\hat{e}_t$ is discussed in 3.3.2.2.

frictions and adjust hours worked. As a consequence, the efficiency wedge increases.

As shown by Chari et al. (2007), input-financing frictions are associated with efficiency wedges. These frictions appear when firms must borrow for an input good and some firms are financially more constrained than others. Such firms have to pay higher interest rates. The loan and guarantee program lowers financial constraints and thus increases the efficiency wedge.
Net exports: The increase in Hermes coverage advances the conditions for exports. Nevertheless, the effects are probably only rather small.

Mapping monetary policy
Government Wedge: Purchasing bonds lowers the bonds' interest rates and this lowers the costs of debt-financed government spending, which may indirectly increase the government wedge.
Durables Wedge: Since refinancing is cheaper, for a given real rate of return, investment increases. Hence, monetary policy changes the intertemporal decision of a household, which is reflected in a higher durables wedge. Furthermore, provision of liquidity also changes the intertemporal decisions of liquidity constrained households, which also reflects in a higher durables wedge.
Investment Wedge: Both mentioned effects of the durables wedge have the same effect on the investment wedge. The provision of liquidity and cheaper refinancing lowers frictions in the investment market.

As already mentioned, Brinca et al. (2016) show how to map an economy with a collateral constrained bank into a the prototype economy with an investment wedge. Lower collateral constraints lower frictions in the investment market. Thus, the slacked collateral requirements by the ECB increase the investment wedge.
Efficiency Wedge: As mentioned above, input-financing frictions are associated with efficiency wedges (see Chari et al., 2007). The friction appears when firms must borrow for input goods and some firms are financially more constrained than others. Those firms have to pay higher interest rates. The Security Markets Program can lower these frictions and thus, increases the efficiency.

3.3.1.3 Calibration

We estimate the elasticity, $\eta_I = \frac{I}{K_I}\Phi_I''$, of the price of capital with respect to the investment to capital ratio as well as the elasticity, $\eta_D = \frac{D}{K_D}\Phi_D''$, of the price of the stock of durables with respect to the new durables to stock of durables ratio in addition to the parameters that characterize the stochastic process $\mathbf{s_t}$. The remaining parameters are calibrated as follows:

The capital elasticity α is set to 0.34. Flor (2014) calculates this as the German capital share from 1991 to 2012. In line with Heer and Maussner (2009, Chapter 1.5), Flor (2014) also provides the discount parameter $\beta = 0.994$ for the German economy. We pin down the annual rate of capital depreciation at the average ratio of gross fixed capital formation and the net stock of fixed assets. The average quarterly capital depreciation rate arises from $\delta_I = 1-(1-\delta_{I,annual})^{\frac{1}{4}}$. In the same manner the rate of durables depreciation δ_D is computed.

The choice of ψ, ϕ and η, which characterize the household's preferences, is more problematic. For ψ and η we follow the baseline calibration from Chari et al. (2007) and fix ψ at 2.24 and η at 1. We calibrate the preference weight of durables ϕ by matching the durable to non-durable consumption ratio with the long-run marginal rate of substitution between consumption and durables. We do not estimate the steady-state values of the different wedges. Instead, we compute them from the model's static equilibrium equations in line with Lama (2011). We fix the steady-state values of output, government consumption, investment in capital as well as in durables to their average shares of output (see Table 3.2). The steady-state labor supply N

is 0.122, which equals the average share of hours worked on the available time budget of a household.[7] Our calibration exercises are summarized in Table 3.4.

Table 3.4: Calibration of the model

Parameter	Description	Value
α	capital share	0.34
β	discount factor	0.994
δ_I	rate of capital depreciation	0.017
δ_D	rate of durables depreciation	0.045
ψ	preference weight of labor	2.24
ϕ	preference weight of consumption	0.879
η	risk aversion	1

3.3.1.4 Identification

We check our prototype economy for strict local identification following Iskrev (2010), who shows that a linearized DSGE model with normally distributed shocks is locally identified for a given set of parameters, if the Jacobian matrix of theoretical first and second moments with respect to these parameters has full rank. To check the identifiability over a sufficiently large parameter space we draw 1,000,000 times from the following distributions for the elasticities of the adjustment costs $\eta_D,\ \eta_I$, for the the off-diagonals $\pi_{ij},\ i \neq j$ of Π, for the diagonals π_{ii} of Π, and the elements $b_{ij},\ i \leq j$ of the lower triangular matrix B with $\Sigma = BB^T$:

$$\eta_D, \eta_I \sim U(0,4), \qquad \pi_{ij} \sim \mathcal{N}(0,0.1), \qquad \pi_{ii} \sim \mathcal{N}(0.8,0.1), \qquad b_{ij} \sim U(-0.05,0.05).$$

The Jacobian of the first and second moments (up to two lags) has full rank at approximately 99.9 percent of the draws. Thus, the model is virtually identifiable in the chosen parameter space.[8]

Brinca et al. (2018) provide and apply strategies for identification strength. They show that weak identification of the stochastic process' parameters is secondary, but this does not hold for structural ones. To address this problem, we compute the likelihood surface of the uncertain deep parameters η_D and η_I to detect a global maximum as well as the likelihood's curvature and execute robustness checks in section 3.4.

3.3.2 The business cycle accounting procedure

The BCA procedure is divided into three separate steps: The estimation of the parameters, the identification of the wedge states, and the assessment of the contribution of a single wedges towards the business cycle.

MLE determines the matrices Π and Σ that characterize the stochastic process $\mathbf{s_t}$ as well as the elasticities η_I and η_D that define the level of adjustment costs. Full-information estimation of DSGE models is typically done with Bayesian methods, although MLE involves less assumptions. Applying Bayesian estimation is usually meaningful, since the researcher has a structural parametrization in mind and, by association, an idea of probable parameter values.

[7] Here we follow (Heer and Maussner, 2009, Chapter 1.5), who assume that the household's maximum working hours amount to $1,440 = 16$ hours per day$\times$90 days per quarter.

[8] In comparison, we proceed similarly for the benchmark economy of Chari et al. (2007) presented in Appendix 3.B. The Jacobian of the first and second moments (up to two lags) has no full rank at 26 parameter draws from 1,000,000.

We would like to stress that the application of BCA requires MLE and any restrictions like the Bayesian approaches, such as Otsu (2010), Chakraborty and Otsu (2013) or Plotnikov (2017) are questionable. The wedges are superpositions and interactions of a variety of market distortions with an underlying reduced-form stochastic process, which complicates the interpretation of the Markov transitions. Furthermore, recall the findings of Nutahara and Inaba (2012) that the VAR(1) strips a potentially more sophisticated stochastic process down. Thus, the estimated parameters are only pseudo-true for the real model. As a consequence, in general the values of the process' parameters cannot be interpreted, and a-priori assumptions of them are meaningless, and even more seriously, may restrict the set of mappable models. Thus, we make a point for MLE and let the data speak through an unrestricted VAR.[9]

After all parameters are pinned down, either by calibration or MLE, we use a state-smoothing algorithm as described in Durbin and Koopman (2012, Chapter 4.4) to predict the wedge's states $\mathbf{s_t}$.

In a last step, in line with Chari et al. (2007), we feed the wedges separately back into the model, while others are set constant, to assess the contribution of each wedge to the quantities of interest.[10]

3.3.2.1 Maximum-likelihood estimation

To evaluate the likelihood function of the linear state-space model (3.3.9)–(3.3.12), most of the literature uses a Kalman-recursion initialized at the unconditional mean and variance of the state vector $[\mathbf{x_0^T}\ \mathbf{s_0^T}]^\mathbf{T}$ (see e.g. DeJong and Dave, 2011, Chapter 8.4)). However, for an asymptotic stable state-space model, the mean squared error (MSE) $\mathbf{P_{t|t}}$ of the point estimate for $[\mathbf{x_t^T}\ \mathbf{s_t^T}]^\mathbf{T}$ conditional on a observed set of data $\{\mathbf{y_1}, \dots, \mathbf{y_t}\}$ converges to a matrix $\mathbf{P}$, the steady-state MSE, as t goes to infinity.[11] Exploiting this property, Chari et al. (2007) use the steady-state MSE $\mathbf{P}$ instead of the unconditional variance to initialize their Kalman-recursion. Further, it can be shown that the steady-state MSE $\mathbf{P}$ is equal zero in BCA prototypes economies like the one presented here.[12] To get the intuition behind the result and for the sake of simplicity, let us consider the case without growth and with zero adjustment costs. In this case, equations (3.3.2) and (3.3.5) rewrite to

$$\begin{aligned} K_{Xt+1} &= X_t + (1-\delta_X)K_{Xt} \\ &= \sum_{i=0}^{t-1}(1-\delta_X)^i X_{t-i} + (1-\delta_X)^t K_{X1},\ X \in \{I, D\}. \end{aligned}$$

Imagine we observe the investment $X_i \in \{I, D\}$ in capital and in durables for all $i = 1, \dots, t$. Assuming that K_{X1} is normally distributed with variance σ_X^2, the variance of K_{Xt+1} conditional on $\{X_1, \dots, X_t\}$ yields $(1-\delta_X)^{2t}\sigma_X^2$. Since $\delta_I, \delta_D \in (0, 1]$, it is straightforward that the uncertainty regarding the endogenous states $\mathbf{x_t}$ disappears as t goes to infinity. Furthermore, assuming $\mathbf{L_s^y}$ is

[9] We would like to point out two technical issues regarding Bayesian methods and BCA. First, to the best of our knowledge, there is no prior that includes all combination parameter values that generate eigenvalues of Π less than one and excludes all combinations that do not have these properties. Second, the posteriors of a VAR-driven DSGE model can be multi-modal. This makes the commonly used RWMH algorithms unsuitable. For a deeper discussion and solution for the latter issue, see Herbst and Schorfheide (2016, Chapter 5, 6.1)

[10] See the technical appendix by Chari et al. (2007) for more details.

[11] For a formal proof, see e.g. Hamilton (1994, Chapter 13).

[12] Fehrle and Huber (2022) show that if $\mathbf{L_s^y}$ is non-singular and $\frac{1-\delta_D}{\gamma_n \cdot g_D}, \frac{1-\delta_I}{\gamma_n \cdot g_I} \in [0, 1)$ the matrix $\mathbf{P} = \mathbf{0}$ reflects the unique and stabilizing solution to the Riccati difference equation that determines the law of motion of the sequence $\left\{\mathbf{P_{t|t}}\right\}_{\mathbf{t=0}}^{\mathbf{N}}$.

non-singular,[13] it follows that

$$\mathbf{s_t} = \left[\mathbf{L_s^y}\right]^{-1}\left(\mathbf{y_t} - \mathbf{L_x^y}\cdot\mathbf{x_t}\right). \tag{3.3.13}$$

Thus, as the uncertainty of the endogenous states $\mathbf{x_t}$ disappears as t goes to infinity, the uncertainty over the exogenous states $\mathbf{s_t}$ disappears as well. Using a Kalman-recursion initialized at the steady-state, with the steady-state MSE $\mathbf{P}$ is therefore equivalent to the assumption that the initial state vector is fixed and known, $[\mathbf{x_0^T}\ \mathbf{s_0^T}]^\mathbf{T} = \mathbf{0}_{nx+ns\times 1}$. There are two major advantages of a fixed and known initialization at the long-run equilibrium. First, the likelihood evaluation can be vectorized and more important, it provides an analytical solution of the MLE for Σ since we can observe the residuals ϵ_t independently of Σ.[14] The solution of the MLE for Σ for a given Π is

$$\hat{\Sigma} = \frac{1}{\mathbf{N}}\sum_{\mathbf{t=1}}^{\mathbf{N}}\left[(\mathbf{s_t} - \Pi\cdot\mathbf{s_{t-1}})\cdot(\mathbf{s_t} - \Pi\cdot\mathbf{s_{t-1}})^\mathbf{T}\right],\ \mathbf{s_0} = \mathbf{0}_{ns\times 1}. \tag{3.3.14}$$

The estimates of a standard Kalman-recursion, which is initialized at the unconditional first and second moments, are more natural, since the initial states are usually unknown. However, note that although the log-likelihood calculated on the basis of a steady-state Kalman-recursion does not reflect the exact or unconditional log-likelihood, the determined maximum-likelihood estimator may (under certain preconditions, see e.g., (Harvey, 1990, pp. 119, 129) have the same large-sample properties as the unconditional maximum-likelihood estimator. Therefore, we use the estimates of the steady-state Kalman-recursion as the initial guess for a second estimation, where we initialize the Kalman-recursion with the unconditional first and second moments.

3.3.2.2 Data manipulation

The observables are GDP, investment, durables, government expenditures, net exports to GDP, and hours worked. Regressions with the logarithm of the first four observables as dependent variable and time as independent variable provide necessary components. The coefficient estimates determine the growth rates and the residuals the relative deviation from the particular growth path. Negative values for net exports prevent logarithmization. A regression with net exports relative to GDP as dependent variable and time as independent variable provides auxiliary variables. The coefficient is the excess growth rate of net exports compared to GDP growth. The residuals are the deviation from the long-run net exports to GDP rate, which is computable in the model. The residuals of these regressions are used for business cycle accounting, the coefficients for growth accounting.

Since hours worked per capita do not include a trend, the relative deviations from the long-run average are used for business cycle accounting. Whereas growth accounting is of course not applicable in this manner.

For a detailed data source, see Appendix 3.C.

[13] Note that for a singular matrix $\mathbf{L_s^y}$ it is not possible to obtain the wedges' states. For a discussion under which circumstances $\mathbf{L_s^y}$ may be singular see Huber (2022). However, this case never occurred in our analysis.

[14] For more details see also Fehrle and Huber (2022).

3.4 Results

3.4.1 Growth accounting

Table 3.5 presents the growth rates of the observables. The GDP annual trend growth rate is 1.32 percent. The amount of durables and investment goods grows slower than GDP, while net exports grow faster. Government consumption grows similar to GDP.

Table 3.5: Growth accounting

Parameter	Description	Value
$\ln(\gamma_n^4)$	annual growth rate of population	0.03%
$\ln(g_Y^4)$	annual growth rate of GDP	1.32%
$\ln(g_I^4)$	annual growth rate of investment	0.93%
$\ln(g_D^4)$	annual growth rate of durables	0.35%
$\ln(g_G^4)$	annual growth rate of gov. cons.	1.40%
$\ln(g_E^4)$	annual growth rate of net exports	1.65%

Similar to the shocks which drive the business cycle, the long-run components of the wedges P_{xt} and γ_z are reduced-form. Since we focus on the business cycle, we discuss only briefly potential causes for different growth rates. Differences in the long-run component of the durables and the investment wedge (P_{Dt}, P_{It}) may occur due to investment-specific technological change as described by Greenwood et al. (1997). The increase in German net exports since the launch of the Euro is investigated by Kollmann et al. (2014). The most important factors, summed up in P_{Et}, are: A higher German savings rate, positive supply shocks, especially due to labor market reforms, as well as a higher demand for German goods of non Euro area members.

Figure 3.4: Maximum-likelihood estimation

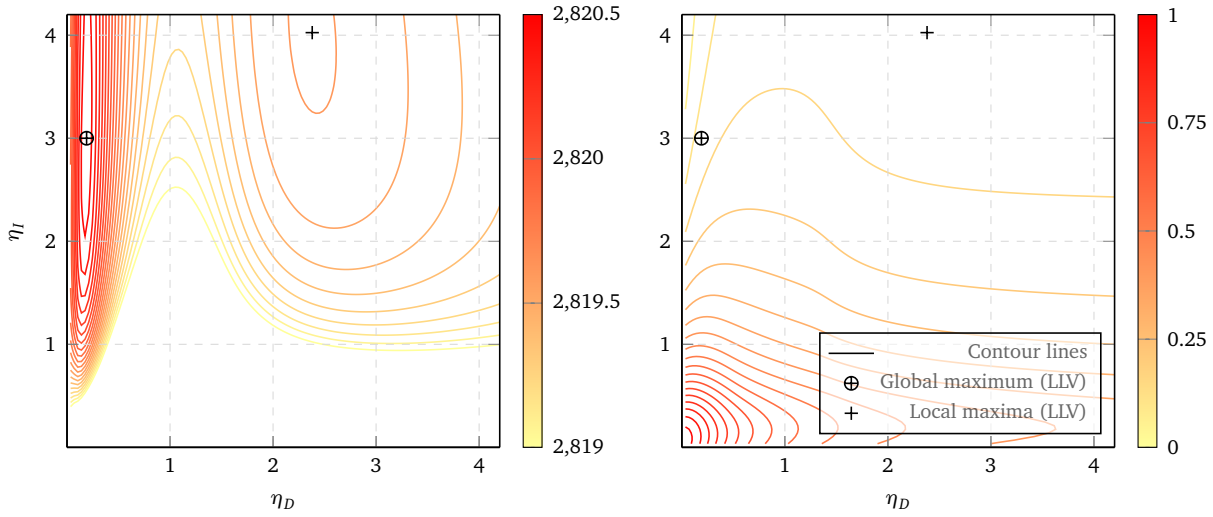

(a) Log-Likelihood (without constant)

(b) Correlation between ϵ_{It} and ϵ_{Dt}

Table 3.6: Estimation of exogenous shock process

Autoregressive Matrix							
Π	$ln(s_A)$	s_N	s_I	s_D	s_E	$ln(s_G)$	
$ln(s_A)$	0.90	0.41	0.00	0.07	-0.21	-0.16	
s_N	0.01	0.83	0.01	-0.02	-0.12	-.01	
s_I	0.70	-1.71	0.96	-0.52	1.44	1.07	
s_D	0.27	-0.05	-0.00	0.66	0.16	-0.01	
s_E	0.06	-0.03	0.01	-0.05	0.62	-0.12	
$ln(s_G)$	-0.05	0.17	-0.01	-0.05	-0.22	0.80	

Correlation and standard errors							
$Corr(\epsilon_i, \epsilon_j)$	ϵ_A	ϵ_N	ϵ_I	ϵ_D	ϵ_E	ϵ_G	$100 \cdot StD(\epsilon_i)$
ϵ_A	1.00						0.94
ϵ_N	0.03	1.00					0.34
ϵ_I	-0.49	-0.06	1.00				7.12
ϵ_D	0.27	-0.83	0.13	1.00			1.44
ϵ_E	0.31	0.70	-0.02	-0.36	1.00		0.59
ϵ_G	-0.10	0.13	-0.19	-0.16	-0.13	1.00	0.80

3.4.2 Estimation

As already mentioned, the MLE includes Π, Σ, η_D and η_I. Panel 3.4(a) illustrates the likelihood function with respect to η_D and η_I, while Π and Σ are the argument maximum of the function for given η_I and η_D. The panel identifies two local maxima. The global is at $\eta_D = 0.19$ and $\eta_I = 3.00$.

Table 3.6 presents the estimates for the autoregressive matrix Π as well as second moments of the innovations ϵ_i. All wedges are highly autoregressive. The investment wedge depends heavily on the other wedges with one lag. The innovations of the investment wedge have the highest volatility and are negatively correlated with the efficiency wedge. There is also a strong negative correlation between the innovations of the durables and the labor wedge. The net export wedge's innovation correlates with the labor wedge.

Panel 3.4(b) illustrates that the innovations of durables and investments are perfectly correlated in the absence of adjustment costs. Fehrle (2019) investigates different investment goods, vector-autoregressive processes and adjustment costs in detail and argues that adjustment costs can be viewed as a underpinning mechanism of reduced-form correlated shocks. Here, e.g. the mentioned high substitutability between durables and investments is prevented either by perfect correlated innovations, adjustment costs or a nest of them. Hence, it is useless to separate investments and durables without adjustment costs, since the corresponding wedges must co-move. Otherwise, as a result of Chang (2000), the high substitutability would lead to an excessive volatility of durables and investments and negative co-movements between them. However, this is contradicted by the data.

3.4.3 Business cycle accounting for the Great Recession and the German fiscal stimulus program, 2008-Q1 – 2011-Q3

The graphical analysis of our BCA exercise is reported in Figure 3.5. In Panels 3.5(a) to 3.5(e) we confront the observations of GDP, its subaggregates and hours worked with the model's prediction when only one wedge is allowed to fluctuate.

Panel 3.5(a) illustrates that the crisis was mainly driven by the efficiency wedge. The invest-

ment and net exports wedge also contributed to the crisis. These three wedges together induced the decrease in GDP. The labor wedge contributed to the crisis from 2009-Q2 to 2009-Q4. Before, the wedge was counter-cyclical and afterwards it introduced the recovery. The durables wedge and government consumption were anti-cyclical. Panel 3.5(b) illustrates that the investment wedge drove the decline in investment mostly, while the efficiency wedge mattered little. The efficiency wedge influenced durables negatively as Panel 3.5(c) shows. The durables wedge on its own increased durables up to almost 50 percent in 2009. Afterwards, the wedge only had a slight impact. Panel 3.5(d) indicates that the efficiency wedge caused the decline in non-durable consumption mostly and the labor wedge partly. The durables and government consumption wedge had little impact on non-durable consumption. Panel 3.5(e) predicts the decline in net exports to GDP and the investment wedge introduced the decline in hours worked. The labor market wedge drove the decline between 2009-Q2 and 2009-Q4. Besides, the labor wedge was counter-cyclical. The other wedges were counter-cyclical. Theory teaches us that the wedges of both investment goods D_t and I_t react similar to monetary policy and financial frictions in general.[15] Thus, Chari et al. (2007) and many others aggregate them. The business investment wedge drove the decline in business investment during the crisis. Financial frictions and other distortions dominated the fiscal and monetary policy measures. This is not true for durables. The only appreciable difference between the wedges during the crises were the car subsidies. Further, the positive impact of the durables wedge occurred simultaneously with the subsidies. The wedge began to stimulate the demand of durable goods with the introduction of the tax exemption for new cars in 2008-Q4. In 2009-Q1 the cash for clunkers program started, while the stimulating effect increased strongly. The stimulus disappeared between 2009-Q4 and 2010-Q1 while the last pay-off took place in 2009-Q4. Hence, we attribute the large increase due to the durables wedge to the car subsidies and can map changes due to the durables as well as government spending wedge to the fiscal stimulus program. The measures in other markets are dominated by frictions. Thus, it is unfortunately impossible to give statements about the measures with the chosen method.

With respect to GDP and hours, we find that the stimulus program due to the durables subsidies and government consumption had a positive effect during the crisis. The model predicts an approximately 2 percent bigger decline in GDP and an approximately 3.5 percent bigger decline in hours without changes in those wedges during the peak of the crisis (2009-Q2). Regarding non-durable consumption and investment the effect of the stimulus program is negative. Nevertheless, during the crisis the stimulus of durables and government consumption increased GDP and was not completely substituted by lower investments and non-durable consumption. Intertemporal substitution of durables investment in the aftermath of the program was small. The bust was driven by the efficiency wedge, which depressed durables over the whole period. The durables wedge virtually did not influence GDP negatively from 2008-Q1 till 2011-Q3.

The labor market wedge mitigated the crisis at the beginning and the end of the crisis. In particular at the end of the crisis, the model predicts an increase of more than 2 percent in GDP and more than 3 percent in hours worked.

The measurement ω_i quantifies the contribution of each wedge to GDP during the Great Recession as

$$\omega_i = \frac{\sum_t (\hat{y}_t^{GDP} - \hat{y}_t^i)}{\sum_j \sum_t (\hat{y}_t^{GDP} - \hat{y}_t^j)} \text{ with } i, j \in \{s_A, s_N, s_I, s_D, s_G, s_E\},\ t \in [\text{2008-Q1}, ..., \text{2011-Q3}],$$

[15] Gertler and Gilchrist (2018) report for the U.S. financial frictions during the Great Recession a big negative impact on the durables market. Benmelech et al. (2016) explain one third of the decline in the U.S. car demand by frictions on the asset-backed commercial paper market. The decline in U.S. house prices weakens the household balance sheets, which also had a negative effect on the U.S. auto market, as shown by Mian et al. (2013).

Figure 3.5: BCA - Results

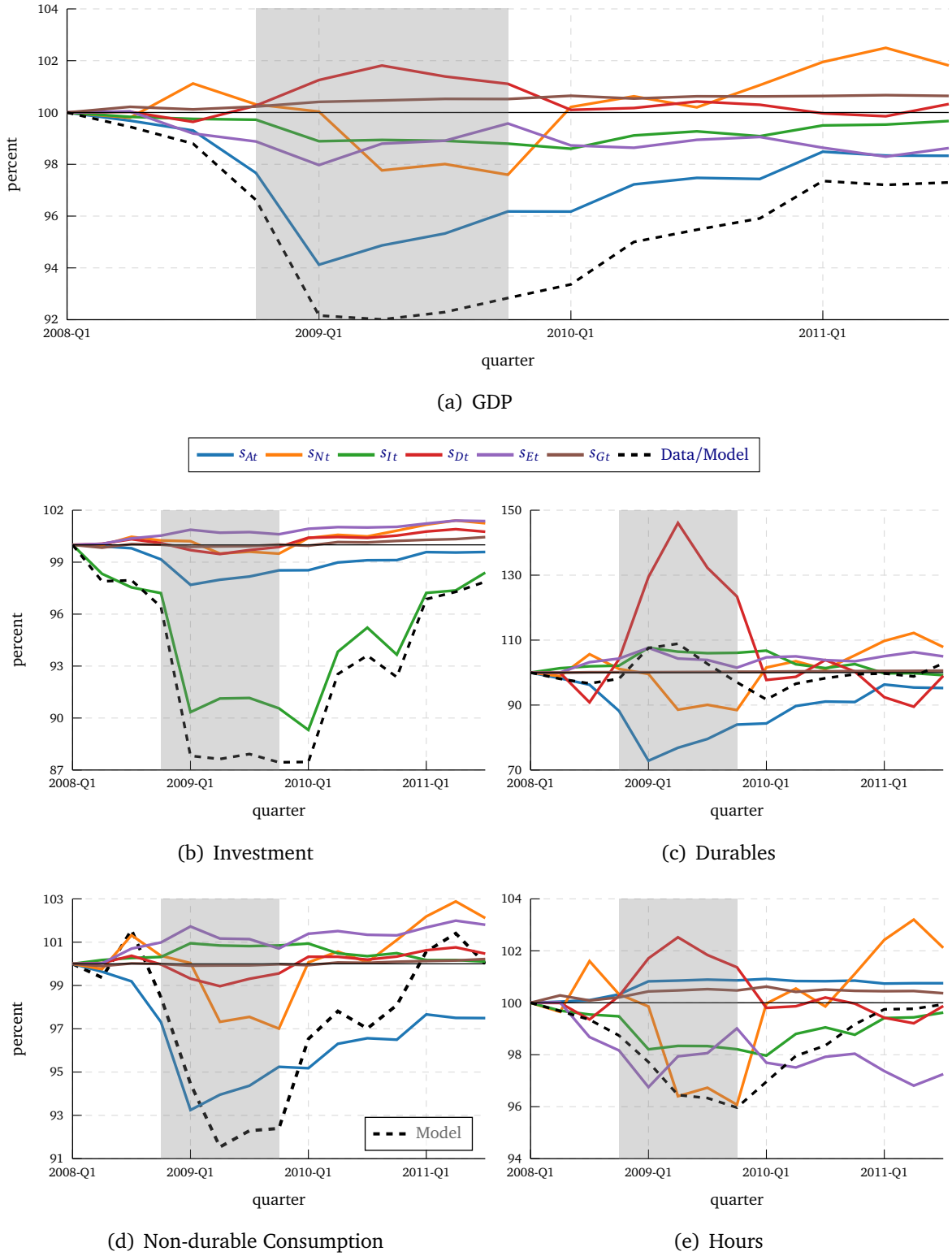

(a) GDP

(b) Investment

(c) Durables

(d) Non-durable Consumption

(e) Hours

Notes: Dashed lines for GDP, investment, durables and hours are the data and the model's outcome. Here they are equivalent. The dashed lines for non-durable consumption is only the model's outcome. The gray area indicates the main effective period of the fiscal stimulus program 2008-Q4 – 2009-Q4.

where $\hat{y}_t^{GDP}$ is the GDP when all wedges are non-changing and $\hat{y}_t^i$ is the model outcome of wedge i alone. Thus, the contribution of all wedges together sums to 1, while the sign of ω_i points out if wedge i has mitigated ($-$) or amplified ($+$) a crisis.

The efficiency wedge accounts for 62 percent of the decline in GDP during this period, net exports for 26 percent, the investment wedge for 19 percent, and the labor market accounts for 3 percent. Government consumption accounts for -5 percent and the durables wedge for -4 percent. Since the effect of the durables wedge during the durables subsidies was at least twice as large as the effect of government consumption and effects throughout the whole crisis were similar but expenditures for these subsidies only made up for about 25 percent of the increase of government consumption, durables subsidies were more efficient to stimulate aggregated demand than government consumption.

With the identifying assumption that the fiscal stimulus program together with monetary policy were the only counter-cyclical distortions, our results represent a lower bound for the impact of fiscal and monetary policy measures as well as for the pro-cyclical distortions.

3.4.4 Robustness and discussion

Robustness in parameters: The results depend potentially on the values of adjustment costs η_I, η_D and on the intertemporal elasticity of substitution η. To evaluate the sensitivity, we calculate ω_i over a grid of the mentioned parameters. Therefore, we reestimate the (remaining) uncertain parameters at each node of the parameter grid.

Figure 3.6 illustrates the contribution of the concerning wedges for different amounts of adjustment costs. The efficiency wedge contributed the most to the decline in GDP, followed by net export for the whole set of adjustment costs. The results for the labor market wedge and government consumption are robust as well. The durables wedge mitigated the crisis for most of the parameter combinations. The contribution would have been pro-cyclical without adjustment costs. As mentioned above, in the absence of adjustment costs a separation of the durables and investment wedge is meaningless. The investment wedge's contribution to the crisis would have been negative for $\eta_I < 1/3$ where the likelihood is the lowest (see Panel 3.4(a)) and positive otherwise.

Subsidies in durables change the intertemporal rate of substitution. Hence, a robustness check to the elasticity of the substitution rate is relevant. Figure 3.7 presents the contribution to the decline in GDP over η. The contributions of the labor, investment, durables and the government consumption wedge are nearly constant. The contribution of net exports declines with a higher elasticity, nevertheless they contributed the second most over the whole domain. The contribution of the efficiency wedge increases with η.

Robustness regarding the benchmark model: The assessment of the joint contribution of the investment and durables wedge as well as the joint contribution of government consumption and net exports maps our economy into the benchmark BCA economy ex post. The left panel of Figure 3.8 illustrates these effects. The right panel plots the impact of the investment and government spending wedge in the Chari et al. (2007) benchmark economy, where durables and investment as well as government spending and net exports are aggregated ex ante.[16] The results are similar, except in the more detailed economy the investment wedge was slightly counter-cyclical during the cash for clunkers program. Thus, the results of the detailed model are not counterfactual to the benchmark BCA model, but provide deeper insights.

Although the impact of the composed investment wedge was negligible during the Great Recession, our results suggest that the decomposed wedges were not. The pro-cyclical effect

[16] Appendix 3.B sketches the model and provides our estimation strategy and results for the Chari et al. (2007) benchmark economy of the presented time series.

Figure 3.6: Adjustment costs specific wedge contribution

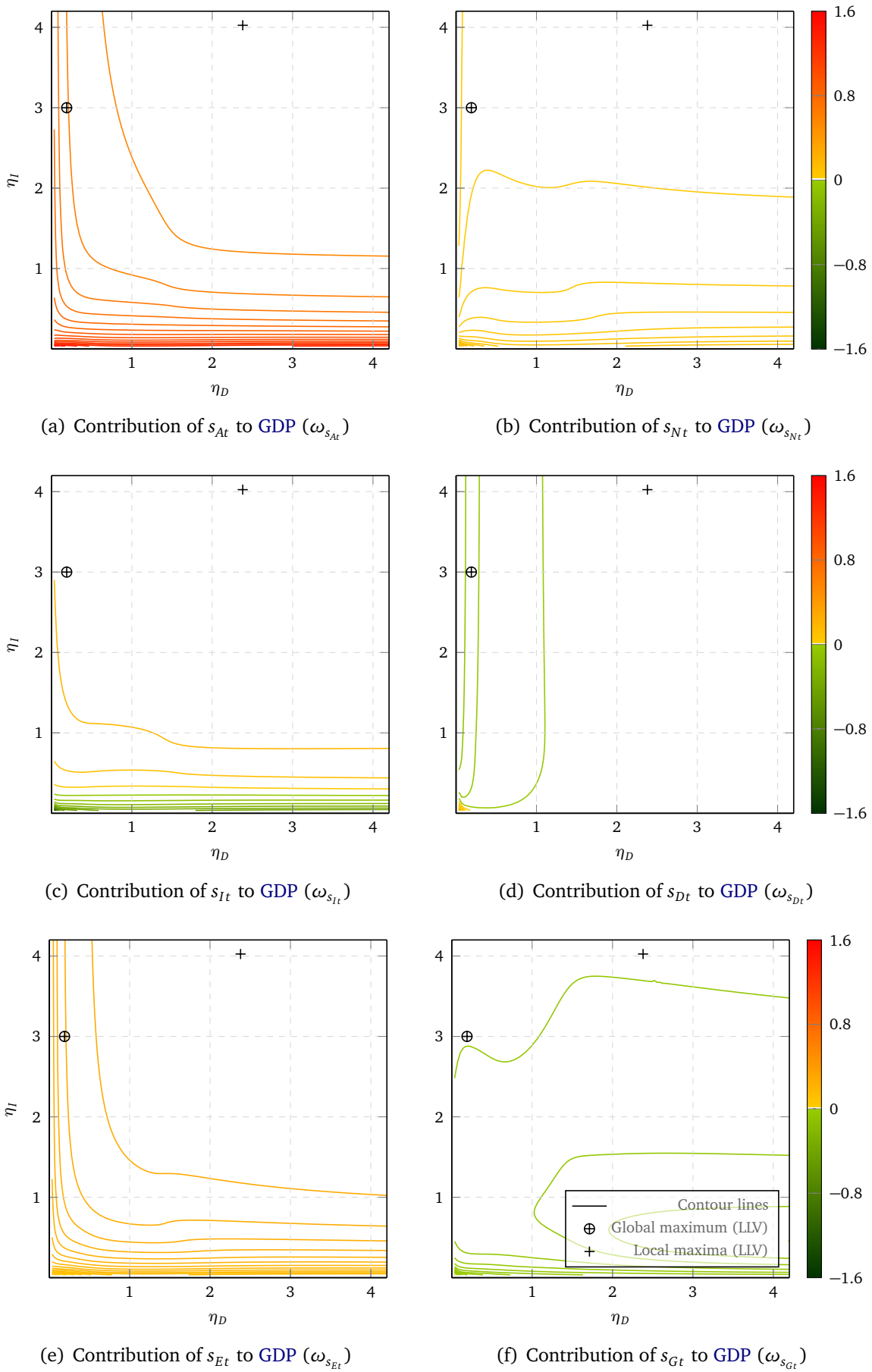

(a) Contribution of s_{At} to GDP ($\omega_{s_{At}}$)

(b) Contribution of s_{Nt} to GDP ($\omega_{s_{Nt}}$)

(c) Contribution of s_{It} to GDP ($\omega_{s_{It}}$)

(d) Contribution of s_{Dt} to GDP ($\omega_{s_{Dt}}$)

(e) Contribution of s_{Et} to GDP ($\omega_{s_{Et}}$)

(f) Contribution of s_{Gt} to GDP ($\omega_{s_{Gt}}$)

Figure 3.7: Inverse elasticity of intertemporal substitution specific wedge contribution

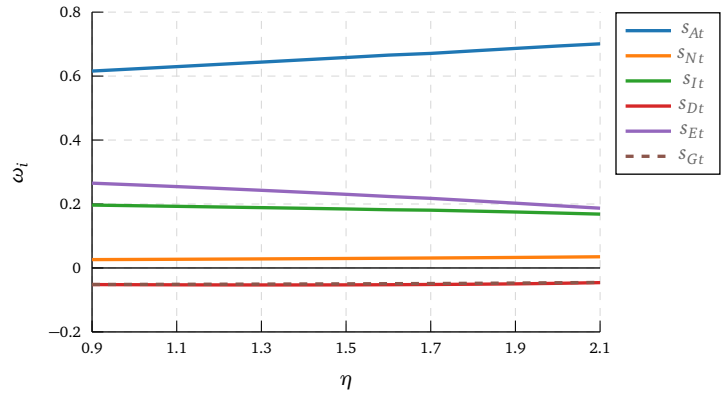

of the investment wedge and the policy-driven counter-cyclical effect of durables wedge offset each other. Hence, without our decomposition the importance of the investment wedge and, by association, the importance of financial frictions during the Great Recession is underrated. For example, the financial frictions of Carlstrom and Fuerst (1997), Kiyotaki and Moore (1997), Bernanke et al. (1999), or Gertler and Kiyotaki (2010) are equivalent to the investment wedge.

Figure 3.8: Robustness to the Chari et al. (2007) benchmark economy

(a) Detailed Economy

(b) Chari et al. (2007) - Benchmark Economy

Comparing two durables boom-bust cycles: As mentioned, there were two boom-bust cycles in the durables market. We compare them in Figure 3.9. Panels 3.9(a) and 3.9(b) show the data and the impact of the durables wedge on durables from 2008-Q1 to 2010-Q4 and from 2006-Q1 to 2007-Q4. The durables wedge accounts during the car subsidies programs for the boom, but only marginally for the bust afterwards. During 2006 a VAT increase announcement passed the institutions and at this time durables investments increased. The introduction of the increase was in 2007-Q1, when the bust took place. The durables wedge caused the whole boom-bust cycle and illustrates intratemporal substitution.

Figure 3.9: The durables boom-bust cycles 2008-2010 and 2006-2007 in comparison

(a) Cash for clunkers program

(b) VAT increase with announcement

3.5 Conclusion

We use the BCA analysis to investigate the impact of the German stimulus program during the Great Recession from 2008-Q1 to 2011-Q3. We extended the prototype economy by two wedges. Wedges correspond to the following variables: *government consumption, durables, investment, labor, net exports, and efficiency*. To account for the fiscal stimulus we map fiscal and monetary policy towards these wedges, thus enabling a policy evaluation.

We introduce two procedures that enable a fast and reliable MLE and the application of tools which help to overcome problems of weak identification. The first procedure separates between growth and business cycle accounting which ensures the stationarity of the underlying stochastic process. The second procedure is a new strategy to find a good guess for the argument maximum of the likelihood function. The applicability of MLE is crucial for, and one of the major advantages of BCA at the same time. Since MLE is difficult, and so Bayesian methods or other restrictions towards the stochastic process are used for BCA, we hope to give new impetus to the use of MLE and BCA with both procedures.

In our BCA analysis we find that the Great Recession in Germany was mainly driven by the efficiency wedge, net exports, and the investment wedge. In contrast, the durables and the government spending wedge acted counter-cyclical. We argue that the latter two collect parts of the German stimulus. The labor market wedge was pro-cyclical between 2009Q2 and 2009-Q4, besides it mitigated the crisis and especially induced the recovery. Due to higher expenditures for government consumption and a similar impact compared to the cash for clunkers program, subsidies for durable goods stimulated aggregated demand more efficiently. We check the robustness of our results to different choices of parameters that determine the elasticity of intertemporal substitution as well as capital and durables adjustment costs. We find that our results are robust for all wedges except the investment wedge. However, the results indicate that previous studies underrate the negative impact of the investment wedge and, as a consequence, the role of investment wedge equivalent financial frictions. We have to mention that BCA is only a first but useful step for the identification of market distortions, and thus we aim to motivate further research on the efficiency of durable goods' subsidies, the role of financial frictions during the Great Recession and the labor market driven recovery in Germany.

Acknowledgment

We are grateful to our Ph.D. advisor Prof. Alfred Maußner for initial ideas and ensuing discussions. We thank Prof. Burkhard Heer, Prof. Loukas Karabarbounis, Prof. Kerstin Roeder, and Dr. Markus Kontny for valuable comments.

Bibliography

BENMELECH, E., R. R. MEISENZAHL, AND R. RAMCHARAN (2016): "The Real Effects of Liquidity During the Financial Crisis: Evidence from Automobiles," *The Quarterly Journal of Economics*, 132, 317–365.

BERGER, D. AND J. VAVRA (2015): "Consumption Dynamics during Recessions," *Econometrica*, 83, 101–154.

BERNANKE, B. S., M. GERTLER, AND S. GILCHRIST (1999): "Chapter 21 - The Financial Accelerator in a Quantitative Business Cycle Framework," in *Handbook of Macroeconomics*, ed. by J. B. Taylor and M. Woodford, Elsevier, vol. 1, 1341–1393.

BRINCA, P., V. CHARI, P. KEHOE, AND E. MCGRATTAN (2016): "Chapter 13 - Accounting for Business Cycles," in *Handbook of Macroeconomics*, ed. by J. B. Taylor and H. Uhlig, Elsevier, vol. 2, 1013–1063.

BRINCA, P., N. ISKREV, AND F. LORIA (2018): "On Identification Issues in Business Cycle Accounting Models," MPRA Paper 90250, University Library of Munich, Germany.

BUNDESGESETZBLATT (2008): "Gesetz zur Umsetzung steuerrechtlicher Regelungen des Maßnahmenpakets "Beschäftigungssicherung durch Wachstumsstärkung"." Tech. Rep. Nr. 64, Bundesanzeiger Verlag, Bonn, Germany, Teil I.

——— (2009): "Gesetz zur Sicherung von Beschäftigung und Stabilität in Deutschland," Tech. Rep. No. 11, Bundesanzeiger Verlag, Bonn, Germany, Teil I.

CARLSTROM, C. T. AND T. S. FUERST (1997): "Agency Costs, Net Worth, and Business Fluctuations: A Computable General Equilibrium Analysis," *The American Economic Review*, 87, 893–910.

CHAKRABORTY, S. AND K. OTSU (2013): "Business Cycle Accounting of the BRIC Economies," *The B.E. Journal of Macroeconomics*, 13, 381–413.

CHANG, Y. (2000): "Comovement, Excess Volatility, and Home Production," *Journal of Monetary Economics*, 46, 385–396.

CHARI, V. V., P. J. KEHOE, AND E. R. MCGRATTAN (2007): "Business Cycle Accounting," *Econometrica*, 75, 781–836.

——— (2009): "New Keynesian Models: Not Yet Useful for Policy Analysis," *American Economic Journal: Macroeconomics*, 1, 242–266.

CHO, D. AND A. DOBLAS-MADRID (2013): "Business Cycle Accounting East and West: Asian Finance and the Investment Wedge," *Review of Economic Dynamics*, 16, 724–744.

CHRISTIANO, L. J. (2002): "Solving Dynamic Equilibrium Models by a Method of Undetermined Coefficients," *Comput. Econ.*, 20, 21–55.

DEJONG, D. N. AND C. DAVE (2011): *Structural Macroeconometrics: Second Edition*, Princeton, NJ: Princeton University Press.

DRYGALLA, A., O. HOLTEMÖLLER, AND K. KIESEL (2020): "The Effects of Fiscal Policy in an Estimated DSGE Model – The Case of the German Stimulus Packages during the Great Recession," *Macroeconomic Dynamics*, 24, 1315–1345.

DURBIN, J. AND S. J. KOOPMAN (2012): *Time Series Analysis by State Space Methods: Second Edition*, Oxford Statistical Science Series, Oxford, UK: Oxford University Press.

EUROPEAN CENTRAL BANK (2010): "Chronology of Monetary Policy Measures of the Eurosystem," *Monthly Bulletin*.

——— (2011): "Chronology of Monetary Policy Measures of the Eurosystem," *Monthly Bulletin*.

FEHRLE, D. (2019): "Housing and the Business Cycle Revisited," *Journal of Economic Dynamics and Control*, 99, 103 – 115.

FEHRLE, D. AND J. HUBER (2022): "Refine and Standardize Business Cycle Accounting Using the Example of the Great Recession in Germany," Mimeo, Augsburg of University.

FLOR, M. (2014): "Post Reunification Economic Fluctuations in Germany: A Real Business Cycle Interpretation," *Review of Business and Economics Studies*, 4, 5–15.

GADATSCH, N., K. HAUZENBERGER, AND N. STÄHLER (2016): "Fiscal Policy during the Crisis: A Look on Germany and the Euro Area with GEAR," *Economic Modelling*, 52, 997–1016.

GEHRKE, B., W. LECHTHALER, AND C. MERKL (2019): "The German Labor Market during the Great Recession: Shocks and Institutions," *Economic Modelling*, 78, 192–208.

GERTH, F. AND K. OTSU (2018): "The Post-Crisis Slump in Europe: A Business Cycle Accounting Analysis," *The B.E. Journal of Macroeconomics*, 18, 1–25.

GERTLER, M. AND S. GILCHRIST (2018): "What Happened: Financial Factors in the Great Recession," *Journal of Economic Perspectives*, 32, 3–30.

GERTLER, M. AND N. KIYOTAKI (2010): "Chapter 11 - Financial Intermediation and Credit Policy in Business Cycle Analysis," in *Handbook of Monetary Economics*, ed. by B. M. Friedman and M. Woodford, Elsevier, vol. 3, 547–599.

GREENWOOD, J., Z. HERCOWITZ, AND P. KRUSELL (1997): "Long-Run Implications of Investment-Specific Technological Change," *The American Economic Review*, 87, 342–362.

HAMILTON, J. D. (1994): *Time Series Analysis*, Princeton, NJ: Princeton University Press.

HANSEN, G. AND L. OHANIAN (2016): "Chapter 26 - Neoclassical Models in Macroeconomics," in *Handbook of Macroeconomics*, ed. by J. B. Taylor and H. Uhlig, Elsevier, vol. 2, 2043–2130.

HARVEY, A. C. (1990): *Forecasting, Structural Time Series Models and the Kalman Filter*, Cambridge, UK: Cambridge University Press.

HEBOUS, S. (2011): "The Effects of Discretionary Fiscal Policy on Macroeconomic Aggregates: A Reappraisal," *Journal of Economic Surveys*, 25, 674–707.

HEER, B. AND A. MAUSSNER (2009): *Dynamic General Equilibrium Modeling: Computational Methods and Applications*, Berlin / Heidelberg, Germany: Springer.

HERBST, E. P. AND F. SCHORFHEIDE (2016): *Bayesian Estimation of DSGE Models*, Princeton, NJ: Princeton University Press.

HUBER, J. (2022): "An Augmented Steady-State Kalman Filter to Evaluate the Likelihood of Linear and Time-Invariant State-Space Models," Mimeo, Augsburg of University.

ISKREV, N. (2010): "Local Identification in DSGE Models," *Journal of Monetary Economics*, 57, 189–202.

KARABARBOUNIS, L. (2014): "The Labor Wedge: MRS vs. MPN," *Review of Economic Dynamics*, 17, 206–223.

KEHOE, T. J. AND E. C. PRESCOTT (2002): "Great Depressions of the 20th Century," *Review of Economic Dynamics*, 5, 1–18.

KERSTING, E. K. (2008): "The 1980s Recession in the UK: A Business Cycle Accounting Perspective," *Review of Economic Dynamics*, 11, 179–191.

KIYOTAKI, N. AND J. MOORE (1997): "Credit Cycles," *Journal of Political Economy*, 105, 211–248.

KOLLMANN, R., M. RATTO, W. ROEGER, J. IN'T VELD, AND L. VOGEL (2014): "What Drives the German Current Account? And How Does It Affect Other EU Member States?" *Economic Policy*, 30, 47–93.

LAMA, R. (2011): "Accounting for Output Drops in Latin America," *Review of Economic Dynamics*, 14, 295–316.

LEUWER, D. AND B. SÜSSMUTH (2018): "Assessing Temporary Product-Specific Subsidies: A Time Series Intervention Analysis," CESifo Working Paper Series 6946, CESifo.

LU, S.-S. (2012): "East Asian Growth Experience Revisited from the Perspective of a Neoclassical Model," *Review of Economic Dynamics*, 15, 359–376.

MIAN, A., K. RAO, AND A. SUFI (2013): "Household Balance Sheets, Consumption, and the Economic Slump," *The Quarterly Journal of Economics*, 128, 1687–1726.

MIAN, A. AND A. SUFI (2012): "The Effects of Fiscal Stimulus: Evidence from the 2009 Cash for Clunkers Program," *The Quarterly Journal of Economics*, 127, 1107–1142.

MULLIGAN, C. B. (2005): "Public Policies as Specification Errors," *Review of Economic Dynamics*, 8, 902–926.

NUTAHARA, K. AND M. INABA (2012): "An Application of Business Cycle Accounting with Misspecified Wedges," *Review of Economic Dynamics*, 15, 265–269.

OECD (2009): *OECD Economic Outlook, Volume 2009 Issue 1*, Paris, France: OECD Publishing.

OHANIAN, L. E. (2010): "The Economic Crisis from a Neoclassical Perspective," *Journal of Economic Perspectives*, 24, 45–66.

OTSU, K. (2010): "A Neoclassical Analysis of the Asian Crisis: Business Cycle Accounting for a Small Open Economy," *The B.E. Journal of Macroeconomics*, 10, 1–37.

PLOTNIKOV, D. (2017): "What Prevents a Real Business Cycle Model from Matching the U.S. Data? Decomposing the Labor Wedge," IMF Working Papers 17/201, International Monetary Fund.

ROSENBERGER, A. (2013): *Krisenmanagement in der Finanz-, Wirtschafts- und europäischen Staatsschuldenkrise*, Aktuelle Fragen der Wirtschaftspolitik, Bayreuth, Germany: Verl. für Nationalökonomie, Management und Politikberatung (NMP).

SOLOW, R. M. (1957): "Technical Change and the Aggregate Production Function," *The Review of Economics and Statistics*, 39, 312–320.

UHLIG, H. (2001): "A Toolkit for Analysing Nonlinear Dynamic Stochastic Models Easily," in *Computational Methods for the Study of Dynamic Economies*, ed. by R. Marimon and A. Scott, Oxford, UK: Oxford University Press, 30–61.

ŠUSTEK, R. (2011): "Monetary Business Cycle Accounting," *Review of Economic Dynamics*, 14, 592–612.

Appendix

3.A Model

The following equations determine the model with stationary variables

$$y_t = k_{It}^{\alpha}(Z_t N_t)^{1-\alpha}, \tag{3.A.1}$$

$$r_t = \alpha \frac{y_t}{k_{It}}, \tag{3.A.2}$$

$$w_t = (1-\alpha)\frac{y_t}{N_t}, \tag{3.A.3}$$

$$\lambda_t = \phi c_t^{\phi(1-\eta)-1} k_{Dt}^{(1-\phi)(1-\eta)} (1-N_t)^{\psi(1-\eta)}, \tag{3.A.4}$$

$$(1-\tau_{Nt}) = \frac{\psi}{\phi}\frac{c_t}{(1-N_t)w_t}, \tag{3.A.5}$$

$$y_t = c_t + i_t + d_t + g_t + e_t, \tag{3.A.6}$$

$$\mu_{It} = \lambda_t \frac{1+\tau_{It}}{1-\Theta'_{It}}, \tag{3.A.7}$$

$$\mu_{Dt} = \lambda_t \frac{1+\tau_{Dt}}{1-\Theta'_{Dt}}, \tag{3.A.8}$$

$$g_I \cdot \gamma_n k_{It+1} = (1-\delta_I)k_{It} + i_t - \Theta_{It} \cdot k_{It}, \tag{3.A.9}$$

$$g_D \cdot \gamma_n k_{Dt+1} = (1-\delta_D)k_{Dt} + d_t - \Theta_{Dt} \cdot k_{Dt}, \tag{3.A.10}$$

$$\mu_{It} = \beta g_{M_I} \mathbb{E}_t \left[\mu_{It+1} \left(1 - \delta_I - \Theta_{It+1} + \frac{i_{t+1}}{k_{It+1}} \Theta'_{It+1} \right) + \lambda_{t+1} r_{t+1} \right], \tag{3.A.11}$$

$$\mu_{Dt} = \beta g_{M_D} \mathbb{E}_t \left[\mu_{Dt+1} \left(1 - \delta_D - \Theta_{Dt+1} + \frac{d_{t+1}}{k_{Dt+1}} \Theta'_{Dt+1} \right) + \lambda_{t+1} \frac{1-\phi}{\phi} \frac{c_{t+1}}{k_{Dt+1}} \right], \tag{3.A.12}$$

with

$$g_{M_I} = g_Y^{\phi(1-\eta)} \cdot g_D^{(1-\phi)(1-\eta)} \cdot g_I^{-1}, \tag{3.A.13}$$

$$g_{M_D} = g_Y^{\phi(1-\eta)} \cdot g_D^{(1-\phi)(1-\eta)-1}, \tag{3.A.14}$$

$$\Theta_{Xt} = \frac{a_X}{2}\left(\frac{x_t}{k_{Xt}} - b_X \right)^2, \tag{3.A.15}$$

$$\Theta'_{Xt} = a_X \left(\frac{x_t}{k_{Xt}} - b_X \right), \tag{3.A.16}$$

$$b_X = x^*/k_X^*, \tag{3.A.17}$$

with $X \in \{I, D\}$, $x \in \{i, d\}$ and where * indicates the steady-state value. The fluctuation in the model is driven by the VAR(1)-process

$$\underbrace{\begin{bmatrix} \ln(s_{At+1}) \\ s_{Nt+1} \\ s_{It+1} \\ s_{Dt+1} \\ s_{Et+1} \\ \ln(s_{Gt+1}) \end{bmatrix}}_{:=\mathbf{s_{t+1}}} = \Pi \underbrace{\begin{bmatrix} \ln(s_{At}) \\ s_{Nt} \\ s_{It} \\ s_{Dt} \\ s_{Et} \\ \ln(s_{Gt}) \end{bmatrix}}_{:=\mathbf{s_t}} + \underbrace{\begin{bmatrix} \epsilon_{At+1} \\ \epsilon_{Nt+1} \\ \epsilon_{It+1} \\ \epsilon_{Dt+1} \\ \epsilon_{Et+1} \\ \epsilon_{Gt+1} \end{bmatrix}}_{:=\epsilon_{t+1}}, \qquad \epsilon_t \sim \mathcal{N}(0, \Sigma). \tag{3.A.18}$$

The stochastic process affects the wedges as follows

$$Z_t = A^* \cdot s_{At}, \tag{3.A.19}$$
$$\tau_{Nt} = \tau_N^* + s_{Nt}, \tag{3.A.20}$$
$$\tau_{It} = \tau_I^* + s_{It}, \tag{3.A.21}$$
$$\tau_{Dt} = \tau_D^* + s_{Dt}, \tag{3.A.22}$$
$$e_t = e^* + s_{Et}, \tag{3.A.23}$$
$$g_t = g^* \cdot s_{Gt}. \tag{3.A.24}$$

3.B Chari et al. (2007) benchmark

3.B.1 Model

$$y_t = k_t^\alpha (Z_t N_t)^{1-\alpha}, \tag{3.B.1}$$
$$r_t = \alpha \frac{y_t}{k_t}, \tag{3.B.2}$$
$$w_t = (1-\alpha)\frac{y_t}{N_t}, \tag{3.B.3}$$
$$\lambda_t = c_t^{(1-\eta)-1}(1-N_t)^{\psi(1-\eta)}, \tag{3.B.4}$$
$$(1-\tau_{Nt}) = \psi \frac{c_t}{(1-N_t)w_t}, \tag{3.B.5}$$
$$y_t = c_t + i_t + g_t, \tag{3.B.6}$$
$$\mu_{It} = \lambda_t \frac{1+\tau_{It}}{1-\Theta'_{It}}, \tag{3.B.7}$$
$$g_I \cdot \gamma_n k_{t+1} = (1-\delta_I)k_t + i_t - \Theta_{It} \cdot k_t, \tag{3.B.8}$$
$$\mu_{It} = \beta g_{M_I} \mathbb{E}_t \left[\mu_{It+1} \left(1 - \delta_I - \Theta_{It+1} + \frac{i_{t+1}}{k_{t+1}} \Theta'_{It+1} \right) + \lambda_{t+1} r_{t+1} \right], \tag{3.B.9}$$

with

$$g_{M_I} = g_Y^{1-\eta} \cdot g_I^{-1}, \tag{3.B.10}$$
$$\Theta_{It} = \frac{a_I}{2}\left(\frac{i_t}{k_t} - b_I\right)^2, \tag{3.B.11}$$
$$\Theta'_{It} = a_I\left(\frac{i_t}{k_t} - b_I\right), \tag{3.B.12}$$
$$b_I = i^*/k^*, \tag{3.B.13}$$

where * indicates the steady-state value.

The fluctuation in the model is driven by the VAR(1)-process

$$\underbrace{\begin{bmatrix} \ln(s_{At+1}) \\ s_{Nt+1} \\ s_{It+1} \\ \ln(s_{Gt+1}) \end{bmatrix}}_{:=\mathbf{s_{t+1}}} = \Pi \underbrace{\begin{bmatrix} \ln(s_{At}) \\ s_{Nt} \\ s_{It} \\ \ln(s_{Gt}) \end{bmatrix}}_{:=\mathbf{s_t}} + \underbrace{\begin{bmatrix} \epsilon_{At+1} \\ \epsilon_{Nt+1} \\ \epsilon_{It+1} \\ \epsilon_{Gt+1} \end{bmatrix}}_{:=\epsilon_{t+1}}, \qquad \epsilon_t \sim \mathcal{N}(0, \Sigma). \tag{3.B.14}$$

The stochastic process affects the wedges as follows

$$Z_t = A^* \cdot s_{At}, \tag{3.B.15}$$
$$\tau_{Nt} = \tau_N^* + s_{Nt}, \tag{3.B.16}$$
$$\tau_{It} = \tau_I^* + s_{It}, \tag{3.B.17}$$
$$g_t = g^* \cdot s_{Gt}. \tag{3.B.18}$$

3.B.2 Observables and data manipulation

The vector of observables reads as follows $\mathbf{y_t} = \begin{bmatrix} \hat{y}_t & \hat{N}_t & \hat{i}_t & \hat{g}_t \end{bmatrix}^{\mathrm{T}}$. In contrast to our modified model government consumption is the sum of government consumption and net exports and investments are the sum of durables and investments.

3.B.3 Calibration and estimation

The calibration and estimation strategy is similar to our modified model. We estimate the elasticity of the price of capital η_I as well as the parameters of the stochastic process. All other parameters are calibrated and the long-run ratios are pined down to their long-run averages. Tables 3.7 and 3.8 present all relevant parameters.

Table 3.7: Calibration and growth accounting for the Chari et al. (2007) economy

Parameter	description	Value
α	capital share	0.34
β	discount factor	0.994
δ_I	rate of capital depreciation	0.0203
ψ	preference weight of labor	2.24
η	risk aversion	1
η_I	elasticity of the price of capital	0.86
$\ln(\gamma_n^4)$	annual growth rate of population	0.03%
$\ln(g_Y^4)$	annual growth rate of GDP	1.32%
$\ln(g_I^4)$	annual growth rate of investment	0.79%

Table 3.8: Estimation of exogenous shock process of the Chari et al. (2007) economy

Autoregressive Matrix					
Π	$ln(s_A)$	s_N	s_I	$ln(s_G)$	
$ln(s_A)$	0.93	0.09	0.05	−0.03	
s_N	−0.01	0.73	0.04	−0.00	
s_I	0.03	2.03	0.67	−0.02	
$ln(s_G)$	0.09	−1.17	0.08	0.84	

Correlation and standard errors					
$Corr(\epsilon_i, \epsilon_j)$	ϵ_A	ϵ_N	ϵ_I	ϵ_G	$100 \cdot StD(\epsilon_i)$
ϵ_A	1.00				0.94
ϵ_N	0.21	1.00			0.29
ϵ_I	−0.27	−0.61	1.00		1.77
ϵ_G	0.43	0.77	−0.34	1.00	2.71

3.C Data

The data is taken from the Fachserie 18: National accounts, domestic product from the German Federal Statistical Office.

- **Pop:** Total Population 1991:I-2018:I

  Source: 2.1.7 Population and labour force participation 1; Seasonally adjusted quarterly results using Census X-12-ARIMA and BV4.1 - Fachserie 18 Reihe 1.3 - 1st Quarter 2018

- **Hours:** Hours worked by persons in employment 1991:I-2018:I

  Source: 2.1.8 Persons in employment, employees and hours worked (domestic concept) 2; Seasonally adjusted quarterly results using Census X-12-ARIMA and BV4.1 - Fachserie 18 Reihe 1.3 - 1st Quarter 2018

- **GDP:** 1991:I-2018:I

  Nominal source: 2.3.1 Use of gross domestic product at current prices 2; Seasonally adjusted quarterly results using Census X-12-ARIMA and BV4.1 - Fachserie 18 Reihe 1.3 - 1st Quarter 2018

  Real source: 2.3.2 Use of gross domestic product, price-adjusted 2; Seasonally adjusted quarterly results using Census X-12-ARIMA and BV4.1 - Fachserie 18 Reihe 1.3 - 1st Quarter 2018

- **PCE:** Private Consumption Expenditures of households 1991:I-2018:I

  Nominal source: 2.3.3 Final consumption expenditure at current prices 3; Seasonally adjusted quarterly results using Census X-12-ARIMA and BV4.1 - Fachserie 18 Reihe 1.3 - 1st Quarter 2018

  Real source: 2.3.4 Final consumption expenditure at , price-adjusted; Seasonally adjusted quarterly results using Census X-12-ARIMA and BV4.1 - Fachserie 18 Reihe 1.3 - 1st Quarter 2018

- **Govern. Consumption:** Government final consumption expenditure (domestic use) 1991:I-2018:I

Nominal source: 2.3.3 Final consumption expenditure at current prices 3; Seasonally adjusted quarterly results using Census X-12-ARIMA and BV4.1 - Fachserie 18 Reihe 1.3 - 1st Quarter 2018

Real source: 2.3.4 Final consumption expenditure at , price-adjusted; Seasonally adjusted quarterly results using Census X-12-ARIMA and BV4.1 - Fachserie 18 Reihe 1.3 - 1st Quarter 2018

- **Investment:** Gross fixed capital formation 1991:I-2018:I

  Nominal source: 2.3.1 gross fixed capital formation at current prices 2; Seasonally adjusted quarterly results using Census X-12-ARIMA and BV4.1 - Fachserie 18 Reihe 1.3 - 1st Quarter 2018

  Real source: 2.3.2 gross fixed capital formation, price-adjusted 2; Seasonally adjusted quarterly results using Census X-12-ARIMA and BV4.1 - Fachserie 18 Reihe 1.3 - 1st Quarter 2018

- **Net Exports:** Balance of exports and imports 1991:I-2018:I

  Nominal source: 2.3.1 Balance of exports and imports at current prices 2; Seasonally adjusted quarterly results using Census X-12-ARIMA and BV4.1 - Fachserie 18 Reihe 1.3 - 1st Quarter 2018

  Real source: 2.3.2 Balance of exports and imports, price-adjusted 2; Seasonally adjusted quarterly results using Census X-12-ARIMA and BV4.1 - Fachserie 18 Reihe 1.3 - 1st Quarter 2018

- **Durables:** Langlebige Güter (Durable Goods) 1991:I-2018:I

  Nominal source: 2.14 Konsumausgaben der privaten Haushalte im Inland nach Dauerhaftigkeit der Güter, Saison- und kalenderbereinigt in jeweiligen Preisen 4; Private Konsumausgaben und Verfügbares Einkommen - 1. Vierteljahr 2018

  Real source: 2.14 Konsumausgaben der privaten Haushalte im Inland nach Dauerhaftigkeit der Güter, Saison- und kalenderbereinigt - preisbereinigt 4; Private Konsumausgaben und Verfügbares Einkommen - 1. Vierteljahr 2018

  (available in German only: Domestic consumer spending on durable goods, seasonally and calendar adjusted 4; Private consumption expenditure and disposable income - 1st quarter of 2018)

Chapter 4

Polynomial Chaos Expansion: Efficient Evaluation and Estimation of Computational Models

— *Daniel Fehrle, Christopher Heiberger and Johannes Huber* —

4.1 Introduction

At an abstract level, computational economic models are mappings from inputs of the model to outputs of the model. The former are the model's parameters, the latter depend on the research question and comprise, e.g., the policy functions of economic agents, the second-moments of model generated time series, or the likelihood implied by a given set of observed data. The model's parameters are typically unknown and plausible values must be derived from observed data, or are even treated as random variables from the Bayesian perspective. Either way, the uncertainty of parameters translates into uncertainty regarding the model's outcomes. Estimation methods, as the generalized method of moments, the matching of impulse responses, or likelihood based methods as well as a careful study of the sensitivity of the model's outcomes for a set of different parameter values requires numerous repeated solutions of the model. Depending on the complexity of the model, estimation and sensitivity analysis can become a time-consuming computational task or even excessive if the time factor is critical, as in high-frequency real-time analyses. Polynomial chaos expansion (PCE), as employed in other scientific disciplines, offers an elegant way to deal with this problem.[1]

PCE is a method that depicts arbitrary elements of a model's solution, the quantity of interest (QoI), in terms of a series expansion of the model's parameters. Given the respective formulae, repeated evaluations are inexpensive in terms of computational time instead of repeated, potentially time-consuming, solutions of the entire model. The present paper provides a theoretical and practical primer of PCE for economists. Without limiting the applicability for other purposes, we focus on parameter estimation of dynamic stochastic general equilibrium (DSGE) models, as we are familiar with the required methods. To the best of our knowledge, applications of PCE in this context have not yet been studied in economic models.[2]

In its general form, the underlying theory of the method rests on the theory introduced by Wiener (1938) and the Cameron and Martin (1947) theorem. Given a family of stochastically independent and normally distributed random variables, which we call germs, the theorem establishes the existence of an orthogonal decomposition—with identity in the L^2 sense—of any random variable with finite second moments and measurable with respect to the germs, into Hermite polynomials in the germs. If we identify the germs with (transformations of) the model's unknown parameters, and if the model's outcome satisfies the required conditions, which apply to most computational economic models, the theory justifies an approximation of

[1] See e.g. Kaintura et al. (2018) for a review on the increasing application of PCE in electronics and electrics.

[2] Harenberg et al. (2019) is the only study we are aware of which has studied PCE in the context of economic models so far. However, different from our work they focus on applications of PCE for structural sensitivity analysis.

the model's outcome by a truncated series of polynomials in the unknown parameters. The so-called truncated PCE can be constructed easily from a limited number of model evaluations, and after construction of the PCE the model's outcome can be obtained uncostly by evaluation of the truncated series instead of repeated solutions of the model.

Ghanem and Spanos (1991) provide first applications of the theory to the problem of uncertain model parametrization. In such applications, we can typically restrict attention to the far easier case with a finite number of germs. In the one-dimensional case where parametrization uncertainty is introduced by means of only one unknown parameter described by a random variable θ with (Borel) probability measure P_θ, the existence of orthogonal decompositions is the direct consequence of the property that the (orthogonal) polynomials with respect to the inner product in $L^2(\mathbb{R}, \mathscr{B}(\mathbb{R}), P_\theta)$ form a complete orthogonal system in L^2. Moreover, the property does not only hold for Hermite polynomials and probability measures of normally distributed random variables but also extends to other commonly used distributions and the corresponding orthogonal polynomials from the Askey scheme. This extension, initially proposed by Xiu and Karniadakis (2002), is also known as generalized polynomial chaos expansion. For a finite number of unknown and stochastically independent parameters θ_i, the property also extends to tensor products of the polynomials and the product probability measure. In consequence, any L^2 mapping can be represented by a Fourier series in the orthogonal polynomials and any random variable with finite second moments which is measurable with respect to the θ_i can be written as a series of polynomials in the θ_i.

For the problem at hand, the L^2 mapping for which the Fourier series must be constructed is identified with the mapping from parameter values to the model's outcome Y. Moreover, the Fourier coefficients are defined by the inner product of this mapping with the orthogonal polynomials. If the inner product cannot be computed analytically, numerical integration rules like Gauss quadratures can be employed which, if the dimensionality of unknown parameters is not too large, require only a comparably small number of model evaluations. As the dimensionality of the problem becomes larger, sparse grid methods, such as Smolyak-Gauss quadrature can help or, alternatively, the coefficients can be obtained from least squares.

After construction of the truncated PCE, it can be used for inexpensive evaluations of the model outcome. First, statistical properties of the model outcome can be derived directly from the PCE and the parameters' distributions. The statistical properties can then be used to quantify the effects of parameter uncertainty. For example, the variance of the model outcome can be used as a first indicator for a sensitivity analysis. Moreover, Harenberg et al. (2019) propose a sensitivity analysis on the basis of Sobol' indices which can be obtained directly from the PCE. The analysis additionally provides necessary conditions for parameter identification in structural estimations. Second, the Fourier expansion can also be used as a point-wise approximation for the mapping between parameters and the QoI. Thus, estimation methods which require repeated recalculations of the model outcome can be sped up significantly. Since Bayesian inference naturally combines the specification of a-priori parameter uncertainty in form of prior distributions with the necessity for repeated model solutions, it provides an especially well-suited setting for the implementation of PCE. The application of PCE in Bayesian inference was first analyzed by Marzouk et al. (2007) in engineering but to the best of our knowledge the method has not yet been studied in economic models.

We apply the method of PCE to the benchmark real business cycle (RBC) model, since this model is suited as illustrative example due to its well-known and simplistic nature. We analyze the convergence behaviour of the PCE—in the sense of the L^2 norm of the approximation error over the parameters' support—as the degree of truncation is increased. Our analysis starts with an example where three parameters are assumed unknown, namely the capital share in production, the coefficient of relative risk aversion and the autocorrelation parameter of total factor productivity, and considers the PCEs of various model outcomes including the model's

linear solution, a projection solution, the variables' second moments and the impulse response function. Although we assume rather "loose" distributions for the unknown parameters, we find linear convergence speed in all cases, and remarkably well approximations can be obtained already with a rather small degree of truncation and a small number of model evaluations. If the model outcome, e.g the linearized policy function, has to be evaluated for a sample of 100,000 parameter values, the PCE with truncation degree 7 provides an approximation with L^2 error of 10^{-3} while the computational time for construction and evaluation is lower by the factor 30 compared to repeated computations.

We extend our example to the higher-dimensional problem where all six model parameters are assumed unknown. Compared to full-grid quadrature rules, sparse-grid quadrature rules and least squares provide less accurate derivations of the PCE coefficients. In consequence, the approximated PCEs require a higher degree of truncation in order to deliver the same accuracy. However, they also require significantly less time for construction. A comparison of computational time versus the approximation's accuracy shows that the PCE constructed from sparse-grid quadrature is most efficient followed by least squares. Yet, for higher degrees of truncation, inaccuracies in the PCE coefficients derived from least squares eventually become dominant and even reverse convergence.

Our analysis continues with Monte Carlo experiments as in Ruge-Murcia (2007) where we gauge the quality of the model's PCE when used for several empirical methods. More specifically, we estimate the model's parameters by generalized method of moments (GMM), simulated method of moments (SMM), maximum-likelihood estimation (MLE) and Bayesian estimation (BE) but use PCE to evaluate the QoI for different parameter values. Compared to the benchmark procedure of repeated solutions, we find that the PCE based method is remarkably efficient and accurate. Estimates deviate only negligibly from the benchmark procedure and most notable, the computation time can be reduced by 99 percent for BE and by 50 percent for GMM, SMM and MLE.

The remainder of the paper is structured as follows. First, we give a simple example to outline the concept of PCE in section 4.2. In section 4.3 we review the basic theory for the existence of polynomial chaos expansions and present the most common practical methods to compute the PCE coefficients. Section 4.4 discusses different applications of the PCE, either to evaluate statistical properties of the model outcome or for point-wise approximation of the mapping from the parameters to the model outcome. We particularly highlight its application to construct surrogates for the model's linear solution or for projection solutions and to approximate gradients. In section 4.5, we apply the method to the benchmark RBC model and discuss the basic results and potential drawbacks. Section 4.6 concludes. More detailed derivations are found in the appendix. MATLAB® code is available from the authors upon request.

4.2 A simple example

Before introducing the theoretical framework of PCE, we first want to outline the concept at hand of a simple example. Since our numerical analysis focuses on discretely-timed models, our example considers the following system of linear first-order difference equations in two real-valued variables $x_{1,t}$ and $x_{2,t}$,

$$\begin{aligned} \vartheta x_{1,t+1} + x_{2,t+1} &= x_{1,t}, \\ x_{1,t+1} + x_{2,t+1} &= x_{2,t}, \end{aligned}$$

for all $t \in \mathbb{N}$, and given $x_{1,0}$ and $x_{2,0}$. Moreover, $\vartheta \in (0,1)$ is an unknown parameter. While the variables' explicit recursion can be derived straightforwardly here by

$$\begin{pmatrix} x_{1,t+1} \\ x_{2,t+1} \end{pmatrix} = H(\vartheta) \begin{pmatrix} x_{1,t} \\ x_{2,t} \end{pmatrix}, \text{ where } H(\vartheta) := \begin{pmatrix} h_{11}(\vartheta) & h_{12}(\vartheta) \\ h_{21}(\vartheta) & h_{22}(\vartheta) \end{pmatrix} = \begin{pmatrix} \frac{-1}{1-\vartheta} & \frac{1}{1-\vartheta} \\ \frac{1}{1-\vartheta} & \frac{-\vartheta}{1-\vartheta} \end{pmatrix},$$

the mapping $\vartheta \mapsto H(\vartheta)$ from the unknown parameter to the (linearized) policy can typically not be derived analytically, but can only be computed numerically, if the system of difference equations is non-linear and stochastic. In consequence, if $H(\vartheta)$ needs to be computed for different parameter values, the underlying numerical methods must eventually be applied repeatedly. PCE, on the other hand, aims to represent the mapping $\vartheta \mapsto H(\vartheta)$ as a truncation from the Fourier series

$$h_{ij}(\vartheta) = \sum_{n=0}^{\infty} \hat{h}_{ij}^{(n)} q_n(\psi^{-1}(\vartheta)),$$

where q_n is the n-th polynomial from a family of orthogonal polynomials, $\psi^{-1}(\vartheta)$ is a transformation of the parameter space into the space of the polynomial orthogonal counterpart's argument, and $\hat{h}_{ij}^{(n)}$ is the corresponding Fourier coefficient of the polynomial. The truncated series expansion is constructed from a limited number of numerical evaluations of the mapping as follows.

First, the uncertainty about the parameter is taken into account by describing it by a random variable θ with suitable probability distribution P_θ. For the present example, suppose that θ is uniformly distributed over the interval $(0, b)$, $0 < b \leq 1$. Second, the series expansion is constructed in a well-known family of orthogonal polynomials, which satisfies orthogonality w.r.t. some weighting function w. Thereby, the appropriate family of orthogonal polynomials is most conveniently chosen in such a way that the weighting function w coincides with the probability density function of the unknown parameter. However, in order to achieve conformity between the weighting function and the density function, a (linear) transformation of the parameter typically becomes necessary. In the present case, Legendre polynomials $\{L_n\}_{n\geq 0}$ are orthogonal w.r.t. the weighting function $w(s) = \mathbb{1}_{(-1,1)}(s)$, i.e. they satisfy

$$\int_{\mathbb{R}} L_n(s) L_m(s) w(s)\, \mathrm{d}s = \begin{cases} 0, & \text{if } n \neq m, \\ \|L_n\|^2 := \frac{2}{2n+1}, & \text{if } n = m. \end{cases}$$

Hence, transformation of the unknown parameter θ to the so-called germ ξ by

$$\xi := \psi^{-1}(\theta) := 2\frac{\theta}{b} - 1 \iff \theta = \psi(\xi) = \frac{(\xi+1)b}{2},$$

yields the desired result, and Legendre polynomials are orthogonal w.r.t. the probability distribution P_ξ of ξ. Given that $b < 1$, the mapping $s \mapsto h_{ij}(\psi(s))$ for each entry h_{ij} of the matrix H is square integrable w.r.t. P_ξ and can be represented by a Fourier series of the form[3]

$$h_{ij}(\psi(s)) = \sum_{n=0}^{\infty} \hat{h}_{ij}^{(n)} L_n(s). \tag{4.2.1}$$

[3]The details in which sense convergence of the series can be established are discussed in the next section.

Moreover, orthogonality implies that the Fourier coefficients $\hat{h}_{ij}^{(n)}$ satisfy

$$\hat{h}_{ij}^{(n)} = \|L_n\|^{-2} \int_{-1}^{1} h_{ij}(\psi(s)) L_n(s)\,\mathrm{d}s.$$

Finally, numerical integration methods are generally required to compute the coefficients $\hat{h}_{ij}^{(n)}$. For example, using Gauss-Legendre-quadrature with M nodes s_i and weights ω_i yields[4]

$$\hat{h}_{ij}^{(n)} \approx \|L_n\|^{-2} \sum_{i=1}^{M} h_{ij}(\psi(s_i)) L_n(s_i)\omega_i.$$

Table 4.1 shows for $b = 0.9$ and $M = 5$ the quadrature weights ω_i, the nodes s_i, the corresponding retransformed parameter values $\vartheta_i := \psi(s_i)$, and for the matrix entry h_{11} the evaluation $h_{11}(\vartheta_i) = \frac{-1}{1-\vartheta_i}$.

Table 4.1: Example

i	ω_i	s_i	ϑ_i	$h_{11}(\vartheta_i)$
1	0.2369	−0.9062	0.0422	−1.0441
2	0.4786	−0.5385	0.2077	−1.2621
3	0.5689	0	0.4500	−1.8182
4	0.4786	0.5385	0.6923	−3.2500
5	0.2369	0.9062	0.8578	−7.0314

Together with $L_0(s_i) = 1, L_1(s_i) = s_i, \|L_0\|^2 = 2$, and $\|L_1\|^2 = \frac{2}{3}$, one can therefore compute, e.g.,[5]

$$\hat{h}_{11}^{(0)} \approx \frac{1}{2}\sum_{i=1}^{5} h_{11}(\vartheta_i)\omega_i = -2.55 \quad \text{and} \quad \hat{h}_{11}^{(1)} \approx \frac{3}{2}\sum_{i=1}^{5} h_{11}(\vartheta_i) s_i \omega_i = -2.70.$$

In this case, the computation of the Fourier coefficients $\hat{h}_{11}^{(n)}$ requires $M = 5$ (numerical) evaluations of the mapping $\vartheta \mapsto h_{11}(\vartheta)$. After computation of the first $N+1$ Fourier coefficients, one

[4] If we additionally write the transformation ψ between parameter and germ in terms of the Legendre polynomials, i.e.

$$\psi(s) = \underbrace{\frac{b}{2}}_{=:\hat{\vartheta}_0} L_0(s) + \underbrace{\frac{b}{2}}_{=:\hat{\vartheta}_0} L_1(s),$$

we equivalently arrive at

$$\hat{h}_{ij}^{(n)} \approx \|L_n\|^{-2} \sum_{i=1}^{M} h_{ij}\left(\hat{\vartheta}_0 L_0(s_i) + \hat{\vartheta}_1 L_1(s_i)\right) L_n(s_i)\omega_i.$$

Note that this expression is identical to the more general form in (4.3.5).

[5] For comparison, exact integration yields

$$\hat{h}_{11}^{(0)} = \frac{1}{2}\int_{-1}^{1} \frac{-1}{1-\frac{(s+1)b}{2}}\,\mathrm{d}s = \frac{\ln(1-b)}{b} = -2.56,\ \hat{h}_{11}^{(1)} = \frac{3}{2}\int_{-1}^{1} \frac{-s}{1-\frac{(s+1)b}{2}}\,\mathrm{d}s = \frac{6-3b}{b^2}\ln(1-b) + \frac{6}{b} = -2.71.$$

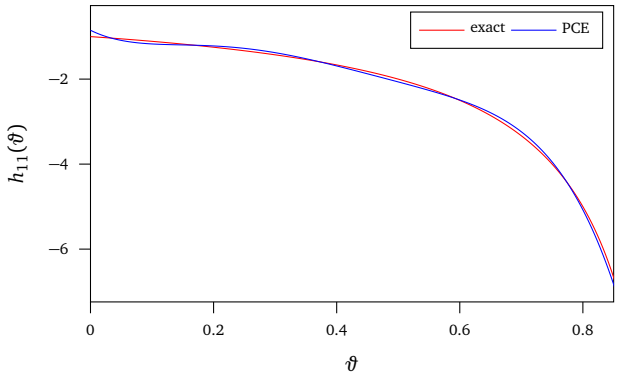

Figure 4.1: Example: Exact evaluation and PCE (numerical integration)

can use the truncated series expansion of (4.2.1), i.e.

$$h_{11}(\vartheta) \approx \sum_{n=0}^{N} \hat{h}_{11}^{(n)} L_n(\psi^{-1}(\vartheta)),$$

in order to (approximately) evaluate $h_{11}(\vartheta)$ for arbitrary parameter values without further need of direct numerical evaluations.[6] Figure 4.1 shows a comparison between exact evaluation of $h_{11}(\vartheta)$ and the truncated PCE with truncation level $N = 5$.

Finally, note already here that an important restriction of the methods is the requirement that the mapping $s \mapsto h_{ij}(\psi(s))$ is square integrable w.r.t. P_ξ, or equivalently w.r.t. the weighting function w corresponding to the family of orthogonal polynomials. In the present example, this condition is fulfilled for $b < 1$. Yet, if $b = 1$, the integrals from which the coefficients are defined are not finite, e.g.,

$$\hat{h}_{11}^{(0)} = \frac{1}{2} \int_{-1}^{1} \frac{-1}{1 - \frac{s+1}{2}} \, \mathrm{d}s = -\infty.$$

4.3 Generalized polynomial chaos expansions

We begin by reviewing the basic idea and theory behind the concept of PCE. While PCE proved useful for a variety of applications, we focus on their implementation to efficiently evaluate computationally expensive model outcomes when one or more of the model's inputs, e.g. model parameters, are uncertain.

Notation and preliminaries: We consider a computational economic model where $\vartheta_i \in \Theta_i, \Theta_i \subset \mathbb{R}, i = 1, \ldots, k$, denotes an arbitrary selection of $k \in \mathbb{N}$ parameters of the model. Moreover, we are interested in some model outcome(s) denoted by a vector $y \in \mathbb{R}^m, m \in \mathbb{N}$. The relation between the input parameters ϑ_i and the model outcome(s) y is determined deterministically, i.e. repeated computation of y with the same inputs ϑ_i to the model produces the same result.[7] This mapping between the ϑ_i and y is described by

$$y = h(\vartheta_1, \ldots, \vartheta_k)$$

[6] Of course, an appropriate choice of the number M of quadrature nodes and, therefore, of the number of numerical evaluations is necessary in order to derive the Fourier coefficients depends on the truncation level N. More details on this topic are provided in the next section.

[7] E.g., if y denotes some second moments of the model, these are derived either from available analytic formulae from the (approximated) model solution or are computed from simulations with the same sample of shocks.

where $h\colon \Theta \to \mathbb{R}^m, \Theta = \bigtimes_{i=1}^{k} \Theta_i \subset \mathbb{R}$. Without loss of generality we consider the case $m = 1$ in the following, and note that for $m \geq 2$ all derivations can be applied separately to each component y_i of y, $i = 1, \ldots, m$, in the same way.

Now further consider the case where the values ϑ_i of the model parameters are subject to some uncertainty to the researcher. In order to account for this uncertainty, we switch from the deterministic representation of the parameters to the perspective of describing them by appropriately distributed random variables. Therefore, let $(\Omega, \mathscr{A}, P)$ denote a sufficiently rich probability space so that any uncertain model input parameter can be described by some real valued random variable $\theta_i\colon \Omega \to \mathbb{R}, i = 1, \ldots, k$, where the real line is equipped with the Borel sigma-algebra $\mathscr{B}(\mathbb{R})$. Moreover, let $\xi_1, \ldots, \xi_k$ denote a family of stochastically independent random variables chosen by the researcher as a basis of the desired polynomial expansions, the so-called germs. In applications, as will be described later, the germs are most commonly either set equal to the uncertain model parameters θ_i or to some natural and convenient transformation of them. We assume:

1. The germs $\xi_1, \ldots, \xi_k$ cover the same stochastic information as the uncertain model parameters, i.e.

   $$\sigma(\xi_1, \ldots, \xi_k) = \sigma(\theta_1, \ldots, \theta_k),$$

   where $\sigma(\cdot)$ denotes the sigma-algebra generated by the random variables.

2. All moments of each ξ_i exist, i.e. $\mathrm{E}[|\xi_i|^n] < \infty$ for all $i = 1, \ldots, k$ and $n \in \mathbb{N}_0$.

Moreover, we write $\boldsymbol{\theta} := (\theta_1, \ldots, \theta_k)\colon \Omega \to \mathbb{R}^k$ and $\boldsymbol{\xi} := (\xi_1, \ldots, \xi_k)\colon \Omega \to \mathbb{R}^k$ for the k-dimensional random vector of the uncertain model parameters and for the random vector of the germs, respectively, where $\mathbb{R}^k$ is also equipped with its Borel sigma-algebra $\mathscr{B}(\mathbb{R}^k)$. For each $i = 1, \ldots, k$, let $P_{\xi_i} := P \circ \xi_i^{-1}$ denote the probability measure of ξ_i on $(\mathbb{R}, \mathscr{B}(\mathbb{R}))$ and analogously let $P_{\boldsymbol{\xi}} := P \circ \boldsymbol{\xi}^{-1} = \bigotimes_{i=1}^{k} P_{\xi_i}$ denote the product probability measure of $\boldsymbol{\xi}$ on $(\mathbb{R}^k, \mathscr{B}(\mathbb{R}^k))$. The Hilbert space (of equivalence classes) of square integrable real valued functions on $(\mathbb{R}, \mathscr{B}(\mathbb{R}), P_{\xi_i})$ is denoted by

$$L_i^2 := L^2(\mathbb{R}, \mathscr{B}(\mathbb{R}), \mathrm{d}P_{\xi_i}) := \left\{ f : \mathbb{R} \to \mathbb{R} \;\middle|\; f \text{ is measurable and } \int_{\mathbb{R}} f^2 \,\mathrm{d}P_{\xi_i} < \infty \right\},$$

where the inner product is defined by

$$\langle f, g \rangle_{L_i^2} := \int_{\mathbb{R}} f\, g \,\mathrm{d}P_{\xi_i} = \mathrm{E}[f(\xi_i) g(\xi_i)] \quad \text{for } f, g \in L^2(\mathbb{R}, \mathscr{B}(\mathbb{R}), P_{\xi_i}).$$

We use the notation $\|\cdot\|_{L_i^2}$ for the induced norm on L_i^2. We introduce the analogous notation, i.e. $L^2 := L^2(\mathbb{R}^k, \mathscr{B}(\mathbb{R}^k), \mathrm{d}P_{\boldsymbol{\xi}})$, for the space of square integrable real valued functions on $(\mathbb{R}^k, \mathscr{B}(\mathbb{R}^k), P_{\boldsymbol{\xi}})$ and write $\langle \cdot, \cdot \rangle_{L^2}$ and $\|\cdot\|_{L^2}$ for the inner product and for the induced norm on L^2. If the distributions of the random variables ξ_i possess probability density functions $w_i\colon \mathbb{R} \to \mathbb{R}_+$, the inner products become

$$\langle f, g \rangle_{L_i^2} = \int_{\mathbb{R}} f(s) g(s) w_i(s) \,\mathrm{d}s,$$

and

$$\langle f, g \rangle_{L^2} = \int_{\mathbb{R}} \ldots \int_{\mathbb{R}} f(s_1, \ldots, s_k) g(s_1, \ldots, s_k) w_1(s_1) \cdot \ldots \cdot w_k(s_k) \,\mathrm{d}s_1 \ldots \mathrm{d}s_k,$$

so that $L_i^2 = L^2(\mathbb{R}, \mathscr{B}(\mathbb{R}), w_i(s)\,\mathrm{d}s)$ and $L^2 = L^2(\mathbb{R}^k, \mathscr{B}(\mathbb{R}^k), w(s)\,\mathrm{d}s)$ where w is the joint probability function $w(s) := \prod_{i=1}^k w_i(s_i)$. Note that Assumption 2 is equivalent to the fact that for each $i = 1, \dots, k$ all univariate polynomials are included in L_i^2 or, again equivalently, that all k-variate polynomials are included in L^2.

Since, by Assumption 1, each θ_i is $\sigma(\boldsymbol{\xi})$-measurable, there exist measurable $\psi_i \colon \mathbb{R}^k \to \mathbb{R}$ which satisfy

$$\theta_i = \psi_i \circ \boldsymbol{\xi}.$$

We write $\boldsymbol{\psi} := (\psi_1, \dots, \psi_k) \colon \mathbb{R}^k \to \mathbb{R}^k$ so that $\boldsymbol{\theta} = \boldsymbol{\psi} \circ \boldsymbol{\xi}$. Moreover, note that $\sigma(\boldsymbol{\xi}) = \sigma(\boldsymbol{\theta})$ also implies the existence of a measurable, inverse mapping $\boldsymbol{\psi}^{-1}$ with $\boldsymbol{\psi} \circ \boldsymbol{\psi}^{-1} = \boldsymbol{\psi}^{-1} \circ \boldsymbol{\psi} = \mathrm{id}$. A further assumption we make is that

3. the second moment of each model input parameter exists, i.e. $\mathrm{E}[\theta_i^2] < \infty$ for $i = 1, \dots, k$. Equivalently, each ψ_i is square integrable on $(\mathbb{R}^k, \mathscr{B}(\mathbb{R}^k), P_{\boldsymbol{\xi}})$, i.e. $\psi_i \in L^2$ for all $i = 1, \dots, k$.[8]

Moreover, as the model input parameters θ_i are now treated as random, the model outcome of interest is random. We therefore adapt its notation to $Y : \Omega \to \mathbb{R}$. Yet, given any elementary event $\omega \in \Omega$ and corresponding realization $\theta_i(\omega)$, the mapping between the model parameters and the model outcome is still determined deterministically by $Y(\omega) = h(\theta_1(\omega), \dots, \theta_k(\omega))$, i.e.

$$Y = h \circ \boldsymbol{\theta} = h \circ \boldsymbol{\psi} \circ \boldsymbol{\xi}, \text{ for some } h \colon \mathbb{R}^k \to \mathbb{R}.$$

The final assumption is that Y is a well-defined random variable with finite second moments, i.e.

4. h is measurable and $h \circ \boldsymbol{\psi}$ is square integrable on $(\mathbb{R}^k, \mathscr{B}(\mathbb{R}^k), P_{\boldsymbol{\xi}})$, i.e. $h \circ \boldsymbol{\psi} \in L^2$.

4.3.1 Single uncertain parameter and germ (k=1)

We begin our description with the simplest case with only one single uncertain input parameter θ and one single germ ξ, i.e. $k = 1$. In general, any arbitrary choice of the germ that satisfies Assumption 2 implies that all polynomials are included in L^2, and therefore allows the construction of an orthogonal system of polynomials $\{q_n\}_{n \in \mathbb{N}_0} \subset L^2$, i.e. a family of polynomials where q_n is of (exact) degree n and

$$\langle q_n, q_m \rangle_{L^2} = \|q_n\|_{L^2}^2 \delta_{m,n} \text{ for all } m, n \in \mathbb{N}_0,$$

where $\delta_{m,n}$ denotes the Knonecker delta. This can generally be achieved by applying, e.g., the Gram-Schmidt process to the sequence of monomials.

In practice, the distribution of the uncertain input parameter is given and one is free to set the germ. It is then convenient to define the germ in such way that i) an easy representation $\theta = \psi(\xi)$ of the parameter in terms of the germ arises and ii) the family of orthogonal polynomials in L^2 corresponds to some well-known class of polynomials. Table 4.2 summarizes the natural choice of the germ and the corresponding family of orthogonal polynomials when the input parameter is normal, uniform, Beta or (inverse) Gamma distributed. More details for these classes are given in Appendix 4.A.

[8] Note that the third assumption is already implied by the second if the germs are set equal to (some polynomial transformation of) the model input parameters.

Table 4.2: Overview: Common distributions and corresponding germs and orthogonal polynomials on L^2

Distribution of θ		Germ		Orthogonal polynomials
Family	Parametric	ξ	ψ	q_n
Normal	$\theta \sim \mathrm{N}(\mu, \sigma^2)$	$\xi := \frac{\theta-\mu}{\sqrt{2}\sigma}$	$\psi(s) = \mu + \sqrt{2}\sigma s$	(physicists) Hermite H_n
Uniform	$\theta \sim \mathrm{U}(0,1)$	$\xi := 2\theta - 1$	$\psi(s) = \frac{s+1}{2}$	Legendre L_n
Beta	$\theta \sim \mathrm{Beta}(\alpha, \beta)$	$\xi := 2\theta - 1$	$\psi(s) = \frac{s+1}{2}$	Jacobi $J_n^{(\beta-1,\alpha-1)}$
Gamma	$\theta \sim \mathrm{Gamma}(\alpha, \beta)$[a]	$\xi := \beta\theta$	$\psi(s) = \frac{s}{\beta}$	General Laguerre $La_n^{(\alpha-1)}$
Inverse Gamma	$\theta \sim \text{Inv-Gamma}(\alpha, \beta)$[a]	$\xi := \frac{\beta}{\theta}$	$\psi(s) = \frac{\beta}{s}$	General Laguerre $La_n^{(\alpha-1)}$

[a] We use the scale-rate notation.

In all of the cases presented in Table 4.2 the respective families of orthogonal polynomials $\{q_n\}_{n\in\mathbb{N}_0}$ form a complete orthogonal system, i.e. lie densely in $L^2 = L^2(\mathbb{R}, \mathscr{B}(\mathbb{R}), P_\xi) = L^2(\mathbb{R}, \mathscr{B}(\mathbb{R}), w(s)\,\mathrm{d}s)$ where w is the corresponding probability density of ξ.[9] More generally, it follows from Riesz (1924) that $\{q_n\}_{n\in\mathbb{N}_0}$ is a complete orthogonal system in L^2 if and only if there exists no other measure μ on $(\mathbb{R}, \mathscr{B}(\mathbb{R}))$ which generates the same moments as P_ξ, i.e. if and only if there is no other measure μ such that

$$\int_{\mathbb{R}} s^n \,\mathrm{d}\mu = \int s^n \,\mathrm{d}P_\xi = \mathrm{E}[\xi^n] \text{ for all } n \in \mathbb{N}_0.$$

If completeness of $\{q_n\}_{n\in\mathbb{N}_0}$ in L^2 can be established, then Assumptions 3 and 4 guarantee the existence of Fourier series expansions of ψ and $h \circ \psi$ in the orthogonal polynomials, i.e. there are coefficients $\{\hat{\vartheta}_n\}_{n\in\mathbb{N}_0}$ and $\{\hat{y}_n\}_{n\in\mathbb{N}_0}$, $\hat{\vartheta}_n, \hat{y}_n \in \mathbb{R}$, so that

$$\psi = \sum_{n=0}^{\infty} \hat{\vartheta}_n q_n \text{ in } L^2 = L^2(\mathbb{R}, \mathscr{B}(\mathbb{R}), P_\xi),$$
$$h \circ \psi = \sum_{n=0}^{\infty} \hat{y}_n q_n \text{ in } L^2 = L^2(\mathbb{R}, \mathscr{B}(\mathbb{R}), P_\xi).$$

Note that identity and convergence is understood in L^2 which also implies point-wise convergence a.e. for a subsequence but not point-wise convergence.[10] Moreover, since $P_\theta = P_\xi \circ \psi^{-1}$, also $h = \sum_{n=0}^{\infty} \hat{y}_n (q_n \circ \psi^{-1})$ in $L^2(\mathbb{R}, \mathscr{B}(\mathbb{R}), P_\theta)$.

Hence, the uncertain model input parameter $\theta = \psi \circ \xi$ as well as our model outcome $Y = h \circ \psi \circ \xi$ can both be expanded exactly by a polynomial series in the germ, i.e. by

$$\theta = \psi(\xi) = \sum_{n=0}^{\infty} \hat{\vartheta}_n q_n(\xi) \text{ in } L^2(\Omega, \mathscr{A}, P), \tag{4.3.1}$$

$$Y = h(\theta) = h(\psi(\xi)) = \sum_{n=0}^{\infty} \hat{y}_n q_n(\xi) \text{ in } L^2(\Omega, \mathscr{A}, P). \tag{4.3.2}$$

[9] See Szegő (1939) for proofs of completeness.
[10] For conditions for point-wise convergence see e.g. Jackson (1941).

These series expansions are called the polynomial chaos expansion (PCE) of θ and Y with respect to the germ ξ. Moreover, orthogonality of $\{q_n\}_{n\in\mathbb{N}_0}$ implies that the Fourier coefficients are determined by

$$\hat{\vartheta}_n = \|q_n\|_{L^2}^{-2}\langle\psi, q_n\rangle_{L^2} = \|q_n\|_{L^2}^{-2}\int_{\mathbb{R}} \psi q_n \,\mathrm{d}P_\xi, \tag{4.3.3}$$

$$\hat{y}_n = \|q_n\|_{L^2}^{-2}\langle h\circ\psi, q_n\rangle_{L^2} = \|q_n\|_{L^2}^{-2}\int_{\mathbb{R}} (h\circ\psi) q_n \,\mathrm{d}P_\xi. \tag{4.3.4}$$

Now in practice, equations (4.3.1)-(4.3.2) justify approximations of the uncertain model input parameter θ as well as of the model outcome Y by their truncated PCE, i.e. by

$$S_N(\theta) = S_N(\psi\circ\xi) := \sum_{n=0}^{N} \hat{\vartheta}_n q_n(\xi),$$

$$S_N(Y) = S_N(h\circ\psi\circ\xi) := \sum_{n=0}^{N} \hat{y}_n q_n(\xi).$$

The approximations then converge to the true random variables, $S_N(\theta)\to\theta$ and $S_N(Y)\to Y$ in L^2 as $N\to\infty$. Yet, equations (4.3.3)-(4.3.4) from which the coefficients are defined can in general not be evaluated analytically. This involves a second approximation for the coefficients $\hat{\vartheta}_n$ and $\hat{y}_n$. The literature on PCE provides a variety of approaches for this task, from which we want to review the most popular ones.

4.3.1.1 Polynomial chaos expansion of the model parameters

Since the germ can be chosen in any desired way that satisfies Assumptions 1 and 2, the following two opposing approaches can be pursued for its specification.

In the first approach, one directly fixes the transformation ψ between the uncertain model parameter and the germ. The germ's distribution then follows from the given distribution of the uncertain input parameter and the chosen definition of ψ. In principal any choice of ψ which satisfies Assumption 2 is possible. One could then construct the family of orthogonal polynomials from the germ's distribution and the expansion coefficients could be derived by numerical integration of (4.3.3) up to any desired order. However, it is typically far more convenient to choose ψ as a simple linear transformation between the uncertain model parameter and the germ which results in a family of well-known orthogonal polynomials in L^2, see e.g. Table 4.2. In this case the expansion (4.3.1) collapses to

$$\theta = \psi(\xi) = \hat{\vartheta}_0 + \hat{\vartheta}_1 q_1(\xi)$$

and the expansion coefficients $\hat{\vartheta}_0$ and $\hat{\vartheta}_1$ are already known exactly.

Conversely, the second approach fixes the distribution of the germ and constructs ψ in such way that it is compatible to the given distribution of the uncertain parameter. This can be achieved as follows. Let F_ξ denote the desired (cumulative) distribution function of ξ and F_θ the given distribution function of θ. Then setting the germ to[11]

$$\xi := F_\xi^{-1}\circ F_\theta\circ\theta$$

[11] We denote by F^{-1} the quantile function.

yields the desired distribution for ξ. Conversely,

$$\psi = F_\theta^{-1} \circ F_\xi$$

and the expansion coefficients can again be computed from (4.3.3) by numerical integration.

4.3.1.2 Polynomial chaos expansion of the model outcome

While the expansion of the model parameter can be directly controlled by the appropriate choice of the germ, the expansion of the model outcome of interest requires some evaluations of the model.

Spectral projection: The first approach derives the polynomial chaos coefficients $\hat{y}_n$ by applying numerical integration methods to (4.3.4). For example, if ξ possesses a probability density function w, then (4.3.4) becomes

$$\hat{y}_n = \|q_n\|_{L^2}^{-2} \int_{\mathbb{R}} h(\psi(s)) q_n(s) w(s)\, \mathrm{d}s.$$

Hence, a Gauss-quadrature with M nodes that corresponds to the weight function w and to the orthogonal polynomials $\{q_n\}_{n\in\mathbb{N}_0}$ yields

$$\hat{y}_n \approx \|q_n\|_{L^2}^{-2} \sum_{i=1}^{M} h(\psi(s_i)) q_n(s_i) \omega_i \approx \|q_n\|_{L^2}^{-2} \sum_{i=1}^{M} h\left(\sum_{m=1}^{N} \hat{\vartheta}_m q_m(s_i)\right) q_n(s_i) \omega_i, \tag{4.3.5}$$

where s_i and ω_i denote the quadrature's nodes and weights, respectively. The Gauss-quadrature rule with M nodes will require to evaluate the model outcome $h(\psi(s_i)) \approx h\left(\sum_{m=1}^{N} \hat{\vartheta}_m q_m(s_i)\right)$ at each of the M nodes. Since the quadrature rule with M nodes is exact for polynomials up to degree $2M-1$, the number of nodes should be chosen appropriately. More specifically, if $h \circ \psi$ is assumed to be well approximated by its truncated partial sum $S_N(h \circ \psi)$ of degree N, the integrand, i.e. $h(\psi(s))q_n(s)$, is well approximated by polynomials of degree not larger than $2N$ for each $n = 1, \ldots, N$. Hence, it should then hold that $M \geq N + 1$.

Least-squares: The second approach treats the ignored higher terms $\epsilon := \sum_{n=N+1}^{\infty} \hat{y}_n q_n(\xi)$ of the truncated PCE as the residual in a linear regression

$$Y = h(\psi(\xi)) = \sum_{n=0}^{N} \hat{y}_n q_n(\xi) + \epsilon.$$

One can then either draw $M \in \mathbb{N}$ i.i.d. sample points $s_j, j = 1, \ldots, M$, from the distribution P_ξ or select them according to regression design principles. After computing the corresponding model outcomes $Y_j = h(\psi(s_j)) \approx h\left(\sum_{m=1}^{N} \hat{\vartheta}_m q_m(s_j)\right)$ the expansion coefficients are determined from

$$(\hat{y}_0, \ldots, \hat{y}_n) = \underset{\hat{y}_0,\ldots,\hat{y}_N}{\arg\min} \sum_{j=1}^{M} \left(Y_j - \sum_{n=0}^{N} \hat{y}_n q_n(s_j)\right)^2.$$

The number of sample (design) points is recommended to be set twice or three times as large as the number of unknown PCE coefficients in the literature, i.e. to $M = 2(N+1)$ or $M = 3(N+1)$.

Stochastic galerkin: For both methods discussed in the preceding paragraphs, the computation of the expansion coefficients is detached from the underlying procedure from which the model outcome is computed. This is different for the third method. Instead of a more general discussion,

we therefore only illustrate this method for the case where the PCE of a model's policy function is constructed. To simplify the notation, suppose that the equations defining the model's solution can be reduced to a sole Euler equation in a single variable. Let $S \subset \mathbb{R}^s$ denote the model's state-space and let $g : S \to \mathbb{R}$ denote the variable's policy function. The Euler equation is typically translated into a functional (integral) equation for g, say

$$R(g, x) = 0 \text{ for all } x \in S.$$

If the functional equation can not be solved analytically, a common approach is to construct an approximation $\hat{g}$ from linear combinations of some basis functions[12], say $\Phi_j, j = 1, \ldots, d$, i.e.

$$\hat{g}(x) = \sum_{j=1}^{d} y_j \Phi_j(x).$$

In order to determine the coefficients y_j in the approximation, which now serve as our model outcome of interest and should not be confused with the Fourier coefficients of the PCE, one can, for example, select d appropriate collocation points $x_1, \ldots, x_d \in S$ and solve the non-linear system of equations given by

$$R\left(\sum_{j=1}^{d} y_j \Phi_j, x_i\right) = 0 \text{ for all } i = 1, \ldots, d$$

for $y_1, \ldots, y_d$.

Now consider the case where one parameter is uncertain and hence described by the random variable θ. If the model's (reduced) Euler equation involves θ, then so does the functional equation for g, i.e. we now write

$$R(g, x; \theta) = 0 \text{ for all } x \in S.$$

Moreover, if one employs the above mentioned solution method, the coefficients y_j will typically also depend on θ, i.e. we have, in slight abuse of notation, $Y_j = h_j(\theta)$. In particular, the mappings h_j between the Y_j and θ arise implicitly from the non-linear system of equations

$$R\left(\sum_{j=1}^{d} Y_j \Phi_j, x_i; \theta\right) = 0 \text{ for all } i = 1, \ldots, d. \tag{4.3.6}$$

In order to avoid the necessity for repeated and potentially computational expensive solutions of this system of equations for different values of θ, one may want to find for each Y_j a PCE in terms of some chosen germ ξ[13]

$$\theta = \psi(\xi) = \sum_{n=0}^{\infty} \hat{\vartheta}_n q_n(\xi),$$

$$Y_j = h_j(\theta) = h_j(\psi(\xi)) = \sum_{n=0}^{\infty} \hat{y}_{jn} q_n(\xi).$$

The PCE of the model's (approximated) policy function with respect to the germ ξ is then given

[12] Most commonly these are selected either as (tensor products of) Chebyshev polynomials or as piecewise linear or cubic polynomials.

[13] Note that in this case we have d model outcomes of interest, namely the coefficients $Y_j = h_j(\theta)$ in $\hat{g}$.

by

$$\hat{g}(x;\xi) = \sum_{j=1}^{d} Y_j \Phi_j(x) = \sum_{j=1}^{d} \sum_{n=0}^{\infty} \hat{y}_{jn} q_n(\xi) \Phi_j(x).$$

Moreover, the Fourier coefficients $\hat{y}_{jn}$ in the PCE can be derived by a Galerkin method if we substitute the Y_j in their implicit definition in (4.3.6) with their PCE and impute the corresponding conditions

$$R\left(\sum_{j=1}^{d}\sum_{n=0}^{\infty} \hat{y}_{jn} q_n(\xi)\Phi_j, x_i; \psi(\xi)\right) = 0 \text{ in } L^2 \text{ for all } i = 1,\dots,d$$

$$\Leftrightarrow \left\langle R\left(\sum_{j=1}^{d}\sum_{n=0}^{\infty} \hat{y}_{jn} q_n(\xi)\Phi_j, x_i; \psi(\xi)\right), q_m(\xi)\right\rangle_{L^2} = 0 \text{ for all } i = 1,\dots,d \text{ and all } m \in \mathbb{N}_0.$$

Hence, we can solve for the $d(N+1)$ unknown coefficients $\hat{y}_{jn}$ in the truncated PCE $Y_j \approx \sum_{n=0}^{N} \hat{y}_{jn} q_n(\xi)$ from the system of equations

$$0 \approx \left\langle R\left(\sum_{j=1}^{d}\sum_{n=0}^{N} \hat{y}_{jn} q_n(\xi)\Phi_j, x_i; \psi(\xi)\right), q_m(\theta)\right\rangle_{L^2} =$$

$$= \int_{\mathbb{R}} R\left(\sum_{j=1}^{d}\sum_{n=0}^{N} \hat{y}_{jn} q_n(\xi)\Phi_j, x_i; \psi(\xi)\right) q_m(\xi)\, \mathrm{d}P_\xi(\xi)$$

for $i = 1,\dots,d$ and $m = 0,\dots,N$. The integral is computed numerically, either from Monte-Carlo draws or from an appropriate Gauss quadrature. Moreover, $\psi(\xi)$ can be substituted by its truncated series expansion as previously described in subsection 4.3.1.1.

4.3.2 Multiple uncertain input parameters ($k \geq 2$)

We now turn to the case where more than one input parameter is uncertain and where more than one germ is used in the polynomial expansions. In brief, the stochastic independence of the germs allows us to apply the procedure from the one-dimensional case to each of the finitely many dimensions.

Since Assumption 2 guarantees that all polynomials are included in each L_i^2, one can again apply the Gram-Schmidt process to the sequence of monomials and construct for each $i = 1,\dots,k$ an orthogonal system of polynomials $\{q_{in}\}_{n\in\mathbb{N}_0} \subset L_i^2$ where q_{in} is a polynomial of (exact) degree n and

$$\langle q_{in}, q_{im}\rangle_{L_i^2} = \|q_{in}\|_{L_i^2}^2 \delta_{m,n} \text{ for all } m,n \in \mathbb{N}_0.$$

For any multi-index $\alpha = (\alpha_1,\dots,\alpha_k) \in \mathbb{N}_0^k$ we define the multivariate polynomial

$$q_\alpha(\xi) := \prod_{i=1}^{k} q_{i\alpha_i}(\xi_i).$$

Since stochastic independence of the ξ_i implies that $P_\xi = \otimes_{i=1}^{k} P_{\xi_i}$, the family of multivariate polynomials $\{q_\alpha\}_{\alpha\in\mathbb{N}_0^k}$ then forms an orthogonal system in L^2. Moreover, if for each $i = 1,\dots,k$ the orthogonal system $\{q_{in}\}_{n\in\mathbb{N}_0}$ is complete in L_i^2, then $\{q_\alpha\}_{\alpha\in\mathbb{N}_0^k}$ is also complete in L^2. In

particular, this is satisfied if each θ_i is distributed according to one of the distributions specified in Table 4.2 and if the germs ξ_i are set accordingly. Then, since $\psi_i \in L^2$ (Assumption 3) and $h \circ \psi \in L^2$ (Assumption 4), there exist coefficients $\{\hat{\vartheta}_{i\alpha}\}_{\alpha\in\mathbb{N}_0^k} \subset \mathbb{R}, i = 1,\dots,k$, and $\{\hat{y}_\alpha\}_{\alpha\in\mathbb{N}_0^k} \subset \mathbb{R}$ such that

$$\psi_i = \sum_{\alpha\in\mathbb{N}_0^k} \hat{\vartheta}_{i\alpha} q_n \text{ in } L^2 = L^2(\mathbb{R}^k, \mathscr{B}(\mathbb{R}^k), P_\xi), \tag{4.3.7}$$

$$h \circ \psi = \sum_{\alpha\in\mathbb{N}_0^k} \hat{y}_\alpha q_\alpha \text{ in } L^2 = L^2(\mathbb{R}^k, \mathscr{B}(\mathbb{R}^k), P_\xi). \tag{4.3.8}$$

The second expansion can again be written equivalently as

$$h = \sum_{\alpha\in\mathbb{N}_0^k} \hat{y}_\alpha (q_\alpha \circ \psi^{-1}) \text{ in } L^2(\mathbb{R}^k, \mathscr{B}(\mathbb{R}^k), P_{\boldsymbol{\theta}}).$$

Therefore, the parameters θ_i and the model outcome Y are again representable in L^2 by a PCE in the germs $\boldsymbol{\xi}$ through

$$\theta_i = \psi_i \circ \boldsymbol{\xi} = \sum_{\alpha\in\mathbb{N}_0^k} \hat{\vartheta}_{i\alpha} q_\alpha(\boldsymbol{\xi}) \text{ in } L^2(\Omega, \mathscr{A}, P), \tag{4.3.9}$$

$$Y = h \circ \boldsymbol{\theta} = h \circ \psi \circ \boldsymbol{\xi} = \sum_{\alpha\in\mathbb{N}_0^k} \hat{y}_\alpha q_\alpha(\boldsymbol{\xi}) \text{ in } L^2(\Omega, \mathscr{A}, P). \tag{4.3.10}$$

Moreover, the expansion coefficients are determined by

$$\hat{\vartheta}_{i\alpha} = \|q_\alpha\|_{L^2}^{-2} \langle \psi_i, q_\alpha \rangle_{L^2} = \|q_\alpha\|_{L^2}^{-2} \int_{\mathbb{R}^k} \psi_i q_\alpha \, \mathrm{d}P_\xi, \tag{4.3.11}$$

$$\hat{y}_\alpha = \|q_\alpha\|_{L^2}^{-2} \langle h \circ \psi, q_\alpha \rangle_{L^2} = \|q_\alpha\|_{L^2}^{-2} \int_{\mathbb{R}^k} (h \circ \psi) q_\alpha \, \mathrm{d}P_\xi, \tag{4.3.12}$$

where $P_\xi = \otimes_{i=1}^k P_{\xi_i}$ implies that $\|q_\alpha\|_{L^2} = \prod_{i=1}^k \|q_{i\alpha_i}\|_{L_i^2}$.

Equations (4.3.11)-(4.3.12) guarantee that if the parameters θ_i and the model outcome Y are approximated by their truncated PCE, the approximations converge to the true random variables in L^2 as the degree of the partial sums is increased. The truncation is typically introduced either by limiting the total degree of the multivariate polynomials

$$S_N^{\text{tot}}(\theta_i) = S_N^{\text{tot}}(\psi_i \circ \boldsymbol{\xi}) := \sum_{\alpha\in\mathbb{N}_0^k, |\alpha|\le N} \hat{\vartheta}_{i\alpha} q_\alpha(\boldsymbol{\xi}),$$

$$S_N^{\text{tot}}(Y) = S_N^{\text{tot}}(h \circ \psi \circ \boldsymbol{\xi}) := \sum_{\alpha\in\mathbb{N}_0^k, |\alpha|\le N} \hat{y}_\alpha q_\alpha(\boldsymbol{\xi}),$$

where $|\alpha| := \sum_{i=1}^k \alpha_i$, or by limiting the maximal degree in each component

$$S_N^{\max}(\theta_i) = S_N^{\max}(\psi_i \circ \boldsymbol{\xi}) := \sum_{\alpha\in\mathbb{N}_0^k, \|\alpha\|_\infty \le N} \hat{\vartheta}_{i\alpha} q_\alpha(\boldsymbol{\xi}),$$

$$S_N^{\max}(Y) = S_N^{\max}(h \circ \psi \circ \boldsymbol{\xi}) := \sum_{\alpha\in\mathbb{N}_0^k, \|\alpha\|_\infty \le N} \hat{y}_\alpha q_\alpha(\boldsymbol{\xi}),$$

where $\|\alpha\|_\infty := \max_{i=1,\dots,k} \alpha_i$.

In order to compute the expansion coefficients from their defining equations (4.3.11)-(4.3.12), it is straightforward to adapt the methods from section 4.3.1.2 to the multidimensional case. However, this typically introduces the curse of dimensionality.

First, this issue becomes particularly problematic if the integrals are computed by Gauss-quadrature rules. If the mapping $h \circ \psi$ can be well approximated by its truncated series expansion S_N, then the integrands $(h \circ \psi) q_\alpha$ in (4.3.12) can be well approximated by multivariate polynomials which rise up to degree $2N$ in each component, indifferent from the fact whether $|\alpha| \leq N$ or $\|\alpha\|_\infty \leq N$ is assumed. Since one-dimensional Gauss-quadrature rules with M nodes provide exact integration rules for polynomials up to degree $2M-1$, it is required to compute (4.3.12) by quadrature rules with $M = N+1$ nodes in each of the k dimensions. Hence, the model outcome must be evaluated for a total of $(N+1)^k$ parameter combinations and the procedure becomes quickly inefficient as k rises. However, sparse grid methods, as e.g. Smolyak-Gauss quadrature which is illustrated in Appendix 4.B and analyzed in the numerical example in section 4.5, can help to reduce the computational effort that is required for similar integration quality.

Second, the burden of higher-dimensional parameter vectors also appears in similar form if the PCE coefficients are determined by least squares. However, while the number of coefficients which must be computed equals $(N+1)^k$ in $S_N^{\max}$, the number of coefficients grows less extremely in S_N^{tot} where it is given by $\binom{N+k}{k}$. Following the recommendation that the number of sample points should be twice or three times as large as the number of unknown coefficients, the model must be evaluated for $2\binom{N+k}{k}$ or $3\binom{N+k}{k}$ parameter combinations in the latter case.

4.4 Applications of generalized polynomial chaos expansions

After its construction, the PCE of the model outcome can be used for computational inexpensive evaluations of the model. On the one hand, statistical properties of the model outcome, as induced by the predefined distribution of the uncertain input parameters, can be derived directly from the PCE. On the other hand, the expansion can also be used as a point-wise approximation of the model outcome for different parameter values.

Evaluation of statistical properties: Convergence in $L^2(\Omega, \mathcal{A}, P)$ of the series expansion in (4.3.10) implies that the distribution of the model outcome Y can be equivalently characterized by its polynomial expansion. In particular, the mean and variance of Y follow directly from the fact that convergence in L^2 also implies convergence of the mean and variance so that orthogonality of the polynomials (and $q_{\mathbf{0}} = 1$ for $\mathbf{0} := (0, \dots, 0) \in \mathbb{N}_0^k$) yields

$$\mathrm{E}[Y] = \sum_{\alpha \in \mathbb{N}_0^k} \hat{y}_\alpha \, \mathrm{E}[q_\alpha(\xi)] = \sum_{\alpha \in \mathbb{N}_0^k} \hat{y}_\alpha \, \mathrm{E}[q_\alpha(\xi) q_{\mathbf{0}}(\xi)] = \sum_{\alpha \in \mathbb{N}_0^k} \hat{y}_\alpha \langle q_\alpha, q_{\mathbf{0}} \rangle_{L^2} = \hat{y}_{\mathbf{0}},$$

and

$$\begin{aligned} \mathrm{Var}[Y] &= \mathrm{E}\left[\left(\sum_{\alpha \in \mathbb{N}_0^k} \hat{y}_\alpha q_\alpha(\xi) - \hat{y}_{\mathbf{0}} \right)^2 \right] = \mathrm{E}\left[\left(\sum_{\alpha \in \mathbb{N}_0^k \setminus \{\mathbf{0}\}} \hat{y}_\alpha q_\alpha(\xi) \right)^2 \right] = \\ &= \sum_{\alpha, \beta \in \mathbb{N}_0^k \setminus \{\mathbf{0}\}} \hat{y}_\alpha \hat{y}_\beta \langle q_\alpha, q_\beta \rangle_{L^2} = \sum_{\alpha \in \mathbb{N}_0^k \setminus \{\mathbf{0}\}} \hat{y}_\alpha^2 \|q_\alpha\|_{L^2}^2. \end{aligned}$$

Moreover, other statistical properties can be computed by Monte-Carlo methods. Large samples of Y can be efficiently constructed by drawing from the germ's distribution and inserting the sample into the expansion of Y. Compared to traditional methods, repeated and costly model

evaluations can thus be avoided.

Using the expansion as point-wise approximation for the model outcome: A truncated version of the Fourier series expansion (4.3.8) can also be used as a point-wise approximation for the mapping h between model input parameters and model outcome

$$h(\vartheta) \approx S_N(h \circ \psi)(\psi^{-1}(\vartheta)) = \sum_{\alpha \in \mathbb{N}_0^k, |\alpha| \leq N} \hat{y}_\alpha q_\alpha(\psi^{-1}(\vartheta)). \tag{4.4.1}$$

Note however that convergence of the series in L^2 as $N \to \infty$ does not imply point-wise convergence on the support of P_ξ but only point-wise convergence a.e. for a subsequence.

The partial sum $S_N(h \circ \psi)$ is the orthogonal projection of $h \circ \psi$ onto the subspace of $L^2(\mathbb{R}^k, \mathscr{B}(\mathbb{R}^k), P_\xi)$ spanned by multivariate polynomials of total degree less or equal to N. If the transformation ψ between germs and parameters is chosen linear, $S_N(h \circ \psi) \circ \psi^{-1}$ is also the orthogonal projection of h onto this subspace in $L^2(\mathbb{R}^k, \mathscr{B}(\mathbb{R}^k), P_{\boldsymbol{\theta}})$.[14] In the sense of the induced metric, it is therefore the best approximation of h by multivariate polynomials of total degree up to N, i.e. it minimizes the mean-squared error over the support of $P_{\boldsymbol{\theta}}$.

Special case: Surrogate of model solution: Consider a discretely-timed model where in any period $t \in \mathbb{N}$ the vector $x_t \in S \subset \mathbb{R}^{n_x}$ denotes the predetermined variables from the state-space S and $y_t \in \mathbb{R}^{n_y}$ is a vector of the non-predetermined variables of the model. Suppose that $\boldsymbol{\theta}$ is a random vector of unknown parameters of the model, and for any possible realization $\vartheta \in \Theta$ the model solution is computed in terms of a policy function $g(.;\vartheta)\colon S \to \mathbb{R}^{n_x+n_y}$ so that

$$\begin{pmatrix} x_{t+1} \\ y_t \end{pmatrix} = g(x_t;\vartheta).$$

If, for any arbitrary $x \in S$ and for a suitable transformation ψ between parameters and germs, the mapping $\vartheta \mapsto g(x;\vartheta)$ satisfies the sufficient condition in assumption 4, then there exists a series expansion by orthogonal polynomials $\{q_\alpha\}$ of the form

$$g(x,\vartheta) = \sum_{\alpha \in \mathbb{N}_0^k} \hat{g}_\alpha(x) q_\alpha(\psi^{-1}(\vartheta)) \text{ in } L^2(\mathbb{R}^k, \mathscr{B}(\mathbb{R}^k), P_{\boldsymbol{\theta}}),$$

$$\hat{g}_\alpha(x) = \|q_\alpha\|_{L^2}^{-2} \int_{\mathbb{R}^k} g(x, \psi(s)) q_\alpha(s) \, \mathrm{d}P_\xi(s).$$

Perhaps the most prevalent approach in the literature to determine the model's policy function is to compute g from a linearized version of the model. In this case

$$g(x;\vartheta) = A(\vartheta)x,$$

and *numeric* implementation of the methods proposed by Blanchard and Kahn (1980), Klein (2000) or Sims (2002) allows to solve for the matrix $A(\vartheta) \in \mathbb{R}^{n_x \times (n_x+n_y)}$ given any arbitrary but fixed $\vartheta \in \Theta$. Since the coefficients in the policy's PCE are here determined by

$$\hat{g}_\alpha(x) = \left(\|q_\alpha\|_{L^2}^{-2} \int_{\mathbb{R}^k} q_\alpha(s) A(\psi(s)) \, \mathrm{d}P_\xi(s) \right) x =: \hat{A}_\alpha x,$$

[14] Otherwise it is the orthogonal projection of h onto the subspace in $L^2(\mathbb{R}^k, \mathscr{B}(\mathbb{R}^k), P_{\boldsymbol{\theta}})$ spanned by multivariate polynomials in ψ^{-1} of total degree less or equal to N.

the series expansion of the linear policy function can be written as

$$g(x,\vartheta) = \sum_{\alpha\in\mathbb{N}_0^k} \hat{g}_\alpha(x) q_\alpha(\psi^{-1}(\vartheta)) = \left(\sum_{\alpha\in\mathbb{N}_0^k} \hat{A}_\alpha q_\alpha(\psi^{-1}(\vartheta)) \right) x.$$

Moreover, the $\hat{A}_\alpha$ coincide with the expansion coefficients from the PCE of the model outcome $A(\vartheta)$. Hence, the PCE of a linear policy is again linear and is represented by the polynomial expansion of the matrix-valued function $\vartheta \mapsto A(\vartheta)$.

A second popular approach to compute the model's policy function are projection methods.[15] In this approach g is constructed as a linear combination of some suitable basis functions Φ_i by

$$g(x;\vartheta) = \sum_{i=1}^{d} c_i(\vartheta)\Phi_i(x).$$

The coefficients in the PCE of g with respect to ϑ then satisfy

$$\hat{g}_\alpha(x) = \sum_{i=1}^{d} \left(\|q_\alpha\|_{L^2}^{-2} \int_{\mathbb{R}^k} q_\alpha(s)\,(c_i(\psi(s)))\,\mathrm{d}P_\xi(s) \right) \Phi_i(x) =: \sum_{i=1}^{d} \hat{c}_{i\alpha}\Phi(x),$$

and the expansion of g can therefore be written as

$$g(x,\vartheta) = \sum_{\alpha\in\mathbb{N}_0^k} \hat{g}_\alpha(x) q_\alpha(\psi^{-1}(\vartheta)) = \sum_{i=1}^{d} \left(\sum_{\alpha\in\mathbb{N}_0^k} \hat{c}_{i\alpha} q_\alpha(\psi^{-1}(\vartheta)) \right) \Phi(x),$$

Now observe that the $\hat{c}_{i\alpha}$ coincide with the coefficients in the polynomial expansion of the model outcome $c_i(\vartheta)$, i.e. with the coefficients in the PCE of the coefficients of the projection solution. Consequently, the PCE of g is again a linear combination of the basis functions Φ_i and the coefficients are represented by the polynomial expansion of $\vartheta \mapsto c_i(\vartheta)$.

Surrogate for gradients: The truncated PCE in (4.4.1) may also be used to approximate the derivatives of the mapping h between parameter values and model outcomes. More specifically, the PCE provides the approximation

$$\frac{\partial h}{\partial \vartheta_i}(\vartheta) \approx \sum_{\alpha\in\mathbb{N}_0^k, |\alpha|\le N} \hat{y}_\alpha \sum_{j=1}^{k} \frac{\partial q_\alpha}{\partial s_k}(\psi^{-1}(\vartheta)) \frac{\partial \psi_j^{-1}}{\partial \vartheta_i}(\vartheta).$$

This approximation can be useful if such derivatives must be evaluated at a potential large number of points. One example may be the method proposed by Iskrev (2010) for conducting local identification analysis which requires differentiation of the linearized policy function with respect to the parameters.

4.5 Numerical analysis

In this section we present the numerical implementation of a PCE for a benchmark RBC model. First, we analyze the convergence behaviour of the series expansion for different model outcomes

[15] See, for instance Judd (1996), Chapter 11, Heer and Maussner (2009), Chapter 6, Judd (1992) or McGrattan (1999).

of interest. More specifically, the model outcomes considered include the linear solution, the second moments and the impulse response functions of the model's variables to a one time shock—both computed from the model's linear policy—as well as a global projection solution. Moreover, we compare different methods to compute the PCE coefficients in terms of accuracy and efficiency. Finally, we perform Monte-Carlo experiments where we evaluate the performance of the PCE for empirical applications as matching moments and likelihood-based approaches.

4.5.1 The model

We consider a benchmark RBC model where the social planner solves the following maximization problem

$$\begin{aligned}
\max_{Y_t,C_t,N_t,I_t,K_{t+1}} \quad & U_0 := \mathbb{E}_0\left[\sum_{t=0}^{\infty}\beta^t \frac{C_t^{1-\eta}(1-N_t)^{\gamma(1-\eta)}}{1-\eta}\right], \\
\text{s.t.} \quad & Y_t = C_t + I_t, \\
& Y_t = e^{z_t}K_t^{\zeta}N_t^{1-\zeta}, \\
& K_{t+1} = (1-\delta)K_t + I_t, \\
\text{given} \quad & K_0, z_0,
\end{aligned}$$

where Y_t, C_t, N_t, I_t and K_t denote output, consumption, working hours, investment and the capital stock, respectively. Moreover, the log of total factor productivity, z_t, evolves according to the AR(1) process

$$z_{t+1} = \rho z_t + \epsilon_{t+1},\ \epsilon_t \sim \text{iidN}(0,\sigma^2).$$

The predetermined state variables x_t and the non-predetermined control variables y_t are

$$x_t := \begin{pmatrix} K_t \\ z_t \end{pmatrix} \text{ and } y_t := \begin{pmatrix} Y_t \\ C_t \\ N_t \\ I_t \end{pmatrix}.$$

4.5.2 Convergence behaviour

First, in order to study the basic convergence behaviour of the PCE for various model outcomes in the benchmark RBC model, we consider an example where we set the uncertain parameters to $\theta := \begin{pmatrix}\zeta & \eta & \rho\end{pmatrix}$. Moreover, we assume the following probability distributions for the (stochastically independent) unknown parameters

$$\zeta \sim 0.15 + 0.3\cdot\text{Beta}(5,7),\ \eta \sim 1 + 7\cdot\text{Beta}(3,7),\ \rho \sim 0.85 + 0.14\cdot U(0,1).$$

The probability density functions with support $\Theta := [0.15;0.45]\times[1;8]\times[0.85;0.99]$ are illustrated in Figure 4.2. The transformations ψ_i between unknown parameters and germs are fixed as in Table 4.2 and the remaining parameters are calibrated as summarized in Table 4.3.

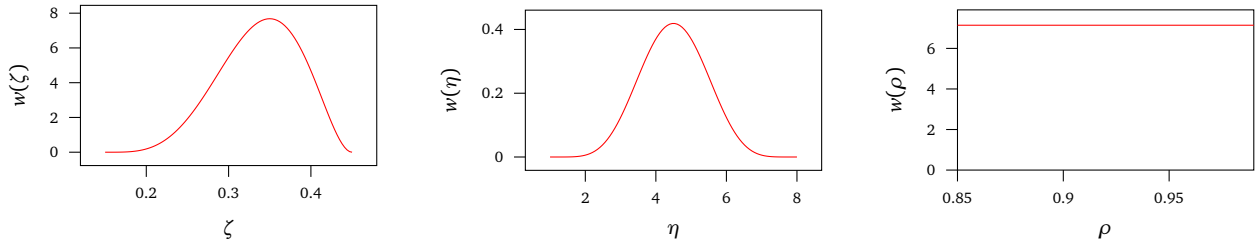

(a) Prior of ζ (b) Prior of η (c) Prior of ρ

Figure 4.2: Distributions of uncertain parameters

Table 4.3: Calibration I

Parameter	Description	Value
β	Discount factor	0.994
δ	Rate of capital depreciation	0.014
N	Steady-state labor supply	0.3
σ	Standard deviation	0.01

Linear policy function: The first model outcome which we consider is the model's linear solution which is of the form

$$\begin{pmatrix} x_{t+1} \\ y_t \end{pmatrix} = A(\vartheta) x_t.$$

Given any parameter values $\vartheta \in \Theta$ the matrix $A(\vartheta) = \big(a_{ij}(\vartheta)\big)_{\substack{i=1,\dots,6 \\ j=1,2}} \in \mathbb{R}^{6\times 2}$ can be easily computed numerically from available methods. As described in section 4.4, the expansion of the linear policy function is again linear and is represented by the polynomial expansion of $A(\vartheta)$. Hence, our task is to construct for each mapping $a_{ij}\colon \vartheta \mapsto a_{ij}(\vartheta)$ the truncated PCE[16]

$$a_{ij}^{(N)}(\vartheta) := S_N^{\text{tot}}(a_{ij}\circ\psi)(\psi^{-1}(\vartheta)) = \sum_{\alpha\in\mathbb{N}_0^3, |\alpha|\le N} \hat{a}_{ij\alpha} q_\alpha(\psi^{-1}(\vartheta)). \tag{4.5.1}$$

Moreover, we first want to abstract from errors in the computation of the expansion coefficients $\hat{a}_{ij\alpha}$ and to focus on the convergence behaviour of $a_{ij}^{(N)} \to a_{ij}$ in L^2 as $N\to\infty$. Therefore, we compute the coefficients from full-grid Gauss-quadrature rules with a sufficiently large number of nodes which should guarantee that integration errors in (4.3.10) (where now $h = a_{ij}$) remain insignificant. More concretely, we apply $N+5$ nodes in each of the three one-dimensional quadrature rules. We compute the coefficients from the quadrature rules and determine the L^2 error from

$$\|a_{ij}^{(N)} - a_{ij}\|_{L^2} = \left(\int_{\mathbb{R}^3} \left(a_{ij}^{(N)}(\vartheta) - a_{ij}(\vartheta)\right)^2 dP_\theta\right)^{1/2} \approx \left(\frac{1}{M}\sum_{i=1}^{M}\left(a_{ij}^{(N)}(\vartheta^{(i)}) - a_{ij}(\vartheta^{(i)})\right)^2\right)^{1/2} \tag{4.5.2}$$

where we draw $M = 10^5$ iid sample points $\vartheta^{(i)}$ from the distribution of θ. The results are presented in Figure 4.2(a) in $\log_{10}$-base for $N=1$ to $N=19$ and suggest linear convergence of the series expansions for each a_{ij}. The L^2 error for all components of the matrix already

[16] We only discuss the mappings $\vartheta \mapsto a_{ij}(\vartheta)$ for $i = 1,3,\dots,6$ and $j = 1,2$ since the expansion of the exogenous AR(1)-process ($i=2$) w.r.t. ρ is trivial.

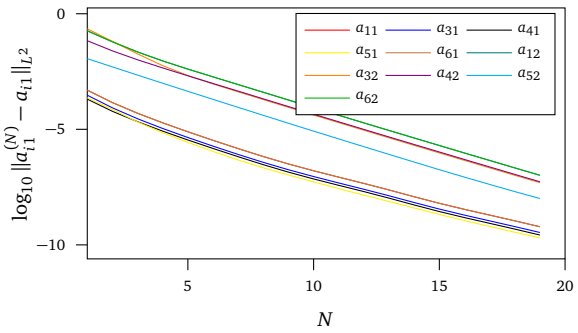

(a) L^2 convergence linear policy

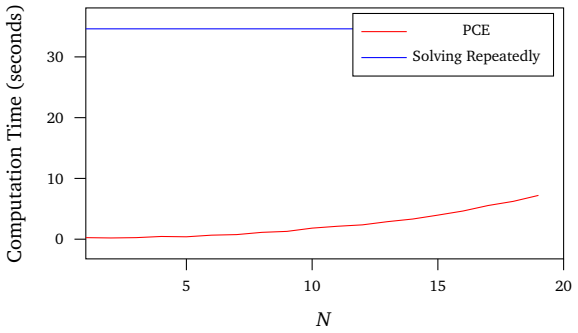

(b) Computation time linear policy

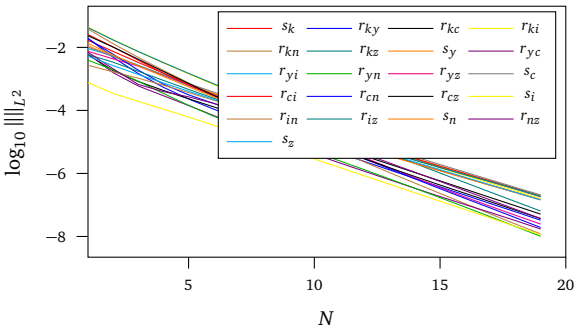

(c) L^2 convergence second moments

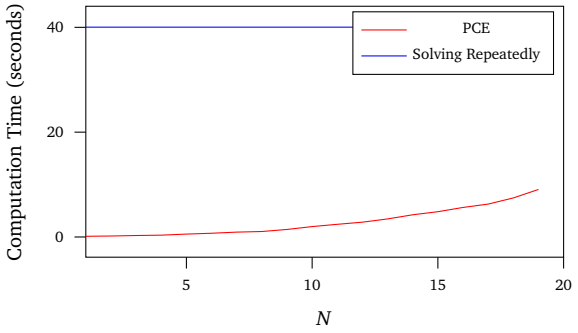

(d) Computation time second moments

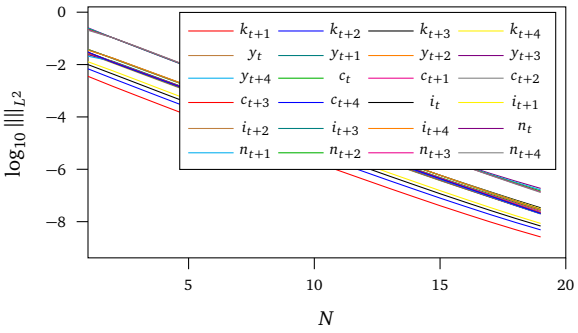

(e) L^2 convergence impulse response function

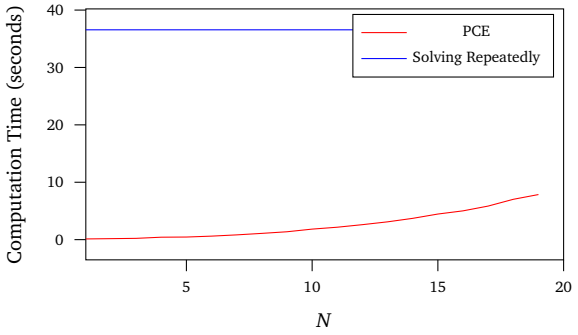

(f) Computation time impulse response function

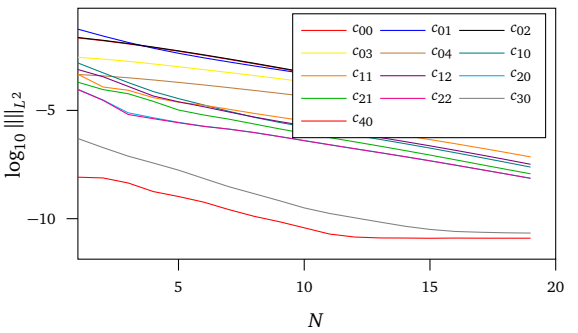

(g) L^2 convergence global solution

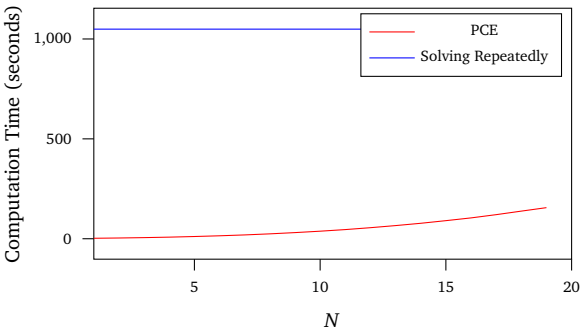

(h) Computation time global solution

Figure 4.3: L^2 convergence of PCE and computation time on an Intel® Core™i7-7700 CPU @ 3.60GHz

falls to the order of magnitude of -3 for $N = 7$ and is as low as -6 for $N = 19$. Moreover, Figure 4.2(b) also shows the time needed for all computations. In case of the PCE, the total time reported includes i) the computation of expansion coefficients $\hat{a}_{ij\alpha}$ from the full-grid quadrature rules which require $(N+5)^3$ model evaluations and ii) the subsequent (trivial) evaluation of the truncated PCE $a_{ij}^{(N)}(\vartheta^{(i)})$ at the 100,000 sample points. For comparison, we also show the computational time which is required to determine the model solution $a_{ij}(\vartheta^{(i)})$ repeatedly at all 100,000 sample points. Most importantly, since even for $N = 19$ the number of model evaluations for the construction of the PCE is significantly smaller at 13824 than the number of evaluation points, the time required by the PCE remains less than one-third of the time needed for repeatedly solving the model.

Second moments: The second model outcome we consider are the model's second moments. More specifically, we consider the variables' standard deviations and the correlations obtained from the model's linear policy. Instead of relying on simulations, we employ available formulae for moments of first-order autoregressive processes to the linear solution. We proceed the same way as in the preceding paragraph and compute for each moment, say x, a series expansion $x^{(N)} := \sum_{\alpha\in\mathbb{N}_0^3,|\alpha|\leq N} \hat{x}_\alpha q_\alpha(\psi^{-1}(\vartheta))$. Importantly, note that we directly construct the PCE of the second moments, i.e. of the mapping $\vartheta \mapsto x(\vartheta)$. An alternative approach to employ PCE for the second moments would be to first construct the PCE of the linear policy and to subsequently use this PCE of the linear policy to compute the second moments.

Figure 4.2(c) again shows linear convergence of the PCEs for each second moment. The L^2 error in the approximation of the model's moments has fallen to the order of magnitude of -3 by $N = 7$ and further declines to -6 by $N = 19$. Moreover, the computation time of the PCE versus the time for repeated computations the model's moments is illustrated in Figure 4.2(d). For the same reasons as before, the time needed by the PCE remains throughout significantly lower than the time required for repeated calculations.

Impulse response function: The next model outcome we discuss are the variables' impulse response functions in response to a one time shock to total factor productivity by one conditional standard deviation. For the sake of exposition, we only consider the variables' outcomes for the next four periods after the shock hits the economy and add the remark that the series expansions become more trivial for later periods where the variables converge back to their stationary values. Hence, we construct PCEs for all variables' outcomes, say X_{t+s}, for periods $s = 0,\dots,4$. Note again that the PCE is constructed directly for each mapping $\vartheta \mapsto X_{t+s}(\vartheta)$.

We show the L^2 errors over the unknown parameters' support in Figure 4.2(e). Convergence is again linear as $N \to \infty$ and the L^2 errors for all variables' outcomes fall to the order of magnitude of -5 by $N = 19$. Furthermore, the computation time of the PCE remains throughout far below the time required for repeated computations of the model's impulse response functions.

Projection solution: The last model outcome for which we want to illustrate the convergence behavior is the model's projection solution computed from Chebyshev polynomials as basis functions. More specifically, we define $k_t := \ln(K_t/K^\star(\vartheta))$ where $K^\star(\vartheta)$ is the capital stock's stationary solution and approximate the policy function for working hours by

$$n_t = g(k_t, z_t; \vartheta) = \sum_{i+j\leq 4} c_{i,j}(\vartheta) T_i\left(2\frac{k_t - \underline{k}}{\bar{k} - \underline{k}} - 1\right) T_j\left(2\frac{z_t - \underline{z}}{\bar{z} - \underline{z}} - 1\right),$$

where we further introduce the transformation $n_t := \ln(N_t/(1-N_t))$. The T_i are Chebyshev polynomials of degree i and $[\underline{k};\bar{k}] \times [\underline{z};\bar{z}] = [\ln(0.8); -\ln(0.8)] \times [-3\frac{\sigma}{\sqrt{1-\rho^2}}; 3\frac{\sigma}{\sqrt{1-\rho^2}}]$ is the domain of the approximation g. The remaining variables are computed analytically from k_t, n_t and z_t and the coefficients $c_{i,j}(\vartheta)$ are determined such way that the model's Euler equation holds

exactly at 13 appropriately selected collocation points.[17]

We discussed in section 4.4 that the expansion of the projection solution is again a linear combination of the same basis functions, i.e. of $T_{i_1} T_{i_2}$ with $i_1 + i_2 \leq 4$, and the coefficients are given by the series expansions of the mappings $\vartheta \mapsto c_{i,j}(\vartheta)$. Hence, we construct truncated PCEs, $c_{i,j}^{(N)} := \sum_{\alpha \in \mathbb{N}_0^3, |\alpha| \leq N} \hat{c}_{ij\alpha} q_\alpha(\psi^{-1}(\vartheta))$ from full-grid quadrature rules with $N+5$ nodes in each dimension. The L^2 error, $\|c_{i,j}^{(N)} - c_{ij}\|_{L^2}$, in log10-basis is again decreasing linearly as $N \to \infty$ as displayed in Figure 4.2(g) and the time for construction and evaluation of the PCEs in Figure 4.2(h) remains throughout significantly smaller than the time for repeated computations of the global solution.

4.5.3 Computation of the polynomial chaos expansion coefficients

In the previous subsection our focus was on the convergence behavior of the PCE when the degree of truncation N was increased. We therefore abstracted from possible errors in the computation of the PCE coefficients and employed a full-grid quadrature rule with sufficiently many nodes. While full-grid quadrature rules have the favorable property that the number of nodes can be easily chosen in such way that they provide exact integration rules for polynomials up to the desired degree, the number of nodes grows exponentially in the dimension of the parameter vector. Hence, they may provide the most convenient way for computation of the PCE coefficients when the number of unknown parameters is not too large, but they become quickly ineffective in higher dimensional problems. If the PCE coefficients are determined from alternative methods, the approximation error of the feasible PCE does not only include the error from truncation of the series expansion but additionally from a potentially less accurate approximation of the PCE coefficients that becomes necessary.

In this section we now switch perspective and analyze the convergence behavior of the PCE when its coefficients are computed from different methods. Next to the benchmark full-grid quadrature rule, the PCE coefficients are additionally approximated by a sparse-grid Smolyak quadrature rule and by least squares. Sparse-grid methods as well as least squares give fundamentals for a rising number of more efficient alternatives. Kaintura et al. (2018) and Harenberg et al. (2019) give a short discussion.

We apply our analysis to the PCE of the model's linear solution but now consider a higher dimensional problem. The vector of unknown parameters expands to $\theta := \begin{pmatrix} \zeta & \eta & \rho & \beta & \delta & \gamma \end{pmatrix}$.[18] The assumed distributions for ζ, η and ρ remain as before in Figure 4.2 and the distributions of the additional unknown parameters are chosen as

$$\beta \sim 0.9 + 0.09 \cdot \text{Beta}(7,4), \ \delta \sim 0.01 + 0.01 \cdot \text{Beta}(3,3), \ \gamma \sim 1.5 + 1 \cdot \text{Beta}(5,4).$$

The probability densities for β, δ and γ are visualized in Figure 4.4.

We compute the truncated PCE (4.5.1) for each mapping $a_{ij} : \vartheta \mapsto a_{ij}(\vartheta)$ in the linear policy $A(\vartheta) = \big(a_{ij}(\vartheta)\big)_{\substack{i=1,\dots,6 \\ j=1,2}} \in \mathbb{R}^{6\times 2}$. The PCE coefficients are now determined either by i) a full-grid Gauss quadrature rule with $N+1$ nodes for each parameter (FGQ), ii) a sparse-grid Smolyak-Gauss quadrature rule with linear growth where the level is set such way that the one-dimensional quadrature rules include the nodes up to degree $N+1$ (SGQ), iii) least squares where the number of sample point is set either twice (LSMC1) or iv) three times as large as the number of unknown PCE coefficients (LSMC2). After construction of the truncated PCE by each of the four methods, we compute the PCE's L^2 error as in (4.5.2) from a draw of $M = 10^5$ iid

[17] The collocation points are combinations of the zeros of the Chebyshev polynomials in the approximation.

[18] These are all of the model's parameters except the standard deviation σ which does not affect the model's linear policy.

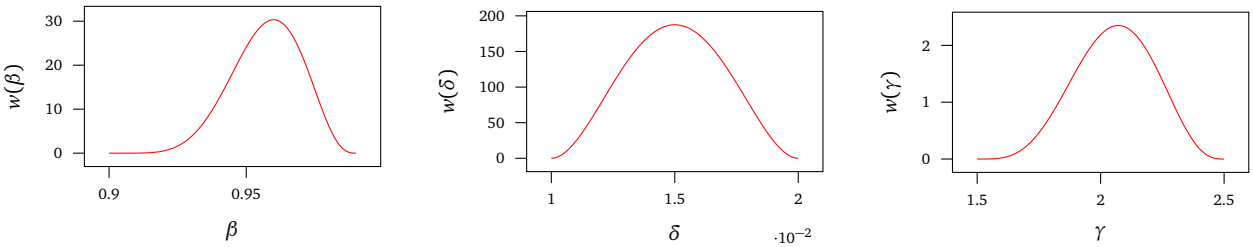

(a) Prior of β (b) Prior of δ (c) Prior of γ

Figure 4.4: Distributions of uncertain parameters

sample points from the parameter's distribution.

Figure 4.5 shows the convergence of the truncated (approximated) PCEs with approximated coefficients for increasing N. As expected, the PCE constructed from a full-grid quadrature rule, which should provide the most accurate determination of the coefficients, also shows the fastest convergence. It is followed by the PCE constructed from the sparse-grid Smolyak quadrature rule while the PCEs where the coefficients are computed by least squares perform worst. In fact, since inaccuracies in the coefficients of higher degree polynomials may have large impact on the L^2 error of the PCE,[19] the PCEs computed from least squares even show increasing errors for larger N. Yet, the necessary computations for the full-grid quadrature method also require by far the most time. Figure 4.4(k) shows that by $N = 5$ the construction and evaluation of the PCE already consumes more time than 100,000 repeated computations of the model solution. In comparison, the sparse-grid quadrature rule is already significantly less computationally costly while the least-squares methods are least expensive to compute and remain less time-consuming than repeated computations of the model solution up to $N = 10$.

Finally, Figure 4.6 provides a more convenient illustration of the different methods' efficiency and plots the PCEs' L^2 error versus the required computation time, both in $\log_{10}$-basis. According to this metric the full-grid quadrature method already performs worst and requires the most computation time to reach the same quality of approximation as the other methods. The most efficient method is the sparse-grid Smolyak quadrature rule. In the present case with six unknown parameters, it reaches an approximation with L^2 error of order of magnitude of -4 before the required time for the PCE's construction exceeds the time for 100,000 repeated computations of the model solution.

4.5.4 Monte Carlo experiments for empirical methods

Design: Our Monte Carlo study follows Ruge-Murcia (2007) and analyzes the performance of PCE when applied to different estimation methods. We set the vector of uncertain parameters to $\theta := (\beta, \rho, \sigma)$ and choose the following probability distributions with support $\Theta := [0.97; 0.999] \times [0.75; 0.995] \times [0.004; 0.012]$ for the unknown parameters:

$$\beta \sim 0.97 + 0.029 \cdot \text{Beta}(2,2),\ \rho \sim 0.75 + 0.245 \cdot \text{Beta}(2,2),\ \sigma \sim 0.004 + 0.008 \cdot U(0,1).$$

Figure 4.7 illustrates the uncertain parameters' probability densities and the remaining parameters are calibrated as summarized in Table 4.4.

[19] Note that the norm of the orthogonal polynomials, $\|q_\alpha\|_{L^2}$, is increasing in $|\alpha|$.

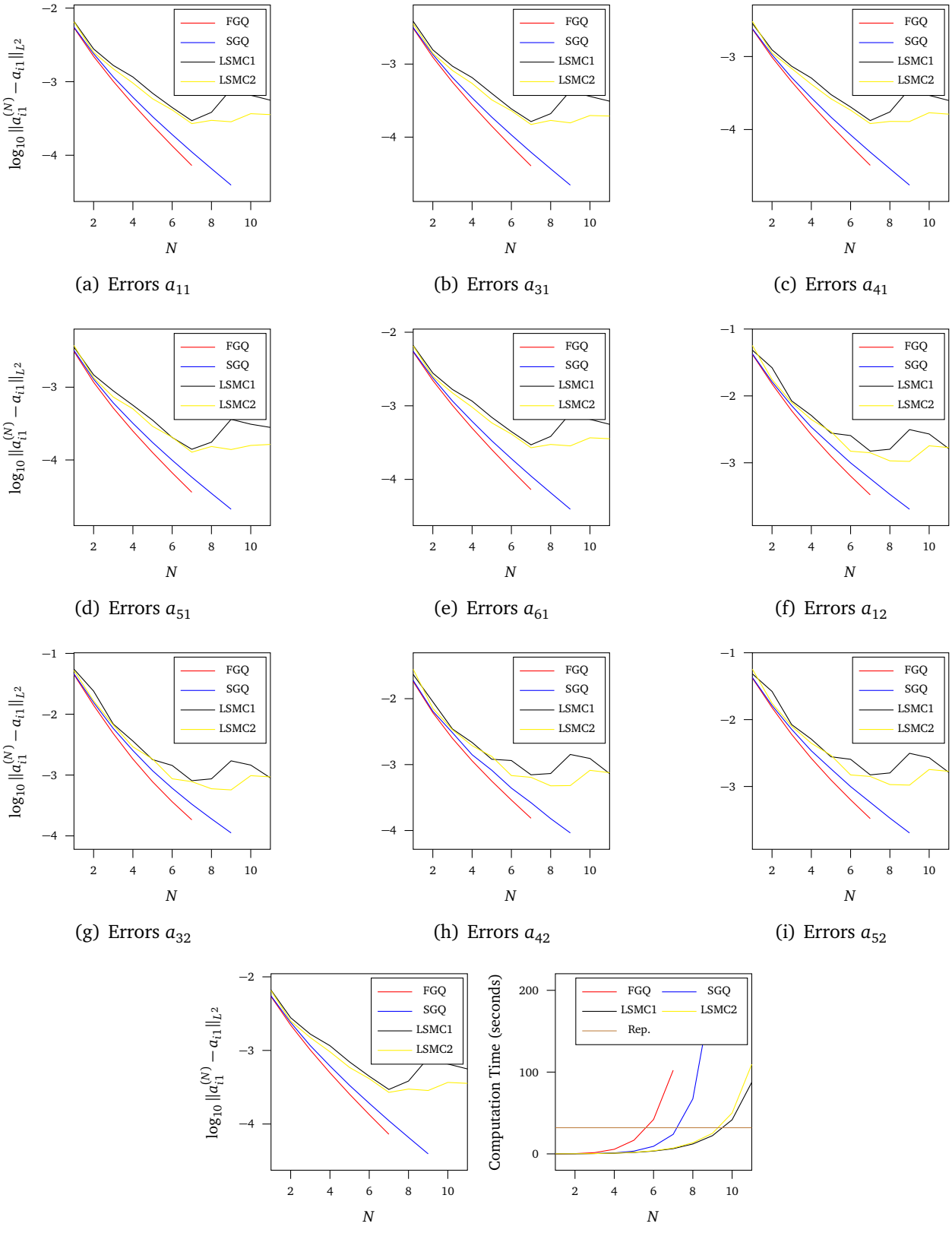

(a) Errors a_{11} (b) Errors a_{31} (c) Errors a_{41}

(d) Errors a_{51} (e) Errors a_{61} (f) Errors a_{12}

(g) Errors a_{32} (h) Errors a_{42} (i) Errors a_{52}

(j) Errors a_{62} (k) Computation time

Figure 4.5: L^2 Convergence of PCE with approximated coefficients and computation time on an Intel® Core™i7-7700 CPU @ 3.60GHz

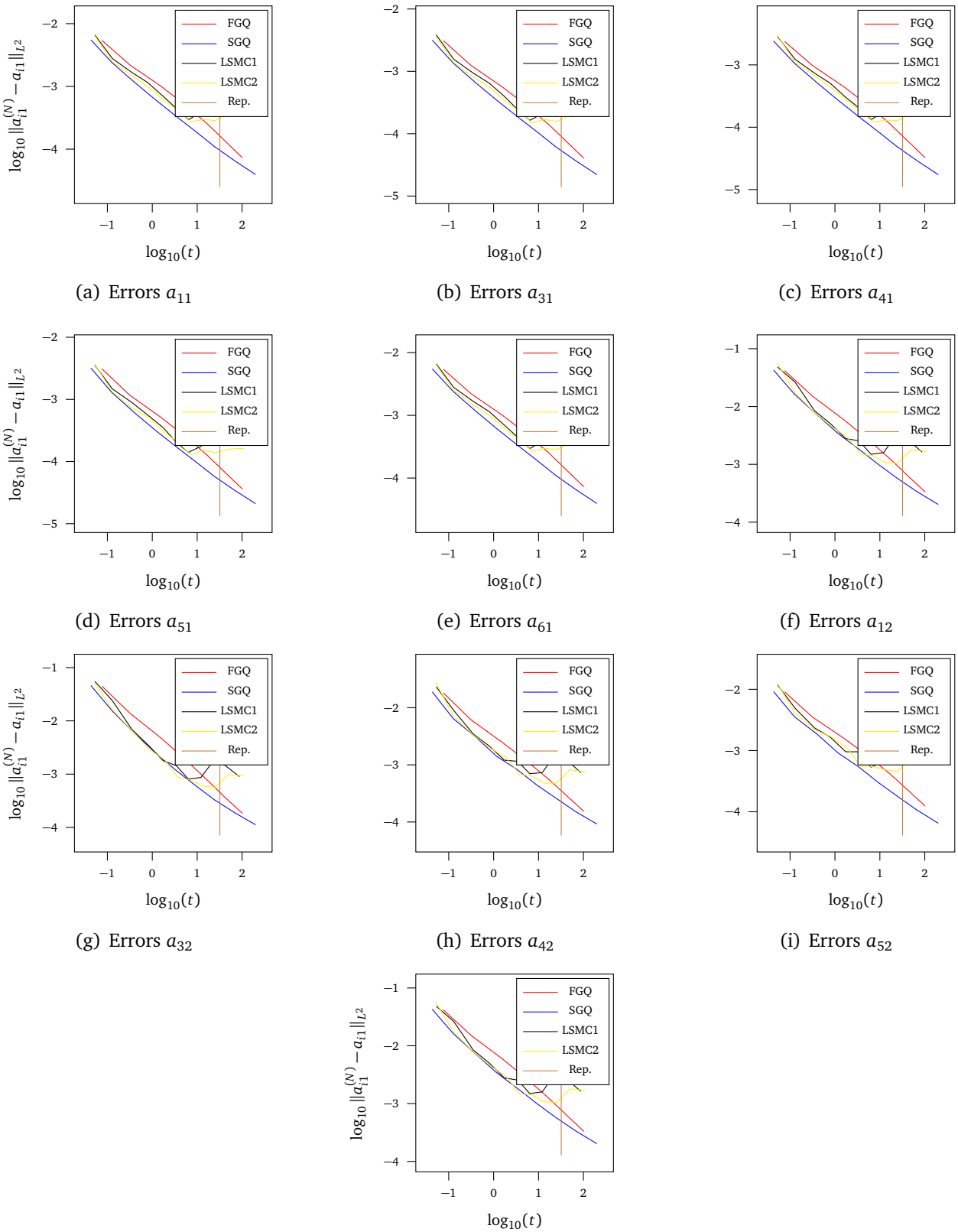

(a) Errors a_{11} (b) Errors a_{31} (c) Errors a_{41}

(d) Errors a_{51} (e) Errors a_{61} (f) Errors a_{12}

(g) Errors a_{32} (h) Errors a_{42} (i) Errors a_{52}

(j) Errors a_{62}

Figure 4.6: L^2 Convergence of PCE with approximated coefficients and computation time on an Intel® Core™i7-7700 CPU @ 3.60GHz

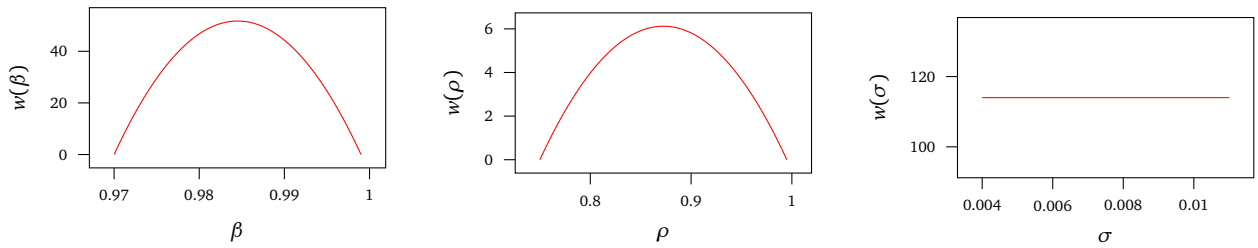

(a) Prior of β (b) Prior of ρ (c) Prior of σ

Figure 4.7: Distributions of uncertain parameters

Table 4.4: Calibration II

Fixed Parameter	Description	Value
ζ	Capital share	0.37
δ	Rate of capital depreciation	0.014
N	Steady-state labor supply	0.3
η	Risk aversion	2
Uncertain Parameters	**Description**	**Distribution**
β	Discount factor	$\beta \sim 0.97 + 0.029 \cdot \text{Beta}(2,2)$
ρ	Persistence	$\rho \sim 0.75 + 0.245 \cdot \text{Beta}(2,2)$
σ	Standard deviation	$\sigma \sim 0.004 + 0.008 \cdot U(0,1)$

Matching moments: To estimate the parameters by matching moments, we choose the following 5 targets: i) the variance of output and of working hours, ii) the autocovariance (lag 1) of output and of working hours, and iii) the covariance between output and working hours. We draw a sample $\vartheta^{(i)}, i = 1,\dots,M$, of size $M = 1,000$ from the distribution of the unknown parameters. In a first step, we compute the linear approximation of the policy function and the second moments for each $\vartheta^{(i)}$ in the sample. Subsequently, we feed the computed second moments as targets to an optimizer and (point) estimate the unknown parameters by the method of matching moments. When minimizing the objective function, we distinguish the following three cases in order to evaluate the model's second moments for different parameter values: i) repeatedly solving the model and computing the second moments (benchmark), ii) constructing the PCE of the linear approximation of the policy function which we then evaluate and use to compute the variables' second moments or iii) constructing the PCE of the model's second moments which we then evaluate. We compute the second moments either from analytic formulae for the linear solution (GMM) or from a simulation with $T = 10,000$ periods (SMM). We adapt the truncation degree and quadrature level manually to achieve a sufficient accuracy to demonstrate the capabilities.[20] After obtaining the parameters' estimate $\hat{\vartheta}^{(i)}$, we define the PCE error by the deviation between the realized point estimate $\hat{\vartheta}^{(i)}_{\text{PCE}}$ from a PCE based method and the estimate $\hat{\vartheta}^{(i)}_{\text{BM}}$ obtained from the benchmark method, i.e.

$$\epsilon^{(i)}_j = 100 \frac{\left|\hat{\vartheta}^{(i)}_{j,\text{PCE}} - \hat{\vartheta}^{(i)}_{j,\text{BM}}\right|}{\vartheta_{j,\max} - \vartheta_{j,\min}}, \; j \in \{\beta,\rho,\sigma\}, \; i = 1,...,M,$$

where j indicates the estimator of the particular parameter and $\vartheta_{j,\max}$ and $\vartheta_{j,\min}$ denote the upper and lower bound of θ_j's prior support.

[20] We discuss heuristics for the choice of the truncation level below.

Table 4.5: Monte Carlo results - GMM

Benchmark (repeated solution)			
	Total average		
Time:	00:01.25		
PCE policy function			
	Total average	PCE	Estimation average
Time:	00:00.5	00:00.05	00:00.45
j	β	ρ	σ
$\bar{\epsilon}_j$	0.04	0.01	0.02
$\epsilon_{j,.05}$	0.00	0.00	0.00
$\epsilon_{j,.5}$	0.03	0.01	0.01
$\epsilon_{j,.95}$	0.11	0.03	0.06
PCE second moments			
	Total average	PCE	Estimation average
Time:	00:03.44	00:03.11	00:00.33
j	β	ρ	σ
$\bar{\epsilon}_j$	0.16	0.02	0.02
$\epsilon_{j,.05}$	0.02	0.00	0.00
$\epsilon_{j,.5}$	0.13	0.02	0.01
$\epsilon_{j,.95}$	0.43	0.06	0.09

Notes: Observable moments: variance of output, variance of hours, covariance between output and hours, autocovariance of output (lag 1), autocovariance of hours (lag 1). $\bar{\epsilon}_j$: mean error, $\epsilon_{j,.05}$: 5 percentile of error, $\epsilon_{j,.5}$: median of error, $\epsilon_{j,.95}$: 95 percentile of error. Errors of PCE based methods are expressed as deviations from the benchmark method of repeatedly solving the policy function in percent of the range of the parameter's distribution. Time: mm:ss.f on an Intel® Core™i7-7700 CPU @ 3.60GHz. The truncation degree and quadrature level of the expanded policy function is 9 and of the second moments 19.

Table 4.6: Monte Carlo results - SMM

Benchmark (repeated solution)			
	Total average		
Time:	01:12.82		
PCE policy function			
	Total average	PCE	Estimation average
Time:	00:34.67	00:00.03	00:34.63
j	β	ρ	σ
$\bar{\epsilon}_j$	0.10	0.02	0.03
$\epsilon_{j,.05}$	0.01	0.00	0.00
$\epsilon_{j,.5}$	0.08	0.01	0.01
$\epsilon_{j,.95}$	0.25	0.04	0.16
PCE second moments			
	Total average	PCE	Estimation average
Time:	00:58.03	00:57.73	00:00.31
j	β	ρ	σ
$\bar{\epsilon}_j$	1.01	0.13	0.10
$\epsilon_{j,.05}$	0.10	0.01	0.01
$\epsilon_{j,.5}$	0.78	0.09	0.06
$\epsilon_{j,.95}$	2.62	0.35	0.30

Notes: Observable moments: variance of output, variance of hours, covariance between output and hours, autocovariance of output (lag 1), autocovariance of hours (lag 1). $\bar{\epsilon}_j$: mean error, $\epsilon_{j,.05}$: 5 percentile of error, $\epsilon_{j,.5}$: median of error, $\epsilon_{j,.95}$: 95 percentile of error. Errors of PCE based methods are expressed as deviations from the benchmark method of repeatedly solving the policy function in percent of the range of the parameter's distribution. Time: mm:ss.f on an Intel® Core™i7-7700 CPU @ 3.60GHz. The truncation degree and quadratur level of the expanded policy function is 7 and of the second moments 13.

Table 4.5 presents the results for GMM. We provide the computation time, the mean, the median, the 5 percentile and the 95 percentile of the PCE error ϵ_j from $M = 1,000$ estimations. We find that the policy function's PCE provides a remarkably well approximation which results in deviations from the benchmark mostly smaller than one permille in comparison to the range of the parameter's distribution. Estimation errors rise if the model's second moments are directly approximated by PCE. However, the average relative errors remain below two permille for all parameters and is almost always less than half a percent, again relative to the parameter's range. Using the PCE of the policy function reduces the computation time on average by 60 percent while the PCE of the second moments is more time consuming than the benchmark. Nevertheless, the pure estimation procedure of the second moments' PCE is on average more than 25 percent faster than the estimation procedure of policy function's PCE.

Since analytic formulae for the model's moments are only available for the linear solution, GMM can only be employed for a linear approximation where computation time is rarely a limiting factor. If the model demands non-linear solutions, one has to resort to simulations in order to derive the model's moments. However, the computation of non-linear solutions and the simulation of model outcomes increase the computational effort significantly. Working with the PCE of the policy function reduces the former burden while working with the PCE of the second moments helps to reduce both burdens. The results for our Monte-Carlo experiment with SMM are summarized in Table 4.6.

We find again that the policy function's PCE provides a remarkably well approximation

which results in errors mostly smaller than 2.5 permille in comparison to the range of the parameter's distribution. Similar to GMM, errors rise if the model's second moments are directly approximated by PCE. However, the average relative errors remain around or below one percent for all parameters and are almost always less than 2.5 percent. Using the PCE of the policy function reduces the computation time on average by 50 percent while the PCE of the second moments reduces them only by 20 percent. However, the pure estimation procedure of the second moments' PCE is on average more than 99 percent faster than the estimation procedure of policy function's PCE. This illustrates the efficiency of PCE once the expansion of the QoI is calculated.

Likelihood-based estimation: We proceed to analyze the performance of PCE in MLE and in BE. More precisely, we now draw a sample of size $M = 500$ from the distribution of the unknown parameters. We approximate linearly the policy function and simulate a time-series of output Y_t for $T = 200$ periods for each $\vartheta^{(i)}$ in the sample.[21] We treat the simulated time-series as observations from which we either (point) estimate the parameters by MLE or conduct BE.

In the case of MLE we distinguish the following three methods to evaluate the observations' likelihood for different parameter values: i) repeatedly solving the model and computing the likelihood (benchmark), ii) constructing the PCE of the linear approximation of the policy function which we then evaluate and use to compute the likelihood or iii) constructing the PCE of the likelihood which we then evaluate. In order to avoid problems with weak identification and in order to focus on the quality of PCE in the estimation procedure, MLE is unusually applied to data in levels instead of the relative deviation from steady-state.

For BE the priors remain the same as in Table 4.4. Moreover, we again consider three methods to evaluate the posterior where the first two are analogous to i) and ii) above while iii) now involves constructing the PCE of the posterior's kernel. For each of the three methods we derive the posterior's mean as well as several quantiles of the posterior distribution from a standard random walk Metropolis-Hasting (RWMH) algorithm with 100,000 draws from the posterior kernel.[22] We measure the accuracy of the PCE based methods for each statistic of the posterior, say x, by computing the deviation between the statistic $\hat{x}^{(i)}_{j,\text{PCE}}$ obtained from the PCE based method and the statistic $\hat{x}^{(i)}_{j,\text{BM}}$ from the benchmark method by

$$\epsilon^{(i)}_{j,\text{PCE}}(x) = 100 \frac{\left|\hat{x}^{(i)}_{j,\text{PCE}} - \hat{x}^{(i)}_{j,\text{BM}}\right|}{\vartheta_{j,\max} - \vartheta_{j,\min}}.$$

Again, we adapt the truncation degree and quadrature level manually to achieve a sufficient accuracy.

[21] More precisely, we generate a sample of size $T = 300$ and burn the first 100 observations.
[22] For the results we burn the first 50,000 draws.

Table 4.7: Monte Carlo results - Maximum-likelihood estimation

Benchmark (repeated solution)			
	Total average		
Time:	00:20.60		
PCE policy function			
	Total average	PCE	Estimation average
Time:	00:18.79	00:00.20	00:18.59
j	β	ρ	σ
$\bar{\epsilon}_j$	0.07	0.08	0.01
$\epsilon_{j,.05}$	0.00	0.00	0.00
$\epsilon_{j,.5}$	0.00	0.00	0.00
$\epsilon_{j,.95}$	0.00	0.01	0.02
PCE likelihood function			
	Total average	PCE	Estimation average
Time:	00:10.81	00:10.36	00:00.44
j	β	ρ	σ
$\bar{\epsilon}_j$	0.08	0.40	0.05
$\epsilon_{j,.05}$	0.00	0.00	0.00
$\epsilon_{j,.5}$	0.00	0.08	0.01
$\epsilon_{j,.95}$	0.03	0.75	0.09

Notes: Observable: Output Y_t. $\bar{\epsilon}_j$: mean error, $\epsilon_{j,.05}$: 5 percentile of error, $\epsilon_{j,.5}$: median of error, $\epsilon_{j,.95}$: 95 percentile of error. Errors of PCE based methods are expressed as deviations from the benchmark method of repeatedly solving the policy function in percent of the range of the parameter's distribution. Time: mm:ss.f on an Intel® Core™i7-7700 CPU @ 3.60GHz. The truncation degree and quadrature level of the expanded policy function is 9 and of the likelihood-function 13.

Table 4.7 displays the results from MLE. First, deviations between the estimates from the method based on the policy function's PCE, the likelihood function's PCE, and from the benchmark version remain remarkably small. The average error concerning the policy function's PCE estimation is smaller than one permille in comparison to the benchmark and relative to the range of the parameter. Furthermore, as the 95 percentile is smaller than the average, the error is mostly smaller than the average. The same holds for the estimation with the likelihood function's PCE. The average error is less than a half percent and the median is less than one permille. Using the PCE of the policy function does not reduce the computation time significantly, because the evaluation of the likelihood-function is the time consuming part. For this reason, using the PCE of the likelihood-function is much more efficient. The total procedure is about 50 percent faster than the benchmark on average and the pure maximization procedure takes less than half a second on average.

Finally, Table 4.8 summarizes the results from the PCE based methods—approximation of the policy function or of the kernel of the posterior—in BE. First, the errors between the two approximations are virtually the same. The average errors of the means and the medians are less than or equal to one fourth of a percent. While deviations slightly increase for estimates of the posterior's lower and upper quantiles, they remain almost always less then 1.25 percent. Recognizing the fact that errors may be partly caused by the RWMH algorithm itself, the deviations between the methods are negligible. Using the PCE of the policy function does not reduce the computation time significantly, because the evaluation of the likelihood-function is likewise the time consuming part. For this reason, the PCE of the likelihood-function is much

more efficient and nearly 99 percent faster than the benchmark.[23]

Table 4.8: Monte Carlo results - Bayesian estimation

Benchmark (repeated solution)									
Time:		Total average 08:36.11							
PCE policy function									
Time:		Total average 07:56.38			PCE 00:00.05		Estimation average 07:56.33		
j	x:	Mean:	Quantile: 5%	10%	25%	50%	75%	90%	95%
β	$\bar{\epsilon}_j(x)$	0.05	0.12	0.08	0.05	0.04	0.05	0.07	0.10
	$\epsilon_j(x)_{.05}$	0.00	0.01	0.01	0.00	0.00	0.00	0.00	0.01
	$\epsilon_j(x)_{.5}$	0.04	0.09	0.05	0.03	0.03	0.04	0.05	0.06
	$\epsilon_j(x)_{.95}$	0.15	0.33	0.23	0.15	0.15	0.14	0.22	0.33
ρ	$\bar{\epsilon}_j(x)$	0.23	0.32	0.28	0.25	0.25	0.30	0.37	0.45
	$\epsilon_j(x)_{.05}$	0.02	0.02	0.02	0.02	0.02	0.02	0.03	0.03
	$\epsilon_j(x)_{.5}$	0.19	0.24	0.24	0.20	0.21	0.25	0.30	0.35
	$\epsilon_j(x)_{.95}$	0.59	0.87	0.71	0.64	0.63	0.77	0.99	1.22
σ	$\bar{\epsilon}_j(x)$	0.09	0.11	0.10	0.09	0.09	0.11	0.15	0.20
	$\epsilon_j(x)_{.05}$	0.01	0.01	0.01	0.01	0.01	0.01	0.01	0.01
	$\epsilon_j(x)_{.5}$	0.07	0.09	0.08	0.07	0.07	0.09	0.12	0.15
	$\epsilon_j(x)_{.95}$	0.24	0.24	0.29	0.25	0.26	0.28	0.41	0.59
PCE posterior-kernel									
Time:		Total average 00:16.82			PCE 00:11.00		Estimation average 00:05.82		
j	x:	Mean:	Quantile: 5%	10%	25%	50%	75%	90%	95%
β	$\bar{\epsilon}_j(x)$	0.05	0.13	0.09	0.05	0.04	0.05	0.07	0.09
	$\epsilon_j(x)_{.05}$	0.00	0.01	0.01	0.00	0.00	0.00	0.00	0.00
	$\epsilon_j(x)_{.5}$	0.04	0.08	0.06	0.03	0.03	0.03	0.04	0.06
	$\epsilon_j(x)_{.95}$	0.16	0.40	0.25	0.15	0.13	0.14	0.19	0.30
ρ	$\bar{\epsilon}_j(x)$	0.21	0.32	0.27	0.24	0.24	0.27	0.36	0.44
	$\epsilon_j(x)_{.05}$	0.02	0.02	0.02	0.01	0.02	0.02	0.02	0.03
	$\epsilon_j(x)_{.5}$	0.16	0.25	0.21	0.20	0.19	0.20	0.27	0.33
	$\epsilon_j(x)_{.95}$	0.59	0.86	0.69	0.59	0.60	0.72	1.01	1.19
σ	$\bar{\epsilon}_j(x)$	0.09	0.12	0.11	0.09	0.09	0.11	0.15	0.19
	$\epsilon_j(x)_{.05}$	0.01	0.01	0.01	0.01	0.01	0.01	0.01	0.01
	$\epsilon_j(x)_{.5}$	0.07	0.09	0.08	0.07	0.07	0.09	0.12	0.13
	$\epsilon_j(x)_{.95}$	0.24	0.32	0.30	0.25	0.24	0.29	0.42	0.55

Notes: Observable: Output Y_t. $\bar{\epsilon}_j$: mean error, $\epsilon_{j,.05}$: 5 percentile of error, $\epsilon_{j,.5}$: median of error, $\epsilon_{j,.95}$: 95 percentile of error. Errors of PCE based methods are expressed as deviations from the benchmark method of repeatedly solving the policy function in percent of the range of the parameter's distribution. Time: mm:ss.f on an Intel® Core™i7-7700 CPU @ 3.60GHz. The truncation degree and quadratur level of the expanded policy function is 9 and of the second moments 13.

[23] It must be mentioned that a higher number of parameters leads to a decrease in efficiency.

Discussion: Our study of PCE in estimation of a standard RBC model shows that the PCE based methods can accurately reproduce the same results as the benchmark method of repeatedly solving the model. Gains in efficiency are larger than 50 percent for matching moments if the PCE of the policy function is used and for MLE if the PCE of the likelihood-function is used. Additionally, we show the gains in efficiency are almost 99 percent for BE with the chosen numbers of parameters, truncation degree, and quadrature level if the PCE of the posterior's kernel is used.

In our specification of the prior distributions we shape and shift the distributions in order to achieve compactness of the support. This procedure is unconventional in BE of DSGE models but helps for PCE. First and foremost, compactness of the support helps to create a setting where the mapping from parameters to the model outcome is square-integrable. Second, it is indispensable for the construction of the PCE coefficients that the model outcome is well-defined and can be computed in a numerically stable way at all nodes of the quadrature rules.[24]

In non-Bayesian approaches, the application of PCE demands the otherwise not necessary specification of prior distributions. Moreover, L^2 convergence of the series expansion is achieved w.r.t. this prior distribution of the parameters. Estimation fails if the true parameter value is at odds to the choice of priors.

Similarly, Lu et al. (2015) show that the use of PCE for BE may be inaccurate in two cases. First, the QoI is represented poorly by a low-order polynomial. Second, the posterior mass is in other regions than the prior mass. To solve these problems, they suggest an adaptive increasing polynomial order by verifying the accuracy at the next evaluation point. As our manual adaption is usually not feasible as it requires the benchmark results, this is also a practical method for determining the truncation level in general. In addition, a small magnitude of the Nth Fourier coefficient is an indicator for a sufficient high truncation level.

Finally, the success of PCE is determined by the ratio of the number of model evaluations necessary in order to compute the coefficients and the number of model evaluations in the estimation method. Hence, PCE works best in cases with a small number of unknown parameters where estimation demands many model evaluations, but PCE loses efficiency in higher dimensional problems.

4.6 Conclusion

The present article discusses the suitability of PCE for computational models in economics. For this purpose, we first provide the theoretical framework for PCE, review the basic theory, and give an overview of common distributions and corresponding orthogonal polynomials. We show how to evaluate statistical properties of the QoI from the PCE and how to use the expansion as a point-wise approximation for the QoI. Further, surrogates for a linearized policy function, for a policy function based on projection methods, and for gradients of the model's QoI are presented.

Second, we analyze PCE when applied to a standard RBC model and provide practical insights. We study convergence behavior for various QoIs and compare the most common methods to compute the PCE coefficients for a lower dimensional and a higher dimensional problem. For the higher dimensional problem with six unknown parameters, sparse-grid quadrature is the most efficient method compared to least squares and a full-grid quadrature. Monte Carlo experiments for different empirical methods show that the PCE based methods can accurately reproduce the same results as the benchmark method of repeatedly solving the model. Gains in efficiency are large, especially for Bayesian inference.

Our discussion addresses potential drawbacks of the method. First, the efficiency of PCE

[24] For example, larger values of the capital share quickly result in numerical problems for the computation of the linear approximation of policy function.

critically suffers from the curse of dimensions in problems with a large number of unknown parameters. Further, poorly chosen priors may affect the accuracy of the estimates.

Despite of these potential drawbacks, PCE is a powerful tool for a broad set of applications. We hope that the article can encourage applications of PCE in economics, especially for parameter inference in complex models where standard techniques are infeasible. Another possible use is real-time analysis of high-frequency data.

Acknowledgment

We are grateful to our academic advisor Prof. Alfred Maußner for his various insightful and detailed remarks on different versions of this article. We thank Michel Bauer for initial ideas and continuing discussions.

Bibliography

BLANCHARD, O. J. AND C. M. KAHN (1980): "The Solution of Linear Difference Models under Rational Expectations," *Econometrica*, 48, 1305–1311.

CAMERON, R. H. AND W. T. MARTIN (1947): "The Orthogonal Development of Non-Linear Functionals in Series of Fourier-Hermite Functionals," *Annals of Mathematics*, 48, 385–392.

GHANEM, R. G. AND P. D. SPANOS (1991): "Spectral Stochastic Finite-Element Formulation for Reliability Analysis," *Journal of Engineering Mechanics*, 117, 2351–2372.

HARENBERG, D., S. MARELLI, B. SUDRET, AND V. WINSCHEL (2019): "Uncertainty Quantification and Global Sensitivity Analysis for Economic Models," *Quantitative Economics*, 10, 1–41.

HEER, B. AND A. MAUSSNER (2009): *Dynamic General Equilibrium Modeling: Computational Methods and Applications*, Berlin / Heidelberg, Germany: Springer.

ISKREV, N. (2010): "Local Identification in DSGE Models," *Journal of Monetary Economics*, 57, 189–202.

JACKSON, D. (1941): *Fourier Series and Orthogonal Polynomials*, Mathematical Association of America.

JUDD, K. L. (1992): "Projection Methods for Solving Aggregate Growth Models," *Journal of Economic Theory*, 58, 410–452.

——— (1996): "Chapter 12 - Approximation, Perturbation, and Projection Methods in Economic Analysis," in *Handbook of Computational Economics*, ed. by H. M. Amman, D. A. Kendrick, and J. Rust, Elsevier, vol. 1, 509–585.

KAINTURA, A., T. DHAENE, AND D. SPINA (2018): "Review of Polynomial Chaos-Based Methods for Uncertainty Quantification in Modern Integrated Circuits," *Electronics*, 7, 30.

KLEIN, P. (2000): "Using the Generalized Schur Form to Solve a Multivariate Linear Rational Expectations Model," *Journal of Economic Dynamics and Control*, 24, 1405–1423.

LU, F., M. MORZFELD, X. TU, AND A. J. CHORIN (2015): "Limitations of Polynomial Chaos Expansions in the Bayesian Solution of Inverse Problems," *Journal of Computational Physics*, 282, 138–147.

MARZOUK, Y. M., H. N. NAJM, AND L. A. RAHN (2007): "Stochastic Spectral Methods for Efficient Bayesian Solution of Inverse Problems," *Journal of Computational Physics*, 224, 560–586.

MCGRATTAN, E. R. (1999): "Application of Weighted Residual Methods to Dynamic Economic Models," in *Computational Methods for the Study of Dynamic Economies*, ed. by R. Marimon and A. Scott, Oxford and New York: Oxford University Press, 114–142.

RIESZ, M. (1924): "Sur le Problème des Moments et le Théorème de Parseval Correspondant," *Scandinavian Actuarial Journal*, 1924, 54–74.

RUGE-MURCIA, F. J. (2007): "Methods to Estimate Dynamic Stochastic General Equilibrium Models," *Journal of Economic Dynamics and Control*, 31, 2599–2636.

SIMS, C. A. (2002): "Solving Linear Rational Expectations Models," *Comput. Econ.*, 20, 1–20.

SZEGŐ, G. (1939): *Orthogonal Polynomials*, American Mathematical Society.

WIENER, N. (1938): "The Homogeneous Chaos," *American Journal of Mathematics*, 60, 897–936.

XIU, D. AND G. E. KARNIADAKIS (2002): "The Wiener–Askey Polynomial Chaos for Stochastic Differential Equations," *SIAM Journal on Scientific Computing*, 24, 619–644.

Appendix

4.A Orthogonal polynomials

We give a short overview for the families of orthogonal polynomials summarized in Table 4.2. More details, in particular regarding their completeness in the respective Hilbert spaces L^2 of square integrable functions, can be found in Szegő (1939).

4.A.1 Hermite polynomials

Hermite polynomials are defined by the recurrence relation

$$H_0(x) = 1,\ H_1(x) = 2x,\ H_{n+1}(x) = 2xP_n(x) - 2nP_{n-1}(x), n \geq 2$$

and form a complete orthogonal system on $L^2(\mathbb{R}, \mathscr{B}(\mathbb{R}), \tilde{w}(x)\,\mathrm{d}x)$ with weighting function

$$\tilde{w}(x) := e^{-x^2}.$$

More specifically,

$$\int_{\mathbb{R}} H_n(x)H_m(x)\tilde{w}(x)\,\mathrm{d}x = 2^n(n!)\sqrt{\pi}\delta_{n,m}$$

The probability density function of a normal distributed random variable $\theta \sim \mathrm{N}(\mu, \sigma^2)$ with mean μ and variance σ^2 is given by

$$f_\theta(\vartheta) = \frac{1}{\sqrt{2\pi}\sigma} e^{-\frac{(\vartheta-\mu)^2}{2\sigma^2}}.$$

Fixing the transformation between the germ and θ in this case to

$$\psi(s) := \mu + \sqrt{2}\sigma s$$

so that the germ ξ is defined by

$$\xi := \psi^{-1}(\theta) = \frac{\theta - \mu}{\sqrt{2}\sigma}$$

implies that ξ has probability density function

$$w(s) = f_\theta(\psi(s))\psi'(s) = \frac{1}{\sqrt{\pi}} e^{-s^2} = \frac{1}{\sqrt{\pi}}\tilde{w}(s).$$

Since w differs from $\tilde{w}$ only by a constant factor, it follows that

$$L^2(\mathbb{R}, \mathscr{B}(\mathbb{R}), \mathrm{d}P_\xi) = L^2(\mathbb{R}, \mathscr{B}(\mathbb{R}), w(s)\,\mathrm{d}s) = L^2(\mathbb{R}, \mathscr{B}(\mathbb{R}), \tilde{w}(s)\,\mathrm{d}s),$$

and that Hermite polynomials also form a complete orthogonal system in $L^2(\mathbb{R}, \mathscr{B}(\mathbb{R}), \mathrm{d}P_\xi)$ with

$$\int_{\mathbb{R}} H_n(s)H_m(s)\,\mathrm{d}P_\xi(s) = \int_{\mathbb{R}} H_n(s)H_m(s)w(s)\,\mathrm{d}s = \frac{1}{\sqrt{\pi}}\int_{\mathbb{R}} H_n(s)H_m(s)\tilde{w}(s)\,\mathrm{d}s = 2^n(n!)\delta_{n,m}.$$

Moreover, given the nodes s_j and weights $\tilde{\omega}_j$ from the common Gauss-Hermite-quadrature rule for weighting function $\tilde{w}$, the Gauss-quadrature rule in terms of weighting function w has the same nodes while the weights are scaled by $\omega_j = \frac{\tilde{\omega}_j}{\sqrt{\pi}}$.

4.A.2 Legendre polynomials

Legendre polynomials are defined by the recurrence relation

$$L_0(x) = 1, \quad L_1(x) = 2x, \quad (n+1)L_{n+1}(x) = (2n+1)xL_n(x) - nL_{n-1}(x),\ n \geq 2$$

and form a complete orthogonal system in $L^2([-1,1], \mathscr{B}([-1,1]), \mathrm{d}x)$, i.e.

$$\int_{-1}^{1} L_n(x)L_m(x)\,\mathrm{d}x = \frac{2}{2n+1}\delta_{n,m}.$$

The probability density function of an uniformly distributed random variable $\theta \sim \mathrm{U}[0,1]$ over $[0,1]$ is given by

$$f_\theta(\vartheta) = \mathbb{1}_{[0,1]}(\vartheta) := \begin{cases} 1, & \text{if } \vartheta \in [0,1] \\ 0, & \text{if } \vartheta \in \mathbb{R} \setminus [0,1] \end{cases}$$

Fixing the transformation between the germ and θ in this case to

$$\psi(s) := \frac{s+1}{2}$$

so that the germ ξ is defined by

$$\xi := \psi^{-1}(\theta) = 2\theta - 1$$

implies that ξ has probability density function

$$w(s) = f_\theta(\psi(s))\psi'(s) = \frac{1}{2}\mathbb{1}_{[-1,1]}(s).$$

Hence, it follows that

$$L^2(\mathbb{R}, \mathscr{B}(\mathbb{R}), \mathrm{d}P_\xi) = L^2(\mathbb{R}, \mathscr{B}(\mathbb{R}), w(s)\,\mathrm{d}s) \simeq L^2([-1,1], \mathscr{B}([-1,1]), \mathrm{d}s),$$

and consequently the Legendre polynomials also form a complete orthogonal system in $L^2(\mathbb{R}, \mathscr{B}(\mathbb{R}), \mathrm{d}P_\xi)$ with

$$\int_{\mathbb{R}} L_n(s)L_m(s)\,\mathrm{d}P_\xi(s) = \int_{\mathbb{R}} L_n(s)L_m(s)w(s)\,\mathrm{d}s = \frac{1}{2}\int_{-1}^{1} L_n(s)L_m(s)\,\mathrm{d}s = \frac{1}{2n+1}\delta_{n,m}.$$

Moreover, given the nodes s_j and weights $\tilde{\omega}_j$ from the common Gauss-Legendre quadrature rule for weighting function $\tilde{w}$, the Gauss-quadrature rule in terms of weighting function w has the same nodes while the weights are scaled by $\omega_j = \frac{\tilde{\omega}_j}{2}$.

4.A.3 Jacobi polynomials

Jacobi polynomials are defined by the recurrence relation

$$J_0^{(\alpha,\beta)}(x) = 1,$$
$$J_1^{(\alpha,\beta)}(x) = \frac{1}{2}(\alpha - \beta + (\alpha + \beta + 2)x),$$
$$a_{1,n}J_{n+1}^{(\alpha,\beta)}(x) = (a_{2,n} + a_{3,n}x)J_n^{(\alpha,\beta)}(x) - a_{4,n}J_{n-1}^{(\alpha,\beta)}(x), n \geq 2$$

where

$$a_{1,n} = 2(n+1)(n+\alpha+\beta+1)(2n+\alpha+\beta),$$
$$a_{2,n} = (2n+\alpha+\beta+1)(\alpha^2-\beta^2),$$
$$a_{3,n} = (2n+\alpha+\beta)(2n+\alpha+\beta+1)(2n+\alpha+\beta+2),$$
$$a_{4,n} = 2(n+\alpha)(n+\beta)(2n+\alpha+\beta+2).$$

They form a complete orthogonal system on $L^2([-1,1], \mathscr{B}([-1,1]), \tilde{w}(x)\,\mathrm{d}x)$ with weighting function

$$\tilde{w}(x;\alpha,\beta) := (1-x)^\alpha(1+x)^\beta.$$

More specifically,

$$\int_{-1}^{1} J_n^{(\alpha,\beta)}(x)J_m^{(\alpha,\beta)}(x)\tilde{w}(x;\alpha,\beta)\,\mathrm{d}x = \frac{2^{\alpha+\beta+1}}{2n+\alpha+\beta+1}\frac{\Gamma(n+\alpha+1)\Gamma(n+\beta+1)}{\Gamma(n+\alpha+\beta+1)n!}\delta_{nm}.$$

The probability density function of a Beta-distributed random variable $\theta \sim \mathrm{Beta}(\alpha,\beta)$ with shape parameters α and β is given by

$$f_\theta(\vartheta;\alpha,\beta) = \frac{1}{B(\alpha,\beta)}\vartheta^{\alpha-1}(1-\vartheta)^{\beta-1}\mathbb{1}_{[0,1]}(\vartheta).$$[25]

Fixing the transformation between the germ and θ in this case to

$$\psi(s) := \frac{s+1}{2}$$

so that the germ ξ is defined by

$$\xi := \psi^{-1}(\theta) = 2\theta - 1$$

implies that ξ has probability density function

$$w(s;\alpha,\beta) = f_\theta(\psi(s);\alpha,\beta)\psi'(s) = \frac{1}{B(\alpha,\beta)}\left(\frac{s+1}{2}\right)^{\alpha-1}\left(1-\frac{s+1}{2}\right)^{\beta-1}\frac{1}{2}\mathbb{1}_{[-1,1]}(s)$$

[25] We denote by $B(x,y)$ the beta function.

$$= \frac{2^{1-\alpha-\beta}}{B(\alpha,\beta)}(s+1)^{\alpha-1}(1-s)^{\beta-1}\mathbb{1}_{[-1,1]}(s) = \frac{2^{1-\alpha-\beta}}{B(\alpha,\beta)}\tilde{w}(s;\beta-1,\alpha-1)\mathbb{1}_{[-1,1]}(s).$$

Since $w(s;\alpha,\beta)$ differs from $\tilde{w}(s;\beta-1,\alpha-1)$ only by a constant factor, it follows that

$$L^2(\mathbb{R},\mathscr{B}(\mathbb{R}),\mathrm{d}P_\xi) = L^2(\mathbb{R},\mathscr{B}(\mathbb{R}),w(s;\alpha,\beta)\,\mathrm{d}s) \simeq$$
$$\simeq L^2([-1,1],\mathscr{B}([-1,1]),\tilde{w}(s;\beta-1,\alpha-1)\,\mathrm{d}s),$$

and that the Jacobi polynomials $\{J_n^{(\beta-1,\alpha-1)}\}_{n\in\mathbb{N}_0}$ also form a complete orthogonal system in $L^2(\mathbb{R},\mathscr{B}(\mathbb{R}),\mathrm{d}P_\xi)$ with

$$\int_{\mathbb{R}} J_n^{(\beta-1,\alpha-1)}(s)J_m^{(\beta-1,\alpha-1)}(s)\,\mathrm{d}P_\xi(s) = \int_{\mathbb{R}} J_n^{(\beta-1,\alpha-1)}(s)J_m^{(\beta-1,\alpha-1)}(s)w(s;\alpha,\beta)\,\mathrm{d}s =$$
$$= \frac{2^{1-\alpha-\beta}}{B(\alpha,\beta)}\int_{-1}^{1} J_n^{(\beta-1,\alpha-1)}(s)J_m^{(\beta-1,\alpha-1)}(s)\tilde{w}(s;\beta-1,\alpha-1)\,\mathrm{d}s =$$
$$= \frac{1}{B(\alpha,\beta)(2n+\alpha+\beta-1)}\frac{\Gamma(n+\beta)\Gamma(n+\alpha)}{\Gamma(n+\alpha+\beta-1)n!}\delta_{nm}.$$

Moreover, given the nodes s_j and weights $\tilde{\omega}_j$ from the common Gauss-Jacobi-quadrature rule for weighting function $\tilde{w}(.,\beta-1,\alpha-1)$, the Gauss-quadrature rule in terms of weighting function $w(.,\alpha,\beta)$ has the same nodes while the weights are scaled by $\omega_j = \frac{2^{1-\alpha-\beta}}{B(\alpha,\beta)}\tilde{\omega}_j$.

4.A.4 Generalized Laguerre polynomials

Generalized Laguerre polynomials are defined by the recurrence relation

$$La_0^{(\alpha)}(x) = 1,$$
$$La_1^{(\alpha)}(x) = 1+\alpha-x,$$
$$(n+1)La_{n+1}^{(\alpha)}(x) = (2n+1+\alpha-x)La_n^{(\alpha)}(x) - (n+\alpha)La_{n-1}^{(\alpha)}(x), n\geq 2$$

They form a complete orthogonal system on $L^2([0,\infty),\mathscr{B}([0,\infty)),\tilde{w}(x)\,\mathrm{d}x)$ with weighting function

$$\tilde{w}(x;\alpha) := x^\alpha e^{-x}.$$

More specifically,

$$\int_0^\infty La_n^{(\alpha)}(x)La_m^{(\alpha)}(x)\tilde{w}(x;\alpha)\,\mathrm{d}x = \frac{\Gamma(n+\alpha+1)}{n!}\delta_{nm}.$$

The probability density function of a Gamma-distributed random variable, denoted by $\theta\sim$ Gamma(α,β), with shape parameter α and rate parameter β is given by

$$f_\theta(\vartheta;\alpha,\beta) := \frac{\beta^\alpha}{\Gamma(\alpha)}\vartheta^{\alpha-1}e^{-\beta\vartheta}\mathbb{1}_{[0,\infty)}(\vartheta).^{26}$$

Fixing the transformation between the germ and θ in this case to

$$\psi(s) := \frac{s}{\beta}$$

so that the germ ξ is defined by

$$\xi := \psi^{-1}(\theta) = \beta\theta$$

implies that ξ has probability density function

$$w(s;\alpha,\beta) = f_\theta(\psi(s);\alpha,\beta)\psi'(s) = \frac{\beta^\alpha}{\Gamma(\alpha)}\left(\frac{s}{\beta}\right)^{\alpha-1} e^{-s}\frac{1}{\beta}\mathbb{1}_{[0,\infty)}(s) = \\ = \frac{1}{\Gamma(\alpha)}\tilde{w}(s;\alpha-1)\mathbb{1}_{[0,\infty)}(s).$$

Since $w(s;\alpha,\beta)$ differs from $\tilde{w}(s;\alpha-1)$ only by a constant factor, it follows that

$$L^2(\mathbb{R},\mathscr{B}(\mathbb{R}),\mathrm{d}P_\xi) = L^2(\mathbb{R},\mathscr{B}(\mathbb{R}),w(s;\alpha,\beta)\,\mathrm{d}s) \simeq L^2([0,\infty),\mathscr{B}([0,\infty)),\tilde{w}(s;\alpha-1)\,\mathrm{d}s),$$

and that the generalized Laguerre polynomials $\{La_n^{(\alpha-1)}\}_{n\in\mathbb{N}_0}$ also form a complete orthogonal system in $L^2(\mathbb{R},\mathscr{B}(\mathbb{R}),\mathrm{d}P_\xi)$ with

$$\int_{\mathbb{R}} La_n^{(\alpha-1)}(s)La_m^{(\alpha-1)}(s)\,\mathrm{d}P_\xi(s) = \int_{\mathbb{R}} La_n^{\alpha-1)}(s)J_m^{(\alpha-1)}(s)w(s;\alpha,\beta)\,\mathrm{d}s \\ = \frac{1}{\Gamma(\alpha)}\int_0^\infty La_n^{(\alpha-1)}(s)La(\alpha-1)_m(s)\tilde{w}(s;\alpha-1)\,\mathrm{d}s \\ = \frac{\Gamma(n+\alpha)}{\Gamma(\alpha)n!}\delta_{nm}.$$

Moreover, given the nodes s_j and weights $\tilde{\omega}_j$ from the common Gauss-Laguerre-quadrature rule for weighting function $\tilde{w}(.,\alpha-1)$, the Gauss-quadrature rule in terms of weighting function $w(.,\alpha,\beta)$ has the same nodes while the weights are scaled by $\omega_j = \frac{\tilde{\omega}_j}{\Gamma(\alpha)}$.

4.B Smolyak-Gauss-quadrature

Suppose that for every $i = 1,\dots,k$ the distribution P_{ξ_i} of ξ_i possesses a probability density function w_i, so that $w := \prod_{i=1}^k w_i$ is the probability density of P_ξ. Then (4.3.12) becomes

$$\hat{y}_\alpha = \|q_\alpha\|_{L^2}^{-2}\int_{\mathbb{R}}\dots\int_{\mathbb{R}} h(\psi(s_1,\dots,s_k))q_{1\alpha_1}(s_1)\dots q_{k\alpha_k}(s_k)w_1(s_1)\dots w_k(s_k)\,\mathrm{d}s_1\dots\mathrm{d}s_k. \qquad (4.B.1)$$

Further suppose that one-dimensional Gauss-quadrature rules corresponding to weighting functions w_i and orthogonal polynomials $\{q_{in}\}_{n\in\mathbb{N}_0}$ are available. For $i = 1,\dots,k$ let $Q_i(M_i)$ denote this one-dimensional Gauss-quadrature rule with M_i nodes $\{s_{i,M_i}^{(j)}\}_{j=1,\dots,M_i}$ and weights

[26] We denote by $\Gamma(x)$ the gamma function.

$\{\omega_{i,M_i}^{(j)}\}_{j=1,\dots,M_i}$, i.e.

$$Q_i(M_i)g := \sum_{j=1}^{M_i} \omega_{i,M_i}^{(j)} g(s_{i,M_i}^{(j)}) \text{ for } g \in L_i^2.$$

Then choose for each $i = 1,\dots,k$ an increasing sequence of natural numbers $\{M_{ij}\}_{j\in\mathbb{N}} \subset \mathbb{N}, M_{ij+1} > M_{ij}$ and define the difference operator by

$$\Delta_{i1} := Q_i(M_{i1}) \quad \text{and} \quad \Delta_{ij} := Q_i(M_{ij}) - Q_i(M_{ij-1}),\ j \geq 2.$$

The Smolyak-Gauss-quadrature rule of order $l \in \mathbb{N}$ and with growth rules given by $\{M_{ij}\}_{j\in\mathbb{N}}$ is defined by

$$Q_l := \sum_{\substack{\nu\in\mathbb{N}^k \\ |\nu|\leq k+l}} \bigotimes_{i=1}^{k} \Delta_{i\nu_i}.$$

or equivalently taking care of duplicate terms in the difference operators

$$Q_l = \sum_{\substack{\nu\in\mathbb{N}^k \\ \max\{k,l+1\}\leq|\nu|\leq k+l}} (-1)^{k+l-1}\binom{k-1}{k+l-|\nu|} \bigotimes_{i=1}^{k} Q_i(M_{i\nu_i}).$$

Applying the Smolyak-Gauss-quadrature rule to (4.B.1) in particular yields the approximation

$$\hat{y}_\alpha \approx \left(\prod_{i=1}^{k} \|q_{i\alpha_i}\|_{L_i^2}^2\right)^{-1} \sum_{\substack{\nu\in\mathbb{N}^k \\ \max\{k,l+1\}\leq|\nu|\leq k+l}} (-1)^{k+l-1}\binom{k-1}{k+l-|\nu|}$$
$$\sum_{j_1=1}^{M_{1,\nu_1}} \dots \sum_{j_k=1}^{M_{k,\nu_k}} \omega_{1,M_{1,\nu_1}}^{(j_1)} \dots \omega_{k,M_{k,\nu_k}}^{(j_k)} h\left(\psi\left(s_{1,M_{1,\nu_1}}^{(j_1)} \dots s_{k,M_{k,\nu_k}}^{(j_k)}\right)\right) q_{1\alpha_1}\left(s_{1,M_{1,\nu_1}}^{(j_1)}\right) \dots q_{k\alpha_k}\left(s_{k,M_{k,\nu_k}}^{(j_k)}\right).$$

This procedure requires to evaluate the model outcome of interest $h\left(\psi\left(s_{1,M_{1,\nu_1}}^{(j_1)} \dots s_{k,M_{k,\nu_k}}^{(j_k)}\right)\right)$ at all sparse-grid points.

Chapter 5

Conclusion

All three essays in this thesis analyze techniques to efficiently evaluate and estimate dynamic stochastic general equilibrium (DSGE) models. We first consider the likelihood-based estimation of (log-) linearized DSGE models. Chapter 2 proposes a modified version of the Kalman filter as a fast option to evaluate the likelihood of these models. In Chapter 3, we provide a two-step procedure for the maximum-likelihood estimation of business cycle accounting (BCA) prototype economies. Investigating the suitability of the generalized polynomial chaos expansion (PCE) in the context of DSGE modeling, Chapter 4 extends the analysis to non-linear and global solution techniques and limited-information estimation methods.

In Huber (2022) (Chapter 2), we propose the augmented steady-state Kalman filter (ASKF) as an efficient algorithm to evaluate the unconditional likelihood of (log-) linearized DSGE models. We find evidence that the ASKF performs well regardless of whether the number of observable time series exceeds the number of states or vice versa. The performance of the ASKF essentially depends on two factors: i) the length of the filtering period and ii) the time needed to determine the equilibrium variance matrix of the model's states. The larger the filtering period, the less the additional computational effort to solve for the equilibrium variance matrix of the model's states will weight compared to the total filtering time.[1] To increase the efficiency of the ASKF for DSGE models without measurement error, we provide conditions under which we may determine the states' equilibrium variance matrix analytically. We compare the performance of the ASKF in terms of an efficient likelihood evaluation to three other variants of the Kalman filter (KF): A textbook version of the KF, the Chandrasekhar recursion (CR) suggested by Herbst (2015), and a filter proposed by Koopman and Durbin (2000) that bases on a univariate treatment of multivariate observation vectors (UKF). Tests in MATLAB® and FORTRAN using a medium-scale DSGE model, namely the model introduced by Smets and Wouters (2007), show that the ASKF is up to three times faster than the CR. Compared to the regular KF and the UKF, the ASKF reduces the computational burden by 60 to 80 percent. Consequently, we consider the ASKF a valid option to reduce the computational burden when evaluating the likelihood of medium- to large-scale DSGE models.

In Fehrle and Huber (2022) (Chapter 3), we perform a BCA analysis for the Great Recession in Germany and the subsequent stimulus measures. To adjust our analysis to the German case, we extend the benchmark prototype economy of Chari et al. (2007) in three ways: First, the wedges include a long- and a short-run component, which allows us to differentiate between growth and business cycle accounting. Second, we distinguish between government spending and net exports, which enables a government spending analysis and accounts for the fact that the German industry strongly depends on foreign trade. Third, we exclude durable consumption goods from aggregated investment in order to consider the cash for clunkers program separately. The resulting prototype economy includes six wedges: a government consumption wedge, a

[1] Note that the filtering period equals either the number of observations or the required periods until it becomes possible to switch to a steady-state Kalman filter (SKF)

durables wedge, an investment wedge, a labor wedge, a net exports wedge, and an efficiency wedge. To estimate the 57 parameters of the wedges' underlying VAR process as well as two structural parameters of our prototype economy, we introduce a reliable and quick procedure to locate the maximum of the likelihood function. Applying this two-step maximum-likelihood estimation (MLE) procedure, we detect two local maxima concerning the estimated structural parameters and identify the global one, for which we illustrate and discuss the results. We find that the efficiency wedge mainly drove the crises, followed by the net exports and the investment wedge. While the labor wedge slightly contributed to the crisis, it also induced a fast recovery. The government consumption wedge and the durables wedge acted counter-cyclically. Discussing our results against different market interventions, we attribute the counter-cyclicality of the government consumption and the durables wedge to measures of the German stimulus program, such as the higher expenditures for government consumption or the cash for clunkers program.

In Fehrle, Heiberger, and Huber (2022) (Chapter 4), we review the method of generalized PCE and its applicability to computational economics and, in particular, DSGE models. As the parameters of those models are typically unknown, one must either assess the effects of the parameter uncertainty on the model's quantity of interest (QoI) (sensitivity/robustness evaluation) or infer plausible values from empirical data (estimation). The required methods are computationally cumbersome since they mostly rely on the repeated computation of the model's solution. PCE offers a promising alternative and has found its way into computational modeling in many disciplines outside of economics. We review the basic theory underlying the PCE and the methods of its practical implementation. At the example of the benchmark real business cycle (RBC) model, we show how to (point-wise) approximate the model's QoIs by a PCE of its parameters. While determining the coefficients of this series expansion requires to evaluate the model's QoI for different parameter values, given the respective formulae, the repeated evaluation of the model's QoI becomes inexpensive in terms of computational time required. We find that the method of generalized PCE particularly suits models with a manageable number of parameters, which are time-consuming to solve but at the same time require frequent evaluation. This is confirmed by our numerical analysis, where we analyze the efficiency of PCE to evaluate and estimate the benchmark RBC model.

Bibliography

CHARI, V. V., P. J. KEHOE, AND E. R. MCGRATTAN (2007): "Business Cycle Accounting," *Econometrica*, 75, 781–836.

FEHRLE, D., C. HEIBERGER, AND J. HUBER (2022): "Polynomial Chaos Expansion: Efficient Evaluation and Estimation of Computational Models".

FEHRLE, D. AND J. HUBER (2022): "Business Cycle Accounting for the German Fiscal Stimulus Program during the Great Recession".

HERBST, E. (2015): "Using the "Chandrasekhar Recursions" for Likelihood Evaluation of DSGE Models," *Comput. Econ.*, 45, 693–705.

HUBER, J. (2022): "An Augmented Steady-State Kalman Filter to Evaluate the Likelihood of Linear and Time-Invariant State-Space Models".

KOOPMAN, S. J. AND J. DURBIN (2000): "Fast Filtering and Smoothing for Multivariate State Space Models," *Journal of Time Series Analysis*, 21, 281–296.

SMETS, F. AND R. WOUTERS (2007): "Shocks and Frictions in US Business Cycles: A Bayesian DSGE Approach," *American Economic Review*, 97, 586–606.